RNI - No. MAHENG/2017/74063
VOLUME 1 (Issue 1) July - December 2017
VOLUME 1 (Issue 2) January - June 2018

ISSN No. 2581-5911
BI-ANNUAL SUBSCRIPTION : Rs. 2000/-

G P GLOBALIZE RESEARCH JOURNAL OF CHEMISTRY

RNI - No. MAHENG/2017/74063

ISSN NO 2581-5911

G P GLOBALIZE RESEARCH JOURNAL OF CHEMISTRY

VOLUME 1 (Issue 1) July - December 2017
VOLUME 1 (Issue 2) January - June 2018

BI-ANNUAL 2017- 2018

CIN U22130MH2016PTC287238
UAN- MH19D0008178

GAURANG PUBLISHING GLOBALIZE PVT. LTD
1,PLOT-72, P. M. M. M. MARG,
TARDEO, MUMBAI-400034.
TEL. 022 23522068 (M) : +91 9969392245
Email : gpglobalize@gmail.com / publish@gpglobalize.com
Web : www.gpglobalize.com

RNI No. MAHENG/2017/74063 ISSN No. 2581–5911

Volume 1 Issue 1 ❖ July – December 2017
Volume 1 Issue 2 ❖ January – June 2018

G P GLOBALIZE RESEARCH JOURNAL OF CHEMISTRY

GAURANG PUBLISHING GLOBALIZE PRIVATE LIMITED, MUMBAI

CIN No. U22130MH2016PTC287238

UAN - MH19D0008178

GP GLOBALIZE RESEARCH JOURNAL OF CHEMISTRY

An International Peer Reviewed Journal of Chemistry

RNI No: MAHENG/2017/74063 **ISSN (Print) No: 2581-5911**

Editor-in-Chief

Dr. D.V. Prabhu
Adjunct Professor and Former Head,
Department of Chemistry, Wilson College, Mumbai - 400 007, India
E-mail : dvprabhu48@gmail.com
Contact: +91 9870 22 68 99

Consulting Editors

Prof. S.M. Khopkar
Professor Emeritus
Department of Chemistry,
IIT-Bombay, Mumbai - 400 076, India
E-mail : khopkarsm@yahoo.com

Prof. Dr. Tulsi Mukherjee
Former Group Director, Chemistry Group,
BARC, Mumbai.
Professor, Homi Bhabha National Institute,
BARC, Mumbai, India
Email: tulsi.mukherjee@gmail.com

Prof. Dr. Irena Kostova
Department of Chemistry,
Faculty of Pharmacy, Medical University,
Sofia, Bulgaria
E-mail : irenakostova@yahoo.com

Publishing Co-ordinator

Mr. Rajan Pendurkar
Gaurang Publishing Globalize Private Limited, Mumbai.
Email: gpglobalize@gmail.com
Contact: +91 9969 392 245

Printed and Published by Gaurang Rajan Pendurkar on behalf of Gaurang Publishing Globalize Private Limited and printed at NIL CREATION, Shop No. 7, 35/55, Bandu Gokhale Path, Mugbhat Cross Lane, Jivanji Maharaj Chawl (Shree Swami Samarth Nagar), Girgaon, Mumbai 400004 and published at Gaurang Publishing Globalize Private Limited 1, Plot 72, P M M M Marg, Tardeo, Mumbai-400034.
Editor-in-Chief Dr. D.V. Prabhu.

Editorial Board

1. Dr. S.K. Aggarwal
   Associate Director, Radiochemistry and Isotope Group,
   BARC, Mumbai, India

2. Prof. Ram K. Agarwal
   Editor-in-Chief, Asian Journal of Chemistry,
   Sahibabad, Ghaziabad, India

3. Prof. Amani S. Awaad
   Department of Chemistry,
   King Saud University, Riyadh, Saudi Arabia

4. Prof. Sultan T. Abuorabi
   Department of Chemistry, Yarmouk University, Jordan
   Secretary General, Association of Arab Universities, Jubeyha, Amman, Jordan

5. Dr. Mahmood M. Barbooti
   Department of Applied Sciences, University of Technology, Baghdad, Iraq

6. Prof. Dr. Satish A. Bhalerao
   Former Head, Department of Botany and Environment, Wilson College, Mumbai, India

7. Prof. Kamala N. Bhat
   Department of Chemistry, Alabama A&M University, Alabama, USA

8. Prof. C.P. Bhasin
   Department of Chemistry, Hem. North Gujarat University, Patan, Gujarat, India

9. Dr. Sheshanath V. Bhosale
   ARC Future Fellow, School of Applied Sciences, RMIT University, Melbourne, Australia
   Department of Chemistry, Goa University Goa, India

10. Prof. Zhigang Chen,
    Director, Jiangsu Key Laboratory of Environment Functional Materials, School of Chemistry, Biology and Materials, Suzhov Univeristy of Science and Technology, Suzhov, Jiangsu, China

11. Dr. Prabodh Chobe
    Regional Director, Yeshwantrao Chavan Maharashtra Open University, Mumbai,
    Former General Manager-Development,
    BASF India Limited, Mumbai, India

12. Prof. Eva Chmiedewska
    Department of Environmental Ecology, Faculty of Natural Sciences,
    Comenius University, Bratislava, Slovak Republic

13. Prof. Abdalla M. Darwish
    School of STEM, Department of Physics
    Dallard University, New Orleans, Louisiana, USA

14. Dr. Ajit Datar
    Adviwor, Shimadzu Analytical (India) Private Limited, Mumbai. India

15. Dr. Ravindra G. Deshmukh
    Associate Dean, Faculty of Science, University of Mumbai, Mumbai,
    Principal, Konkan Gyanapeeth Karjat College of Arts, Science and Commerce, Karjat, Raigad District, India.

16. Prof. K.R. Desai
    Director, Department of Chemistry
    Director, C.G. Bhakta Institute of Biotechnology,
    Uka Tarsadia University, Surat, India

Editorial Board

17. Dr. Shivani S. Dhage
Former Deputy Director, CSIR National Environmental Engineering Research Institute,
Mumbai, India

18. Prof. E.S. Dragan
Petruponi Institute of Macromolecular Chemistry, Aleea Grigore Voda, Iasi, Romania

19. Dr. Priy Brat Dwivedi
Chemistry Faculty, Caledonian College of Engineering, Muscat, Oman

20. Dr Chandrakant Gadipelly
Research Scientist, RIL-VMD Tech. Group Reliance Industries, Mumbai, India

21. Prof. Shankar Lal Garg,
Director, World Research Journals Group, Patron, World Researchers Associations, Indore, India

22. Prof. Kallol K. Ghosh
Head, Department of Chemistry, Pandit Ravi Shankar Shukla University,
Raipur, India

23. Dr. Pushpito Ghosh
K.V. Mariwala-J.B. Joshi Distinguished Professor, Institute of Chemical Technology, Mumbai, India
Former Director, CSIR Central Salt and Marine Chemical Research Institute, Bhavnagar, India

24. Prof. Falah H. Hussein
Professor of Physical Chemistry, College of Science, University of Babylon, Babylon, Iraq

25. Prof. Sudha Jain
Former Head, Department of Chemistry, University of Lucknow, Lucknow, India

26. Prof. Shehdeh Jodeh
Department of Chemistry, Najah National University, Nablus, Palestine

27. Prof. S.B. Jonnalagadda
Department of Chemistry, University of Kwazulu – Natal, Durban, South Africa

28. Dr. Hidemitsu Katsura
University of Tsukuba, Sakado, Japan,
Universiti Kuala Lumpur IPROM, Kuala Lumpur, Malaysia

29. Prof. Olga Kovalchukova
Department of General Chemistry, People's Friendship University of Russia, Moscow, Russia

30. Dr. Sudhir Kapoor
Head, Nanochemistry Section, Radiation and Photochemistry Division, BARC, Mumbai, India
Professor, Homi Bhabha National Institute, BARC, Mumbai, India

31. Dr. Anna D. Kudryavtseva
P.N. Lebedev Physical Institute,
Russian Academy of Sciences, Moscow, Russia

32. Prof. R.S. Lokhande
Head, Department of Chemistry
Director, University Research Cell,
Jaipur National University, Jaipur, India

Editorial Board

33. Prof. Mahendra Mahanti
Visiting Professor, School of Chemical Sciences, NISER, Bhubaneswar, India
Retired Professor, Department of Chemistry, North Eastern University, Shillong, Meghalaya, India

34. Prof. Jyotsna Meshram
Head, Department of Organic Chemistry, School of Chemical Sciences, North Maharashtra University, Jalgaon, India

35. Dr. Seema Mishra
Director, SIES Indian Institute of Environment, Navi Mumbai, India

36. Prof. Jose R. Mora
Universidad San Francisco de Quito, Ecuador
Venezuelan Institute for Science Research, Centre of Chemistry, Caracas, Miranda, Venezuela

37. Prof. Subhash C. Mojumdar
External Faculty, Trencin University of A Dubcek, Serbia (SR), EU

38. Prof. Gurunath Mukherjee
Sir Rashbehary Ghosh Professor (Retired), University of Calcutta, Kolkata, India

39. Dr. D.B. Naik
Radiation and Photochemistry Division, BARC, Mumbai, India

40. Dr. Reji Nair
Scientist, HPLC, Trace-Ability, Inc., Los Angeles, CA, USA

41. Dr. Venkat Narayan
Polymer Research Group, De Puy Orthopaedics, Johnson & Johnson, USA

42. Dr. R. Nagaraj
NASI Senior Scientist and J.C. Bose Fellow, CSIR Centre for Cellular and Molecular Biology, Hyderabad, India

43. Dr. Sunil S. Patil
Head, Department of Chemistry, CKT College, Panvel, India

44. Dr. Harichandra A. Parbat
Department of Chemistry, Wilson College, Mumbai, India

45. Prof. Sourav Pal
Director, IISER-Kolkata, Kolkata, India
Former Director, CSIR National Chemical Laboratory, Pune, India

46. Dr. Pradnya J Prabhu
Department of Chemistry, K.J. Somaiya College of Science and Commerce, Mumbai, India

47. Prof. Surendra Prasad
School of Biological and Chemical Sciences, University of South Pacific, Suva, Fiji

48. Dr. G. Ramakrishnan
Director, SIES Institute of Chromatography and Spectroscopy, Navi Mumbai, India
President, Chromatographic Society of India

49. Dr. A.V.R. Reddy
Former Head, Analytical Chemistry Division, BARC, Mumbai, India
Professor, Homi Bhabha National Institute, BARC, Mumbai, India

50. Prof. C. Suresh Reddy
Department of Chemistry, S.V. University, Tirupati, India

Editorial Board

51. Prof. Genserik Reniers
Department of Chemistry, University of Antwerpen, Antwerp, Belgium

52. Prof. Anil Kumar Singh
Department of Chemistry, IIT-Bombay, Mumbai, India
Former Vice-Chancellor, University of Allahabad, Allahabad, India

53. Prof. A.D. Sawant
Department of Chemistry, Institute of Science, Mumbai, India
Former Vice-Chancellor, University of Rajasthan, Jaipur, India

54. Prof. M.S. Sadjadi,
Professor of Chemistry, Tehran Science and Research Branch, Islamic Azad University, Tehran, Iran

55. Prof. Sri Juari Santosa
Department of Chemistry, Faculty of Mathematics and Natural Sciences, Gadjah Mada University, Yogyakarta, Indonesia

56. Prof. Pradeep K. Sharma
Head, Department of Chemistry, J.N.V. University, Jodhpur, India

57. Prof. Sanjay K. Sharma
Editor-in-Chief, Rasayan Journal of Chemistry, Jaipur
Head, Department of Chemistry, JECRC University, Jaipur, India

58. Prof. R.K. Sharma
Coordinator, Green Chemistry Network Centre,
Department of Chemistry, University of Delhi, Delhi, India

59. Dr. S. Sivaram
INSA Senior Scientist, IISER – Pune
Former Director, CSIR National Chemical Laboratory, Pune, India

60. Prof. Alok Srivastava
Head, Department of Chemistry, Panjab University, Chandigarh, India

61. Prof. Toyohide Takeuchi
Department of Chemistry, Faculty of Engineering, Gifu University, Gifu, Japan

62. Prof. Sunil Kumar Talapatra
Former Head, Department of Chemistry, University of Calcutta, Kolkata, India

63. Dr. S. Vasudevan
Principal Scientist, Electroinorganics Division, CSIR-Central Electrochemical Research Institute, Karaikudi, India

64. Prof. Suresh Valiyaveettil
Materials Research Laboratory, Department of Chemistry, National University of Singapore, Singapore

65. Prof. Shuli You
Shanghai Institute of Organic Chemistry, Chinese Academy of Sciences, China

G P GLOBALIZE RESEARCH JOURNAL OF CHEMISTRY

RNI No: MAHENG/2017/74063 **ISSN No (Print): 2581-5911**

GUIDELINES TO AUTHORS

GP Globalize Research Journal of Chemistry is an international peer reviewed journal which publishes full length research papers, short communications, review articles and book reviews covering all areas of Chemistry including Environmental Chemistry. G P Globalize Research Journal of Chemistry is a biannual journal published in English in print and online versions.

(1) Manuscript preparation

a) Page Layout: A4 (21 cm x 29.7 cm) leaving 2.5 cm margin on all sides of the text. All the text should be in Times New Roman font, double spaced and pages should be numbered consecutively.

b) Use MS word (2003-2007) for text and TIFF, JPEG or Paint for figures.

c) The first page should contain title in bold, 14 point size, name/s of author/s in bold, 12 point size, affiliation/s-address, email id and contact number in 11 point size, abstract-up to 200 words in 11 point size, keywords-between 5 to 10 keywords in 11 point size.

d) Main Text- The paper should be divided into the following sections:

Introduction, Materials and Methods, Results and Discussion, Conclusions, Acknowledgement and References.

Tables and Figures of good resolution (600 dpi) should be numbered consecutively and given in the order of their appearance in the text and should not be given on separate pages.

e) References- References should be cited in the text as superscript numbers in order of appearance.

References at the end of the paper should be listed in serial order to match their order of appearance in the text. Names of journals should be in italics and volume number should be in bold.

Reference to papers e.g. Ganesh R.S., Pravin S. and Rao T.P., 2005, *Talanta,* **66,** 513.

Reference to books e.g. Lee J.D., 1984, A New Course in Inorganic Chemistry, 3rd ed., ELBS and Van Nostrand Reinhold (UK) Co. Ltd., p.268-269.

f) Abbreviations should be explained at first appearance in the text.

g) Nomenclature should be as per **IUPAC** guidelines.

h) SI units should be used throughout.

(2) Manuscript Submission

Manuscripts should be submitted online at dvprabhu48@gmail.com. The paper will be accepted for publication after review. All correspondence should be made to the Editor-in-Chief at dvprabhu48@gmail.com.

(3) Proofs

Galley proofs will be sent online to the corresponding author on request and should be returned to the Editorial office within seven working days.

(4) Plagiarism

GP Globalize Research Journal of Chemistry is committed to avoid plagiarism and ensure that only original research work is published.

The Editorial Board and panel of reviewers will check and prevent plagiarism in the manuscripts submitted for publication.

(5) Copyright

Publication of a paper in GP Globalize Research Journal of Chemistry automatically transfers copyright to the publisher. Authors can share free eprints of their published papers with fellow researchers.

(6) Circulation and Subscription rates

Issue No. 1 in July to December

Subscription rates are as follows:

Library/Instituional charges (In India)	₹ 2000/-
Individual charges (In India)	₹ 2000/-
Library/Instituonal charges (Outside India)	US $ 150
Individual charges (Outside India)	US $ 150

Subscription charges:
Review of Research papers is done free of charge. Subscription to the Journal is expected.

Mode of Payment

Demand draft/Multicity cheque payable at Mumbai in favour of
"Gaurang Publishing Globalize Pvt. Ltd. Mumbai"

For Online payment:

Name of the Bank:	**Axis Bank**
Branch Name:	**Tardeo, Mumbai (MH)**
Account No.	**916020066451552**
IFSC Code:	**UTIB0001345**

For further details please contact:

Dr. D.V. Prabhu, Editor-in-Chief,
Email: dvprabhu48@gmail.com
Mobile: 09870 226 899

Mr. Rajan Pendurkar, Publishing Co-ordinator,
Email: gpglobalize@gmail.com
Mobile: 09969 392 245

A Request to Authors

We thank you for sending your research paper to G P Globalize Research Journal of Chemistry (RNI No. MAHENG/2017/74063 ISSN No. (Print): 2581-5911

*You are requested to send a DD/Multicity Cheque for ₹ 2000/- in favour of "**Gaurang Publishing Globalize Pvt. Ltd., Mumbai**" payable at Mumbai. If the Editorial Board accepts your paper for publication after review, then your DD/cheque will be deposited and a receipt will be sent for the same, otherwise the DD/Cheque will be returned to you at the earliest.*

We would appreciate if you help us in our efforts to promote academic excellence.

G P GLOBALIZE RESEARCH JOURNAL OF CHEMISTRY

RNI No. MAHENG/2017/74063 ISSN No. (Print) 2581-5911

Volume 1 Issue 1 ❄ July-December 2017

CONTENTS

Papers

1. Synthesis, characterization and antimicrobial activities of some new methylene based Schiff bases containing benzothiazole derivatives **1 - 7**
   Divyanshu D. Patel and Keshav C. Patel

2. An efficient constriction of Quinolin-4(1H)-one by the use of mediated proton ionic liquid under nitrogen atmosphere **8 - 15**
   Praveen Kumar, Ashok Yadav and Saurabh Singh

3. Stability study of Anthocyanins from Banana bracts (*Musa paradisiacal* L.) of Indian origin extracted by Microwave Extraction **16 - 27**
   Mitali Kulkarni and Ajit Datar

4. Bionics – inspiration in nature for design of new adsorbents and their potential in removal of pharmaceuticals **28 - 33**
   Eva Chmielewská

5. Separation of Anions with Capillary Liquid Chromatography using Polymethacrylate based Monolithic Capillary Columns modified with Arginine **34 - 44**
   Oksil Venriza, Lee Wah Lim, and Toyohide Takeuchi

6. Antimicrobial Poly(*N*-vinyl carbazole)/Carbon Multiwalled Nanotubes (PVK/MWNTs) CPN nanocomposite film as coatings on conducting surfaces **45 - 53**
   Karina Milagros Cui-Lim

7. Kinetics and mechanism of oxidation of D-xylose and D-arabinose by N-Bromonicotinamide **54 - 60**
   L. Pushpalatha

8. Development and Validation of HPTLC Method for Quantitation of Trigonelline from M*irabilis jalapa* Linn. leaves and Enhancement in Extraction Yield of Trigonelline from Ultra Fine Powder **61 - 71**
   Padma S. Sathe and Vidya V. Dighe

9. SERS study of two organophosphates: Dimethoate and methyl parathion **72 - 78**
   Praveen S.G., Asenath Benitta T, Sudhir Kapoor, Jayakumar V.S., Bansal C and Kumaran J. T. T.

Conference Alerts **79 - 81**

RNI No. MAHENG/2017/74063
ISSN No. (Print) 2581-5911

Synthesis, characterization and antimicrobial activities of some new methylene based Schiff bases containing benzothiazole derivatives

Divyanshu D. Patel and Keshav C. Patel
Department of Chemistry, Veer Narmad South Gujarat University,
Surat - 395007, Gujarat, India
E-mail: pateldivyanshu@rediffmail.com

Abstract
A series of 6,6'-methylene bis (N-substituted benzylidene-4,7-dichloro benzo[d]thiazole-2-amine) compounds have been synthesized by the condensation of 6,6'-methylene bis (4,7-dichlorobenzo[d]thiazol-2-amine) and various substituted aromatic aldehydes. All the synthesized compounds were characterised by elemental analysis, IR spectra and ^{1}H NMR spectra. They were screened for in vitro antibacterial (E. coli, P. aeruginosa, S. aureus, S. pyogenes) and antifungal activities (C. albicans, S. cervecieaceae and A. clavatus).

Keywords: *4,4'-Methylene bis (2,5-dichloro aniline), potassium thiocyanate, bromine, aromatic aldehydes, antimicrobial activity.*

Introduction

Chemistry of heterocyclic compounds is one of the leading lines of investigations in Organic Chemistry. Heterocyclic compounds are widely distributed in nature and are essential for life. They play a vital role in the metabolism of all living cells. There are a vast number of pharmacologically active heterocyclic compounds, many of which are in regular clinical use.

Nitrogen, sulphur and oxygen containing five member heterocyclic compounds have assumed importance in drug discovery processes. Benzothiazole derivatives exhibit a wide range of biological activities, such as antifungal [1-2], antibacterial [3], antitumor [4-5], anti-inflammatory [6], anticonvulsant [7-8], anticancer [9-10] and antiturbercular [11]. We report herein the synthesis and comparative microbial activities of five member heterocyclic derivatives (benzothiazole).

Materials and Methods

Synthesis of 4,4'-methylene bis (2, 5-dichloro aniline) (3)

4-4'-Methylene bis (2,5-dichloro aniline) (3) was synthesized by the method described in literature [12].

Synthesis of the 6,6'-methylene bis (4,7-dichlorobenzo [d]thiazol-2-amine) (4)

4,4'-Methylene bis (2,5-dichloro aniline) (3.36 g, 0.01 mol) (3) and potassium thiocynate (19.44 g, 0.2 mol) were added to 40.0 mL of precooled acetic acid at 5^0C temperature. To this solution, 6.0 mL of bromine in 24.0 mL of glacial acetic acid was added carefully so that the temperature did not rise beyond 0^0C. After all the bromine had been added (120 minutes), the solution

was stirred for an additional 2 hours at 0^0C temperature. It was allowed to stand overnight to give an orange precipitate. Water (25.0 mL) was added quickly and the slurry was heated at 85^0C on a steam bath and filtered. The orange residue was placed in a reaction flask and treated with 10.0 mL of glacial acetic acid and again heated to 85^0C and filtered. The combined filtrate was cooled and neutralized with concentrated ammonia solution to pH 6 to give dark yellow precipitate of 6,6'-methylene bis (4,7-dichlorolbenzo [d]thiazol-2-amine) and recrystallized from toluene. Yield 85%, m.p. 265^0C[13-14].

General synthesis of the compounds (5a- j)

6,6'-Methylene bis (*N*-substituted benzylidene-4,7-dichloro benzo[*d*]thiazol-2-amine) compounds were synthesized by reaction of 6,6'-methylene bis (4,7-dichlorobenzo [*d*]thiazol-2-amine) (4.50g, 0.01 mol) with various substituted aromatic aldehyde (0.02 mol). Each reactant was dissolved in a minimum amount of methanol, mixed together and a few drops of glacial acetic acid catalyst were added. The solution was refluxed for 10 hours then cooled to atmospheric room temperature and poured into ice cold water to give solid product. It was filtered, washed with water, dried and recrystallised from ethanol [15-16].

Scheme-1: Synthetic route for 6,6'-methylene bis (*N*-substituted benzylidene-4,7-dichloro benzo[*d*]thiazol-2-amine) from 2,5-dichloro aniline (5a- j).

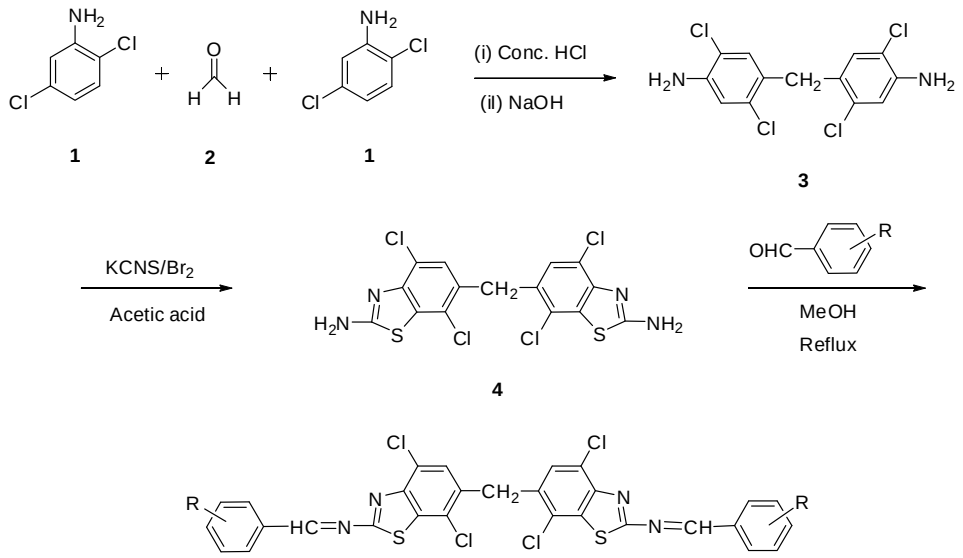

where, R = a. 4-OH, b. 4-CH_3, c. H, d. 2-CH_3, e. 2-OH, f. 2-NO_2, g. 2-F, h. 4-F, i, 4-Cl, j. 2-Cl.

6,6'-Methylene bis(N-4-hydroxybenzylidene-4,7-dichlorobenzo[d]thiazole-2-amine) 5a

Brown colour solid powder, mp 106^0C, yield 71%; IR (KBr, cm^{-1}): 3400 (O-H stretching, Ar-OH), 3060 (C-H stretching, aromatic), 2935, 2850 (C-H stretching, -CH_2-group), 1635 (C=N stretching, Schiff base), 1585 (C=N stretching, benzothiazole), 1505 (C=C stretching, aromatic), 1470, 1430 (C-H bending, -CH_2- group), 1330 (O-H bending, Ar-OH), 720 (C-Cl stretching, chloro); ^{1}H NMR (400.1 MHz, DMSO): δ_H 3.84 (s, 2H, CH_2), 6.85-7.79 (m, 10H, Ar-H), 8.50 (s, 2H, HC=N), 9.80 (s, 2H, OH); Anal. Calcd for: $C_{29}H_{16}Cl_4N_4O_2S_2$ (685.40); Found (C, 52.97), requires (C, 52.90); Found (H, 2.38),

requires (H, 2.45); Found (N, 8.45), requires (N, 8.51).

6,6'-Methylene bis(N-4-methylbenzylidene-4,7-dichlorobenzo[d]thiazole-2-amine) 5b

Light yellow colour solid powder, mp 126^{0}C, yield 68%; IR (KBr, cm^{-1}): 3060 (C-H stretching, aromatic), 2930, 2855 (C-H stretching, -CH_2- group), 2920, 2870 (C-H stretching, -CH_3 group), 1620 (C=N stretching, Schiff base), 1590 (C=N stretching, benzothiazole), 1510 (C=C stretching, aromatic), 1475, 1430 (C-H bending, -CH_2- group), 1380 (C-H bending, -CH_3), 740 (C-Cl stretching, chloro); ^{1}H NMR (400.1 MHz, DMSO): δ_H 2.23 (s, 6H, -CH_3), 3.92 (s, 2H, CH_2), 6.90-7.69 (m, 10H, Ar-H), 8.60 (s, 2H, HC=N); Anal. Calcd for: $C_{31}H_{20}Cl_4N_2S_2$ (654.46); Found (C, 56.83), requires (C, 56.89); Found (H, 3.14), requires (H, 3.08); Found (N, 8.49), requires (N, 8.56).

6,6'-Methylene bis(N-benzylidene-4,7-dichlorobenzo [d]thiazole-2-amine) 5c

Orange colour solid powder, mp 144^{0}C, yield 72%; IR (KBr, cm^{-1}): 3060 (C-H stretching, aromatic), 2930, 2855 (C-H stretching, -CH_2- group), 1628 (C=N stretching, Schiff base), 1600 (C=N stretching, benzothiazole), 1515 (C=C stretching, aromatic), 1470, 1430 (C-H bending, -CH_2- group), 745 (C-Cl stretching, chloro); ^{1}H NMR (400.1 MHz, DMSO): δ_H 3.95 (s, 2H, CH_2), 6.95-7.83 (m, 12H, Ar-H), 8.50 (s, 2H, HC=N); Anal. Calcd for: $C_{29}H_{16}Cl_4N_4S_2$ (626.41); Found (C, 55.65), requires (C, 55.60); Found (H, 2.51), requires (H, 2.57); Found (N, 8.89), requires (N, 8.94).

6,6'-Methylene bis(N-2-methylbenzylidene-4,7-dichlorobenzo[d]thiazole-2-amine) 5d

Light yellow colour solid powder, mp 123^{0}C, yield 68%; IR (KBr, cm^{-1}): 3065 (C-H stretching, aromatic), 2930, 2850 (C-H stretching, -CH_2- group), 2925, 2870 (C-H stretching, -CH_3 group), 1625 (C=N stretching, Schiff base), 1595 (C=N stretching, benzothiazole), 1515 (C=C stretching, aromatic), 1475, 1440 (C-H bending, -CH_2- group), 1385 (C-H bending, -CH_3), 760 (C-Cl stretching, chloro); ^{1}H NMR (400.1 MHz, DMSO): δ_H 2.25 (s, 6H, -CH_3), 3.90 (s, 2H, CH_2), 6.92-7.69 (m, 10H, Ar-H), 8.75 (s, 2H, HC=N); Anal. Calcd for: $C_{31}H_{20}Cl_4N_2S_2$ (654.46); Found (C, 56.94), requires (C, 56.89); Found (H, 3.15), requires (H, 3.08); Found (N, 8.50), requires (N, 8.56).

6,6'-Methylene bis(N-2-hydroxybenzylidene-4,7-dichlorobenzo[d]thiazole-2-amine) 5e

Brown colour solid powder, mp 134^{0}C, yield 73%; IR (KBr, cm^{-1}): 3405 (O-H stretching, Ar-OH), 3065 (C-H stretching, aromatic), 2935, 2855 (C-H stretching, -CH_2- group), 1620 (C=N stretching, Schiff base), 1590 (C=N stretching, benzothiazole), 1505 (C=C stretching, aromatic), 1470, 1435 (C-H bending, -CH_2- group), 1335 (O-H bending, Ar-OH), 750 (C-Cl stretching, chloro); ^{1}H NMR (400.1 MHz, DMSO): δ_H 3.91 (s, 2H, CH_2), 6.85-7.70 (m, 10H, Ar-H), 8.60 (s, 2H, HC=N), 9.85 (s, 2H, OH); Anal. Calcd for: $C_{29}H_{16}Cl_4N_4O_2S_2$ (685.40); Found (C, 52.95), requires (C, 52.90); Found (H, 2.38), requires (H, 2.45); Found (N, 8.57), requires (N, 8.51).

6,6'-Methylene bis(N-2-nitrobenzylidene-4,7-dichlorobenzo[d]thiazole-2-amine) 5f

Yellow colour solid powder, mp 96^{0}C, yield 69%; IR (KBr, cm^{-1}): 3055 (C-H stretching, aromatic), 2925, 2845 (C-H stretching, -CH_2- group), 1627 (C=N stretching, Schiff base), 1605 (C=N stretching, benzothiazole), 1580, 1350 (N=O stretching, -NO_2), 1525 (C=C stretching, aromatic), 1477, 1440 (C-H bending, -CH_2- group), 760 (C-Cl stretching, chloro); ^{1}H NMR (400.1 MHz, DMSO): δ_H 3.96 (s, 2H, CH_2), 6.89-7.85 (m, 10H, Ar-H), 8.80 (s, 2H, HC=N); Anal. Calcd for: $C_{29}H_{14}Cl_4N_6O_4S_2$ (716.40); Found (C, 48.56), requires (C, 48.62); Found (H, 1.90), requires (H, 1.97); Found (N, 11.79), requires (N, 11.73).

6,6'-Methylene bis(N-2-fluorobenzylidene-4,7-dichlorobenzo[d]thiazole-2-amine) 5g

Brown colour solid powder, mp 128^{0}C, yield 67%; IR (KBr, cm^{-1}): 3060 (C-H stretching, aromatic), 2930, 2855 (C-H stretching, -CH_2- group), 1635 (C=N stretching, Schiff base), 1610 (C=N stretching, benzothiazole), 1520 (C=C stretching, aromatic), 1465, 1435 (C-H bending, -CH_2- group), 1105 (C-F stretching, Fluoro), 760 (C-Cl

stretching, chloro); ^{1}H NMR (400.1 MHz, DMSO): δ_H 3.95 (s, 2H, CH_2), 6.90-7.86 (m, 10H, Ar-H), 8.90 (s, 2H, HC=N); Anal. Calcd for: $C_{29}H_{14}Cl_4F_2N_2S_2$ (662.38); Found (C, 52.65), requires (C, 52.58); Found (H, 2.21), requires (H, 2.13); Found (N, 8.53), requires (N, 8.46).

6,6'-Methylene bis(N-4-fluorobenzylidene-4,7-dichlorobenzo[d]thiazole-2-amine) 5h

Brown colour solid powder, mp 141^{0}C, yield 65%; IR (KBr, cm^{-1}): 3050 (C-H stretching, aromatic), 2935, 2850 (C-H stretching, -CH_2- group), 1630 (C=N stretching, Schiff base), 1585 (C=N stretching, benzothiazole), 1520 (C=C stretching, aromatic), 1465, 1435 (C-H bending, -CH_2- group), 1100 (C-F stretching, Fluoro), 730 (C-Cl stretching, chloro); ^{1}H NMR (400.1 MHz, DMSO): δ_H 3.84 (s, 2H, CH_2), 6.92-7.95 (m, 10H, Ar-H), 8.53 (s, 2H, HC=N); Anal. Calcd for: $C_{29}H_{14}Cl_4F_2N_2S_2$ (662.38); Found (C, 52.50), requires (C, 52.58); Found (H, 2.20), requires (H, 2.13); Found (N, 8.38), requires (N, 8.46).

6,6'-Methylene bis(N-4-chlorobenzylidene-4,7-dichlorobenzo[d]thiazole-2-amine) 5i

Green colour solid powder, mp 130^{0}C, yield 68%; IR (KBr, cm^{-1}): 3055 (C-H stretching, aromatic), 2945, 2850 (C-H stretching, -CH_2- group), 1628 (C=N stretching, Schiff base), 1585 (C=N stretching, benzothiazole), 1525 (C=C stretching, aromatic), 1460, 1435 (C-H bending, -CH_2- group), 750 (C-Cl stretching, chloro); ^{1}H NMR (400.1 MHz, DMSO): δ_H 3.89 (s, 2H, CH_2), 6.89-7.55 (m, 10H, Ar-H), 8.65 (s, 2H, HC=N); Anal. Calcd for: $C_{29}H_{14}Cl_6N_4S_2$ (695.30); Found (C, 50.18), requires (C, 50.10); Found (H, 2.09), requires (H, 2.03); Found (N, 8.12), requires (N, 8.06).

6,6'-Methylene bis(N-2-chlorobenzylidene-4,7-dichlorobenzo[d]thiazole-2-amine) 5j

Light yellow colour solid powder, mp 145^{0}C, yield 71%; IR (KBr, cm^{-1}): 3060 (C-H stretching, aromatic), 2935, 2845 (C-H stretching, -CH_2- group), 1620 (C=N stretching, Schiff base), 1580 (C=N stretching, benzothiazole), 1520 (C=C stretching, aromatic), 1460, 1430 (C-H bending, -CH_2- group), 740 (C-Cl stretching, chloro); ^{1}H NMR (400.1 MHz, DMSO): δ_H 3.90 (s, 2H, CH_2), 6.88-7.47 (m, 10H, Ar-H), 8.60 (s, 2H, HC=N); Anal. Calcd for: $C_{29}H_{14}Cl_6N_4S_2$ (695.30); Found (C, 50.04), requires (C, 50.10); Found (H, 2.07), requires (H, 2.03); Found (N, 8.14), requires (N, 8.06).

Results and Discussion

All the synthesized compounds were recrystallized and purified. The structures of the newly synthesized compounds were determined on the basis of their FTIR and ^{1}H NMR spectra data. Methyl and methylene C-H stretching vibrations were observed near 2926 cm^{-1} and 2853 cm^{-1} respectively. Broad absorption bands observed in the region between 3080-3030 cm^{-1} and 1620-1480 cm^{-1} indicated the presence of aromatic C-H stretching and C=C stretching respectively. The absorption band observed in the region of 1615-1565 cm^{-1} confirmed the presence of C=N stretching of benzothiazole ring. The ^{1}H NMR spectra of the synthesized compound showed chemical shifts, which are characteristic of the expected structure of compounds. A singlet observed at d 3.84 was attributed to -CH_2- and d 8.60 to -N=CH- of Schiff base.

For antibacterial activity, the newly synthesized compounds were screened against gram positive bacteria *S. aureus* (MTCC-96) and *Streptococcus pyogenes* (MTCC-443) and gram negative *E.Coli* (MTCC-442) and *Pseudomonas aeruginosa* (MTCC-2488)]. Antibacterial activity was carried out by serial broth dilution method [17-18]. The compounds **(5a-j)** were screened for their antibacterial activity in triplicate against *E. coli*, *S. aureus*, *P. aeruginosa*, and *S. pyogenes* at different concentrations of 1000, 500, 250, 125, 62.5 µg/mL as shown in **(Table 1)**. The drugs which were found to be active in primary screening were similarly diluted to obtain 125, 62.5 µg/mL concentrations. The standard drug used in this study were 'Norfloxacin, Ciprofloxacin and Chloramphenicol' for evaluating antibacterial activity which showed (100, 50, 25, and 12.5 µg/mL) MIC against *E. coli*, *P. aeruginosa*, *S. aureus*, and S. *pyogenes* respectively.

Antimicrobial activity:

Antibacterial activity

Table 1: Antibacterial activity of compounds [5a to 5j]

Compound	Minimum Inhibitory Concentrations (µg/mL)			
	Gram negative bacteria		Gram positive bacteria	
	E. coli	*P. aeruginosa*	*S. aureus*	*S. pyogenus*
5a	250	500	125	250
5b	250	62.5	250	250
5c	125	250	500	250
5d	250	250	500	250
5e	250	250	500	250
5f	500	125	250	250
5g	500	250	500	250
5h	250	500	250	250
5i	500	500	125	250
5j	125	250	250	500
Norfloxacin	50	50	50	50
Ciprofloxacin	50	50	50	50
Chloramphenicol	50	50	50	50

Antifungal activity

Table 2: Antifungal activity of compounds [5a to 5j].

Compound	Minimum Inhibitory Concentrations (µg/mL)		
	Fungus		
	C. albicans	*S. cervecieaceae*	*A. clavatus*
5a	1000	1000	1000
5b	1000	500	1000
5c	500	500	1000
5d	1000	500	1000
5e	500	500	1000
5f	500	500	500
5g	500	250	1000
5h	500	500	500
5i	1000	500	1000
5j	1000	1000	500
Nystatin-B	100	100	100
Gresiofulvin	100	100	100

Same compounds were tested for antifungal activity in triplicate against *C. albicans*, *S. Cervecieaceae* and *A. clavatus* at various concentrations of 1000, 500, 200 and 100 µg/ml as shown in **Table 2**. The results were recorded in the form of primary and secondary screening. The synthesized compounds were diluted to

1000 µg/mL concentration, as a stock solution. The synthesized compounds which were found to be active in the primary screening were further tested in a second set of dilution against all microorganisms. The lowest concentration, which showed no growth after spot sub-culture was considered as MIC for each drug. The highest dilution showing at least 99% inhibition was taken as MIC. The test mixture containing 10^8 spores/mL MIC. "Nystatin-B" and "grisiofulvin" was used as a standard drug for antifungal activity, which showed MIC against *C. albicans*, *S. cervecieaceae*, and *A. clavatus*, respectively. The results of antimicrobial evaluation of derivatives (5a-j) are shown in Table 2.

Conclusions

A variety of benzothiazole derivatives have been successfully synthesized in excellent appreciable yields and screened in vitro for their antimicrobial activities against both strains of Gram-positive, Gram-negative bacteria and fungal strains. The spectral analysis data confirmed the proposed structures for these newly synthesized compounds.

Acknowledgement

The authors are thankful to Prof. Keshav C. Patel, Head of the Department of Chemistry, V.N.S.G. University, Surat, India for providing all the laboratory facilities. Special thanks go to UGC-BSR Research fellowship (SAP) for providing financial support during the research work and also SAIF, Punjab University, Chandigarh for spectral data.

References

1. Alessia C., Ivana D., Marilena M., Antonio C., Francoise V.B., Antonio R., Filomena C. and Carlo F., 2013, *Eur. J. Med. Chem.*, **64**, 357-364.

2. Mehlika D.A., Zafer A.K., Gulhan T.Z., Ahmet O., Fatih D., Gokalp I. and Gilbert R., 2014, *Synthe. Commu.*, **41**, 2234-2250.

3. Russo F., Romeo G., Santagati N.A., Caruso A., Cutuli V. and Amore D., 1994, *Eur. J. Med. Chem.*, **29**, 569-578.

4. Lion C.J., Matthews C.S., Wells G., Bradshaw T.D., Stevens M.F.G. and Westwell A.D., 2006, *Bioorg. Med. Chem. Lett.*, **16**, 5005-5008.

5. Racane L., Stojkovic R., Kulenovic V.T. and Zamola G.K., 2006, *Molecules*, **11**, 325.

6. Sharma N.K. and Jha K.K., 2010, *Int. J. Curr. Pharma. Res.*, **2(2),** 01-06.

7. Siddiqui N., Pandeya S.N, Khau S.A., Stables J., Rana A.R., Alan M., Md-Arshad F. and Bhat M.A., 2007, *Bioorg. Med. Chem.*, **17**, 225-259.

8. Hisamoddin S.Z.K., Sanchaity P., Sharma P.Y. and Patel N.U., 2014, *Pharma Science Monitor*, **5(1)**, 207-225.

9. Huang S.T., Hsei I.J. and Chen C., 2006, *Bioorg. Med. Chem.*, **14**, 6106-6119.

10. Xuan-Hong S., Zhao W., Yong X., Ting-Hong Y., Mei D., You-Zhi X., Yu-Quan W. and Luo-Ting Y., 2012, *Molecules*, 17, 3933-3944.

11. Desai K.G., Raval J.P. and Desai K.R., 2006, *J. Iranian Chem. Soc.*, **3**, 233.

12. Patel D.D., Patel M.S., Patel V.S. and Patel K.C., 2014, *Int. J. Adv. Res.*, **2(3)**, 1048-1054.

13. Shashank D., Vishawanth T., Balasubramaniam V., Nagendra A., Perumal P. and Suthakaran R., 2009, *Int. J. Chem. Res.*, **1(4)**, 1224-1231.

14. Barot H.K., Mallika G., Sutariya B.B., Shukla J. and Nargund L.V., 2010, *Res. J. Pharm. Bio. & Chem. Sci.*, **1(1)**, 124-129.

15. Ibrahim M.N., Hamad K.J. and Al-Joroshi S. H., 2006, *Asian J. Chem.*, **18(3)**, 2404-2406.

16. Baliani A., Baeno G.J., Stewart M.L. and Brun R., 2005, *J. Med. Chem.*, **48**, 5570.

17. Ghalem B.R. and Mohamed B., 2009, *African J Pharm. Pharmacol.*, **3**, 92-96.

18. Desai N.C. and Trivedi P., 1993, *Indian J. Chem.*, **33B**, 97-500.

RNI No. MAHENG/2017/74063
ISSN No. (Print) 2581-5911

An efficient constriction of Quinolin-4(1H)-one by the use of mediated proton ionic liquid under nitrogen atmosphere

Praveen Kumar[1], Ashok Yadav[1] and Saurabh Singh[2*]
[1]Department of Chemistry, University of Rajasthan, Jaipur-302055, India
[2*]Department of Chemistry, M. L.V. Govt. College, Bhilwara-311001, Rajasthan, India
Emai: praveenkaler@gmail.com, saurabhsingh.chem@gmail.com

Abstract
An eco-friendly methodology for the synthesis of Quinolin-4(1H)-one and its derivatives in the presence of ionic liquid [BMIM]Br has been suggested and the reaction carried out between substituted arylamine with Meldrum's acid (2, 2-dimethyl- 1,3-dioxane-4,6-dione) and trimethyl orthomate under nitrogen atmosphere at 45±2°C.

Keywords: ***S****ubstituted arylamine, Meldrum's acid (2, 2-dimethyl-1,3-dioxane-4,6-dione), trimethyl orthoformate, Ionic liquid (1-butyl-3-methylimidazolium bromide)[BMIM]Br.*

Introduction

Quinolones constitute an important framework of nitrogen containing heterocycles, which have contributed to society from the biological and industrial view points to help understand life processes.[1,2] Thus, quinolone nucleus represents a pharmaceutically important class of compounds because of its diverse biological and pharmaceutical activities like, anti-viral[3,4], anti-platelet[5], anti-tumor[6], anti-inflammatory[7], anti-hypertensive[8], anti-HIV[9,10], positive cardiac effects[11] and tyrokinase PDGF-TRK inhibiting agents.[12] Further, these nuclei have been exploited as precursors for anti-caner[13] and anti-malarial agent.[14] The antibiotics, *viz.* norfloxacin[15] [1], ciprofloxacin[16-18] [2], Levofloxacin[19] [3], Gatifloxacin[20] [4], and ofloxacin[21,22] [5] *etc.* have been found to possess Quinolin-4(1H)-one (4[1H]-quinolone nuclei). Norfloxacin [1] and ciprofloxacin [2] have also been show to inhibit topoisomerase-II (Gyrase-a subunit).[23, 24]

Due to their remarkable pharmacological properties and potential for biological activities, a number of methods for the synthesis of quinolone derivatives[25-31] have been worked up. The literature survey[32-44] reveals that the synthesis of quinolone derivatives suffers from serious disadvantages, like involvement of hazardous chemicals, long reaction times and often poor yields. Hence we planned to develop environmentally friendly methodology for the synthesis of quinolones using ionic liquids.

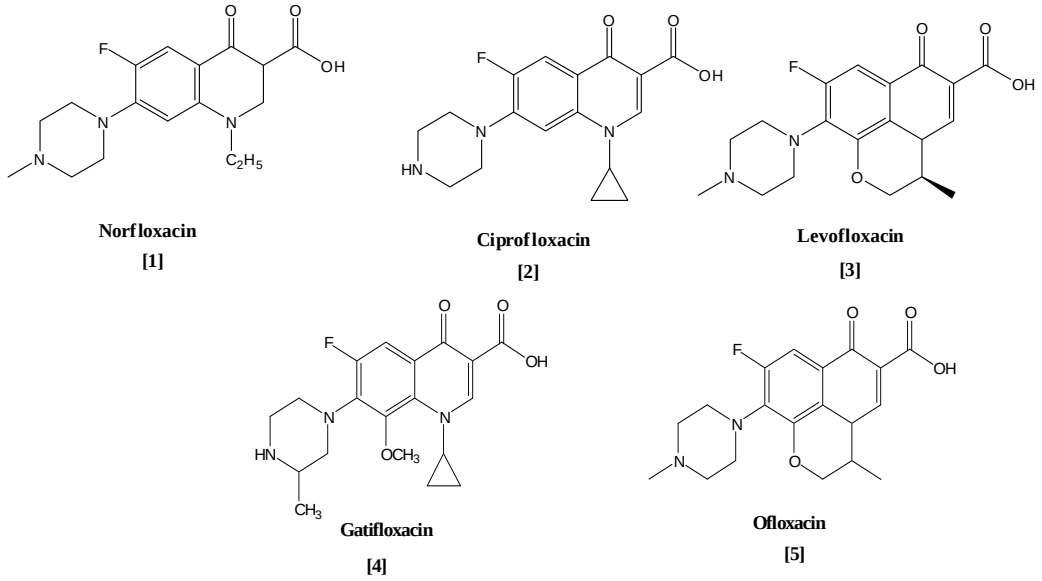

Scheme - 1

Materials and Methods

(a) Typical experimental procedure for the synthesis of 4a-h

A mixture of aniline **1** (5 mmol), Meldrum's acid **2** (6 mmol), trimethyl orthoformate **3** (15 mmol) and [BMIM]Br (3 mL) was taken in a round bottomed flask -with the provision to perform the reaction under nitrogen atmosphere. The contents of the flask were stirred magnetically at 45 ± 2°C. The progress of the reaction was monitored on a TLC plate (Merck Silica gel $60F_{254}$) in pet.ether–ethyl acetate (8:2) and the visualization was accomplished in an iodine chamber/UV-light. After the completion of the reaction, water (10 mL) was added. The organic compound precipitate was filtered on a Buckner funnel applying vacuum. The product, so obtained, was purified by crystallization with methanol/ column chromatography (Merck Silica gel 60–120 mesh) and elution of the product was carried out by pet.ether–ethylacetate (8:2).

Characterization data of the compounds 4a-h:

5-[Phenyl-2-ylamino]-2,2-dimethyl-1,3-dioxane-4,6-dione (4a): yellow solid, 75% yield, m.p. 120-122°C. IR (KBr pellet, cm^{-1}): 3187, 3089, 2998, 1735, 1685, 1632, 1608, 1447, 1265, 1121. ^1H NMR (300 MHz, $CDCl_3$) δ = 1.69 (s, 6H, 2×CH_3), 7.35(d, 1H, J=6.1Hz, Ar), 7.40 (t,1H, J=2.1,Ar)7.48 (t, 1H, J= 0.58, Ar), 8.62 (d, 1H, =CH), 11.36 (d, 1H,J=11.1Hz, NH). ^{13}C NMR (75 MHz, $CDCl_3$): δ = 27.2 (2×CH_3), 87.6 (OCC_4) 116.2, 128.5, 129.1, 129.4, 131.1, 131.7, 152.7, 152.3, 165.1. Anal. calcd. for $C_{13}H_{10}NO_4$ C, 63.93; H, 4.09; N, 5.73%. Found C, 63.88; H, 4.04; N, 5.68%.

5-{[(4-chloro, 2-nitrophenyl amino)]methylene}-2,2-dimethyl-1,3-dioxane4-6-dione (4b) : colour less solid, 78% yield, m.p. 190-192°C. IR (KBr, pellet, cm^{-1}): 3148, 3075, 2999, 724, 1685, 1618, 1443, 1289, 1206. ^1H NMR (300 MHz, $CDCl_3$): δ = 1.77 (s, 6H, 2×CH_3), 7.23 (s, 1H, J=5.3Hz, Ar), 7.29 (d,1H, J=2.8,Ar), 7.32 (d, 1H, J= 0.58, Ar), 8.62 (d, 1H, =CH), 11.36 (d, 1H, J=11.1Hz, NH).^{13}C NMR (75 MHz, $CDCl_3$) : δ = 27.2 (2×CH_3), 89.4 ($OCCH_3$), 105.5, 117.5, 125.2, 127.7, 130.1, 131.9, 133.8, 148.9, 162.50. Anal. calcd. for $C_{13}H_{11}N_2O_6Cl$; C, 47.78; H, 3.36; N, 8.57%; Found C, 47.72; H, 3.28; N, 8.52%.

5-{[4-Methyl,2-nitrophenyl)amino]methylene}-2,2-dimethyl-1,3-dioxane-4,6-dione(4c) : colour less solid, 81% yield, m.p. 194-196°C. IR (KBr pellet, cm^{-1}) : 3149, 3072, 2976, 1730, 1680, 1622, 1439, 1285, 1105. ^1H NNR (300 MHz, $CDCl_3$) : δ = 1.75 (s, 6H, 2×CH_3), 1.58 (s, 3H, Me), 7.33 (m, 2H, Ar), 7.52 (s, 1H, Ar), 8.62 (d, 1H, =CH), 11.60 (d, 1H, -NH). ^{13}C NMR (75 MHz, $CDCl_3$) : δ = 27.3 (2×CH_3), 88.7 ($OCCH_3$), 105.7, 119.3, 124.6, 126.9, 129.8, 133.8, 148.9, 162.4. Anal. calcd. for $C_{14}H_{14}N_2O_6$; C, 50.29; H, 4.19; N, 16.76%; Found C, 50.33; H, 4.11; N, 16.70%.

5-{[(2,4,5-trichlorophenyl)amino]methylene}-2,2-dimethyl-1,3-dioxane-4,6-dione(4d) : colourless solid, 77% yield, m.p. 188-190°C. IR (KBr pellet, cm^{-1}) : 3148, 3076, 2960, 1740, 1685, 1619, 1445, 1290, 1109. ^1H NMR (300 MH, $CDCl_3$) : δ = 1.73 (d, 6H, 2×CH_3), (s, 1H, Ar), 7.36 (s, 1H, Ar), 8.69 (d, 1H, 999=CH), 11.65 (d, 1H, -NH). 13C NMR (75 MHz, $CDCl_3$) : δ = 26.9 (2×CH_3), 89.1 ($OCCH_3$), 106.3, 118.7, 125.1, 126.8, 129.4, 134.1, 148.9, 163.6. Anal. calcd. for $C_{13}H_{10}NO_4Cl_3$. C, 44.50; H, 2.85; N, 3.99%; Found C, 44.46; H, 2.78; N, 3.80%.

5-{[(2-Methylphenyl)amino]methylene}-2,2-dimethyl-1,3-dioxane-4,6-dione (4e): Yellow solid, 83% yield, mp 142-144°C. IR (KBr pellets, cm^{-1}) : 3165, 3058, 2985, 1722, 1672, 1640, 1609, 1440, 1270, 1025. ^1H NMR (300 MHz, $CDCl_3$) δ = 1.76 (s, 6H, 2×CH_3), 3.33 (s, 3H, CH_3), 7.02 (d, 1H, J= 7.6 Hz, Ar), 7.15 (dd, 2H, Ar), 7.19 (d, 1H J = 7.6 Hz, Ar), 8.65 (d, 1H, J = 13.9Hz, Ar), 7.15 (dd, 2H, Ar),. ^{13}C NMR (75 MHz, $CDCl_3$) : δ = 21.21 27.1, 87.1, 105.3, 117.4, 124.8, 127.5, 131.3, 136.7, 137.5, 152.7, 163.6, 165.7. Anal. calcd. for $C_{14}H_{15}NO_4$: C, 64.36; H, 5.74; N, 5.36%. Found : C, 64.28; H, 5.79; N, 5.44%.

5-{[(3-methylphenyl)amino]methylene}-2,2-dimethyl-1,3-dioxane-4,6-dione (4f) : yellow solid, 82% yield, m.p.=160-162°C. IR (KBr pellet, cm^{-1}) : 3142, 3076, 2933, 1740, 1680, 1680, 1618, 1440, 1292, 1136. ^1H NMR (300 MHz, $CDCl_3$) : δ = 1.72 (s, 6H, 2Me), 1.53 (s, 3H, Me), 7.28 (s, 1H, Ar), 7.32-7.36 (m, 3H, Ar), 8.65 (d, 1H,=CH), 11.58 (d, 1H, NH). ^{13}C NMR (75 MHz, $CDCl_3$) : δ = 26.8, 30.4, 89.8, 106.4, 119.1, 124.9, 127.1, 129.4, 135.2, 148.9, 162.7. Anal. calcd. for $C_{14}H_{15}NO_4$. C, 64.36; H, 5.74; N, 5.36%; Found C, 64.32; H, 5.68; N, 5.26%.

5-{[(2-Nitrophenyl)amino]methylene}-2,2-dimethyl-1,3-dioxane-4,6-dione (4g) : Yellow solid, 74% yield, m.p. 190-192°C. IR (KBr pellets, cm^{-1}) : 3148, 3075, 2999, 1724, 1685, 1618, 1445, 1290, 1206. ^1H NMR (300 MHz, $CDCl_3$) δ = 1.77 (s, 6H, 2×CH_3), 7.35-7.38 (m, 4H, Ar), 8.63 (d, 1H, =CH), 11.65 (d, 1H, -NH). ^{13}C NMR (75 MHz, $CDCl_3$) δ = 27.2, 89.4, 105.4, 117.5, 125.3, 127.6, 130.1, 131.9, 133.8, 148.9, 162.5. Anal. calcd. for $C_{13}H_{12}N_2O_6$: C, 53.43; H, 4.10; N, 9.58%. Found : C, 53.39; H, 4.13; N, 9.52%.

5-{[(2,5-dimethyl phenyl)amino]methylene}-2,2-dimethyl-1,3-dioxane-4,6-dione (4h): yellow solid, 78% yield, m.p.=165-167°C. IR (KBr pellet, cm^{-1}) : 3155, 3089, 2933, 1439, 1685, 1622, 1443, 1295, 1135. ^1H NMR (300 MHz, $CDCl_3$) : δ = 1.71 (s, 6H, 2Me), 1.48 (s, 3H, Me), 1.43 (s, 3H, Me), 7.26 (d, 2H, Ar), 7.35 (s, 1H, Ar), 8.61 (d, 1H, = CH), 11.56 (d, 1H, NH). ^{13}C NMR (75 MHz, $CDCl_3$) : δ = 26.8, 29.6, 30.4, 89.8, 106.3, 120.2, 124.7, 128.2, 129.4, 135.2. Anal. calcd. for $C_{15}H_{17}NO_4$. C, 65.45; H, 6.18; N, 5.09%; Found C, 65.41; H, 6.12; N, 4.98%.

(b) Typical experimental procedure for the cyclization of compound 5a-h :

Compound **4a-h** (5 mmol) and [BMIM]BF_4/OTf (3 mL) were taken in a round bottomed flask having provision to carry out the reaction under nitrogen atmosphere. The contents of the flask were stirred magnetically at 90 ± 2°C. The progress of the reaction was monitored on a TLC plate in pet.ether–ethyl acetate (8:2). After completion of the reaction, the product was extracted with ethyl acetate (3×10 mL). The solvent was recovered under reduced pressure (5 mm of Hg). The pasty mass thus obtained was extracted with diethyl ether (3×10 mL), dried over anhydrous sodium sulphate and ether was distilled out. The product so obtained was

purified by crystallization with ethanol/column chromatography (Merck Silica gel 60–120 mesh) and eluting the TLC product with pet.ether– ethylacetate (8:2).

Characterization data of the compounds 5a-h:

Quinolin-4(1H)-one (5a) : brownish solid, 76% yield, m.p. 228-230°C. IR (KBr pellet, cm^{-1}): 3096.5, 2917, 2813, 1625, 1560, 1423, 1245, 110. ^{1}H NMR (300 MHz, $CDCl_3$) : δ = 6.23 (d, 1H, J = 6.8Hz, CH), 6.86 (s, 1H, Ar), 7.21 (s, 1H, Ar), 7.58 (d, 1H, CH); 11.70 (d, 1H, NH). ^{13}C NMR (75 MHz, $CDCl_3$) : δ = 111.5, 117.8, 123.5, 129.5, 139.4, 142.4, 143.5, 183.7. Anal. calcd. for C_9H_7NO. C, 74.48; H, 4.82; N, 9.65%; Found C, 74.44; H, 4.77; N, 9.60%.

4-chloro, 8-nitroquinolin-4(1H)-one (5b) : brownish solid, 80% yield, m.p. 280-282°C. IR (KBr pellet, cm^{-1}) : 3072, 2945, 2813, 1620, 1565, 1425, 1250. ^{1}H NMR (300 MHz, $CDCl_3$) : δ = 6.23 (d, 1H, J = 7.1Hz, CH), 7.10 (s, 1H, Ar), 7.18 (s, 1H, Ar), 7.78 (d, 1H, CH); 11.75 (d, 1H, NH). ^{13}C NMR (75MH, $CDCl_3$) δ = 111.7, 118.3, 123.2, 129.4, 139.7, 142.7, 143.8, 184.9. Anal. calcd. for $C_9H_5N_2O_3Cl$. C, 46.05; H, 6.39; N, 11.9%; Found C, 45.98; H, 6.32; N, 11.4%.

6-methyl, 8-nitroquinolin-4(1H)-one (5c): brownish solid, 83% yield, m.p. 278-280°C. IR (KBr pellet, cm^{-1}) : 3062, 2913, 2815, 1628, 1572, 1419, 1240, 1123. ^{1}H NMR (75 MHz, $CDCl_3$) δ = 2.42 (s, 3H, Me), 6.15 (d, 1H, J = 6.9Hz,CH), 7.13 (s, 1H, Ar), 7.16 (s, 1H, Ar), 7.58 (d, 1H, CH), 11.68 (d, 1H, NH). ^{13}C NMR (75 MHz, $CDCl_3$) : δ = 16.9 (CH_3), 1090, 121.5, 126.3, 127.7, 129.6, 131.8, 134.5, 139.7, 176.1. Anal. calcd. for $C_{10}H_8N_2O_3$ C, 58.82; H, 3.9; N, 13.7%; Found C, 58.78; H, 3.5; N, 13.2%.

5,6,8-trichloroquinolin-4(1H)-one (5d): brownish solid, 79% yield, m.p. 282-284°C. IR (KBr pellet, cm^{-1}) : 3142, 3082, 2933, 1625, 1562, 1510, 1213, 1080. ^{1}H NMR (300 MHz, $CDCl_3$) : δ 6.17 (d, 1H, J = 6.32Hz, CH), 7.69 (s, 1H, Ar), 7.76 (d, 1H, CH), 11.72 (d, 1H, NH). ^{13}C NMR (75 MHz, $CDCl_3$) : δ 108.7, 122.6, 126.7, 127.3, 130.5, 134.9, 139.4, 177.9. Anal. calcd. for $C_9H_4NOCl_3$. C, 43.46; H, 1.6; N, 5.6%; Found C, 43.42; H, 1.2; N, 5.1%.

8-Methylquinolin-4(1*H*)-one (5e) : Brownish solid, 82% yield, m.p. 188-190°C. IR (KBr pellets, cm^{-1}) : 3172, 3102, 2968, 1609, 1565, 1517, 1450, 805. ^{1}H NMR (300 MHz, $CDCl_3$) δ = 6.24 (d, 1H, J = 7.3Hz,, CH), 6.89 (d, 1H, Ar), 6.92 (d, 1H), 7.26 (d, 2H), 7.75 (d, *J* = 7.3Hz, 1H, CH). ^{13}C NMR (75 MHz, $CDCl_3$) : δ = 19.4, 111.6, 125.2, 125.9, 127.3, 134.6, 139.2, 139.4, 141.7, 183.9. Anal. calcd. for $C_{10}H_9NO$: C, 75.47; H, 5.66; N, 8.80%. Found : C, 75.39; H, 5.61; N, 5.78%.

7-methylquinolin-4(1*H*)-one (5f): brownish solid, 78% yield, m.p. 206-208°C. IR (KBr pellets, cm^{-1}) : 3172, 3104, 2970, 1613, 1565, 1518, 1452, 1022. ^{1}H NMR (300 MHz, $CDCl_3$) δ = 2.39 (s, 3H, 3H, Me), 6.21 (s, 1H, J = 7.11Hz, CH), 7.02 (s, 1H, Ar), 7.15-7.22 (d, 2H, Ar), 7.71 (d, 1H, CH), 11.69 (d, 1H, NH). ^{13}C NMR (75 MHz, $CDCl_3$) δ = 23.9, 111.3, 116.8, 123.5, 129.4, 139.4, 141.2, 143.5, 184.1. Anal. calcd. for $C_{10}H_9NO$. C, 75.47; H, 5.6; N, 8.8%; Found C, 75.40; H, 5.1; N, 8.3%.

8-Nitroquinolin-4(1*H*)-one (5g) : Brownish solid, 78% yield, mp 170-172°C. IR (KBr pellets, cm^{-1}) : 3187, 3036, 1635, 1580, 1522, 1305, 1104, 1085, 716. ^{1}H NMR (300 MHz, $CDCl_3$) δ = 6.31 (d, 1H, J = 7.6Hz, CH), 7.51 (m, 1H), 8.02 (d, 1H), 8.09 (d, 1H), 8.54 (d, 1H, CH). ^{13}C NMR (75 MHz, $CDCl_3$) δ = 111.3, 123.2, 126.9, 128.3, 130.9, 131.7, 137.7, 141.9, 178.1. Anal. calcd. for $C_9H_6N_2O_3$: C, 56.84; H, 3.15; N, 14.73%. Found : C, 56.69; H, 3.11; N, 14.76%.

5,8-dimethyl quinolin-4(1*H*)-one (5h) : brownish solid, 78% yield, m.p. 216-218°C. IR (KBr pellets, cm^{-1}) : 3172, 3104, 2975, 1615, 1562, 1521, 1450, 1215, 1025. ^{1}H NMR (300 MHz, $CDCl_3$), δ = 2.41 (s, 3H, Me), 2.43 (s, 3H, Me), 6.18 (d, 1H, J = 7.02Hz, CH), 6.92 (d, 2H, Ar), 7.75 (d, 1H, CH), 11.68 (d, 1H, NH). Anal. calcd. for $C_{11}H_{11}NO$. C, 76.30; H, 6.3; N, 8.0%; Found C, 76.24; H, 6.0; N, 7.76%.

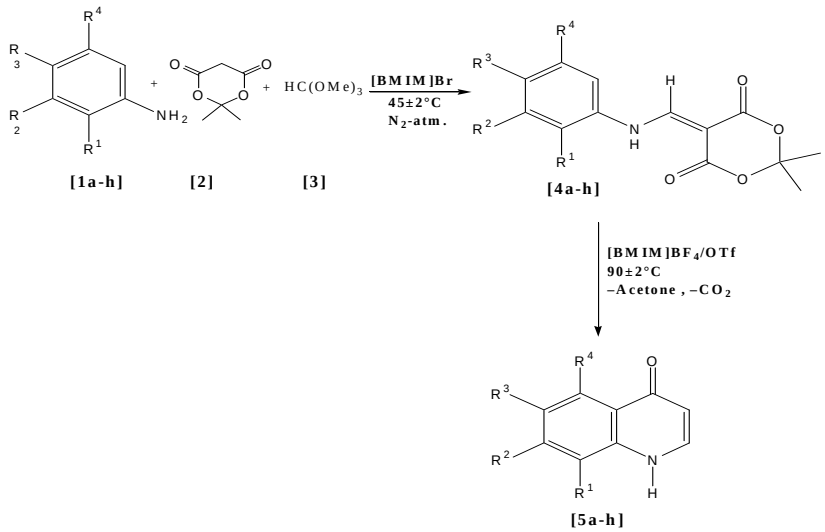

Scheme - 1I

Table 2 Yields of the compounds 5a–h in different ionic liquids

Product	R^1	R^2	R^3	R^4	Yield(%)Time(min.)	
					[BMIM]BF_4	[BMIM]OTf
5a	H	H	H	H	74/120	76/120
5b	NO_2	H	Cl	H	79/120	80/120
5c	NO_2	H	Me	H	80/120	83/120
5d	Cl	H	Cl	Cl	78/120	79/120
5e	Me	H	H	H	81/120	82/120
5f	H	Me	H	H	81/120	80/120
5g	NO_2	H	H	H	76/120	77/120
5h	Me	H	H	Me	77/120	79/120

A plausible mechanism of the reaction process is depicted in Scheme-3

We have studied the recyclability of the regenerated ionic liquids for the products **4a** and **5a**. The yields of the products in two cycles are presented in **Table 3**.

Table 3 Recyclability data for product 4a and 5a

Product	Cycles	Yield(%)Time(min.)		
		[BMIM]Br	[BMIM]BF_4	[BMIM]OTf
4a	0	75/120	–	–
	1	72/120	–	–
	2	69/120	–	–
5a	0	–	74/120	76/120
	1	–	71/120	73/120
	2	–	68/120	71/120

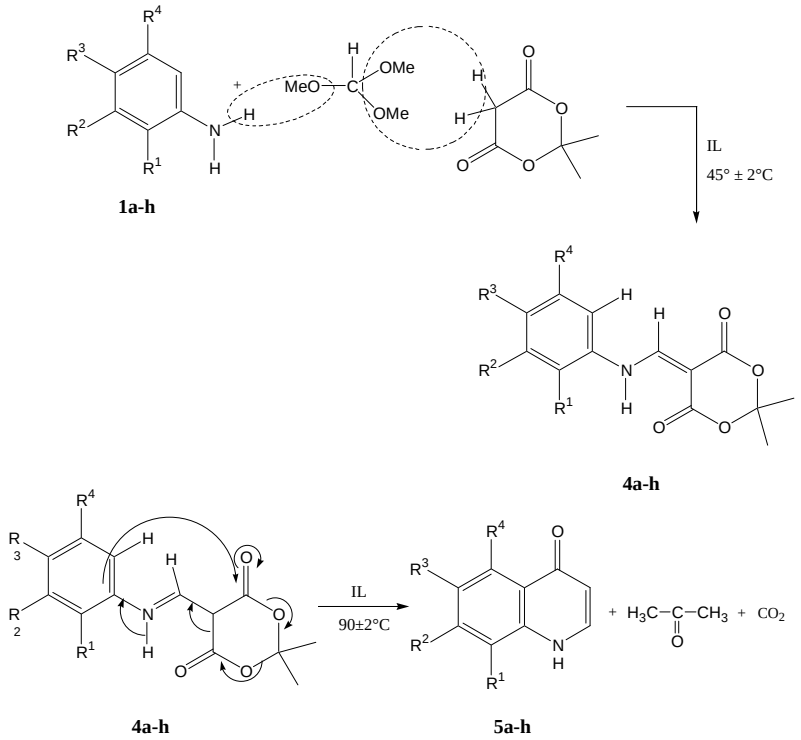

Scheme - 1II

Results and Discussion

In our work, we have carried out the reaction between substituted arylamine **1a-h** with Meldrum's acid (2,2-dimethyl-1,3-dioxane-4,6-dione) in which nucleophilic attack takes place at C-4 and C-6, while electrophilic attack takes place at C-5 position) **2** and trimethyl orthoformate **3** in presence of ionic liquid, *viz.*, 1-butyl-3-methylimidazolium bromide [BMIM]Br. The reaction was carried out by stirring the contents of the flask under nitrogen atmosphere at 45±2°C. The products obtained were arylaminomethylene-1,3-dioxane-4,6-dione **4a-h (Table-1, Scheme-2)**.

Table 1 Yields of the comkpounds in ionic liquid

Product	R^1	R^2	R^3	R^4	Yield(%)Time(min.) [BMIM]Br *
4a	H	H	H	H	75/120
4b	NO_2	H	Cl	H	78/120
4c	NO_2	H	Me	H	81/120
4d	Cl	H	Cl	Cl	77/120
4e	Me	H	H	H	83/120
4f	H	Me	H	H	82/120
4g	NO_2	H	H	H	74/120
4h	Me	H	H	Me	78/120

Compounds 4**a-h** were then cyclized under nitrogen current at 90±2°C in ionic liquids, *viz.* [BMIM]BF_4/OTf to afford 4(1*H*)-quinolones **5a-h** in excellent yields **(Scheme-2 and Table-2)**.

Conclusions

A series of derivatives of novel quinolone have been synthesized by the use of eco-friendly route in minimum time with good yields.

References

1. (a) Krchnak, V. and Holladay, M.W., 2002, *Chem. Rev.*, **61**, *102*.

   (b) Thompson, L.A. and Ellman, J.A., 1996, *Chem. Rev.*, ***96***, 555.

   (c) Terrett, N.K., Gardner, M., Gordon, D.W., Kobylecki R.J. and Steele, J., 1995, *Tetrathedron*, ***51***, 8135.

2. Gracia, M. and Torroba, T., 2005, *Molecules.*, ***10***, 318-320.

3. Balkumar, C., Lamba, P., Kishor, D.P., Narayana, B.L., Rao, K.V., Rajwinder, K., Rao, A.R., Shireesha, B. and Narsaiah, B., 2010, *Eur. J. Med. Chem.*, ***45***, 4904.

4. Alafeefy, A.M., Kadi, A.A., Al-Deeb, O.A., El-Tahir, K.E.H. and Al-Jaber, N.A. 2010, *Eur. J. Med. Chem.*, ***45***, 4947.

5. Selvam, T.P. and Kumar, P.V., 2010, *Bull. Korean Chem. Soc.*, ***31***, 3265.

6. Kabri, Y.; Azas, N.; Dumetre, A.; Hutter, S.; Laget, M.; Verhaghe, P.; Gellis, A. and Vanlee. 2010, *Eur. J. Med. Chem.*, ***45***, 616.

7. Leatham, P.A.; Bird, H.A.; Wright, V.; Seymour, D. and Gordon, A., 1983, *Eur. J. Rheumatol. Inflamm.*, ***6***, 209.

8. Muraganantham, N.; Sivakumar, R.; Anbalagan, N.; Gunasekaran, V. and Leonard, J. T., 2004, *Biol. Pharm. Bull.*, ***27***, 1683.

9. Wilson, W.D., Zhao, M., Patterson, S.E., Wydra, R.L., Janda, L. and Strekowski, L., 1992, *Med. Chem. Res.*, ***2***, 102.

10. Strekowski, L., Mokrosz, J.L., Honkan, V.A., Czarny, A., Cegla, M.T., Patterson, S.E., Wydra, R.L. and Schinazi, R.F., 1991, *J. Med. Chem.*, ***34***, 1739.

11. Tiwari, R. and Chhabra, G., 2010, *Asian J. Chem.* ***22***, 5981.

12. Maguire, M.P.; Sheets, K.R.; McVety, K.; Spada, A.P. and Ziberstein, A.J., 1994, *Med. Chem.*, ***37***, 2129.

13. Noolvi, M.N., Patel, H.M., Bhardwaj, V. and Chauhan, A., 2011, *Eur. J. Med. Chem*, ***46***, 2327.

14. Selvam, T.P.; Kumar, P.V. and Prakash, C.R.; 2010, *Int. J. Pharm. and Pharmaceutical Sci.*, ***2***, 118.

15. Koga, H., Ito, A., Murayama, S., Suzue, S. and Irikura, T., 1980, *J. Med. Chem.*, ***23***, 1358.

16. Jaber, L. A., Bailey, E. M. and Rybak, M. J., 1989, *Clin. Pharm.*, ***8***, 97.

17. Wise, R., Andrews, J. M. and Edwards, L. J., 1983, *Antimicrob. Agents Chemother.* ***23***, 559.

18. Sato, K., Matsuura, Y., Inoue, M., Une, T., Osada, Y., Ogawa, H. and Mitsuhashi, S., 1982, *Antimicrob. Agents Chemother.*, ***22***, 548.

19. Atarashi, S., Yokahama, S., Yamazaki, K., Sakano, K., Imamura, M. and Hayakawa, I., 1987, *Chem. Pharm. Bull.*, ***35***, 1896.

20. Blondeau, J. M., 2000, *Expert Opin. Invest. Drugs* ***9***, 1877.

21. Hayakawa, I., Hiramitsu, T. and Tanaka, Y., 1984, *Chem. Pharm. Bull.* ***32***, 4907.

22. Chaudhary, R.P. and Gupta, R., 1984, *Phosphorus, Sulfur and Silicon*, ***187***, 735.

23. Nightingale, C. H., 2000, *Pharmacotherapy*, ***20***, 245.

24. Selvam, T.P. and Kumar, P.V., 2010, *Drug. Discoveries and Therapeutics*, ***4***, 392.

25. Shao, J., Huang, X., Hong, X., Liu, B., Xu, B., 2012, *Synthesis*, **44**, 1798-1808.

26. Zhao, T. and Xu, B., 2010, *Org. Lett.*, ***12***, 212-215.

27. Zhou, C., Dubrovsky, A. V. and Larock, R.C., 2006, *J. Org. Chem.*, ***71***, 1626-1632.

28. Bernini, R., Cacchi, S., Fabrizi, G. and Sferrazza, A., 2009, *Synthesis*, 1209-1219.

29. Jan Tois, Mikko Vahermo and Ari Koskinen, 2005, ***46(5)***, 735.

30. Jens Lange, Alex C. Bissember and Martin G. Banwell, Ian A. Cade 1999.

31. Abdullah, Faiz Mohd. and Singh, A.K., 2013, *J.Org. Chem.* ***29***, 609.

32. Panda, S. S. and Jain, S.C., 2013, *Med. Chem. Lett.* ***23***, 3225-3229.

33. Roberta Berrino, Sandro Cacchi, Giancarlo Fabrizi and Antonella Goggiamani, 2012, *J. Org. Chem.*, ***77***, 2537-2542.

34. Abeer Ahmed[a] and Mohsen Daneshtalab *J. Pharm. Pharmaceut. Sci.*, 2012, 152-72.

35. Kappe Th., Aigner R., Hohengassner P. and Stadlbauer W., 1994, *J. Prakt. Chem.*, ***336***, 596-601.

36. Steinschifter W.; Fiala, W. and Stadlbauer, W., 1994, *J. Heterocycl. Chem.*, ***31***, 1647-1652

37. Yushchenko, D.A.; Bilokin', M.D.; Pyvovarenko, O.V.; Duportail, G.; Mely, Y. and Pivovarenko, V.G. 2006, *Tetrahedron Lett.*, ***47***, 905-908.

38. Yushchenko, D.A., Shavadchak, V.V., Klymchenko, A.S., Duportaill, G., Mely, Y. and Pivovarenko, V.G. 2006, *New J. Chem.*, ***30***, 774-781.

39. Thomas Kappe, Abdel S. Karem and Walfgang Stadlbaver, 1988, *J. Heterocyclic Chem.*, ***25***, 857.

40. Thomas Kappe, Rodolf Aigner, Peter Hohengassner and Walfgang Stadlbaver, 1994, *J. Prakt. Chem.*, ***336***, 596-601.

41. Gould, R. Jr. and Jocobs, W.A, 1939, *J. Am. Chem. Soc.*, ***61***, 2890.

42. Aruna, G.; Jyostna T.S. and Achaiah, G., 2010, *International Journal of Pharmaceutical Science and Nenotechnology*, ***3(I)***.

43. Wube A.A., Hufner A., Thomaschitz, C., Blunder M., Kouroser M., Baver R. and Bucar F., 2011, *Biorganic & Medicinal Chemistry*, ***19***, 567-579.

44. Tois, J., Vahermo M. and Koskinen A., 2011, *Tetrahedron Letters*, ***46***, 735-737.

RNI No. MAHENG/2017/74063
ISSN No. (Print) 2581-5911

Stability study of Anthocyanins from Banana bracts (*Musa paradisiacal* L.) of Indian origin extracted by Microwave Extraction

Mitali Kulkarni and Ajit Datar
Guru Nanak Institute of Research and Development,
G. N. Khalsa College, Matunga, Mumbai-400019, Maharashtra, India
Email: kmitalis@gmail.com

Abstract
*Anthocyanin pigments were extracted from Banana bracts (*Musa paradisiaca *L.) of Indian origin by Microwave Extraction (MAE) using 0.1% acidified ethanol as extraction solvent. The extracted and semi-purified anthicyanin pigments were then subjected to a number of environmental conditions, which could destabilize the anthocyanin molecules. These environmental conditions were: range of pH of solutions (starting from pH 1 to pH 10), various temperatures (starting from -20ºC up to -121ºC) and exposure to various light conditions (sun light, day light and dark). The results of the study showed that changes occurred in the anthocyanin stability as pH, temperature and exposure to light increased.*

Keywords: *Stability, anthocyanins, MAE, SPE*

Introduction

The trend of emerging lifestyle towards living natural has given great impetus to the study of nature derived products. Colour, being the integral part of any product, influences not only the perception of flavor, but also affects attraction and quality after consumption. At present environmentally benign products are becoming the top priority or choice due to increased awareness about the ill effects of synthetic dyes on human beings. Thus requirement of natural dyes has risen tremendously. Although natural colorants are widely distributed in nature, the main obstacle for their introduction as food-pigmenting agents or colour additives in cosmetics or other utility products is that they require high investment. Of special interest to the food, pharmaceutical and cosmetic industry is the limited availability of red pigments; therefore research into natural sources of red pigments has increased recently[1].

Thus, Anthocyanins hold an important place in the natural colourants research field. These are sub-group of flavonoids and are very delicate in nature; but most attractive hues starting from pink, red, orange, blue to purple are exhibited by anthocyanins only. The anthocyanins are regarded as flavonoid compounds since they possess the characteristic C6C3C6 carbon skeleton and have the same biosynthetic origin as other natural flavonoids. The anthocyanidins are the basic structures of the anthocyanins. These anthocyanidins (aglycones) consist of an aromatic ring [A] bonded to a heterocyclic ring [C] that contains oxygen, which is also bonded by a carbon-carbon bond to a third aromatic ring [B]. When the anthocyanidins are found in their glycoside form (bonded to a sugar moiety) they are known as anthocyanins.

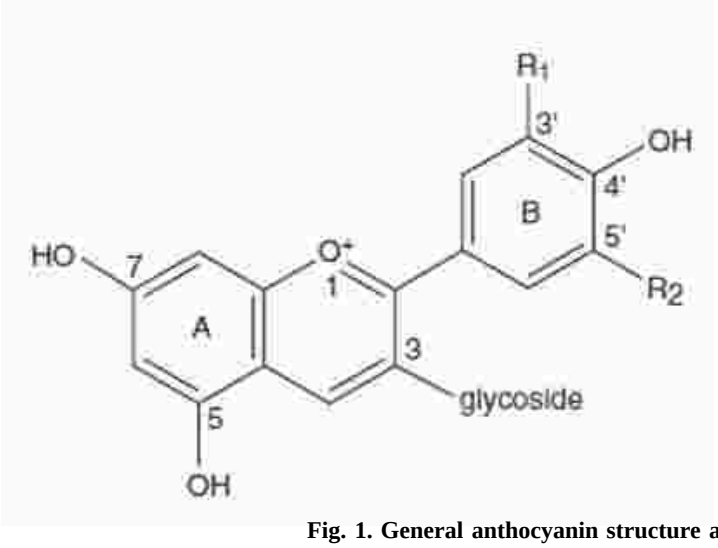

R_1=R_2=H	Pelargonidin
R_1= OH, R_2=H	Cyanidin
R_1=OCH_3, R_2=H	Peonidine
R_1=R_2=OH	Delphinidin
R_1=OCH_3, R_2=OH	Petunidin
R_1=R_2=OCH_3	Malvidin

Fig. 1. General anthocyanin structure and common substitutions

Degradation may occur during extraction/purification/ storage of anthocyanins in extract or in products. The knowledge of factors governing anthocyanin stability and putative degradation mechanisms is vital for efficient extraction/purification of anthocyanins. The major factors affecting stability of anthocyanins are pH, temperature and the presence of oxygen, enzymatic conditions etc [2].

Effect of pH, temperature and light exposure on the anthocyanin extract was studied. The results obtained from these experiments gave important information about the stability of banana bract anthocyanins from *Musa paradisiaca* L. extracted using a novel technique, MAE. Thus, in turn it helped in proving the suitability of MAE for extraction of anthocyanins from banana bracts. The suitable conditions for extract handling during storage as well as during product development were also derived based on the observations from these experiments.

Effect of pH, Temperature and Light exposure on anthocyanins

pH

Anthocyanins undergo reversible changes in different pH conditions (refer Fig. 2). The presence of the oxonium ion adjacent to the C-2 position in anthocyanins is responsible for their characteristic amphoteric nature. Non-and monoacylated anthocyanins thus behave somewhat like pH indicators, existing as either an acid or base, depending on pH. Anthocyanin-containing solutions generally display their most intense red coloration at acid pH. With increasing pH, aqueous anthocyanin extracts normally fade to the point where they may appear colourless before finally changing to purple or blue at high pH[2]. The anthocyanin extract obtained from banana bracts was subjected to different pH conditions and the change in colour of the extract was assessed. The stability of the anthocyanins was observed based on changes in wavelength maxima and absorbance.

Temperature

As with most chemical reactions the stability of anthocyanin and the rate of their degradation, in natural and model system, is markedly influence by temperature. The thermal stability of anthocyanin varies with their structure, pH , the presence of oxygen and interaction with other components in the system. In general, structural feature that lead to increased pH-stability also lead to increased thermal stability, i.e. hydroxylation of aglycon decrease stability, while methoxylation, glycosulation and acylation have the opposite effect. In the presence of oxygen, maximum thermal stability of anthocyanidin 3-glycosides has been observed at pH1.8 to 2.0, while that of anthocyanin 3,5-diglycosides has

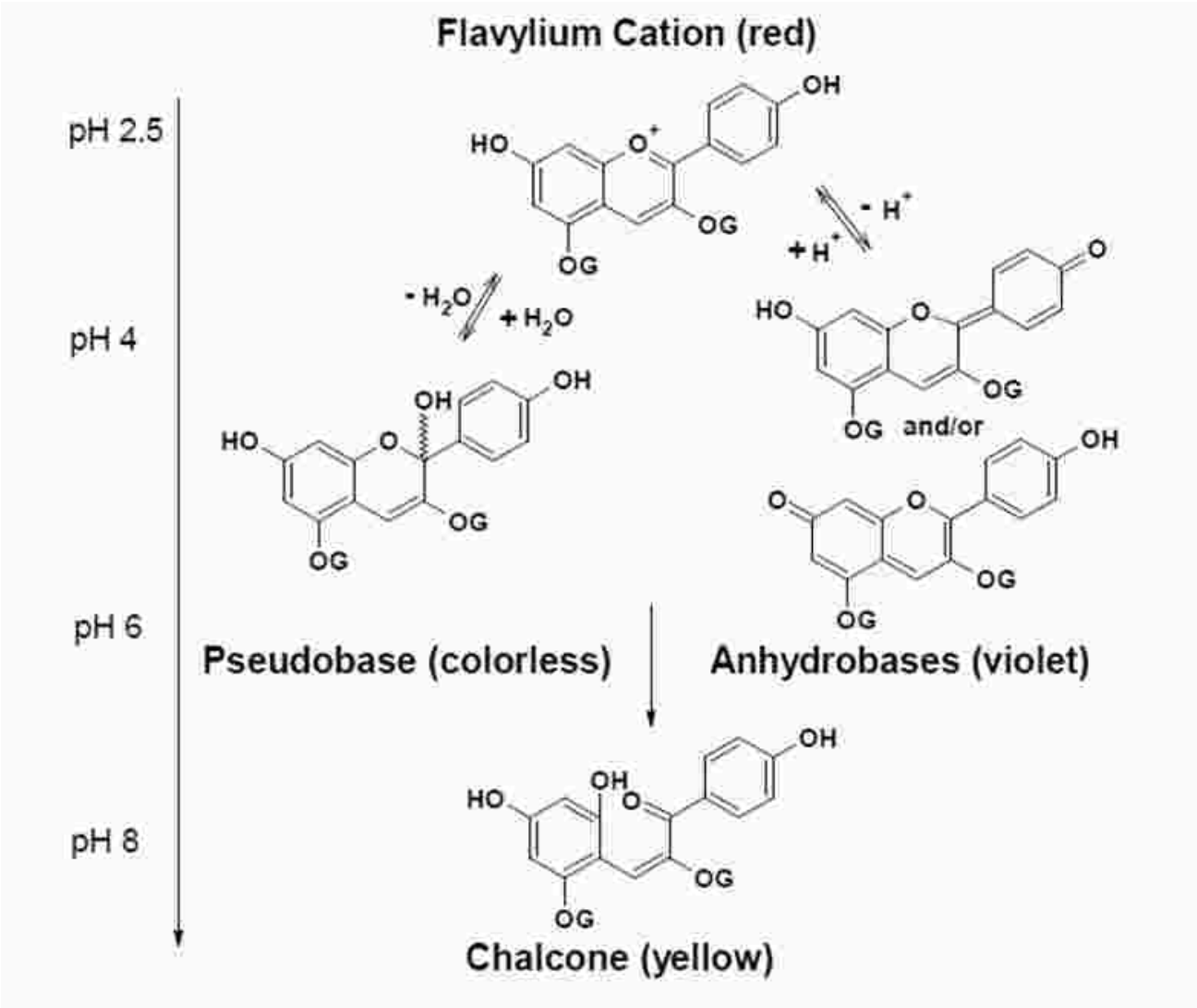

Fig. 2. Effect of various pH on Anthocyanin structure

been observed at pH 4.0 to 5.0. Anthocyanin degradation is virtually pH-independent at pH 2.0 to 4.5 in the absence of oxygen. Anthocyanin containing banana bract extract was subjected to various temperatures starting from as low as -20ºC up to 121ºC. Samples at low temperatures were stored at the specified temperatures for 7 days and readings were taken at various intervals mentioned below. To achieve the temperatures from 50ºC to 100ºC, a water bath was used. The samples were subjected to highest temperature under study viz. 121ºC by keeping them in an autoclave. Effect of temperature was checked by observing changes in λmax and absorbance value. The dilution of sample was chosen such that the absorbance value falls in the linear range of spectrophotometer [2].

Light

Anthocyanin decomposition would appear to be mainly photo-oxidative since p-hydroxybenzoic acid has been identified as a minor photo-oxidative product. Antho-

cyanins substitute at the C-5 hydroxyl group, which is known to fluoresce and hence are more susceptible to photochemical decomposition than the unsubstituted anthocyanins. In this project, stability of extracted anthocyanins was checked under various light conditions; such as day light, sun light, and in dark [2].

Materials and Methods

Sample Preparation: Banana bracts were obtained from local market in Matunga, Mumbai, India. The purple coloured petaloids of the bracts were plucked and washed clean with water and pat dried using tissue paper. These were cut into small pieces and were subjected to microwave assisted extraction. Extraction was carried out at 100W irradiation power for 9 minutes. 0.1% acidified ethanol was used as extraction solvent. Coloured ethanolic extract was then concentrated using rotary vacuum evaporator at 35ºC and reconstituted in 0.1% acidified distilled water; which was then purified by SPE on C-18 cartridges. The semipurified extract was used for further study.

Chemicals and Reagents: All chemicals and reagents used were analytical grade. Ethanol was procured from Changshu Yangyuan Chemical, China and HCl from Merck (11.3N). All the glassware used viz. pipette, conical flasks, and standard volumetric flasks; were of 'B' class. Micropipettes were used where appropriate.

pH solutions: a range of pH solutions were prepared starting from pH 1 up to pH 11 using, HCl, KCl, Na-acetate. $3H_2O$, NaOH, $NaH_2PO_4.2H_2O$ in standardizing proportions.

Apparatus: UV-V is spectrophotometer Shimadzu 1650PC, Rotary vacuum evaporator Buchhi, balance Shimadzu AX 200, SPE manifold, C-18 cartridges Thermo Scientific Hypersep C-18, sorbent 500mg, volume 3mL, Water bath.

Experimental procedure and observations

A. Sample preparation for determination of effect of pH on stability of anthocyanins:

100µL of extract was added in 2900µL pH solution of each strength. This dilution of sample was chosen such that the absorbance value falls in the linear range of the spectrophotometer. Sample was allowed to equilibrate for 30 minutes and readings were taken. The samples were stored for 24 hours and readings for the same were again taken.

Table.1 Observation of behavior of anthocyanins under various pH

pH value	Day1		Day2		Colour observed at various pH values
	λmax (nm)	OD	λmax (nm)	OD	
1	513.00	1.140	514.00	1.096	Dark red
2	513.00	1.014	513.00	1.035	Medium dark red
3	512.00	0.631	513.00	0.600	Pale red
4	506.00	0.361	507.00	0.342	Faint red
5	_	_	_	_	Faint violet
6	_	_	_	_	Violet
7	552.00	0.564	_	_	Violet
8	565.00	0.680	_	_	Faint violet-almost colourless
9	565.00	0.735	_	_	Yellow
10	378.00	1.518	_	_	Yellow
11	368.00	1.199	_	_	Yellow

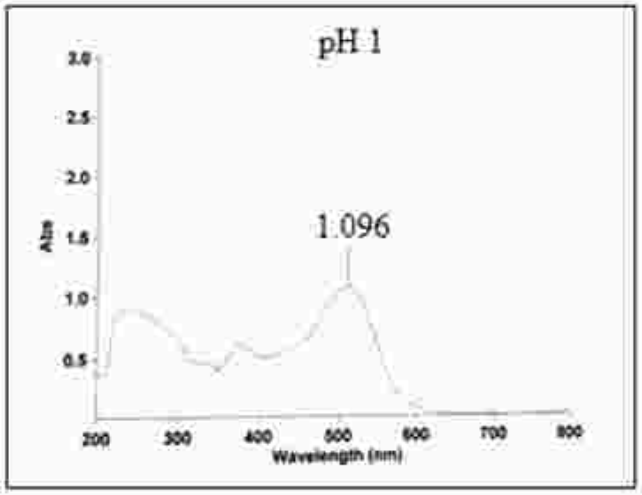
pH 1
1.096
Abs
Wavelength (nm)

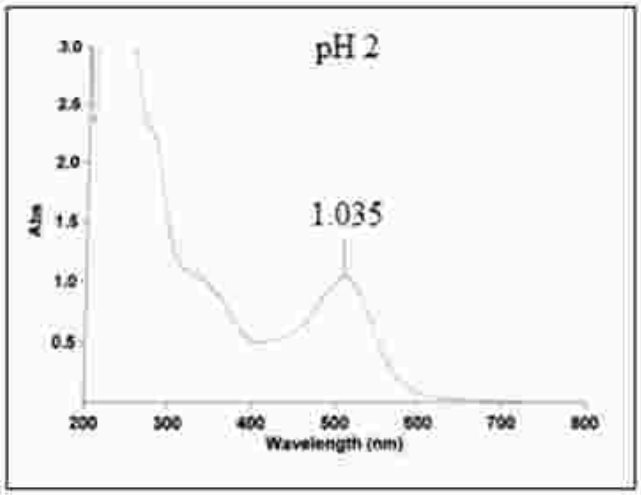
pH 2
1.035
Abs
Wavelength (nm)

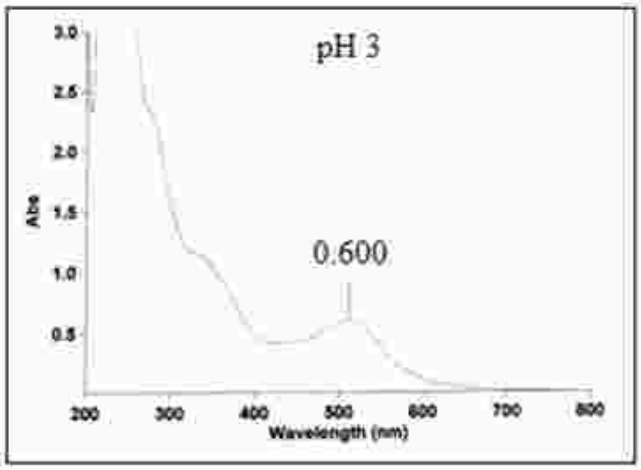
pH 3
0.600
Abs
Wavelength (nm)

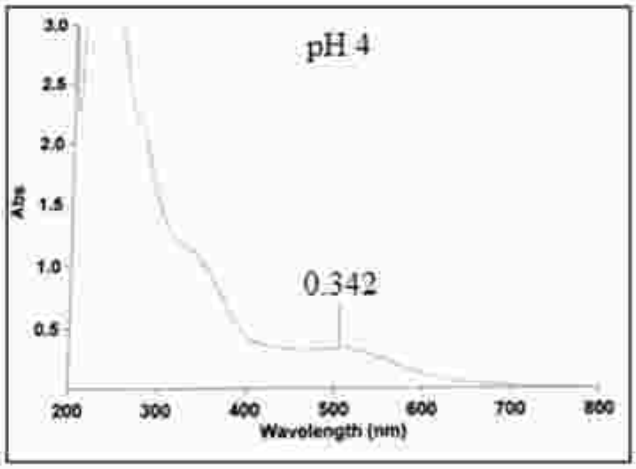
pH 4
0.342
Abs
Wavelength (nm)

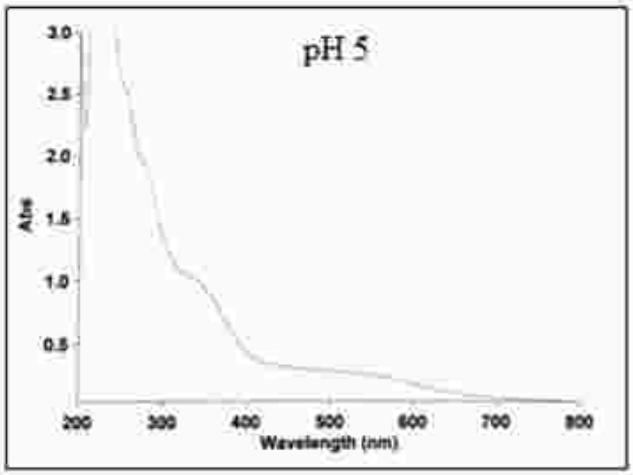
pH 5
Abs
Wavelength (nm)

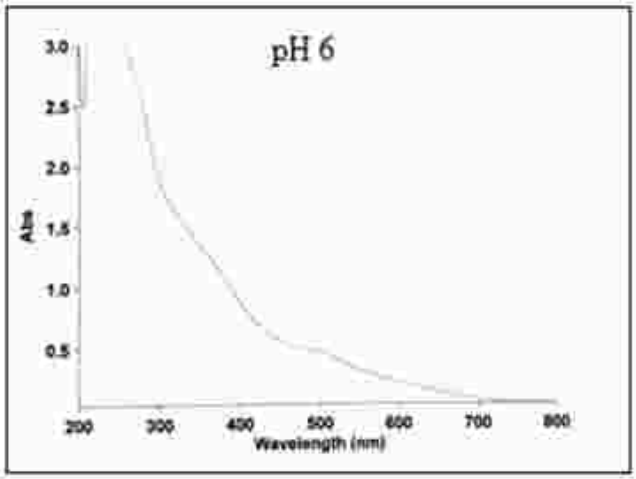
pH 6
Abs
Wavelength (nm)

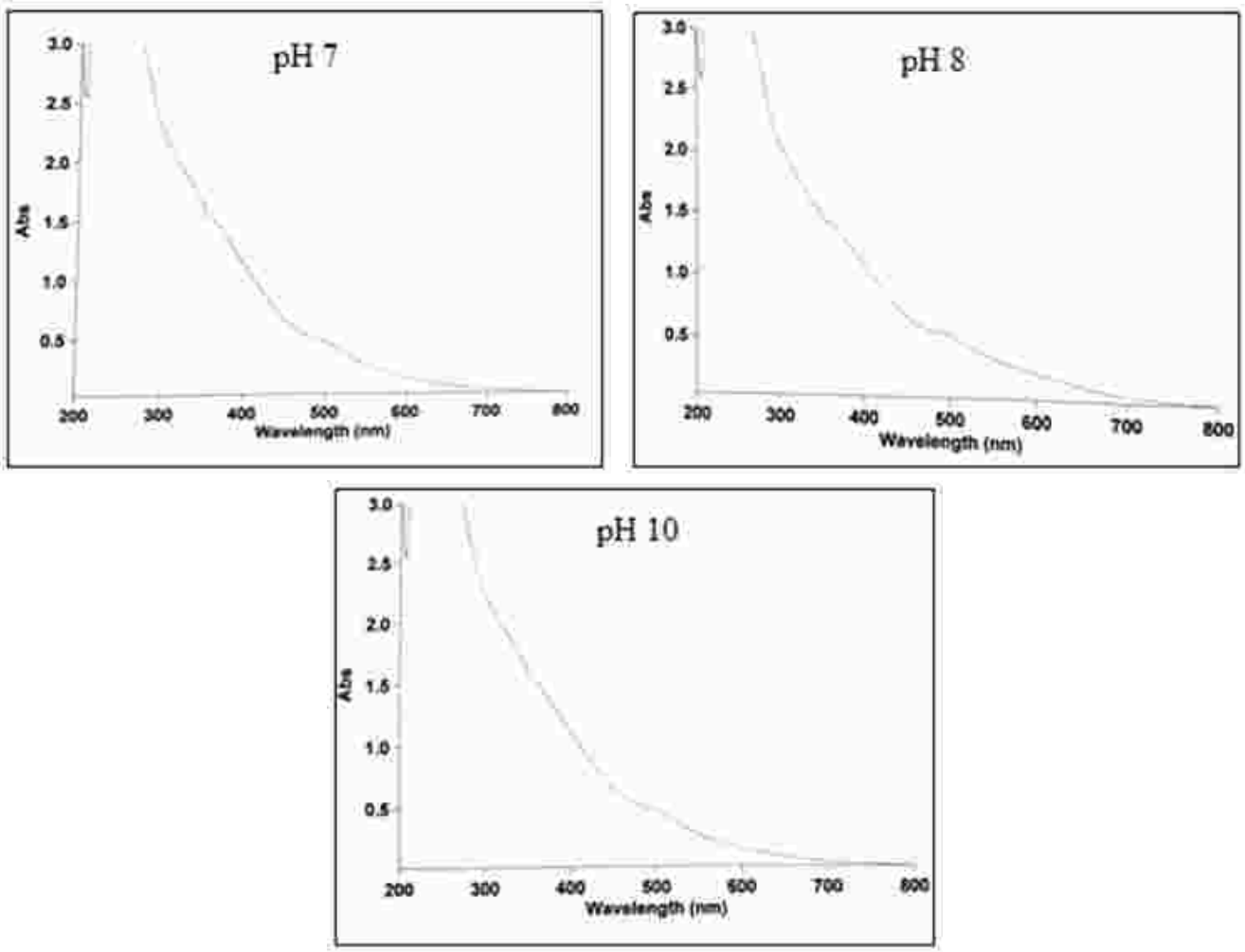

Fig. 3: UV-Visible spectra at different pH (from 1 to 8 and at 10)

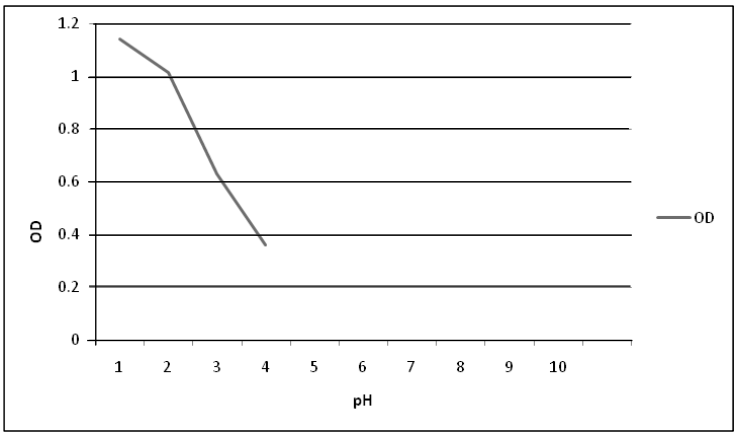

Graph 1. Decrease in stability of anthocyanins with increasing pH

B. Sample preparation for determination of effect of Temperature on stability of anthocyanins

A wide range of temperatures was selected starting from -20ºC up to 121ºC. Understanding the stability of anthocyanins under various temperature conditions would help in taking decisions about storage temperature and conditions and processing temperatures in product development process.

Samples were prepared in pH 1 buffer since it was observed from the pH stability study that the colour of the anthocyanins is most stable under low pH conditions. 100µL of extract was added in 2900µL pH 1 buffer (0.2M HCl and 0.2M KCl in appropriate proportion) and were subjected to various temperature conditions. Effect of temperature was checked by observing changes in λmax and absorbance value. This dilution of sample was chosen such that the absorbance value falls in the linear range of spectrophotometer. Samples at low temperatures were stored at the specified temperatures for 7 days and readings were taken at various intervals mentioned below. To achieve the temperatures from 50ºC to 100ºC a water bath was used. The samples were subjected to highest temperature under study viz. 121ºC by keeping them in an autoclave.

Table 2. Observations of change in absorption values under range of temperatures

Temperature (˚C)	Day	Λmax	OD
-20	1	513.00	1.165
	4	513.00	1.168
	7	513.00	1.171
4	1	513.00	1.157
	4	513.00	1.158
	7	513.00	1.171
10	1	513.00	1.165
	4	513.00	1.164
	7	513.00	1.176
RT	1	514.00	1.157
	4	514.00	1.150
	7	514.00	1.152
50	1	513.00	1.137
70	1	513.00	1.195
100	1	513.00	1.030
121	1	513.00	0.710

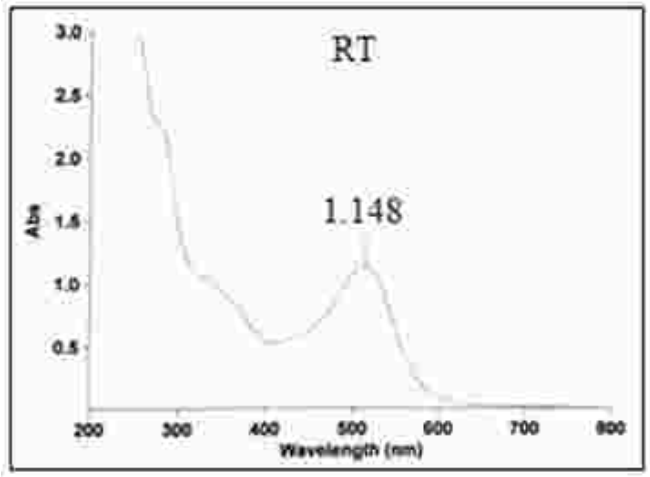

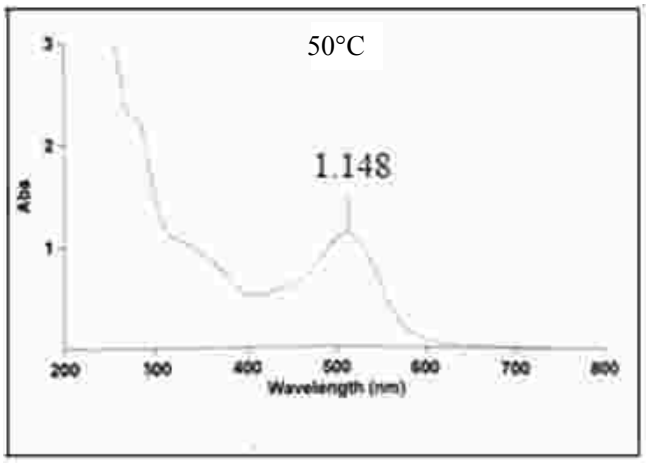

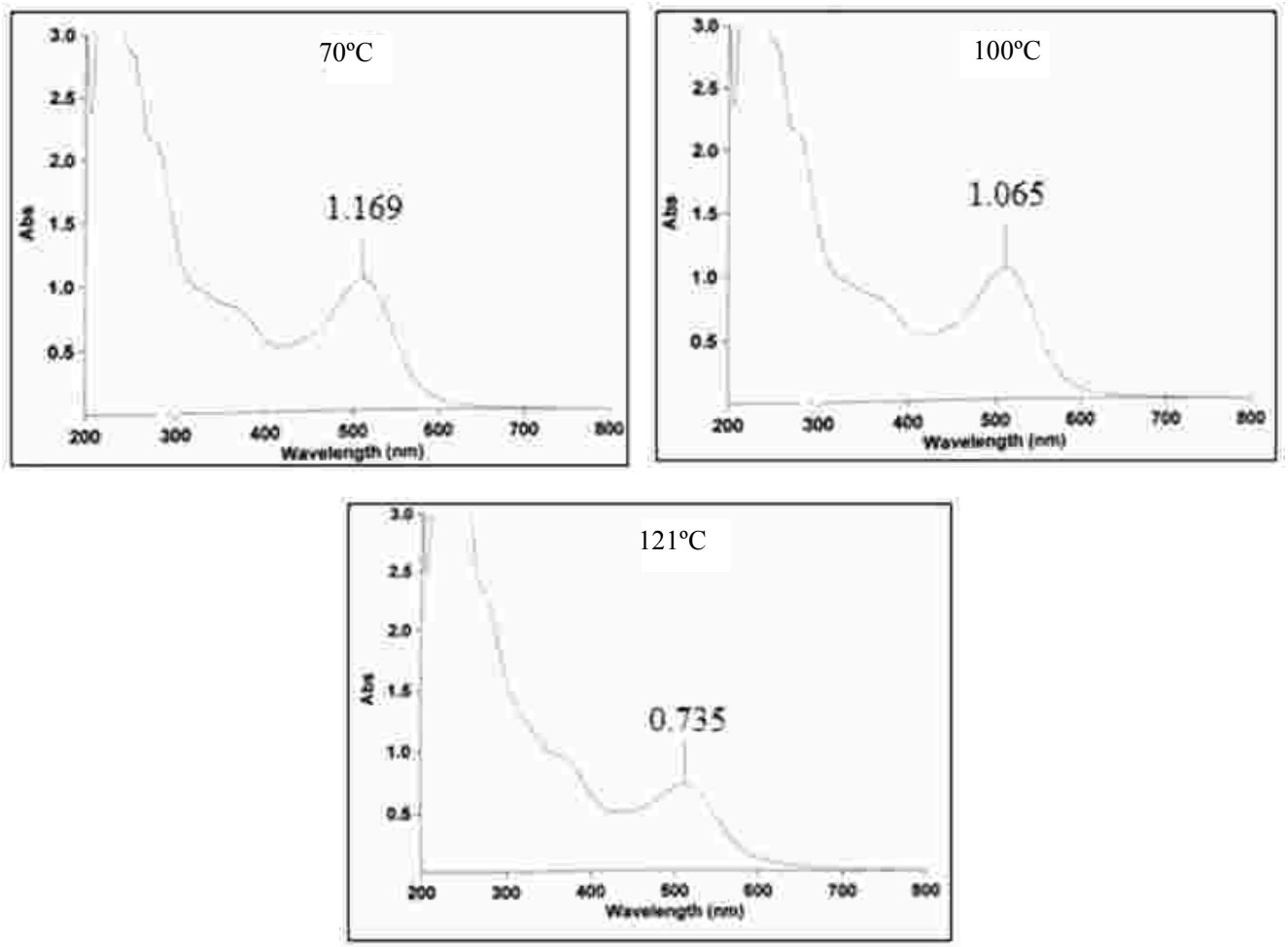

Fig. 4 : UV-Visible spectra at different temperatures (from -20ºC to 121ºC)

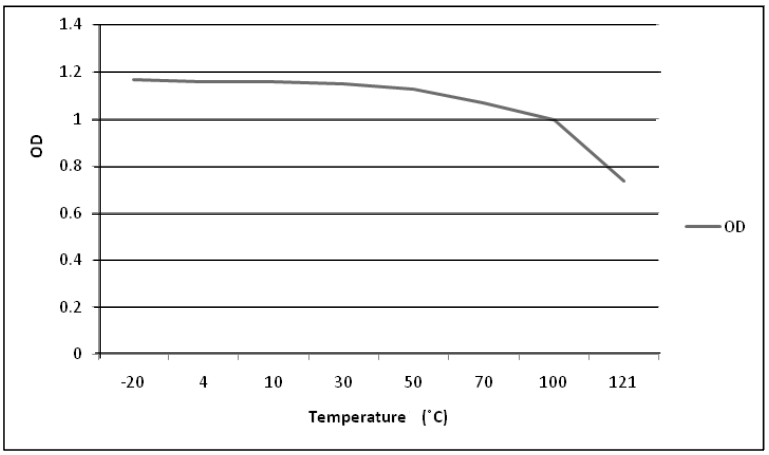

Graph 2. Decrease in stability of anthocyanins with increasing temperature.

C. Sample preparation for determination of effect of Light exposure on stability of anthocyanins

Stability of extracted anthocyanins was checked under various light conditions such as day light, sun light, dark. In order to find out the effect of various light conditions the sample concentration was adjusted, so that absorbance value would fall in the linear range. Every day 3mL of sample aliquot was taken and the change in the absorbance readings was noted. The samples were prepared by adding 100µL of extract in 2900µL pH 1 buffer (0.2M HCl and 0.2M KCl in appropriate proportion). The observations of effect of light would help in finding out the handling and storage conditions for product development.

Table 3. Observations for change in absorption for various light exposure conditions

Light condition	Day	λmax	OD
Day light	1	513.00	1.162
	4	513.00	1.164
	7	513.00	1.159
Sun Light	1	513.00	1.168
	4	513.00	1.150
	7	513.00	1.121
Dark	1	513.00	1.183
	4	513.00	1.217
	7	513.00	1.148

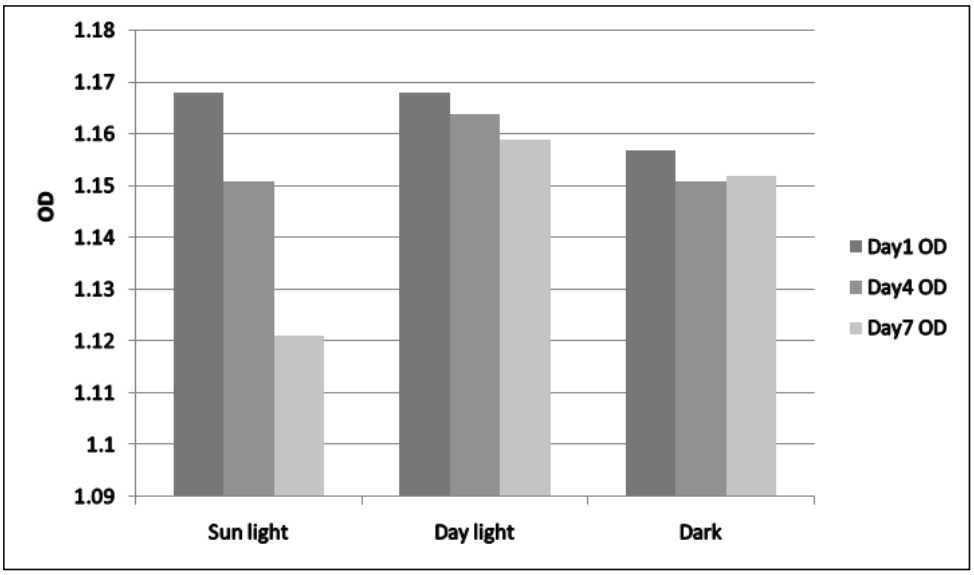

Graph 3. Decrease in stability of anthocyanins with changing light exposure conditions

Results and Discussion

Effect of pH on stability:

It was noted as early as 1914 that an individual anthocyanin species can have different colours. The colour of anthocyanins depends on their structure, the acidity of the environment, and the presence of metals. It was observed (refer Table 1) that at pH below 2.5, the anthocyanins were present in the flavylium cation state, the primary structure of the compound, and a red color was observed. In weakly acidic solutions, where the pH was between 4 and 7, the compound favored a secondary structure, a mixture of anhydrobases and pseudobases. The initially formed purple anhydrobases (in the pH range 4-6) underwent rapid decolorization to colourless (above pH 6) which then changed to yellow chalcone form (above pH 8) caused by nucleophilic attack from water on pyran ring.

Effect of Temperature on stability

The thermal stability of anthocyanin varies with their structure, pH, the presence of oxygen and interaction with other components in the system. Maximum thermal stability of anthocyanidin 3-glycosides has been observed at pH1.8 to 2.0. This supports the findings from the above experiments of pH and temperature stability since measurements were taken under low pH conditions. The experiment was performed covering the whole range of temperatures starting from as low as -20ºC to 121ºC. Observations (refer Table 2) for low temperature conditions were taken over 7 days in order to understand whether degradation takes place with time, irrespective of storage of extract in low temperature conditions.

It was observed (refer Table 2) that λmax and absorbance value did not change over 7days when samples were stored under low temperatures such as -20ºC, 4ºC and 10ºC and at room temperature the change was minuscule. Then at higher temperatures such as 50ºC and 70ºC no significant change in the absorbance was observed; this indicates that anthocyanins extracted from banana bracts can withstand temperature up to 70ºC but at 100ºC and 121ºC degradation was noted in terms of decrease in absorbance value by 11% and 39% respectively. Thus anthocyanins from banana bracts are proved to be fairly stable up to the temperature of 70ºC and above that degradation of the components take place.

Effect of Light exposure on stability

Light exposure of any type is generally found to be detrimental to anthocyanin stability. p-hydroxybenzoic acid has been identified as a minor photo-oxidative product which could be due to photo chemical decomposition of anthocyanins. In this project, banana bract anthocyanins from *Musa paradisiacal L.* was subjected to various light exposure conditions such as day light, direct sun light, in dark, for 7 days and ultraviolet light for 30 minutes. The effect of light was checked as changes in λmax and absorbance values.

Effect of Day light exposure: It was observed that there is no significant change in the λmax and absorbance values even after 7 days exposure (refer Table 3). It indicates that the extracted banana bract anthocyanins are fairly stable when exposed to day light in atmospheric conditions. This in turn indicates that the anthocyanins can withstand routine atmospheric conditions which would be characteristic of any industrial plant.

Effect of Sun light exposure: Sun light or any ionizing radiations have proved to be damaging to the anthocyanin stability. There was decrease in the absorption by approximately 28%. It indicates that sun light has a negative effect on the anthocyanin stability and hence this can be considered as a storage condition for processing product and handling extract.

Effect of storage in dark: It is known that anthocyanins undergo photo-oxidation, thus keeping them in dark would have positive effect on stability of anthocyanins. Similarly it was observed that negligible degradation occurred when samples were stored in dark for 7 days. This indicates that, keeping anthocyanins in dark environment will protect their structure from photo-oxidation.

Conclusions

In recent years, people are becoming more aware regarding the safety of the products. A trend is being seen 'whatever is natural; is safe'. The identity and origin of the product components are mandatory to be mentioned on almost all utility goods and food products. Thus nowadays people prefer products bearing tags as 'natural' or 'herbal'. Thus, the demand for nature based products is increasing tremendously. Since colour is an integral part of any product, research in the field of finding newer and stable natural colourant sources is the need of the hour. Among all the colours, red or shades of red are the most attractive options required in food, pharma as well as cosmetic industries. Red colour can be obtained from a group of natural colorants, Anthocyanins. They are responsible for all the attractive hues displayed by nature. They are water soluble, easy to

incorporate and give brilliant colour to the products. But they come with a price; they are delicate and easily affected by many degradation mechanisms.

Anthocyanins undergo reversible reaction under different pH environments. The coloured flavylium form was observed at low pH which changed to mixture of pseudobases and anhydrobases which showed purple colour in the medium pH range and finally in alkaline pH range, was converted to chalcone form which is yellow in colour. Thus it can be concluded that colour of the anthocyanins can be best maintained at low pH. Hence the banana bract anthocyanins can be used in the food products such as jams, jellies, sugar confectionaries, sauces etc. which are acidic in nature; and also in creams or ointments or hair colours having acidic or citric ingredients such as anti-aging creams and heel creams in case of cosmetic products. The anthocyanins can be stabilized by complexing reactions and can be utilized in coloured cosmetics.

The second aspect studied was the effect of temperature. It was observed that colour of banana bract anthocyanins was not lost in substantially high temperature up to 70ºC. Thus it can be inferred that anthocyanins would withstand higher temperatures employed during processing conditions. It was also observed that anthocyanins are best maintained at low temperatures. The study was carried out for 7 days, and indicated stability of colour over time. This indicates that colour of the anthocyanins can remain constant for longer time if stored at low temperatures. This information is very important, since the decisions for storage and high processing temperatures for banana bract anthocyanins were taken based on these observations.

Another important parameter studied was exposure of banana bract anthocyanins to various light conditions over a period of 7 days. It was observed that direct sun light has harmful effect on the anthocyanin colour stability since it reduced by 27% of the original colour. Secondly it was observed that day light has lesser degradation effect on colour and in dark, the degradation was least. This indicated that anthocyanins should be stored at low temperatures and away from the light.

All of the above points finally can be concluded that banana bract anthocyanins from *Musa paradisiac* L. show fair colour stability under low pH, they can withstand processing temperatures up to 70ºC and can sustain colour for a longer time when stored at low temperatures in a dark environment. Thus these inferences are very helpful in the process of designing a product using these anthocyanins. Hence banana bract anthocyanins show great potential as source of natural colourant for food as well as cosmetic products.

References

1. Oluwaniyi, O.O., Dosumu, O.O., Awolola, G.V. and Abdulraheem, A. F., 2009, *Journal of Feed Technology,* **4(5)**, 218-225.

2. Hendry G.A.F. and Hougston, J.D., 1992, Natural Food Blackie Glasgow and London, Published in USA by 'AVI'.

3. Veridiana Vera de Rosso and Adriana Z. Mercadante, 2007, *Innovative Food Science and Emerging Technologies,* **8,** 347–352

4. David Del Pozo-Insfran, Carmen H. Brenes, and Stephen T. Talcott, 2004, *J. Agric. Food Chem.*, ***52***, 1539-1545.

5. Laleh, G.H., Frydoonfar, H., Heidary, R., Jameei R. and Zare, S., 2006, *Pakistan Journal of Nutrition* **5 (1)**, 90-92.

6. Lucimara Salvat Vanini, Talita Akemi Hirata, Angela Kwiatkowski and Edmar Clemente, 2009, *Braz. J. Food Technol*., **12(3)**, 213-219.

7. Eliana Ferreira Ozela, Paulo César Stringheta, and Milton Cano Chauca, 2007, *Cien. Inv. Agr.,* **34(2)**, 85-90.

8. Janna O A, Khairul A, Maziah M and Mohd Y., 2006, *African Journal of Biotechnology* **5 (2)**, 170-174.

9. Stéphanie Guillotin, Philippe Sanoner and Catherine M.G. C. Renard, 2009, *Journal of Horticultural Science & Biotechnology,* ISAFRUIT Special Issue, 96–99.

10. Thermo Spectronic, Basic UV-Vis theory, Concepts and Applications, www.molecularinfo.com/MTM/UV.pdf

11. Daniel, M., 2008, Herbal Technology- concepts and approaches, © Satish Serial Publishing House.

12. Krish Moorthy, 2008, Fundamentals of Biochemical Calculations, Second edition, CRC press ©.

RNI No. MAHENG/2017/74063
ISSN No. (Print) 2581-5911

Bionics – inspiration in nature for design of new adsorbents and their potential in removal of pharmaceuticals

Eva Chmielewská
Faculty of Natural Sciences, Department of Environmental Ecology,
Comenius University, Mlynská dolina B2, 842 15 Bratislava, Slovak Republic,
Email: chmielewska@fns.uniba.sk

Introduction

Current industrial adsorbents consist of a broad variety of chemical substances and different geometrical structures. In today's society environmental requirements are becoming important since there is an increased interest in the industrial use of renewable resources. "*Green*" designates a novel advanced adsorbent fabricated from Nature bioinspiring (basically polysaccharide) materials and synthesis to mimic the exceptional features of natural species [1,2].

Actually, biopolymers present fascinating templates for creating bioinorganic materials, e.g. starch that is stored in plants, meets all the required criteria. Combined with the traditional chemical techniques, the biopolymer assisted synthesis may prove a promising route to prepare a "*new generation*" of biomineral adsorbents guiding oriented growth of organic substances on the surface. Some interesting remarks of living cells are based on excretion of biogenic surfactants or specific biopolymeric acids like alginic acid and their salts. Alginate is a copolymer of the isomers, mannuronic and guluronic acids enabling the dense packing of submicrometer-sized particles in suspensions in order to enhance their colloidal stability [1-3].

To promote the zeolite performance and to prepare more effective adsorbent for specific post-treatment processes, flexible component, i.e. alginate with a rigid component, (powdered) zeolite was crosslinked using Fe(III) and Ca(II) ions. While incorporated Fe(III) cations in new adsorbent were responsible for electrostatic interactions "oxyanionic pollutants vs. biopolymer pelletized zeolite", Ca ions were responsible for exchange of metallic cations. Finally, such alginate-zeolitic adsorbents showed during examination, considerable enhanced adsorption capacity towards metallic pollutants [3].

Using the hydrophilic, expandable and permeable hydrogels with low interfacial tension for the novel adsorbent synthesis, substances which resemble soft living tissues, is another excellent example of advanced surface treatment strategy how to enhance clinoptilolite tuff performance. Various aspects regarding above mentioned surfactant octadecylammonium (ODA) clinoptilolite have been reviewed and highlighted in literature [1,3,4,5].

Iron oxides are effective, low cost adsorbents for heavy metals and radionuclides removal, respectively. Their sorption process is mainly controlled by complexation. When their particle size is reduced to below 20 nm, the adsorption capacity increases by 10 to 100 times, suggesting a "nanoscale effect". While nanomaterials embedded in a solid matrix like zeolite may expect minimum release into the environment, research is needed to develop simple, low cost techniques to immobilize nanomaterials without significantly impacting their adsorption performance. Based upon the recent encouraging results of Slovakian natural clinoptilolite producer, and necessity to immobilize a nanosized iron oxide onto

solid surfaces, we studied various routes to prepare environmentally viable as well as economically feasible adsorbent with zeolite matrix [4,5].

Emerging contaminants in Environment

Pharmaceuticals, currently called emerging contaminants (ECs), can enter the environment by a number of pathways and can be further distributed in various environmental media. One prominent pathway could be the use of wastewater sludge or waste water for field fertilization and irrigation. In water environments, a large variety of these compounds and their metabolites have been detected and also soil could be an important source of water contamination [6-9].

The presence and distribution of pharmaceuticals in the soil vai land application are far from known because of a lack of appropriate methodologies. Liquid chromatography combined with mass spectrometry (LC-MS) or with tandem mass spectrometry (LC-MS/MS) is a popular technique currently being used in pharmaceutical analyses. The latter allows detection of extremely low concentrations (ng/L or ng/g) of these compounds in various complex liquid or solid matrices.

The presence of ECs in the environment is mainly attributed to the discharge of treated wastewater from water treatment facilities. Conventional secondary processes (activated sludge and trickling filters) represent the most extensively used and studied processes. An increase in drug use may be anticipated during music festivals, public holidays, major sporting events and by students during exam periods [6-9]. However, above mentioned bioprocesses are not designed to remove ECs resulting in their discharge to receiving surface waters including rivers, lakes and coastal discharge. e.g. during anaerobic digestion, biosolids (or treated sludge) are generated. These are often applied to agricultural land as a fertiliser in many countries. Despite lengthy digestion (on an avarage 4 weeks) and outdoor storage for up to six months following treatment, some ECs have been found to persist.

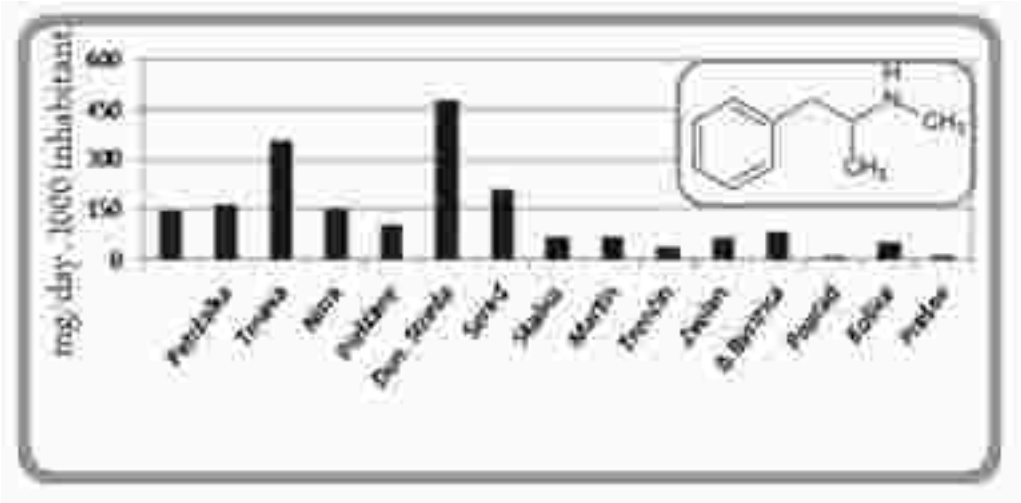

Fig.1: Methamphetamine consumption in Slovakian towns

The presence of these chemicals in the environment is more serious considering that they do not appear individually, but as a complex mixture, which could lead to unwanted synergistic effects. Parent chemicals are often excreted from the human body with a number of associated metabolites. As an example, Ibuprofen is excreted as the unchanged drug. Approximately 70 pharmaceuticals, belonging to a variety of therapeutic classes, have been reported in UK waters [6]. The analgestic tramadol has been observed in river water at the highest concen-

tration up to a maximum of 7731 ng /L [6,10]. The hallucinogen 3,4-methylenedioxy-N-methylamphetamine (MDMA) and the stimulant cocaine have been observed in river water in concentrations of 25 and 17 ng /L, respectively [6,12-14]. To date, more than 200 different pharmaceuticals alone have been reported in river waters globally, with concentrations up to a maximum of 6.5 mg/L for the antibiotic ciprofloxacin [6,10,11].

Methamphetamine (locally called pervitin) is an extremely addictive stimulant drug that is chemically similar to amphetamine[15]. It is a white, odorless, bitter-tasting crystalline powder. Methamphetamine is taken orally, smoked, snorted, or dissolved in water or alcohol and injected. Smoking or injecting the drug delivers it very quickly to the brain, where it produces an immediate, intense euphoria. According to monitoring provided by the national water authorities and researchers, consumption of this chemical in Czech and Slovak Republics is the highest in the world (Table 1) [15].

An attempt to remove antibiotics by polishing or posttreatment of water using adsorption

Nevertheless, removal of environmental pollutants released or discharged over a vast area of the world, require relatively cheap, cost effective or economically viable technology. Current treatment processes for contaminated waste streams are mostly chemical precipitation, membrane filtration, ion exchange and adsorption. Among those different techniques, adsorption based processes have drawn much interest as in the past due to the relatively simple approach for the removal of several environmental pollutants. Activated carbon, clay minerals, biomass, natural zeolites and even some industrial solid waste have been widely used as adsorbents for removal of ions and organics from contaminated waters. The excellent selectivity of natural zeolites to different adsorbates as well as worldwide abundance of these precious tuffaceous materials, has popularised their utilization in environmental cleanup technologies since 1960´s. Most of the reported applications of natural zeolites in the past decades have focused on the removal of ammonium and heavy metals. Nevertheless, the unique chemical and structural characteristics of natural zeolites made them appropriate for several environmental applications, where effectivness and low cost of materials are needed [16]. Today, hundreds of zeolitic applications related to water treatment and purification processes are available. However, recent literature reports the state of the art mainly in zeolite surface modification using the hydrophobization (sol-gel technique for coating the zeolitic surface by different surfactants, moreover with zero valent iron (ZVI-) addition), metal doping or peletization of zeolite matrices with some biopolymeric eco-friendly carbohydrates. Since the last decade, several new surface modified or hybridized zeolite adsorbents have been succesfully synthesized whose performance has been excellent.

In general for water and wastewater treatment, a significant majority of recent developments relate to biological processes and treatment technologies using advanced adsorption and filtration media. Adsorption is the capability of all solid substances to attract to their surfaces, molecules of gases or solutions with which they are in close contact. Due to their high specific surface area, nano adsorbents show a considerably higher rate of adsorption for organic compounds as compared to granular or powdered activated carbon. They have great potential for novel, more efficient, and faster decontamination processes aimed at removal of organic and inorganic pollutants like heavy metals and micropollutants [11]. Nanometals and zeolites benefit from their cost-effectiveness and compatibility with existing water treatment systems since they can be implemented in pellet and bead forms for fixed absorbers. Evidently, the photocatalytic degradation of organic pollutants including ECs by TiO_2 supported solid matrices belong to the latest in the field (AOP). Titanium dioxide has been widely used as photocatalytic material in the removal of toxic chemicals from waters, but due to its fine sized grains (4-30 nm), it aggregates rapidly by loosing efficiency. TiO_2 is not porous and its surface exhibits polar property, however when immobilized on porous solids

(semiconductor graded solids) using mostly the sol-gel route, provides higher specific surface area and facilitates more effective adsorption sites than bare TiO_2 [17,18]. Prophylaxis antibiotic (cefazoline) removal using aqueous solution and stationary (batch) system was applied to compare several adsorbents like native, ODA- and carbonized zeolite (clinoptilolite-rich tuff), montmorillonite, German commercial GEH, active coke and beringite (Fig.2). Aqueous model solutions of cefazoline were analysed by means of Diode Array (UV-VIS) Spectrometer Hewlett Packard 8452A at the wavelength 272 nm.

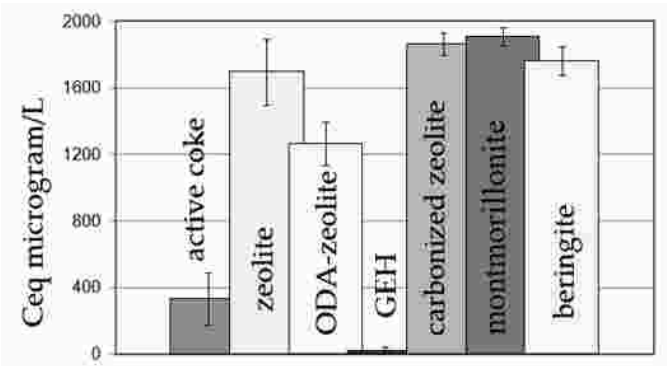

Fig.2: Average equilibrium concentrations of cefazoline removal onto some selected adsorption materials

Cefazoline is an antibiotic used for the treatment of a number of bacterial infections. The drug is usually administered by either injection into a muscle or into a vein. It is listed in the World Health Organization's List of Essential Medicines - the most important medications needed for a basic health system (Table 1).

According to the above graphical plot, the highest capacity towards cefazoline was shown by GEH and active coke. ODA-surfactant coated zeolite exhibited acceptable uptake performance. Beringite is basically aluminium silicate rock made up of albite, barkevite and orthoclase. Fig.3 presents a broader range of selected adsorbents for examination of cefazoline uptake. German provenience silcarbon, industrial ashes chezacarb (amorphous carbon) from Chemopetrol Litvínov (Czech Republic), German granulated ferric hydroxide (GEH) with the main components of akaganeite (ß–FeOOH) and goethit [α-FeO(OH)], montmorillonite from the deposit in Slovak Republic, obtained from the rock after sedimentation and purification procedures and commercial Happy End (Great Britain), mostly natural resources derived and mixed products denoted as SK1, SK2, DN2 and CB18 were compared. SK1 and SK2 contain the mixture of cellulose, calcium carbonate and clays, while

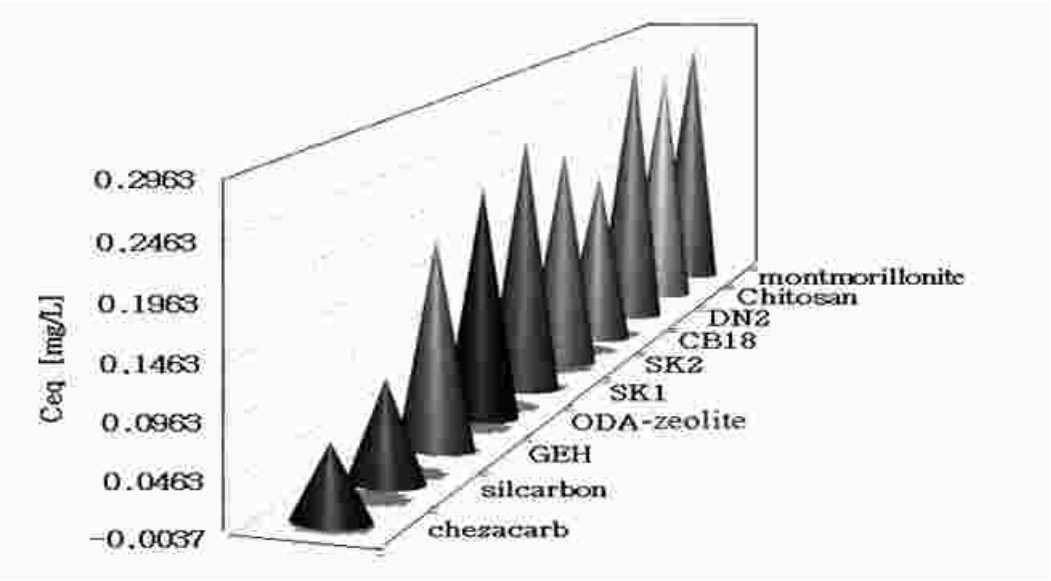

Fig.3: A broader range of selected adsorbents for examination of cefazoline uptake

DN2 is manufactured mainly from natural silicate resources based on the former commercial Absodan and CB18 with a high quality peat (Table 1). Peat contains lignin, cellulose, fulvic and humic acids as major constituents that have polar functional groups, such as alcohols, aldehydes, ketones, phenolic hydroxides and ethers, using them in chemical bonding [16].

According to Figures 2 and 3, ODA-zeolite has removal efficiency for unpolar heavily substituted carboxylic acid cefazoline (Table 1). As can be seen, carbon based adsorbents (chezacarb and silcarbon) showed the best removal performance besides GEH and ODA-zeolite while for cefazoline removal Happy End products under SB18 (peat) were preferred.

Tab.1: Commercial products Absodan and Spilkleen manufactured from natural materials and applied for cefazoline removal (left); structure formula of cefazoline (right)

	SK1 denotes a mixture of natural resources, mostly the cellulose, calcium carbonate and clays
	Spilkleen SK2 is a commercial product similar like SK1
	CB18 means a high quality peat
	DN2 is manufactured mainly from natural silicate resources based on the former commercial Absodan

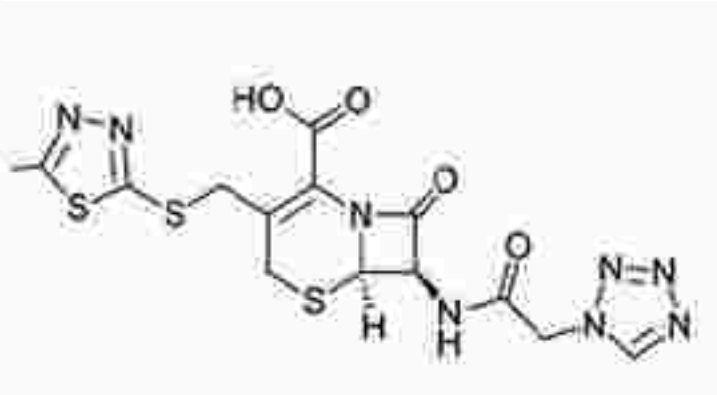

Conclusions

The presence of pharmaceuticals (ECs) in the environment has been a topic of concern. Most environmental data focus on the occurrence, fate, and transport of these compounds in wastewater or receiving waters. Their presence in source waters and drinking water is particularly problematic as this pathway represents a vector for human exposure. Several promising options for pharmaceutical removal from water are available, and many technologies employ an advanced oxidation process (AOP). AOPs have been shown to be better suited for removing recalcitrant pharmaceuticals from water as compared to conventional treatment processes.

Although numerous adsorbents have been developed and examined for water treatment, their potential needs to be further assessed on pilot scale with real surface/ground water or/and wastewater. Development of some synthetic, hybrid and nano-scale adsorbents shows high efficiency towards removal of specific pollutants, but more research is needed prior to their use an full-scale in water and wastewater treatment.

The development of wastewater treatment systems using oyster shells as the biological growth media that shows enhanced affinity to microorganisms or for even trace concentrations of ECs in water, development of biomimetic adsorbents imitating lipids from white whales, arctic wolves, South African fur seals, marketable fish and mussels, based on high accumulation affinity of organism´s lipids towards ECs, has to be mentioned.

References

1. Biomimetic Materials Chemistry. S. Mann (Ed.) John Wiley & Sons, Inc. Bath (United Kingdom) 1996. ISBN: 1-56081-669-4. p.383.
2. Handbook of Biomineralization, Biomimetic and Bioinspired Chemistry. P. Behrens and E. Bauerlein (Eds.) Wiley-VCH Verlag GmbH & Co. KgaA, Weinheim 2007. ISBN: 978-3-527-31805-6. p.415.
3. Chmielewská, E. and Xu, F., 2015, *Current Green Chemistry*, **2(4)** 362-370.
4. Altshuller, G., 1999, The innovation algorithm, TRIZ, systematic innovation and technical creati-vity. Technical Innovation Center Inc., Worcester, Massachusetts, USA.
5. Favret, E.A. and Fuentes, N.O. Functional Properties of Bio-Inspired Surfaces**,** Characterization and Technological Applications, © World Scientific Publishing Co. Pte. Ltd., 416 p. 2009.
6. Petrie, B., Barden, R. and Kasprzyk-Hordern, B., 2015, *Water Research* **72,** 3-27.
7. Sabourin, L., Duenk, P., Bonte-Gelok, S., Payne, M., Lapen and D.R.,Topp, E., 2012. *Sci. Total Environ*., **431**, 233e236. http:// dx.doi.org/10.1016/j.scitotenv.2012.05.017.
8. Ort, C., Lawrence, M.G., Reungoat, J. and Mueller, J.F., 2010. *Environ. Sci. Technol.*, **44**, 6289e6296. http://dx.doi.org/10.1021/es100778d.
9. Miao, X.S., Yang, J.J. and Metcalfe, C.D., 2005. *Environ. Sci. Technol.*, **39,** 7469e7475. http://dx.doi.org/10.1021/es050261e.
10. Heal, D.J., Smith, S.L., Gosden, J. and Nutt, D.J., 2013, *J. Psychopharmacol.*, **27**, 479e496. http://dx.doi.org/10.1177/0269881113482532.
11. Gehrke, I., Geiser, A. and Somborn-Schulz, A., 2015, *Science and Applications*. **8,** 1–17.
12. Gottschalk F, Sonderer T., Scholz R.W. and Nowack B., Modeled environmental concentrations of engine 2009, *Environ Sci Technol*., **43**, 9216–9222.
13. European Chemicals Bureau. Technical Guidance Document on Risk Assessment. Dublin, UK: Institute for Health and Consumer Protec-tion, European Commission; 2003. Available from: http://echa.europa.eu/documents/10162/16960216/tgdpart2_2ed_en.pdf. Accessed July 24, 2014.
14. European Protection Agency. Office of Research. Nanomaterial case study: nanoscale silver in disinfectant spray. EPA/600/R-10/081F, 2012. Available from: http://cfpub.epa.gov/ncea/cfm/recordisplay.cfm?deid=24166. Accessed July 24, 2014.
15. Mackuak, T. et al., 2014, *Sci. Total Environment* **494,** 158-165.
16. Chmielewská, E., Environmental zeolites and aqueous media. Examples of practical solutions. Bentham Science Publishers (Bentham eBooks), ISBN: 978-1-60805-933-1, p.220, 2014. http://ebooks.benthamscience.com/book/9781608059324.
17. Bhatnagar, A., Application of adsorbents for water pollution control. A note on the advances in adsorption technology for water treatment: Progress and challenges. eISBN 978-1-60805-269-1, 523-528, Bentham Sci.Publ. Ltd., 2013.
18. Ternes, T.A., Meisenheimer, M., Mc Dowell, D., Sacher, F., Brauch, H.J., Haist-Gulde, B., Preuss, G., Wilme, U. and Zulei-Seibert, N., 2002, *Envron. Sci. Technol.*, **36**, 3855-3863.

RNI No. MAHENG/2017/74063
ISSN No. (Print) 2581-5911

Separation of Anions with Capillary Liquid Chromatography using Polymethacrylate based Monolithic Capillary Columns modified with Arginine

Oksil Venriza, Lee Wah Lim and Toyohide Takeuchi*
Department of Chemistry and Biomolecular Science, Faculty of Engineering,
Gifu University, 1-1 Yanagido, Gifu 501-1193, Japan
Email: take-t@gifu-u.ac.jp

Abstract
The organic methacrylate based monolith column was prepared and modified with arginine in organic solvent under acidic condition. Organic mixture solvent under acidic condition could improve the reaction of arginine with the epoxy groups of the poly(glycidyl methacrylate (GMA)-ethylene dimethacrylate (EDMA)). The GMA-EDMA-arginine monolith column was prepared with isopropanol and decanol as the porogenic solvents, GMA as monomer and EDMA as crosslinker in one solution and the second solution was 250 mM arginine in dimethylformamide and methanol as organic solvent, in acidic solution. Performance of a 0.32 mm. i.d x 10 cm polymer methacrylate monolith column was evaluated for separation of anions such as 1.0 mM each of IO_3^-, BrO_3^-, NO_2^-, Br^-, and NO_3^-, with 200 mM NaCl in the 0.1 M phosphate buffer as mobile phase at 210 nm wavelength and flow rate 3 µL/min, although bromide and nitrate were still overlapped. This method has a good permeability of 1.9 x 10^{-14} m^2, excellent linearity with the correlation coefficient (approximately one) and excellent repeatability performance with values less than 5 %, and finally could be applied for real river water samples.

Keywords: *Capillary Column, Organic Polymer Monolith Column, L-Arginine, Inorganic Anion*

Introduction

In the last decade the developments in the field of ion chromatography (IC) were aimed at increasing the efficiency, sensitivity and rapidity of analysis, as well as improving separation selectivity.[1,2,3] Since selectivity and efficiency to the large extent depend on the surface chemistry of the stationary phase, the development of polymer monolith anion exchangers remains one of the priority tasks in modern IC. The knowledge about the surface chemistry of anion and cation exchangers can provide understanding of the trends in selectivity and efficiency changes, as well as help in the choice of the stationary phase type suitable for solving a particular analytical task.[4,5] The newly explored application of metal organic gel has been used increasing separation in liquid chromatography.[6] Monolith columns have been widely applied in capillary liquid chromatography (CLC) and capillary eletrochromatography (CEC) due to their easy preparation, unique hydrodynamic property and high performance compared with the traditional particle-packed column or the open tubular column. During the evolution of CEC in the past 10 years, the attention slowly shifted from the separation of mixtures of well selected model compounds, typically aromatic hydrocarbons due to their good visibility with a UV detector to real samples. In situ polymerisation was done in silica monolith column bonding cyanopropyl[7,8,9] and the silica

hybrid monolith column was synthesized for multiple interactions including hydrophobicity, hydrophilicity, as well as cation exchange interaction.[10.11.12] Due to the zwitterionic nature of the resultant stationary phase, the modified monolithic column contained both cation and anion exchange capacity with amino acid, such as lysine[13.14] and also a polar copolymerized method.[15.16.17] Amino acid compound was investigated in CLC for anion and cation separation on silica hybrid monolithic column.[18.19] The technology for the preparation of such porous beads is very well developed and an excellent control over bead size, porosity and surface chemistry can be achieved. Amino acid compound in most recent innovations was made to achieve high performance with open tubular separation method, focusing on the ingenious chemical and physical solution made to increase the surface and equip the stationary phase with exploitable selectivity of monolith column.[20.21] Polymerization temperatures gave impact for separation of organic analytes such as alkyl benzenes, aryl amines, carboxylic acids, a mixture of phenols and carbonyl compounds by CLC.[22] But chromatographic polymer monolith column method is important for L-arginine, which is one of the three amino acids with basic side chains, and is very hydrophilic in character. Studies of interaction of L-arginine with toluene/water have been done.[23] It contains a guanidine group in the side chain, and this moiety is protonated at physiological pH. Upon functionalization with these amino acids, the polymers become positively charged and their interaction with the negatively charged molecule is much more efficient. The L-arginine molecule can highly facilitate the interaction of nano particles with biological macromolecules with adding an organic solvent and an acid catalyst for reaction of the amino acid with epoxy group of polymer. For the characterization of prepared polymer scanning electron microscopy (SEM) technique is used. SEM technique is based on the principle of scanning probe consisting of a focused electron beam emitted from an electron gun, which scans the surface of the specimen. Also some researchers used FTIR for doing a polymer characterization.[24]

Materials and Methods

Experimental Instrumentation

The chromatographic measurements were carried out by using a CLC system constructed by an L.TEX-8301 Micro Feeder (L.Tex Corporation, Tokyo, Japan) equipped with an MS-GAN 050 gas-tight syringe (0.5 mL; Ito, Fuji, Japan) as a pump, a model 7520 micro-injection valve with an injection volume of 0.20 µL (Rheodyne, Cotati, CA, USA) as an injector, a 0.320 mm i.d. x 100 mm microcolumn, and a UV-2070C UV detector (JASCO, Tokyo, Japan). The UV detector was operated at 210 nm. A capillary flow cell (75 µm; JASCO) was attached to the UV detector. The data were acquired by a CDS data processor (LA soft, Chiba, Japan). The inlet pressure was monitored by an L.TEX-8150 Pressure sensor (L.TEX). The separation column was dipped in a water bath. The measurements were carried out at room temperature (21-22˚C)

Reagents and Materials

The reagents employed were of guaranteed reagent grade and were obtained from Wako (Osaka, Japan), unless otherwise noted. Purified water was produced in the laboratory by using a Millipore Simplicity UV water distillation system (Millipore, Molsheim, France). Glycidyl methacrylate (GMA), ethylene dimethacrylate (EDMA), 3-(trimethoxysilyl)propyl methacrylate (γ-MAPS, 98%), methanol, isopropanol, decanol, azobisiso-butyronitrile (AIBN), acetone, hydrochloric acid (1 mol/L), sodium chloride, sodium hydroxide (0.1 mol/L) and dimethylformamide (DFA) were employed.

Pre-treatment of fused-silica capillary

Prior to the polymerization, the capillary column was pretreated using the following procedure : the capillary column with a length of 12 cm was rinsed with 0.1M NaOH for 30 minutes and then with water until the outflow reached pH 7.0. This was followed by flushing with 1 M HCl for 30 minutes. The capillary was filled with silanization solution containing 50% (v/v) Y-MAPS

in acetone, and injected into the capillary with a 0.5 mL syringe. Then, the capillary was sealed with PTFE at both ends and then submerged in water bath at 60°C overnight (24 hours). After silanization, the capillary was flushed with acetone to flush out the residual reagent and then dried by passing nitrogen gas. Thereby, Si-O-Si-C bonds were formed between the capillary wall and the reactive methacryloyl groups, which were available for subsequent attachment of monolith to the wall during the polymerization reaction.[25]

Co-polymerization of anion-exchange monolith column

The monolithic columns were prepared from polymerization reaction of mixtures, consisting of the monomers GMA, EDMA, the porogens of isopropanol and decanol using AIBN (0.3%, w/w, with respect to the monomers) as an initiator. 0.5 mL of this solution and 0.5 mL of arginine solution were mixed. The polymerization mixtures were sonicated for 5 min to obtain homogeneous solution, and then purged with nitrogen for 30 min. After the pretreated capillaries were completely filled with the mixture, they were sealed at both ends with PTFE. The sealed capillaries were submerged in a water bath or oven and allowed to react at 60-100°C for 12 hours. The resultant monolithic capillary columns were washed with methanol for about 2 h using an HPLC pump to remove the unreacted monomers and the porogenic solvents. For amino acid, organic solvent was used under acidic condition.[26] Finally, the structure of polymer column has a positive charge of arginine, as shown in Figure 1. The morphology of monolith column was evaluated by using scanning electron microscopy (SEM; S-4800, Hitachi, Tokyo, Japan).

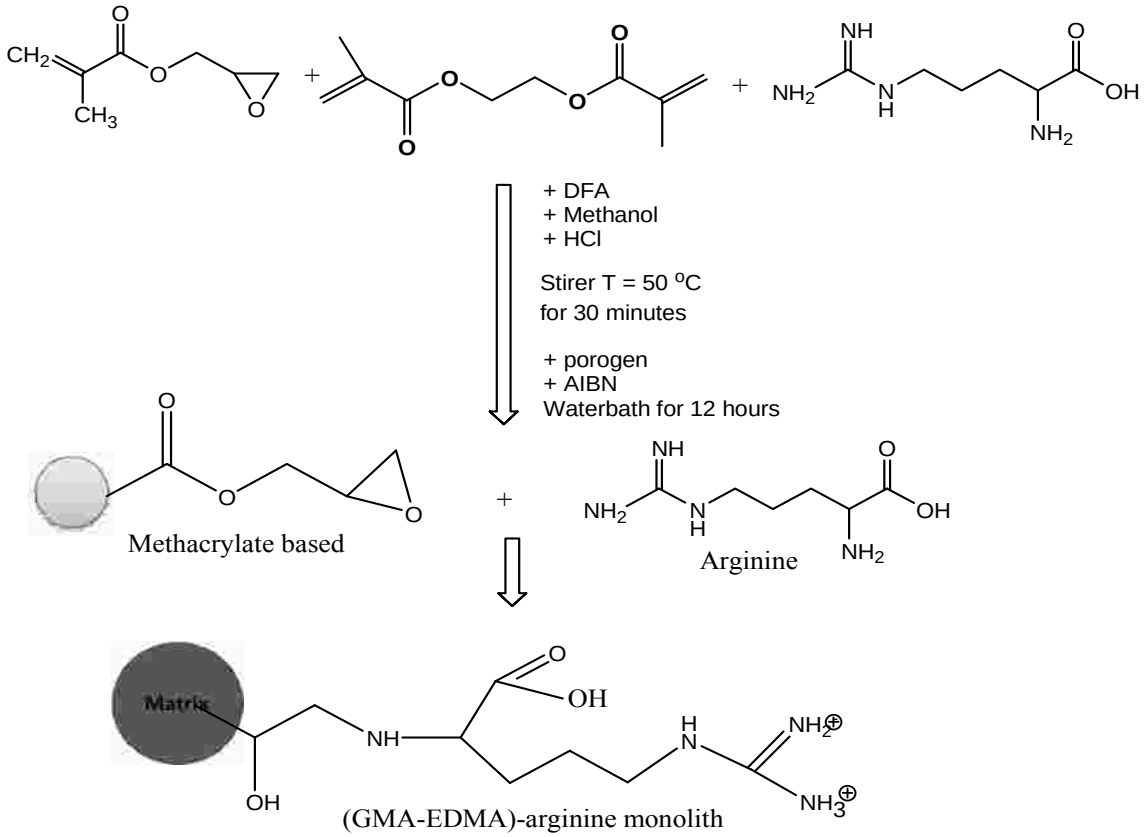

Fig. 1 Schematic diagram of the expected reaction for preparation of poly(GMA-EDMA)-arginine monolith column

Results and Discussion

Effect of composition of porogen and crosslinker for monolith column poly(GMA-EDMA)-arginine

In this research, poly(GMA-EDMA) anion exchange monolith column was produced by a two-step procedure, just like an organic polymer monolith column for separation of DNA.[27,28] The GMA-EDMA-arginine monolith column was prepared with isopropanol and decanol as porogenic solvents, GMA as monomer and EDMA as crosslinker in one solution and the second solution was 250 mM arginine in DFA as organic solvent in acidic solution. The ratio between the monomer and the porogen phases influences the flow-through pore size within a broad range and the morphology of the monolith columns depends on the composition of the porogenic solvent. Solvent in arginine solution like methanol, DFA and water may affect the structure of pores.

The porosity of the poly(GMA-EDMA)-arginine can be controlled by changing the ratio of monomer and porogen, as shown in Table 1.

Tabel 1. Constitution of reaction mixtures

Column	Monomer mixture (mL)		Porogen mixture (mL)		Ratio monomer/porogen	250 mM arginine solution (mL)
	GMA	EDMA	Isopropanol	Decanol		
A	0.070	0.030	0.28	0.12	20/80	0.5
B	0.105	0.045	0.245	0.105	30/70	0.5
C	0.14	0.06	0.21	0.09	40/60	0.5
D	0.105	0.045	0.105	0.245	30/70	0.5
E	0.045	0.105	0.245	0.105	30/70	0.5

All columns had same length of 10 cm and were evaluated using methanol as mobile phase with a flow rate of 3 μL/min. The experimental results obtained showed that the mobile phase cannot flow through for the columns D and E. The pressures of columns A, B and C were 0.9, 2.4 and 3.9 MPa, respectively. These results show that the column with the higher ratio of porogen has a good porosity. In this case, the chosen ratio of monomer mixture versus porogen mixture was 30/70. Figure 2 shows the SEM images of poly(GMA-EDMA)-arginine monolithic column.

Effect of organic solvent and acid solvent in arginine solution

Once the chemical reaction equilibrium condition of arginine was established in the acidic solution, the reaction becomes maximal in the presence of an acid catalyst such as hydrochloric acid.[29] For the prepared poly (GMA-EDMA)-arginine, hydrochloric acid solution (0.10 mmol/L) was used, which affects the reaction of arginine with the epoxy side of monomer. Figure 3 shows the separation of anions by poly(GMA-EDMA)-arginine with and without hydrochloric acid in the solution.

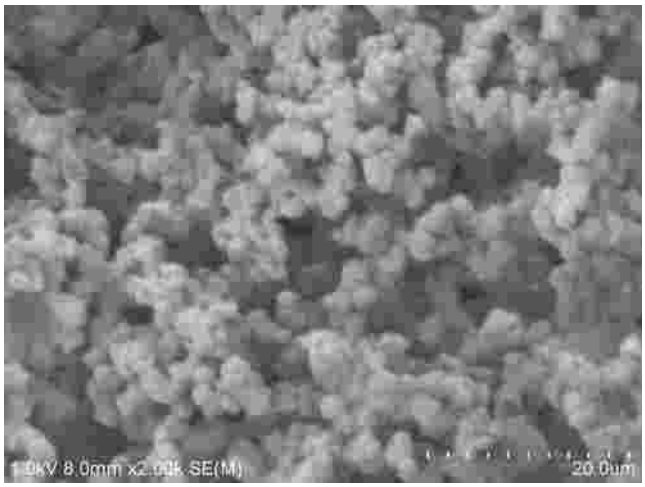

Fig. 2. SEM images of poly(GMA-EDMA) modified with arginine in organic solvent under acidic condition.

As shown in Figure 3, column A was prepared without organic solvent under acidic condition and anions cannot be separated, while column B was prepared with

hydrochloric acid in the polymer solution that gave separation of anions. Column C was prepared with the DFA as organic solvent for arginine under acidic condition with HCl. It is observed that column C gave a better separation of anions than columns A and B.

Optimization of polymerization of monolith column
Based on effect of organic and acidic solvents, the monolithic column poly(GMA-EDMA)-arginine was prepared with methanol also as the organic solvent for increasing solubility of arginine in the solution. That meant finding the equilibriums condition of polymerization of monolith arginine column was necessary. Table 2 shows various columns prepared. Combination of organic solvent, in this case methanol and DFA gave good selectivity of the monolith poly(GMA-EDMA)-arginine column and 5 anions sample could be separated.

Table 2. The composition of polymerization of poly(GMA-EDMA)-arginine with various organic solvent

Column	Monomer mixture		Porogen mixture (mL)		% Porogen	250 mM arginine solution 0.5 mL		Result
	GMA	EDMA	Isopropanol	Decanol		Methanol	DFA	
A	0.105	0.045	0.315	0.035	70	0.5	0	good
B	0.105	0.045	0.315	0.035	70	0.25	0.25	good
C	0.105	0.045	0.315	0.035	70	0.15	0.35	good
D	0.105	0.045	0.315	0.035	70	0.35	0.15	No good

Table 2 shows that two types of columns could be used for separation demonstration, involving columns A and B. Arginine was more easily dissolved in solutions for columns A and B than in solution for column C. Use of methanol and DFA as organic solvents could increase the equilibrium reaction of arginine. The separations of anions using columns A, B and C are shown in Figure 4. For column D, anions cannot be separated, because the eluent could not pass out through the hard column.

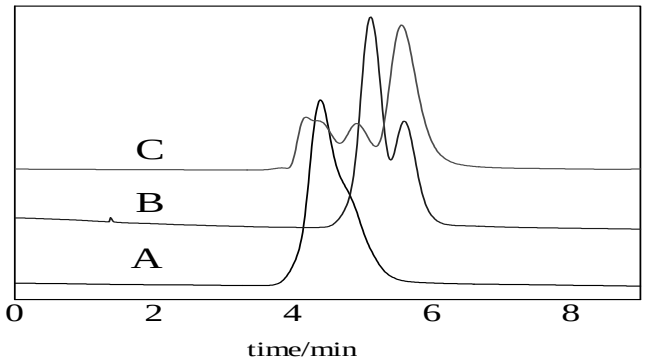

Fig 3. Chromatograms for various organic and acid solvent (A. without acid and organic solvent, B. 10 % 0.1 mol/L of HCl, C, 45 % of DFA) for separation of anions (1.0 mM each of IO_3^-, BrO_3^-, Br^-, NO_3^-, I^-), with eluent 50 mM NaCl. Experimental conditions : poly(GMA-EDMA)-arginine monolith column (100 x 0.32 mm i.d); UV detector at 210 nm; flow rate : 3 µL/min.

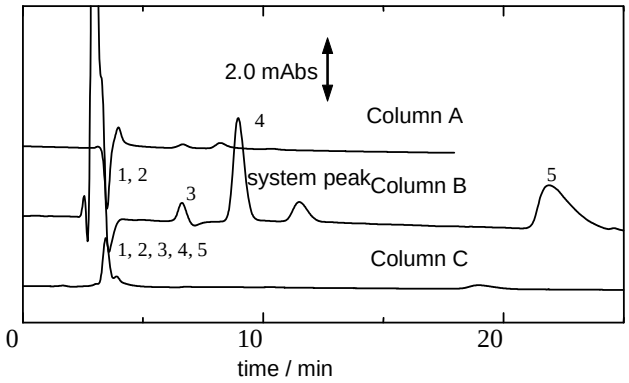

Fig. 4 Separation of anions (1.0 mM each of 1. IO_3^-, 2. BrO_3^-, 3. Br^-, 4. NO_3^-, 5. I^-), using 50 mM NaCl as the eluent for different methanol concentration. Column: as in Table 2. Other experimental conditions as in Figure 3.

Finally, the composition of column B was chosen and 10% 0.1 mol/L hydrochloric acid was added as acid catalyst for preparation of poly(GMA-EDMA)-arginine. The addition of acid catalyst in the solution resulted in more introduction of arginine on surface of epoxy group than without acid catalyst. The monolith poly (GMA-EDMA)-arginine has a good anion separation, as shown in Figure 5.

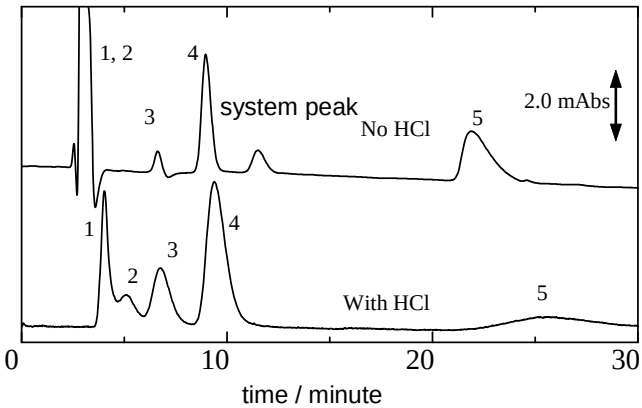

Fig. 5 Anion separation

Optimum temperature for poly(GMA-EDMA)-arginine column

Reaction temperature of polymerization is important for getting a good monolith column. The decrease of reaction temperature gives better performance for separation of 5 anions with iodide in the sample. Figure 6 shows the separation of 4 anions (IO_3^-, BrO_3^-, NO_2^-, NO_3^-) at different polymerization temperatures 60, 80 and 100°C, respectively. Lower temperature polymerization gave more arginine attached on the epoxy group of monomer, and could produce mesopore and macropore of monolith poly(GMA-EDMA)-arginine.

Effect of eluent cation on retention of anions

The positive charge of arginine as coated on poly(GMA-EDMA) works as the anion exchange site for separation of 5 anions. The retention behavior of 5 anions using aqueous solution with different cations as the eluent was evaluated. Different eluent cations gave the different elution time for anions. The retention of anions decreased if hydrated cation with smaller size was

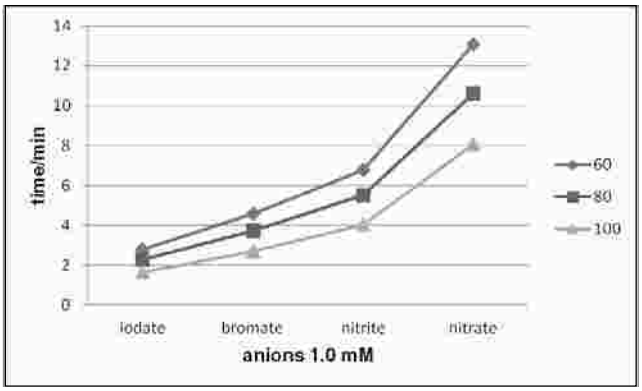

Fig. 6 Chromatograms for separation of anions (1.0 mM each of 1. IO_3^-, 2. BrO_3^-, 3. NO_2^-, 4. NO_3^-,) at 3 different polymerization temperatures. Operation condition; using 200 mM NaCl as the eluent at poly(GMA-EDMA)-arginine monolith column (100 x 0.32 mm i.d); UV detector at 210 nm; flow rate : 3 µL/min.

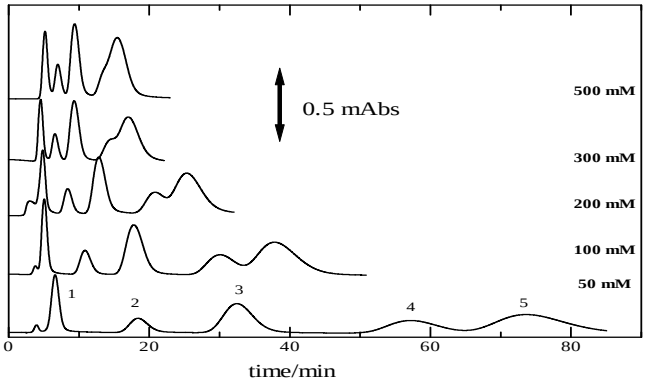

Fig. 7 Effect of eluent cation on the retention of anions (1.0 mM each of IO_3^-, BrO_3^-, NO_2^-, Br^-, NO_3^-,), using 200 mM each salt solution as the eluent. Other experimental conditions as in Figure 3.

used as the eluent. In this condition using monolith poly(GMA-EDMA)-arginine, sodium chloride (NaCl) showed better seperation of anions, but peaks of Br^- and NO_3^- were still overlapped. Logarithm of retention time of anions for some salt aqueous solution as NaCl, KCl, RbCl, CsCl, NH_4Cl, $MgCl_2$, $SrCl_2$ and $CaCl_2$ is shown in Figure 7. For the divalent cation i.e.. Mg^{2+}, the logarithm of retention time of anions was nearly the same as Ca^{2+} and Sr^{2+} although the Mg^{2+} has a smaller size than Ca^{2+} and Sr^{2+}. NaCl was chosen as the optimum salt

mobile phase for separation of anions using monolith poly(GMA-EDMA)-arginine, because it provides good anion separation than the other salt mobile phase, but Br^- and NO_3^- were not separated completely.

In order to find the optimum concentration of NaCl as eluent 50 mM, 100 mM, 200 mM, 300 mM and 500 mM were tried. Figure 8 shows the effect of NaCl concentration on the retention time, and that Br^- and NO_3^- were separated on the poly(GMA-EDMA)-arginine column by using lower concentration of NaCl as the eluent, leading to long time separation and peak broadening.

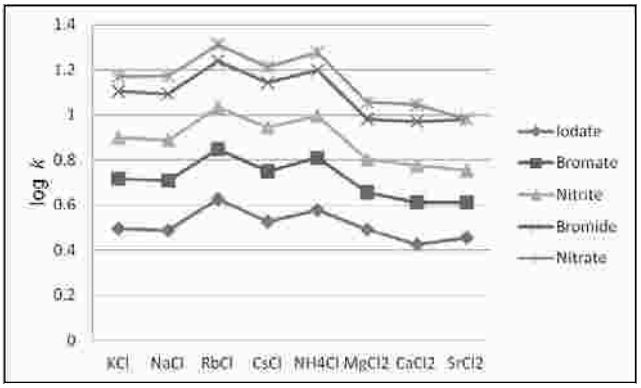

Fig. 8 Effect of NaCl concentration on separation of anions (1.0 mM each of 1. IO_3^-, 2. BrO_3^-, 3. NO_2^-, 4. Br^-, 5. NO_3^-,). Other experimental conditions as in Figure 3 except for the eluent concentration.

Effect of acid and organic solvent in the eluent

Poly(GMA-EDMA)-arginine was evaluated for separation of 5 anions using 200 mM NaCl as the eluent. Positive charge of arginine makes it work as the weak anion exchanger type. It seems that Br^- and NO_3^- did not separate completely. In order to investigate the hydrophobic property of amino acid monolith column, ACN was added in the mobile phase[30,31] and also hydrochloric acid. The addition of 5% 0.1 M HCl and 10% acetonitrile in the mobile phase slightly decreased retention time of 5 anions. Both of them could not solve the problem and separation of Br^- and NO_3^- on poly(GMA-EDMA)-arginine monolith column was not complete,

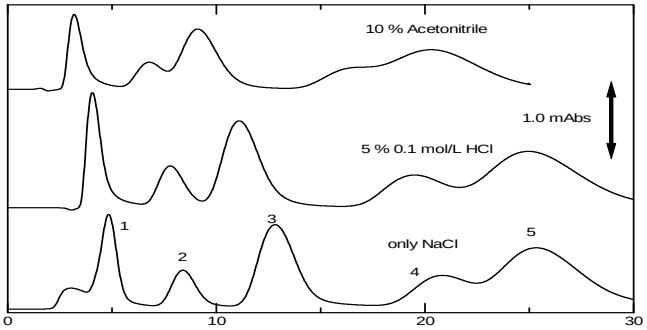

Fig. 9 Chromatograms for separation of anions (1.0 mM each of 1. IO_3^-, 2. BrO_3^-, 3. Br^-, 4. NO_3^-, 5. I^-), using 200 mM NaCl eluent with acetonitrile and HCl effect. Other experimental conditions as in Figure 3.

as shown in Figure 9 unlike crown ether bonded column in capillary IC.[32]

Effect of phosphate buffer as mobile phase

Since the pl of arginine is 10.76, the amine columns are expected to be positively charged under pH lower than pl. In this study, phosphate buffer at pH 6.8 was used to increase the anion interaction on the amine column with lower ion capacity.[33] The result was not successful because the retention time of 5 anions under optimum NaCl concentration became longer without using phosphate buffer as the mobile phase. This may be because the pH of NaCl solution without the buffer is lower than 6.8 leading to less protonation of poly(GMA-EDMA)-arginine with phosphate buffer and the elution strength of the eluent increased, which means selectivity of column also deteriorated by using phosphate buffer, as shown in Figure 10.

Characterization of poly(GMA-EDMA)-arginine monolith column

Parameters of any chromatographic column for discussing characteristics of polymer monolith column are its permeability (controlled by the average size of its through pores and by its external porosity), its efficiency (controlled by the average sizes of its domain and ion exchange capacity), theoretical plates and SEM analysis. In this section, we will discuss the structure

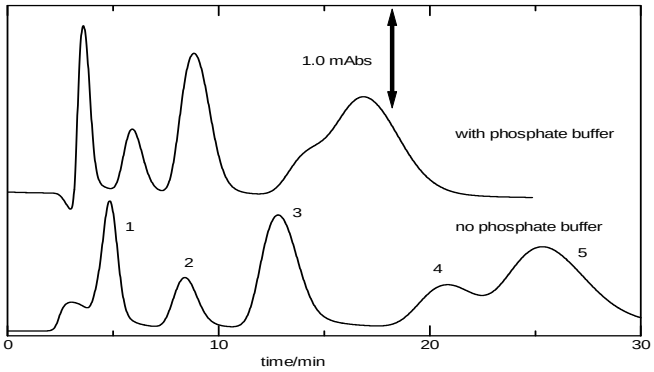

Fig. 10 Chromatograms for separation of anions (1.0 mM each of 1. IO_3^-, 2. BrO_3^-, 3. Br^-, 4. NO_3^-, 5. I^-), using 200 mM NaCl eluent with or without 0.1 mol/L phosphate buffer. Other experimental conditions as in Figure 3.

and performance of poly(GMA-EDMA)-arginine monolith column prepared for IC.

To force the percolation of a stream of mobile phase at constant velocity through a porous bed e.g., a chromatographic column, a certain pressure, ΔP, must be maintained at the column inlet. The flow rate of 75% methanol as mobile phase was evaluated versus inlet pressure on poly(GMA-EDMA)-arginine column. The flow rates 0.5, 1.0, 2.0, 3.0, 4.0 and 5.0 µL/min were evaluated, as shown in Figure 11.

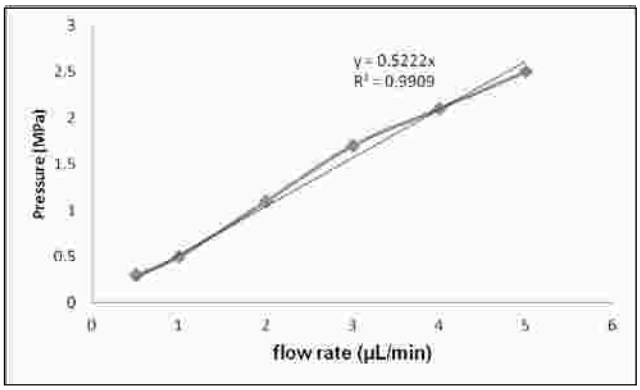

Fig. 11 Relationship between flow rate and inlet pressure using 50 % methanol eluent. Other experimental conditions as in Figure 3.

Figure 11 shows that increase of flow rate of mobile phase results in the increase of pressure. This shows that the permeability of the poly(GMA-EDMA)-arginine monolith is good, because the linearity of plot of flow rate versus pressure is nearby one. This result indicated that the poly(GMA-EDMA)-arginine organic monolith column could be used for a fast, efficient analysis at a higher flow rate and less pressure. The permeability of poly(GMA-EDMA)-arginine is 1.9 x 10^{-14} m^2, and its values are in the range 0.15 to 8.14x10^{-14} m^2.[34] for polymer methacrylate base monoliths.

The relative standard deviations (RSD) of retention time, peak height and peak area of four anions were calculated under the same operating conditions. The results of this condition are provided in Table 3. The relative standard deviations for n = 7 were less than 5% for all the analyte anions. These values show the poly(GMA-EDMA)-arginine monolith column has a good repeatability.

Table 3. Relative standard deviation of retention time, peak area and peak height.

RSD (%) n = 7			
	Retention	Peak Area	Peak Height
IO_3^-	1.67	2.81	1.29
BrO_3^-	1.48	2.32	1.89
NO_2^-	1.47	1.49	0.96
NO_3^-	1.58	2.05	1.30

Due to their porous characteristics, they could be used in different processes, such as stationary phase for different types of chromatography. In this study, the morphology of the poly(GMA-EDMA)-arginine monolith column was evaluated with SEM. In this monolith column, isopropanol was used as a porogen solvent to produce the mesopores and decanol was used to produce the throughpores in the polymer, and could give the best flow-through characteristic,[35] as shown in Figure 12.

Fig. 12 SEM images of poly(GMA-EDMA)-arginine monolithic column prepared with organic solvent under acidic condition with the optimum condition polymerization.

Standard calibration curve

Under the optimum operation conditions for separation of four anions, the linearity of concentration versus peak area was evaluated with standard calibration curve. The concentration of anions (IO_3^-, BrO_3^-, NO_2^-, NO_3^-) were 0.05 mM, 0.1 mM, 0.2 mM, 0.5 mM and 1.0 mM each, respectively. The relative coefficient is approximately one, which means that the method has an excellent linearity, as shown in Figure 13.

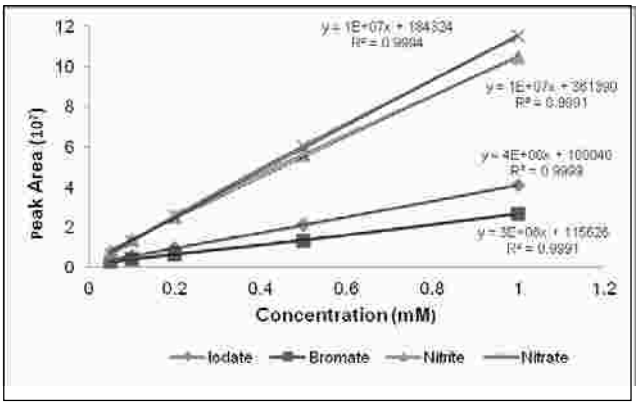

Fig. 13 Calibration curve of anions for optimum condition reaction using 200 mM NaCl eluent. Other experimental conditions as in Figure 3.

Application to real samples

For the evaluation of ability of this method, the river water samples were collected in Gifu prefecture, and were called river 1, 2 and 3, and then used as sample application. The water samples were filtered through a 0.45 µm membrane filter for IC. By using optimum operation condition, nitrate concentration determined in the river water sample 2 was 1.68 ppm and river water sample 3 was 1.8 ppm, as shown in Figure 14.

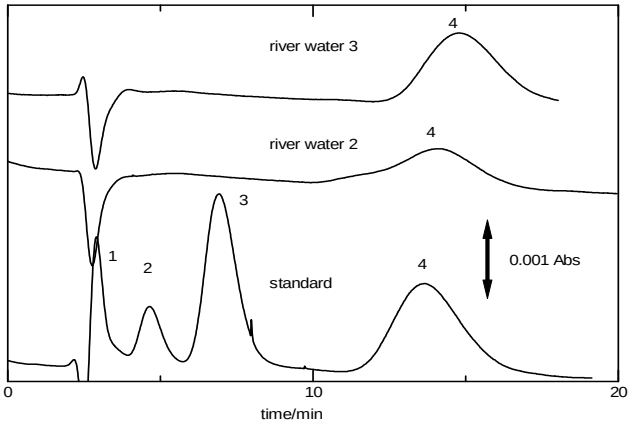

Fig. 14 Separation of anions contained in river water samples. Operation condition as in Figure 6.

Conclusions

Polymethacrylate based anion-exchange monolithic columns were prepared by thermal copolymerization of GMA as monomer, EDMA as crosslinker using binary porogenic solvents in the fused silica capillary with diameter of 0.32 mm. In this work, L-arginine was dissolved in organic solvent and was attached on the surface polymer using hydrochloric acid as catalyst. Poly(GMA-EDMA) modified with 250 mM arginine was optimised for the separation of anions with 200 mM NaCl in the 0.1 M phosphate buffer as eluent. This method has been successfully applied for the separation of four anions such as IO_3^-, BrO_3^-, NO_2^-, NO_3^- with good linearity and excellent repeatability.

References

1. Jiang, H., Yuan, H., Qu, Y., Liang, Y., Jiang, B., Wu, Q., Deng, N., Liang, Z., Zhang, L. and Zhang., Y., 2016, *Talanta*, **146**, 225.
2. Li, Q., Lu, C. and Liu, Z., 2013, *J. Chromatogr. A.*, **1305**, 123.
3. Wei, Y., Huang, X., Liu, R., Shen, Y. and Geng, X., 2006, *J. Sep. Sci.*, **29**, 5.
4. Zatirakha, A.V., Smolenkov, A.D. and Shpigun, O.A., 2016, *Anal. Chim. Acta*, **904**, 33.
5. Currivan S. and Jandera, P., 2014, *Chromatogr.*, **1,** 24.
6. Guihen E. and Glennon, J. D., 2004, *J. Chromatogr. A.*, **1044**, 67.
7. Guiochon, A., 2007, *J. Chromatogr. A.*, **1168**, 101.
8. Aydogan, C., 2015, *J. Chromatogr. A.*, **1392**, 63.
9. Zou, H., Huang, X., Ye, M. and Luo, Q., 2005, *J. Chromatogr. A.*, **954**, 5.
10. Lin, Z., Tan, X., Yu, R., Lin, J., Yin, X., Zhang, L. and Yang, H., 2014, *J. Chromatogr. A.*, **1355**, 228.
11. Wei, Y., Huang, X., Liu, R., Shen, Y. and Geng, X., 2006, *J. Sep. Sci.*, **29**, 5.
12. Wang, X., Zheng, Y., Zhang, C., Yang, Y., Lin, X., Huang, G. and Xie, Z., 2012, *J. Chromatogr. A.*, **1239**, 56.
13. Sugrue, E., Nesterenko, P.N. and Paull, B., 2005, *J. Chromatogr. A.*, **1075**, 167.
14. Watanabe, Y., Ikegami, T., Horie, K., Hara, T., Jaafar, J. and Tanaka, N., 2009, *J. Chromatogr. A.*, **1216**, 7394.
15. Zhang, F., Li, Y., Guo, Z., Liang, T., Yang, B., Zhou, Y. and Liang, X., 2011, *Talanta*, **85**, 112.
16. Chuang, S.C., Chang, C.Y. and Liu, C.Y., 2004, *J. Chromatogr. A.*, **1044**, 229.
17. Bayramoglu, G., Bitirim, V., Tunali, Y., Arica, M.Y. and Akcali, K.C., 2013, *Mat. Sci. Eng. C.*, **33**, 801.
18. Ou, J., Lin, H., Zhang, Z., Huang, G., Dong, J. and Zou, H., 2013, *J. Electrophor.*, **34**, 126.
19. Xu, H., Xu, Z., Yang, L. and Wang, Q., 2011, *J. Sep. Sci.*, **34**, 2314.
20. Guihen E. and Glennon, J. D., 2004, *J. Chromatogr. A.*, **1044**, 67.
21. Nesterenko, E.P., Nesterenko, P. N. and Paull, B., 2009, *Anal. Chim. Acta*, **652**, 3.
22. Lubbad S.H. and Buchmeiser, M.R., 2010, *J. Chromatogr. A.*, **1217**, 3223.
23. Giri, A., Goswami, N., Lemmens, P. and Pal, S.K., 2012, *J. Mat. Res.*, **47**, 1912.
24. Li, D., li, Y., Li, X., Bie, Z., Pan, X., Zhang, Q. and Liu, Z., 2015, *J. Chromatogr. A.*, **1384**, 88.
25. Carreto, J. I., Carignan, M.O. and Montoya, N.G., 2005, *M. Biol.*, **146**, 237.
26. Monzo, A., Rejtar, T., Guttman, A., 2009, *J. Chromatogr. Sci.*, **47**, 467.
27. Tasfiyati, A.N., Iftitah, E.D., Sakti, S.P. and Sabaruddin, A., 2016, *Anal. Chem. Res.*, **7**, 9.
28. Tischer, A., Lilie, H., Rudolph, R. and Lange, C., 2010, *J. Protein Sci.*, **19**, 1783.
29. Paull, B., Nesterenko, P.N., 2005, *TrAC.*, **24**, 295.

30. Shediac, R., Ngola, S.M., Throckmorton, D.J., Anex, D.S., Shepodd, T.J. and Singh, A.K., 2001, *J. Chromatogr. A.*, **925**, 251.

31. Xu, H., Xu, Z., Yang, L. and Wang. Q. 2011, *J. Sep. Sci.*, **34**, 2314.

32. Takeuchi, T., Tokunaga, K. and Lim, L.W., 2013, *Anal. Sci.*, **29**, 423

33. Iverson, C.D., Gu, X. and Lucy, C.A., 2016, *J. Chromatogr. A.*, **1458**, 82

34. Moravcova, D., Jandera, P., Urban, J. and Planeta, J., 2004, *J. Sep. Sci.*, **27**, 789

35. Arrua, R.D., Strumia, M.C. and Igarzabal, C.I.A., 2009, *Materials.*, **2**, 2429.

RNI No. MAHENG/2017/74063
ISSN No. (Print) 2581-5911

Antimicrobial Poly(*N*-vinyl carbazole)/Carbon Multiwalled Nanotubes (PVK/MWNTs) CPN nanocomposite film as coatings on conducting surfaces

Karina Milagros Cui-Lim[1,2]
[1]Department of Physical Sciences, College of Science, University of Eastern Philippines,
[2]Research Office, University of Eastern Philippines,
Catarman N. Samar, 6400, PHILIPPINES
Email: karina_cui@yahoo.com

Abstract
*In this work, the preparation of poly(*N*-vinyl carbazole) (PVK) and carbon nanotubes (CNTs) or PVK/CNTs CPN nanocomposites film was carried out by an electrochemical approach. Solutions of the CNTs or multi-walled carbon nanotubes (MWNTs) with the PVK were prepared using mixed solvents aided by sonication which resulted in exfoliation and deaggregation of the MWNTs into the PVK polymer matrix. Cyclic voltammetry (CV) was carried out from spin-coated films of this homogeneous dispersion which resulted in the formation of a conjugated polymer network (CPN) nanocomposite film, i.e. anodic electro-polymerization or crosslinking of the carbazole units. The spectroscopic and electrochemical characteristics of the nanocomposites films were also analyzed using CV. FT-IR-ATR spectroscopy were used to prove the wrapping/cross-linking of MWNTs outer surfaces by the PVK polymer. The antibacterial property of the electrodeposited PVK/CNTs CPN films was then tested against* Escherichia coli *K12 MG1655 (*E. coli*).*

Keywords: *antibacterial coatings, PVK/CNTs CPN films, electropolymerized surfaces, conducting polymers, CNTs*

Introduction

Biofilm formation on conducting materials (metal, metal alloys, metal oxides, and electrodes) has emerged as a significant problem in the long-term use of bioimplants, biosensors, and marine and industrial instrumentations.[1-3] Strategies for controlling bacterial colonization have focused on improving and developing antimicrobial materials and designs to inhibit biofilm formation. Some examples of antimicrobial agents previoulsy used as surface coatings and showing reduced bacterial adhesion are antibiotics,[4-7] quaternary ammonium salts,[8] cationic peptides,[9] and metal ions[10]. However, problems related to the development of microbial resistance,[11] surface coating difficulties, and relatively high costs make these approaches unsuitable for antimicrobial coatings.

The incorporation of CNTs on conducting surfaces is an alternative method to prevent bacterial colonization. This extremely thin nanomaterial[12-14] has been reported to show promising antibacterial activity.[13,14] Furthermore, compared to other antibacterial surfaces, it is relatively cheap and possesses very high electrical conductivity, mechanical stiffness[15-17] and extraordinary electronic transport property[18-22]. Despite many advantages that it

has to offer, the investigation of CNTs as an antimicrobial coating film has not been established. To our knowledge, most of the antibacterial investigations were conducted either in solution [13] or as free-standing CNTs[14]. In the present study, we investigate the antimicrobial properties of coated surfaces with CNTs. At present, the major challenges of working with CNTs are its nondispersibility in either aqueous or organic solvents, direct immobilization on surfaces and processability which leads to the difficulty of working with CNTs. To address these issues, our group has developed a method of fabricating a more stable and well dispersed CNTs organic matrix composed of CNTs wrapped with poly(N-vinyl carbazole) (PVK) and consequently electrochemically cross-linked to form PVK/CNTs CPN nanocomposite film.[23] CNTs which is readily dispersible in cyclohexyl pyrrolidone (CHP) solvent and PVK on dichloromethane (DCM) on the other hand forms a pi-pi stacking interaction with CNTs that stabilizes the dispersion of the nanocomposite (NC) and creates a conducting polymer network (CPN) that can be immobilized and patterned on any conducting substrate via electrochemical methods.[24-30]

In this study, we present the immobilization of well dispersed CNTs on conducting surface as an antimicrobial coating. Specifically, we tethered PVK/CNTs nanocomposite via electrodeposition on indium tin oxide (ITO) and stainless steel substrate. Cyclic voltammetry (CV), attenuated total reflectance infrared (FTIR-ATR) spectroscopy, and atomic force microscopy (AFM) were used to monitor its deposition. The antibacterial property of the electrodeposited PVK/CNTs CPN films was then tested against *Escherichia coli* K12 MG1655 (*E. coli*).

Materials and Methods

Preparation of PVK/CNTs nanocomposite films

The preparation of the PVK/CNTs nanocomposite films were done according to previously reported procedure.[23] Indium tin oxide (ITO) (0.5 in x 0.5 in) was used as the substrate for PVK/CNTs nanocomposites and PVK/CNTs CPN film fabrication. The surface was first cleaned by sequentially sonicating in deionized water, isopropanol, hexane and toluene, each for 15 minutes and then dried in an oven or under a stream of N_2. A drop of PVK/CNTs solution (2 ug/mL PVK/0.06 ug/mL CNTs) was then spin-coated onto the substrate at 1500 rms for 60 seconds to deposit a film in surface. After the spin-coating deposition, the PVK/CNTs nanocomposite films were thoroughly dried in a vacuum oven for 24 hours at 70^0C to remove any solvent. Electrodeposition was accomplished by using cyclic voltammetry (Princeton Applied Research Parstat 2263) experiments with a three (3) electrode set-up from a solution of 0.1 M tetrabutyl ammonium hexafluoro-phosphate (TBAH) dissolved in acetonitrile (ACN). The coated ITO surface was used as the working electrode (WE), Pt wire as the counter electrode (CE) and Ag/AgCl as the reference electrode (RE). Electrochemical cross-linking of PVK and GO was accomplished by repeatedly cycling an electrode potential between the limits 0 to 1.4 V for up to 50 cycles at a potential scan rate of 50 mV/s. The CPN film being insoluble in ACN solvent was thoroughly washed with ACN and was dried in nitrogen before the analysis of the film to remove excess PVK.

Surface Characterizations

Atomic Force Microscopy: The morphology before and after electropolymerization of PVK/CNTs on ITO glass substrates were characterized by AFM. Atomic force microscopy (AFM) imaging was done under ambient conditions with a PicoSPM II (PicoPlus, Molecular Imaging - Agilent Technologies) in the Magnetic AC mode (MAC mode) using a magnetic field to drive a magnetically coated cantilever in the top-down configuration. Type II MAC levers with a spring constant of 2.8 nN/M with about 10 nm tip radius were used for all scans.

Attenuated Total Reflectance Fourier Transformed Infrared (ATR FTIR): The ATR FTIR spectra were

obtained on a Digilab FTS 7000 equipped with HgCdTe detector from 4000 to 600 (cm^{-1}). All spectra were taken with a nominal spectral resolution of 4 cm^{-1} in absorbance mode. All films were measured under ambient and dry conditions for several trials at different areas of the sample surface.

Antibacterial Measurements

Bacterial Culture: A single isolated *Escherichia coli* K12 MG1655 (*E. coli*) colony was inoculated in 5 mL Tryptic Soy Broth (TSB) overnight at 35°C. The bacterial culture was centrifuged at 3000 rpm for 10 minutes, and the bacteria pellet was resuspended in TSB. The optical density of the suspension was adjusted to 0.5 at 600 nm, which corresponds to a concentration of 10^7 colony forming units per milliliters (CFU/mL).

Treatment of samples with bacterial culture: Aliquots of 180 µL of bacterial suspensions (10^7 CFU/mL) were placed in an Eppendorf tube containing 20 µL of sample (CNTs, PVK/CNTs, and pure PVK) at different concentrations in DI water (1000 µg/mL, 500 µg/mL, 100 µg/mL). Control samples contained 180µL of bacterial suspensions with 20 µL of DI water. The tubes were shaken at 50 rpm for 1 hour at room temperature.

Antimicrobial Activity determined by growth curve measurements: The antimicrobial property of CNTs, PVK/CNTs, and pure PVK samples were evaluated by examining the bacterial growth curves via OD_{600} after 1 hour exposure to these materials [31]. The mixtures of bacteria and samples were transferred into 5 mL TSB broth, and incubated at 37°C. Bacterial growth was monitored by measuring the OD_{600} after every hour using Spectrophotometer (Perkin Elmer, Place). The OD curves were generated by plotting the OD values versus growth time. The fast or slow increase in OD during the incubation represents the ability of *E.coli* to survive and grow in the presence of the different nanomaterials.

Antibacterial measurements on stainless steel substrates: PVK/CNTs CPN film, PVK, CNTs-modified films and unmodified ITO substrate were individually placed in a 12 well-plate (Falcon). To each well was added 1.0 mL of bacterial culture and then incubated at 37°C (without shaking) for 2 hours. The samples were then removed and immediately prior to viewing were stained for 10 minutes with 3.0 µL of L 7007 Life-dead stain solution, obtained from Molecular Probes (Leiden, The Netherlands), containing a green fluorescent dye (Syto 9) marking viable bacteria cells and red fluorescence dye (PI) for detection of dead cells. The surfaces were placed in microscope slides, covered with a cover slip and imaged using BX 51 Olympus Fluorescent Microscope equipped with a DP72 digital camera under 100 *x* objective. All images were acquired and analyzed using cell Sens Dimension software. Percent dead was expressed as the percent of the ratio of the total number of dead cells to the total number of bacteria attached.

Results and Discussion

The preparation of the PVK/CNTs nanocomposite film was carried out by electrodeposition on the ITO interface. Figure 1 shows the CV plot monitoring the immobilization of PVK/CNTs on the surface. Figure 1, shows the cyclic voltammograms of pure PVK scanned at 50 mV/s for 50 cycles and PVK/MWNTs films at different scan rates in order to cross-link the PVK film forming the CPN film.[31] For pure PVK, an irreversible oxidation peak at about 0.9-1.0 V and reduction peak at 0.7 V were observed in the voltammogram which suggest the formation of the carbazolylium radical cation, and a cross-linked material having a higher electrical conducting behaviour compared to the PVK precursor. This essentially represents the formation of a CPN control film. The shapes of the voltammogram were clearly different when the MWNTs were added to the electrochemically cross-linkable PVK. A downshift in the reduction peak was observed for PVK/MWNTs and this could be due to the doping behaviour of the negatively charged MWNTs. No anodic peak was observed regardless of the number of cycles employed on the PVK/MWNTs film deposited in ITO glass substrate.

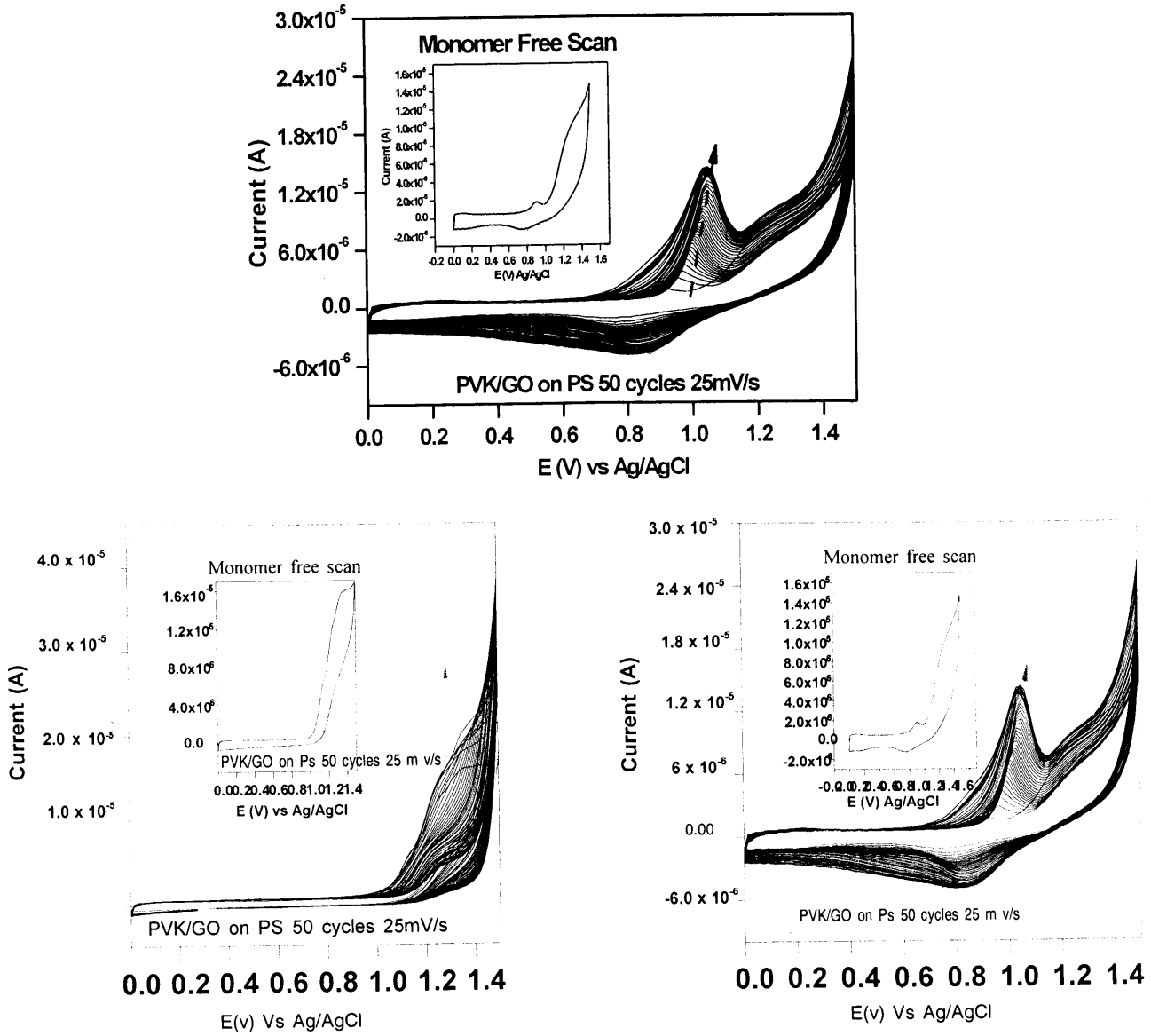

Fig. 1: Cyclic voltammograms of the pure PVK and PVK/CNTs CPN nanocomposite film. The inset is the monomer free scan CV data for the pure PVK and PVK/CNTs.

FTIR-ATR was used to verify the presence of the electrodeposited PVK/CNTs on ITO. The FTIR-ATR spectra for the PVK and PVK/CNTs modified surfaces are depicted in Figure 2. For the electropolymerized pure PVK, assignment of the main absorption peaks are as follows: 3100 cm^{-1} (aromatic C-H stretch), 2900- 3000 cm^{-1} (aliphatic C-H stretch from the polymer backbone), 1600 cm^{-1} (C=C stretching), 1226 cm^{-1} (C-N stretching of vinyl carbazole), 1100-1150 cm^{-1} (in plane –C-H aromatic), and 700-800 cm^{-1} (out of plane –C-H aromatic). While all these peaks were observed on the PVK/CNTs CPN nanocomposite film, the presence of interaction on the surface was verified by the appearance of a slight shift of the peaks from 1600 to 1610 cm^{-1} and 1226 to 1230 cm^{-1} which could be due to the interaction between the PVK and CNTs CPN nanocomposite.

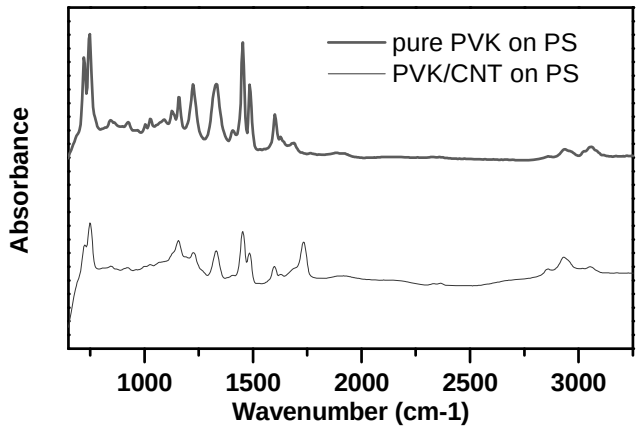

Fig, 2: FTIR-ATR analysis pure PVK and PVK/CNTs CPN nanocomposite film.

The homogeneity of the deposited film was determined by Atomic Force Microscopy (AFM) (Figure 3). The electrodeposited films (PVK and PVK/CNTs) revealed excellent well defined surface coverage with a root mean squared (rms) value of 3.45 nm and 6.23 nm for the PVK and PVK/CNTs, respectively. The average grain size was about 160 nm typical of the grain size observed for the presence of PVK on the surface.[27]

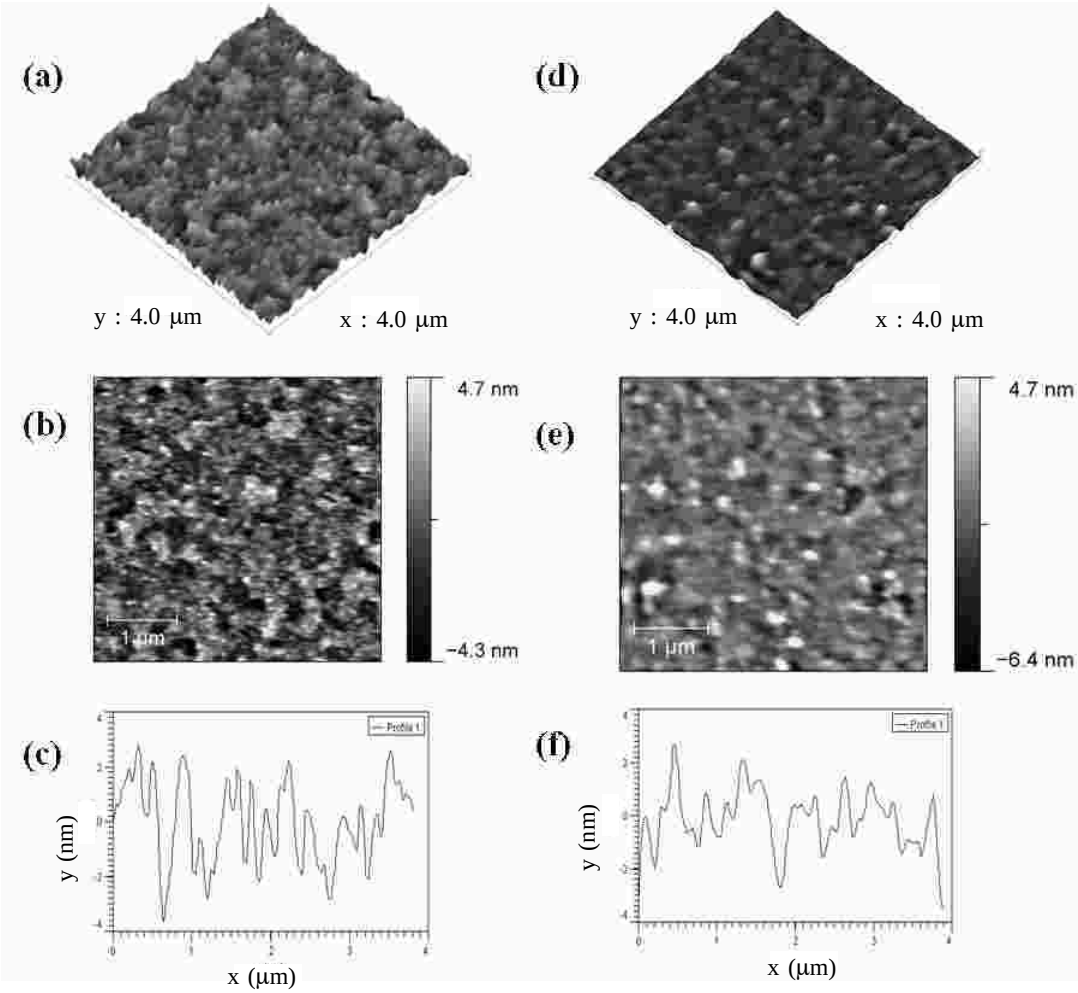

Fig. 3: AFM (a,d) topography,(b, e) phase and (c,f) line profile measurements of PVK/CNTs CPN nanocomposite film (a, b, c) and pure PVK (d, e, f). Note: CV deposition at 0V-1.5V, 50 mV/s, 50 cycles.

Prior to testing bacterial toxicity on modified surfaces, the antibacterial property of the nanocomposite, PVK/CNTs, CNTs, and pure PVK were evaluated by incubating each solution with *E. coli* cells for 1 hour. The growth curves of bacterial-treated with PVK/CNTs CPN nanocomposite film, CNTs and PVK samples were examined via optical density (OD) measurements, which correspond to the number of live cells that are able to grow after 1 hour of exposure to the samples. In general, compared to the control, samples containing CNTs were observed to be antibacterial. This was shown by the low OD values observed for all measured samples (Figure 4A). To evaluate the antimicrobial effectiveness of the different nanomaterials, we measured for each of the growth curves the time required to reach 10^7 CFU/mL, which corresponds to an OD_{600} of 0.5. All the CNTs-containing samples took longer time to reach OD of 0.5 as compared to the untreated samples (control) and the pure PVK samples (Figure 4B). CNTs is already known to be toxic to bacteria,[13,14] however, the addition of PVK resulted in an increased dispersion of CNTs in the solution [23] providing a greater aspect ratio, thereby resulting in an increased interaction with the bacteria and higher toxicity.

After testing the antibacterial properties of the composites in solution, we tested the effects of modified films

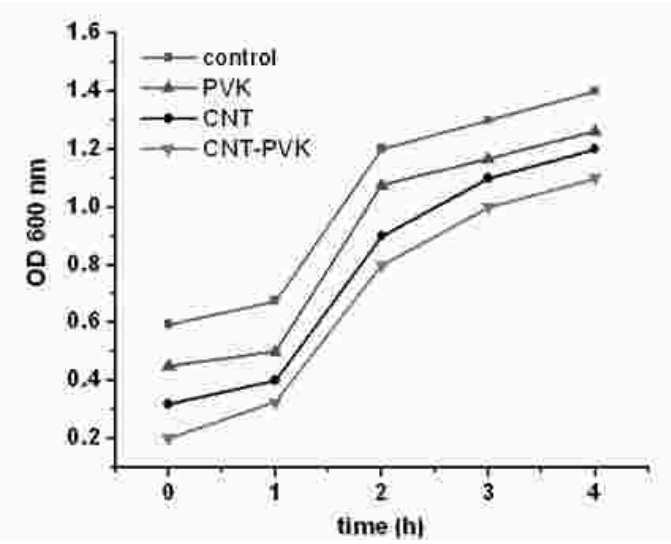

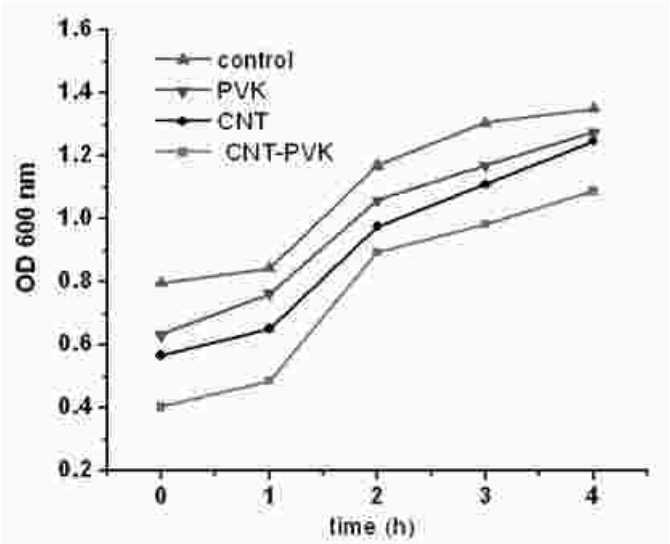

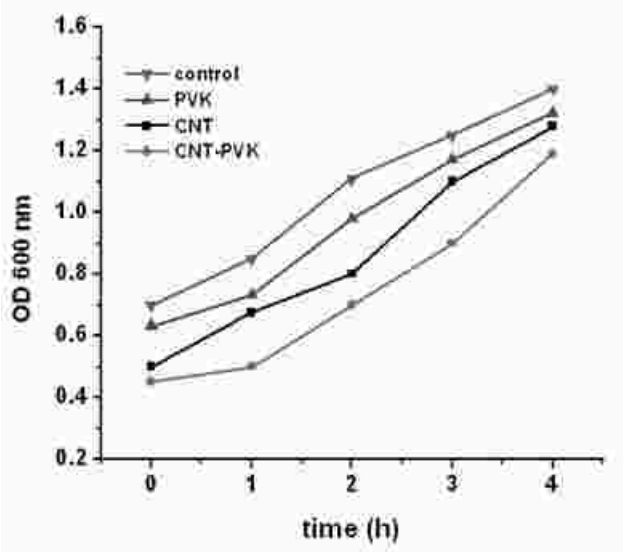

Fig. 4: (a) OD growth curves of E. coli cells (10^7 cfu/mL) that were exposed to CNTs, PVKCNTs nanocomposite, and pure PVK at different concentration for 1 h prior to their growth on TSB. (b) The time required by the bacteria to reach an OD_{600} nm of 0.5 for samples treated with each of the above conditions

of PVK, PVK/CNTs, and CNTs on *E. coli*. *In situ* live-dead staining of the bacterial organisms attached to the differently modified surfaces were performed to determine the ratio of dead bacteria versus the total number of bacteria. SYTO 9 dye was used to show both the live and dead cells, while the dead bacteria with compro-

mised membranes were stained only by propidium iodide (PI). Fluorescence images of the surface reveal that after incubation almost similar number of total bacteria was adsorbed on each of the surface (Figure 5). However a more pronounced antibacterial activity was observed for the CNTs-modified surfaces than the unmodified and PVK films. In fact, the PVK/CNTs and CNTs-modified surfaces were successful in inactivating *E. coli* by approximately 85% and 90%, respectively. This result showed that CNTs remained effective even after surface immobilization. It is worth noting that the addition of PVK did not hinder its efficacy but showed an enhanced bacterial toxicity than the CNTs alone. We suggest that the improved dispersion caused by the presence of PVK led to the results observed.

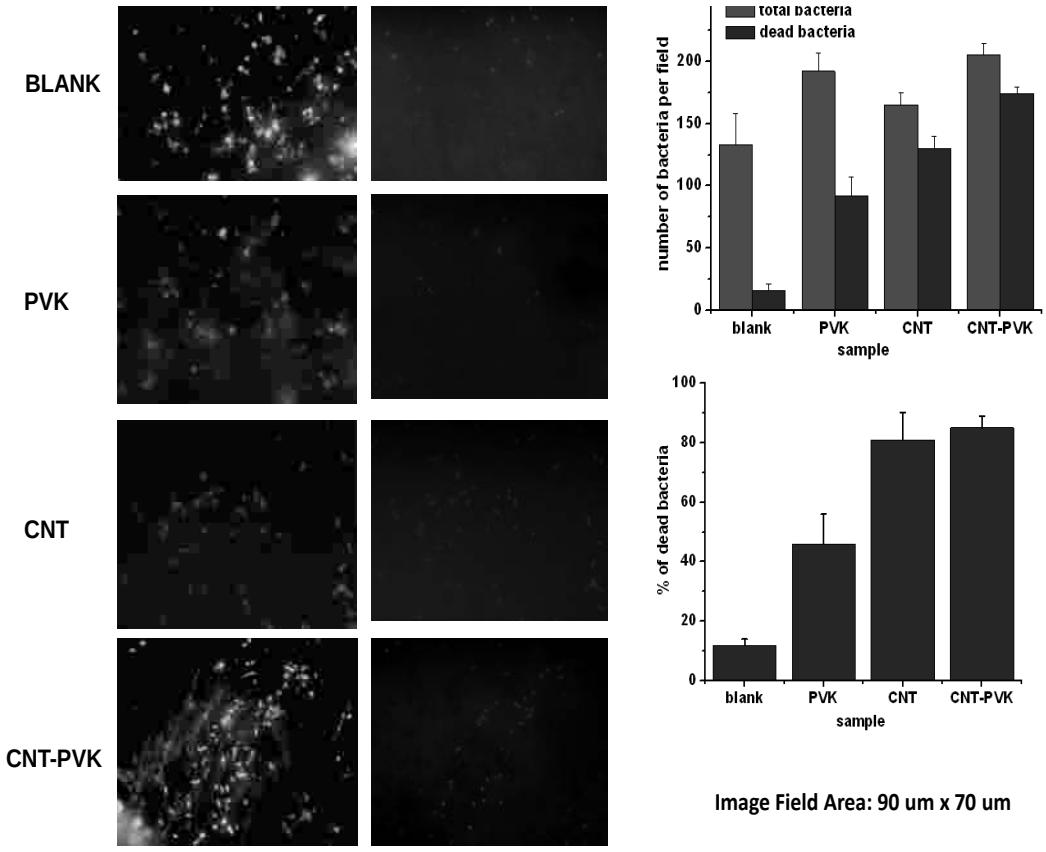

Fig. 5: Fluorescence images of the *E. coli* on (a) unmodified ITO, (b) electrodeposited PVK, (c) spin-coated CNTs, and (d) electrodeposited PVK/CNTs films. Images were obtained with a 100x oil immersion objective using a FITC filter for green fluorescence from SYTO 9 in all bacteria presented on the left column and a TRITC filter for red fluorescence from PI in membrane-compromised bacteria presented on the right column. (e) Plot of the total number of bacteria (green) and among them the number of PI-positive bacteria (red) on the field of view (90×70 ìm^2), which were adsorbed on the modified surfaces. The blank is the unmodified ITO substrate as the control. (f) Correlation of the % non-viable E. coli (% PI-positive) attached on each of the surfaces. Note: Data were expressed as the mean number of bacteria ± standard deviation of four experiments (4 replicates prepared at 2 different times).

Conclusions

We have presented the antibacterial property of a PVK/CNTs electropolymerized nanocomposite on ITO surface and steel substrate. We fabricated an alternatively simple, but robust antimicrobial coating that can be applied on any electrically conducting substrates. The inclusion of PVK allowed the immobilization of a well-defined and homogeneous film via electropolymerization on the ITO surface. Antibacterial properties of the CNTs-containing films and solutions resulted in increase bacterial inactivation, relative to the control. Even in the presence of PVK, the nanocomposite maintained its bacterial toxicity. This result shows the potential of the PVK/CNTs nanocomposite to be used as a useful and alternative antimicrobial coating for conducting materials that are widely used in biomedical and industrial fields.

Acknowledgement

The author would like to thank the College of Science and the University Research Office, University of Eastern Philippines, Philippines for support.

References

1. Donlan, R. M., 2001, *Emerg. Infect. Dis.*, **7**, 277.
2. Pavithra, D. and Doble, M., 2008, *Biomed. Mater.*, **3**.
3. Cole, N., Hume, E. B. H., Vijay, A. K., Sankaridurg, P., Kumar, N. and Willcox, M. D. P., 2010, *Invest. Opthalmol. Visual Sci.*, **51**, 390.
4. Darouiche, R.O., Raad, I. I., Heard, S. O., Thornby, J. I., Wenker, O. C., Gabrielli, A., Berg, J. and Khardori, N., 1999, *N. Engl J. Med.*, **340**, 1.
5. Kamal, G. D., Pfaller, M. A., Rempe, L. E. and Jebson, P. J., 1991, *J.A.M.A.*, **265,** 2364.
6. Bach, A., Darby, D., Bottiger, B., Bohrer, H., Motsch, J. and Martin, E., *Int. Care Med.* **122**, 1066.
7. Thornton, J., Todd, N. J. and Webster, N. R., 1996, *Anaesthesia*, **51**, 1018.
8. Ravikumar, T., Murata, H., Koepsel, R. R. and Russel, A. J., 2006, *Biomacromolecules*, ***7,*** 2762.
9. Gabriel, M., Nazmi, K., Veerman, E. C., Amerongen, A. V. N., Zentner, A., 2006, *Bioconjugate Chem.*, **17**, 548.
10. Maki, D.G., Cobb, L., Garman, J.K., Shapiro, J.M., Ringer, M. and Helgerson, R.B., 1988, *Am. J. Med.*, **85**, 307.
11. Neu, H.C., 1992, *Science*, **257,** 1064.
12. Geim, A. K. and Novoselov, K. S., 2007, *Nat. Mat.*, **6,** 183.
13. Akhavan, O. and Ghaderi, E., 2010, *ACS Nano*, **4,** 5731.
14. Hu, W., Peng, C., Luo, W., Lv, M., Li, X., Li, D., Huang, Q. and Fan, C., 2010, *ACS Nano*, **4,** 4317.
15. Lee, C., Wie, X. and Kysar, J. W. and Hone, J., 2008, *Science*, **321**, 385.
16. Stankovich, S., Dikin, D. A., Dommett, G. H. B., Kohlhaas, K. M., Zimney, E. J., Piner, R. D., Nguyen, S. T. and Ruoff, R. S., 2006, *Nature*, **442,** 282.
17. Baladin, A. A., Ghosh, A., Bao, W., Calizo, I., Teweldebrhan, D., Miao, F., Lau, C. N., 2008, *Nano Lett.*, **8**, 902.
18. Novoselov, K. S., Geim, A. K., Morozov, S. V., Jiang, D., Zhang, Y., Dubunos, S. V., Grigorieva, I. V. and Firsov, A. A., 2004, *Science*, **306**, 666.
19. Novoselov, K. S., Geim, A. K., Morozov, S. V., Jiang, D., Katsnelson, M. I., Grigorieva, I. V.,

Dubunos, S. V. and Firsov, A. A., 2005, *Nature*, **438**, 197.

20. Zhang, Y., Tan, Y.-W., Stormer, H. L., Kim, P., 2005, *Nature*, **438**, 201.

21. Geim, A. K., 2009, Science, **324**, 1530.

22. Li, D., Muller, M. B., Gilje, S., Kaner, R. B., Wallace, G. G., 2008, *Nat. Nanotechnol.*, **3**, 101.

23. Cui, K. M., Tria, M. C., Pernites, R., Binag, C. A. and Advincula, R. C., 2011, submitted.

24. Xia, C., and Advincula, R. C., 2001, *Chem. Mater.*, **13**, 1682.

25. Baba, A., Onishi, K., Knoll, W., Advincula, R. C., 2008, *J. Phys. Chem. B.*, **108**, 18949.

26. Taranekar, P., Fulghum, T., Baba, A., Patton, D., Ponnapati, R. and Clyde, G., 2007, *J. Am. Chem. Soc.*, **129**, 12537.

27. Fulghum, T., Taranekar, P. and Advincula, R. C., 2008, *Macromolecules*, **41**, 5681.

28. Xu, Y., Bai, H., Lu, G., Li, C. and Shi, G., 2008, *J. Am. Chem. Soc.*, **130**, 5856.

29. Stankovich, S.; Piner, R. D.; Nguyen, S. T.; Ruoff, R. S., 2006, *Carbon*, **44**, 3342–3347.

30. Bourlinos, A. B., Gournis, D., Petridis, D., Szaboì, T., Szeri, A., and Deìkaìny, I., 2003, *Langmuir*, **19**, 6050.

31. Yang, C., Mamouni, J., Tang, Y. and Yang, L., 2010, *Langmuir*, **26**, 160.

RNI No. MAHENG/2017/74063
ISSN No. (Print) 2581-5911

Kinetics and mechanism of oxidation of D-xylose and D-arabinose by N-Bromonicotinamide

L. Pushpalatha
Postgraduate and Research Department of Chemistry,
National College, Trichy – 620 001, Tamil Nadu, India.
E-mail : lathaa_ramesh@yahoo.com

Abstract
Kinetic investigation of oxidation of D-xylose and D-arabinose, by aqueous alkaline solution of N-Bromonicotinamide (NBN) has been carried out in the temperature range 308-328K.The reaction shows first order with respect to [alkali] and [substrate] and zero order with respect to oxidant. Addition of Nicotinamide (NA) has no effect on the rate of oxidation Increase in ionic strength of the medium does not change the rate. Effect of temperature on the rate of oxidation has been studied to show the validity of Arrehenius equation and various activation parameters have been computed. The stoichiometry of the reaction was found to be 1:1. 1,2-enediol was found to be the reactive intermediate. Xylonic acid and arabinonic acid were the products of oxidation for xylose and arabinose respectively.

Keywords: *Xylose, Arabinose, N-Bromonicotinamide, oxidation, mechanism.*

Introduction

The kinetics of oxidation of sugars has been the subject of extensive research in recent years. This is attributed to the economic and biological importance of carbohydrates to living organisms. The oxidations have been carried out in both acidic and alkaline media using oxidants as transition metal ions, inorganic acids, organometallic complexes and enzymes. Carbohydrates are a major sources of energy for living organisms and understanding of the oxidation of sugars is therefore of immense importance. The oxidation of sugars especially the mono and disaccharides has been the subject of extensive research. Sugar oxidation occurs under different conditions of pH, temperature and ionic strength giving products that depend on the oxidants used. The kinetics and mechanism of oxidation of monosaccharides and disaccharides have been studied in both acidic and alkaline media, employing different transition metal ions, inorganic acids, complex ions and hydrogen peroxide as oxidants. The results show that the mechanism may depend on the nature of the substrates, in some cases it involves the formation of intermediate complex, free radical or transition states.

Mukhtar Singh[1] reported the apparent molar volumes and viscosities of mono and disaccharides in water and in (DMF+water) mixed solvent systems at 293.15, 303.15 and 313.15K.

Sheila Srivastava[2] investigated the kinetics of Ru(III) catalysed oxidation of galactose and cyclopentanol by potassium bromate in alkaline medium.

H. K. Okoro[3] and E. O. Odebunmi reported the kinetics and mechanism of oxidation of sugar and sugar alcohols by potassium permanganate.

Katre Yokraj[4] followed the micelle catalyzed oxidation of mannose by N-bromophthalimide in the presence of sulfuric acid.

N-halo reagents like N-halo derivatives of amines, amides, imides, urea, saccharins, sulfonamides, sulfonimides are widely used in organic synthesis for their potential to promote important reactions such as halogenation, oxidation, and protection as well as formation of C-X, C-O, and C=O bonds. They play a key role in the chemistry of natural compounds. N-Bromonicotinamide(NBN) is chosen as oxidant for its easy method of synthesis, easy handling, higher rate of oxidation, longer shelf life and versatility.

Our earlier study on the oxidation of amino acids had focused attention on the kinetic aspects of oxidation by NBN[5] in aqueous acetic acid medium.

In our continuing efforts to exploit NBN as oxidant, the present study investigates the kinetics of oxidation of xylose and arabinose in aqueous alkaline medium.

Materials and Methods

N-Bromonicotinamide (NBN) was prepared by the reported method[6]. Standard solution of NBN(m.p.210°C) was prepared afresh in water and its purity was checked iodometrically. The standard solutions of xylose and arabinose(Aldrich) were always prepared afresh in double distilled water. The other chemicals used were sodium hydroxide, sodium perchlorate, mercuric acetate etc. All chemicals used were of A.R. grade. Mercuric acetate was added to suppress the formation of free bromine which otherwise would have vitiated the results. Mercuric acetate did not interfere with the results[5]. Ionic strength of the medium was kept at 0.1 mol dm^{-3} by employing concentrated aqueous solution of sodium perchlorate (Merck).

Kinetic measurements

The solution of substrates (xylose and arabinose)and oxidant were kept in black coated bottles separately. These solutions were kept in the thermostat to attain the thermostatic temperature. The appropriate quantity of oxidant was added to the substrate containing other reagents and the reaction bottle was shaken well. The reaction was followed potentiometrically by setting up a cell made up of the reaction mixture into which platinum electrode and reference electrode (SCE) were dipped. The e.m.f. of the cell was measured periodically using a Equip-Tronics (EQ-DGD) potentiometer. Effects of concentrations of substrates (xylose and arabinose), oxidant (NBN), sodium hydroxide, sodium perchlorate and nicotinamide and temperature on the oxidation rate were studied. The reaction was carried out under pseudo-first order condition ([substrates] >>[NBN]). The pseudo-first order rate constants computed from the linear ($r^2 > 0.9990$) plots of log (E_t-E_∞) against time. Duplicate kinetic runs showed that the rate constants were reproducible within ±3%. The course of the reaction was studied for more than two half-lives.

Stoichiometry

N-Bromonicotinamide was taken in large excess as compared to xylose in different ratios. Reaction mixture containing xylose, sodium hydroxide and N-bromonicotinamide (in excess) were equilibrated for 42 hours at room temperature(~30°C). After the reaction was complete, the excess of NBN was determined iodometrically and indicated 1:1 stoichiometry. The overall stoichiometry of the oxidation reaction may be represented as

$$\underset{\text{Xylose(n=5)}}{C_nH_{2n}O_n} + NBN + H_2O \rightarrow \underset{\text{Xylonic acid}}{C_nH_{2n}O_{n+1}} + Br^- + NA$$

Similar procedure was done for arabinose, taking reaction mixture containing arabinose, sodium hydroxide and N-bromonicotinamide. 1:1 stoichiometry was observed. The overall stoichiometry of the oxidation reaction may be given as

$$\underset{\text{Arabinose (n=5)}}{C_nH_{2n}O_n} + NBN + H_2O \rightarrow \underset{\text{Arabinonic acid}}{C_nH_{2n}O_{n+1}} + Br^- + NA$$

Product analysis

In a typical experiment, a mixture of freshly prepared xylose (1 mol dm^{-3}) and NBN (1.5g, 0.2 mol dm^{-3}) was made up to 50 mL with water. The mixture was allowed to stand for 12 hours in the dark to ensure completion of the reaction. Similar procedure was carried out for arabinose. The products of oxidation were xylonic acid for xylose and arabinonic acid for arabinose. Nicotinamide was the by-product in both the cases. The products were identified by spot test analysis[7] and paper chromatography. The products were also identified by the following method: a little amount of the product was added to 1mL of 5% sodium bicarbonate solution. Evolution of carbon dioxide with effervescence indicated the presence of acidic group in the compound. Evidence for the formation of an enediol is furnished by observed ability of alkaline solution of carbohydrates to decolorize solution of 2,6-dichlorophenolindophenol.

Results and Discussion

The kinetic results for the oxidation of xylose and arabinose by N-Bromonicotinamide (NBN) can be summarized as follows. The kinetic studies were carried out under pseudo-first order conditions with [substrate] >> [NBN].

Effect of varying [oxidant]

The constancy of pseudo-first order rate constant at different [NBN] at constant [substrate] indicated that the reaction exhibits zero order with respect to the oxidant (Table 1).

Table 1 Effect of [NBN] on reaction rate

[substrate]=0.025 mol dm^{-3} [NaOH]=0.02 mol dm^{-3}, $[NaClO_4]$=0.1mol dm^{-3}, $Hg(CH_3COO)_2$=0.005 mol dm^{-3}, Temp. =308 K

[NBN] 10^4 moldm^{-3}	10^6 k_{obs} s^{-1}	
	Xyl	Ara
25	30.20	9.42
35	30.18	9.43
45	30.19	9.42
55	30.20	9.41
75	30.21	9.41

Effect of substrate

At constant $[OH^-]$ and [NBN], the plot of $\log(E_t - E\infty)$ (where E_t is the e.m.f. of the cell at time t and E_∞, the corresponding value at the completion of the reaction) vs time was linear, indicating a first order dependence of rate on [substrate]. The rate constant increases with the concentration of reducing sugar, proving that the reaction was of first order with respect to [substrate]. Both oxidations show same trend (Table 2) (Fig.1).

Table 2 Effect of [Substrate] on reaction rate

[NBN] = 0.0025 mol dm^{-3} [NaOH] = 0.02 mol dm^{-3}, $[NaClO_4]$ = 0.1mol dm^{-3}, $Hg(CH_3COO)_2$= 0.005 mol dm^{-3}, Temp.=308K

[Substrate] 10^3 moldm^{-3}	10^6 k_{obs} S^{-1}	
	Xyl	Ara
25	30.20	9.42
35	35.88	13.73
45	40.79	17.98
55	45.52	22.65
75	53.58	32.37

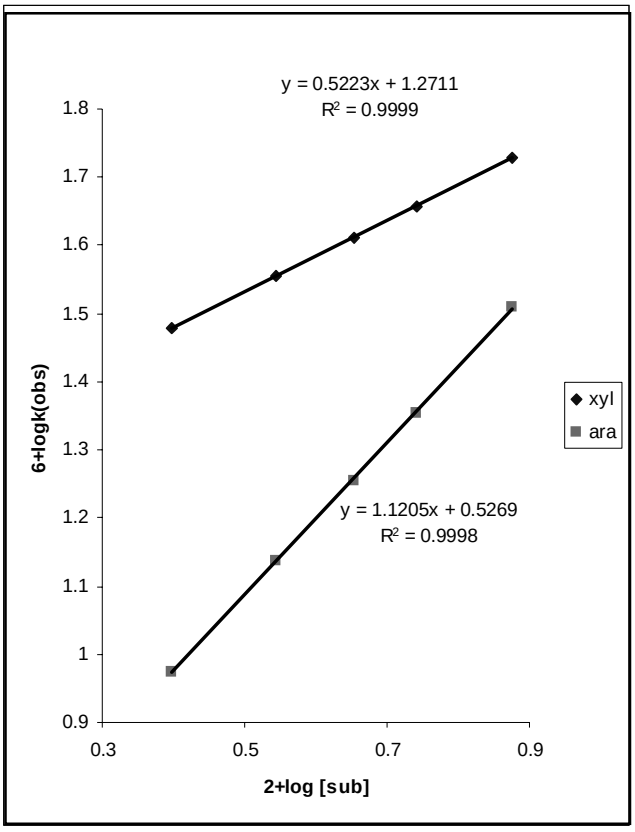

Fig. 1: Effect of [Substrate] on reaction rate

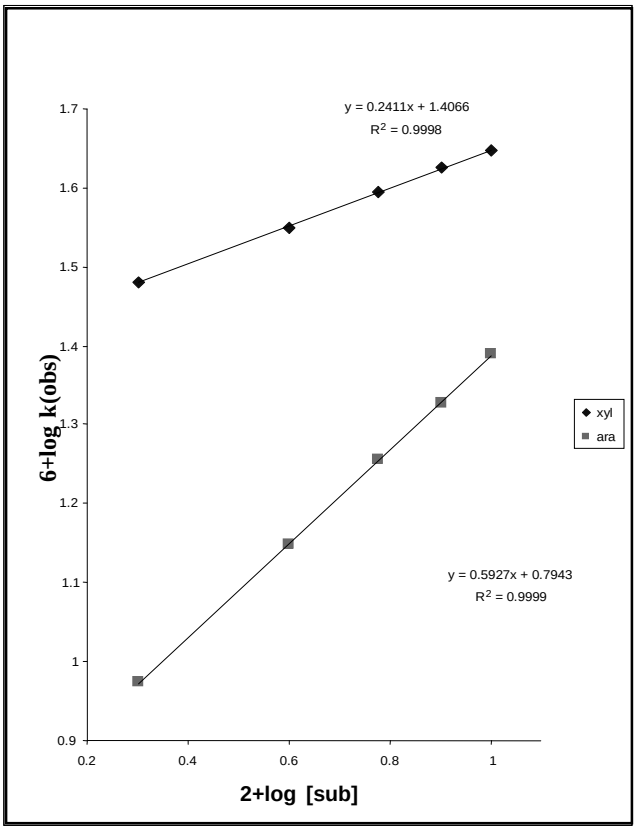

Fig. 2: Effect of [OH$^-$] on reaction rate

Effect of varying [OH$^-$]

Table 3 shows that for both substrates, the rate increases proportionally with the increase in [NaOH]. The plot of log k_{obs} versus log [OH$^-$] was linear with a unit slope indicating first order dependence on [sodium hydroxide] (Table 3) (Fig.2).

Table 3: Effect of [OH$^-$] on reaction rate

[NBN]=0.0025 mol dm^{-3} [substrate]=0.025mol dm^{-3}, [$NaClO_4$]=0.1mol dm^{-3}, $Hg(CH_3COO)_2$=0.005 mol dm^{-3}, Temp. =308 K

[NaOH] 10^2 moldm^{-3}	10^6 k_{obs} S^{-1}	
	Xyl	Ara
2.0	30.20	9.42
4.0	35.49	14.10
6.0	39.29	17.99
8.0	42.18	21.29
10.0	44.43	24.51

Effect of addition of nicotinamide

The effect of one of the product of the reaction has been studied by adding various concentrations of nicotinamide, keeping concentration of sugar and NBN constant. There was no significant change in the rate of reaction.

Effect of ionic strength

The effect of ionic strength was studied by carrying out investigations in the presence of different amounts of sodium perchlorate. No appreciable salt effect was detected.

Effect of added salts

Added salts like $BaCl_2$, KCl, Na_2SO_4 and K_2SO_4 did not have any effect on the rate.

Test for free radicals

The possibility of free radical intervention in the NBN oxidation reaction was tested by the following procedure, the reaction mixture containing acrylonitrile scavenger was kept for 24 hours in an inert atmosphere and then diluted. On dilution, formation of precipitate was not observed indicating the absence of free radical intervention in the reaction.

Effect of temperature

Increase in temperature increases the rate of oxidation and plot of log k_{obs} vs reciprocal of temperature was linear. The oxidation of xylose and arabinose by NBN was studied at different temperatures (308to 328K) (Table 4) (Fig.3) and the activation parameters were evaluated (Table 5) (Fig.4).

Table 4 Effect of Temperature on reaction rate

[substrate]=0.025 mol dm^{-3} [NaOH]=0.02 mol dm^{-3}, [NBN]=0.0025 mol dm^{-3} [$NaClO_4$]=0.1mol dm^{-3}, $Hg(CH_3COO)_2$=0.005 mol dm^{-3}

Temperature K	10^6 k_{obs} s^{-1}	
	Xyl	Ara
308	30.20	9.42
313	34.32	13.27
318	38.92	18.24
323	44.32	24.99
328	44.79	33.20

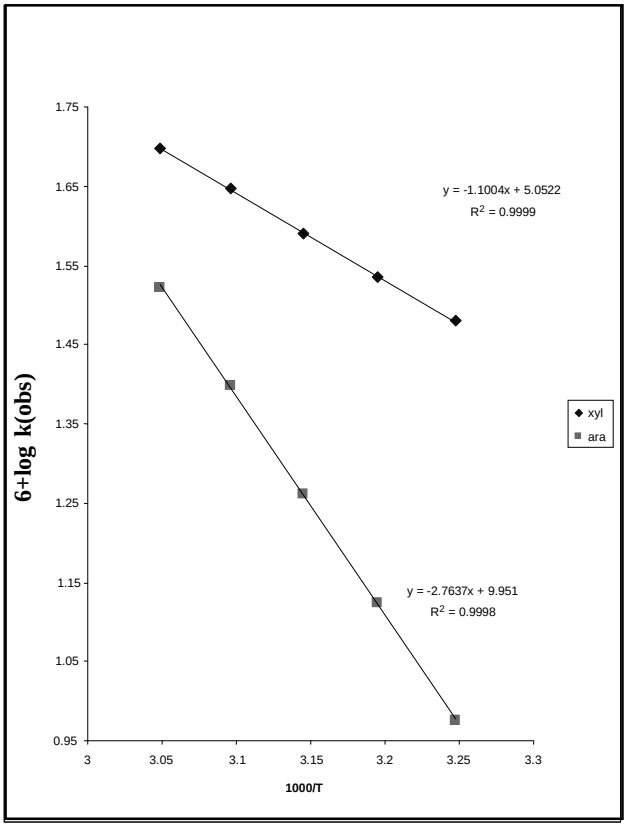

Fig. 3: Effect of Temperature on reaction rate

Table 5 Activation Parameters

Substrate	E_a $kJmol^{-1}$	$\Delta H^{\#}$ $kJmol^{-1}$	$\Delta S^{\#}$ $J\ K^{-1}mol^{-1}$	$\Delta G^{\#}$ $kJmol^{-1}$
Xylose	11.71	9.15	– 192.10	68.32
Arabinose	25.54	22.98	– 151.36	69.60

Discussion

The possible oxidizing species in alkaline medium are NBNBr, Br_2 and HOBr[5]. The observed zero order dependence of the reaction rate on NBN rules out NBNBr and molecular bromine as the reactive oxidizing species. Addition of nicotinamide having no effect on the rate indicates that HOBr may not be the oxidizing species. H_2OBr may be discarded because of negligible

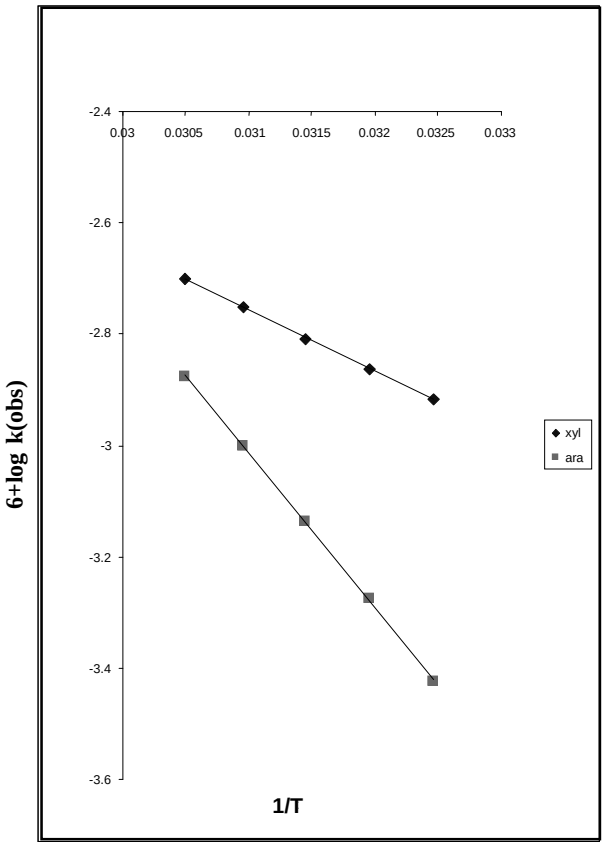

Fig. 4: Activation parameters

effect of addition of nicotinamide on reaction rate. A careful study of the kinetics of oxidation of above sugars shows that the rate expression is of the form.

$$-\frac{d[NBN]}{dt} = k\,[\text{substrate}]\,[OH]$$

which implies that the rate of reaction is independent of the concentration of [NBN], while the reaction is of first order both with respect to sugar as well as alkali. In cases where the concentration of sugar as well as alkali is large as compared to the concentration of [NBN], the rate expression becomes

$$-\frac{d[NBN]}{dt} = k_s = \Delta\chi / \Delta t$$

where ks = k[substrate] [$O\bar{H}$]

Mechanism

On the basis of the above experimental results, it appears that the first slow step involves a reaction between hydroxide ion and the reducing sugar, leading to the formation of an intermediate reactive form:

$$S + H\bar{O} \underset{k_{-1}\,(\text{slow})}{\overset{k_1}{\rightleftharpoons}} H - C\,(OH) = CR(OH) + H_2O$$

1, 2 Enediol (E) ..... (I step)

where S represents the reducing sugar. The fact that this step is slow explains the first order of the reaction with respect to reducing sugar. Further, this intermediate reactive form, which is called, 1,2 enediol, is subsequently oxidized by NBN to form nicotinamide and other reaction products.

$$\text{en (E)} + \text{HBN} \xrightarrow[\text{fast}]{k_2} \text{products} + \text{NA}\ldots\ldots \quad \text{(II step)}$$

{Products- xylonic acid and arabinonic acid for xylose and arabinose respectively}

where " en " represents 1,2 enediol. The fact that the second step is fast explains the zero order of the reaction with respect to [NBN].

It may be pointed out that in the present study, oxidation by bromine was completely suppressed as the oxidative studies were carried out in presence of mercuric acetate which combines with bromide ions formed in the reaction[25]. Thus kinetics of only NBN oxidation were followed.

The involvement of the substrate molecule in the rate-determining step leads to different values of k_{obs} for different initial concentrations of xylose and arabinose.

Conclusions

The reaction rates are enhanced by increase in [substrate], [alkali] and temperature. Nicotinamide has no effect on the rate. The oxidation of xylose is faster than

that of arabinose oxidation. 1,2-Enediol form of sugar is the reactive intermediate leading to products. Xylonic acid and arabinonic acid are the products of oxidation of xylose and arabinose respectively. The products were identified. Suitable mechanism in accordance with experimental observations was proposed and the rate laws were derived. NBN can be used as a better oxidant for the facile oxidation due to its easy method of synthesis and handling, higher rate of oxidation, longer shelf life and versatility.

Acknowledgements

The author gratefully acknowledges her husband Mr. A. Ramesh's moral support and help at all times.

References

1. Vineeta, Radha RanI Gupta and Mukhtar Singh, 2010, *J. Indian Chem. Soc.,* **87**, 1087.
2. Sheila Srivastava, Parul Srivastava, Lakshmi Chaudhary, Ashish Kumar, Shalini Singh, 2009, *J. Indian Chem. Soc*., **86**, 58.
3. Okoro H. K. and Odebunmi E. O., 2009, *International Journal of Physical Sciences*, **4(9)**, 471.
4. Katre Yokraj, Singh Minu, Patil Sangeeta and Singh Ajaya K., 2009, *Acta Phys. Chim. Sin*., **25(2),** 319.
5. (a) Pushpalatha L., 2014, *Oxid. Commun*., **37(1)**, 121.

   (b) Pushpalatha L., 2015, *International Letters of Chemistry, Physics And Astronomy,* **57**, 95.

   (c) Pushpalatha L., 2015, *International Letters of Chemistry, Physics and Astronomy,* **52**, 111.

   (d) Pushpalatha L., 2015, *Int. J. Chem.,* **4(1)**, 33.
6. Hauser C.R. and Renfrow Jr W.B., 1923, *J. Am. Chem. Soc*., **59,** 121.
7. Feigl F. 1966 - Spot Tests in Organic Analysis, 3rd ed., Elsevier, New York, p 325.

RNI No. MAHENG/2017/74063
ISSN No. (Print) 2581-5911

Development and Validation of HPTLC Method for Quantitation of Trigonelline from M*irabilis jalapa* Linn. leaves and Enhancement in Extraction Yield of Trigonelline from Ultra Fine Powder

Padma S. Sathe* and Vidya V. Dighe
Department of Chemistry, Ramnarain Ruia College, Matunga, Mumbai 400019, India.
Email: ***padmasathe@gmail.com***

Abstract
A simple HPTLC method has been developed and validated for determination of trigonelline in methanolic extract of Mirabilis jalapa *Linn. (Nyctaginaceae) leaves using n-butanol: methanol: water (6.0:2.0:2.0 v/v/v) as mobile phase. Detection and quantification were performed by densitometry at ë = 254 nm. Validated method shows linear response over concentration range of 1.5µg per band to 3.5µg per band of trigonelline. The LOD and LOQ values were found to be 0.05µg per band and 1.5µg per band respectively. This method was found to be precise and accurate. Ultra fine powder of leaves of M*irabilis jalapa *Linn. was prepared using simple stepwise powdering method. Coarse grinding of the dried leaves of* Mirabilis jalapa *Linn. was done using ice jacketed domestic mixer. This powder was sieved through a BSS 85 mesh sieve and used as micro powder. Further fine grinding was done by jet milling, followed by ball milling. This powder was used as ultra fine powder. The amount of trigonelline obtained using methanol extract of* Mirabilis jalapa *Linn. ultra fine powder was found to be 1.1147 mg/g compared to amount of trigonelline obtained in the methanol extract of micro powder of* Mirabilis jalapa *Linn. which gave 0.7356 mg/g of trigonelline.*

Keywords: *Mirabilis jalapa, Nyctaginaceae, trigonelline, HPTLC, ultra fine powder.*

Introduction

Mirabilis jalapa Linn., is a popular ornamental plant grown worldwide for the beauty of its flowers.[1] It is popularly known as four o'clock, as the flowers open in the late afternoon or early evening.

Mirabilis jalapa Linn. from family Nyctaginaceae is known to possess various bioactivities, including antimicrobial,[2] antibacterial and antifungal[3] antiviral & antiviroid,[4] anthelmintic,[5] antinociceptive,[6] anti-inflammatory,[7] wound healing,[8] hepato-protective,[9] hypoglycemic[10] & hypolipidemic,[11] antiallergic and antiasthamatic.[12]

Trigonelline is known to be an important bioactive alkaloid, proposed as a protective dietary agent in human health. It possesses both potential insulin sensitivity and shows hypoglycemic and hypolipidemic effects. [13] In *Mirabilis jalapa* Linn. plant, trigonelline was found in leaves, stems, flowers, roots and seeds. [14] Dried roots of *Mirabilis jalapa* containing trigonelline have been used in traditional Chinese medicine.[15]

HPTLC, due to its simplicity and minimum sample clean-up requirement has been widely used as a quality con-

trol tool for the phytochemical evaluation of herbal drugs. HPTLC methods have been reported in literature for quantitation of trigonelline in herbal extracts, [16] in leaves of *Abrus precatorius* L., [17] and from seeds of *Trigonella Foenum graecum* L.[18&19]

HPTLC finger print profile has been reported in literature from *Mirabilis jalapa* Linn. Flowers.[20] But no HPTLC method has been reported for quantitation of trigonelline from *Mirabilis jalapa* Linn. Hence in the present research work, a precise and accurate HPTLC method has been developed and validated using International Conference on Harmonization (ICH) guidelines for quantitation of trigonelline which may be used as a fast and relatively cheap method for determination of trigonelline from dried leaf powder of *Mirabilis jalapa* Linn. Further, it is reported in literature that grinding the plant powder to very fine size enhances the content of phytoconstituents.[21, 22] Methods like jet milling and ball milling are optimised and reported for grinding to very fine size.[23, 24]

In the present work, a method for grinding dried leaf powder to very fine size is developed, and the developed HPTLC method is used for quantitation of trigonelline from dried leaf micro powder and ultra fine powder of *Mirabilis jalapa* Linn. It is established that grinding the plant powder to a very fine size enhances the amount of trigonelline.

Materials and Methods

Reagents and Standard

The solvents n-butanol and methanol were of AR grade with 99.5% and 99.7% purities respectively. The solvents and distilled water used were procured from LiChrosolv Merck, India. Trigonelline hydrochloride standard of Lot No. BCBH 2677V was procured from Sigma-Aldrich Chemie Gmbh (Aldrich Division; Steinheim, Federal Republic of Germany). Its reported purity was 98.3% in the Certificate of Analysis.

Plant Material

Leaves of *Mirabilis jalapa* Linn. were collected from a domestic garden in Dombivli, Dist. Thane, Maharashtra, India. Its herbarium was prepared and authenticated from Botanical Survey of India, Pune, Maharashtra, India. (Certificate No. BSI/WC/Tech/2012/70) Duplicate herbarium was prepared and preserved in Ramnarain Ruia College, Mumbai.

The collected leaves of *Mirabilis jalapa* Linn. were washed, dried in shade, finely ground using a specially fabricated domestic mixer with an outer ice bath; the leaf powder was sieved through a BSS 85 mesh sieve. This powder was used as micro powder.

This powder was further ground to an ultra fine size, by passing it thrice through a jet mill, having 4 inch chamber and two jets of air at pressure of around 8 kg per cm^2, particle size obtainable was up to one micron. The particle size was monitored using Malvern Mastersizer 2000 analyser.

About 400 g jet milled plant powder was ball milled. About 1600 grams of 3.2 mm chrome balls were used. Milling was done at 980 rpm for three cycles of forty five minutes each. Liquid nitrogen was used for cooling. This powder was used as ultra fine powder. The particle size was monitored using Malvern Mastersizer 2000 analyser, and then using a Field Emission Scanning Electron Microscope.

The bulk density, tapped density and specific surface area of both micro powder and ultra fine powder were determined. Both micro powder and ultra fine powder were stored in airtight containers at room temperature (28°C± 2°C).

Preparation of standard solution of trigonelline (1000 µg/mL)

Accurately weighed 63.36 mg of trigonelline hydrochloride equivalent to 50.0 mg of trigonelline standard was transferred to a 50 mL standard volumetric flask.

It was dissolved in 20 mL of methanol and the contents of the flask were sonicated in an ultrasonic bath (Model: TRANS-O-SONIC, Frequency: 50 Hz) for 5 minutes

for complete dissolution of trigonelline. The contents were then diluted up to the mark with methanol to obtain stock solution of trigonelline with concentration of 1000.0 µg/mL.

Preparation of the sample solutions

About 1.0 g micro powder of the leaves of *Mirabilis jalapa* Linn., was accurately weighed and transferred to 50.0 mL stoppered conical flask.10.0 mL of methanol was added to it and the flask was sonicated in an ultrasonic bath for 15 minutes. Further, sample solution was filtered through Whatman filter paper no.41. The filtrate was evaporated to dryness and then finally reconstituted in 10 mL of methanol.

The solution was then finally filtered using 0.45 ìm nylon filters (Millipore) before the analysis. Exactly similar procedure was followed for preparing sample solution of ultra fine powder of the leaves of *Mirabilis jalapa* Linn.

Chromatographic Conditions

Chromatography was performed on 20.0 cm x 10.0 cm TLC plates which were cut from 20.0 cm x 20.0 cm TLC aluminum plates precoated with 200 ìm layers of silica gel 60 F 254 (E. Merck, Mumbai, India). 0.05 to 5.0 µL of the standard solution of trigonelline and five and ten µL of each of sample solutions were applied, as bands, with the help of CAMAG Linomat V sample applicator with a 100 EL syringe (Hamilton, Bonaduz, Switzerland)., at a distance of 20.0 mm from the bottom edge of the chromatographic plate, as bands of 8.0 mm width, at a distance of 11.4 mm from each other. The mobile phase was prepared by mixing n-butanol: methanol: water (6.0:2.0:2.0 v/v/v) in a stoppered conical flask. It was then vortexed for 5.0 minutes.

Linear ascending development was carried out in a twin-trough glass chamber (Camag, Muttenz, Switzerland) saturated with mobile phase.

The optimized chamber saturation time for the mobile phase was 20 minutes at room temperature (25±2^{0}C). The plates were developed to a distance of 70 mm from the bottom edge of the plate.

After plate development, the plate was air dried and the response of the solutions was monitored using CAMAG III TLC Scanner with Win CATS software version 1.4.2., set at a wavelength, λ = 254 nm, in absorbance mode under Deuterium light.

Results and Discussion

Linearity

10.0 µL of each of the fifteen working standard solutions of trigonelline, in the concentration range of 0.05 µg/band to 5.0 µg/band, were applied in order of increasing concentrations, as 8 mm bands on the TLC plate by means of CAMAG Linomat V automatic sample applicator. The plate was developed to a distance of 70 mm from the bottom edge of the plate under specified chromatographic conditions. After plate development, the plate was air dried and the response of the trigonelline standard solutions was monitored using CAMAG III TLC Scanner with Win CATS software version 1.4.2., set at a wavelength, λ=254 nm, in absorbance mode under Deuterium light.

The peak areas of trigonelline were recorded for each concentration of trigonelline. The data pairing technique was applied to determine if there was any significant variation in peak areas of trigonelline solutions of same concentration recorded in duplicate. No significant statistical difference was observed between each pair of solutions of same concentration. The response factor was found to be constant in the concentration range of 1.5 µg/band to 3.5 µg/band. Five different concentrations (1.5 µg/band to 3.5 µg/band) of trigonelline were applied in triplicate to a plate, developed and the detector response at different concentrations was measured at wavelength, λ=254 nm, in absorbance mode under Deuterium light.

The calibration curve of trigonelline was obtained by plotting a graph of mean peak area vs. applied concentration of trigonelline in the concentration range of 1.5 µg/band to 3.5 µg/band and it was found to be linear in

this concentration range. The data was subjected to regression analysis to calculate the calibration equation and correlation coefficient. The regression equation was Y= 2265X -31.84. (R^2= 0.999, n=5) The results listed in Table 1, show that within the concentration range indicated, there was a good correlation between mean peak area and corresponding concentrations of standard. Limit of Detection (LOD) & Limit of Quantitation (LOQ). The limit of detection (LOD) and limit of quantitation (LOQ) were determined at a signal to noise ratio of 3:1 and 10:1 respectively. The LOD and LOQ values obtained are listed in Table 1.

Precision

The method was validated in terms of instrumental precision, repeatability, and intermediate precision. Instrumental precision was studied by repetitive analysis (n = 10) of the standard solution of trigonelline (2.0 µg/mL), using the proposed method and the peak areas of trigonelline were recorded.

The repeatability was carried out in same laboratory, on same day, by analyzing six sample solutions of dried leaf micro powder and ultra fine powder of leaves of *Mirabilis jalapa* Linn. under the specified chromatographic conditions. The peak areas of trigonelline were recorded.

The intermediate precision of the method was evaluated by analyzing six sample solutions each of micro powder and ultra fine powder of dried leaves of *Mirabilis jalapa* Linn. on three different days under the specified chromatographic conditions. The peak areas of trigonelline were recorded. The results were expressed as percentage relative standard deviation of peak area of trigonelline and are listed in Table 1. The results indicate that the proposed method is precise and reproducible.

System suitability

System suitability was carried out to verify that the resolution and reproducibility of the system were acceptable for the analysis. System suitability test was carried out by applying 10 µL of standard solution of trigonelline, with concentration of 2.0µg/mL. as a band in six replicates on the same chromatographic plate under specified chromatographic conditions. The chromatograms were recorded. The values of percent relative standard deviation of peak area and retention factor of standards were taken as an indicator of system suitability. All the values for standard solution of trigonelline were found to lie within the acceptable range with values of percent relative standard deviation less than 2, indicating suitability of the system.

Estimation of trigonelline in dried leaf powder of *Mirabilis jalapa* Linn.

10.0 µL of each sample solution prepared by extracting about 1.0 g of dried leaf micro powder of *Mirabilis jalapa* Linn. with methanol as described earlier, was applied as bands in seven replicates, on a precoated silica gel 60 F_{254} TLC plate. The plate was developed and scanned as mentioned above. The values of peak areas and mean of peak area of trigonelline were recorded. Percent relative standard deviation of peak area of trigonelline was determined.

From the calibration curve, the amount of trigonelline present in the sample solution of *Mirabilis jalapa* Linn. was calculated.

Exactly same procedure was followed for the ultra fine powder. The assay results are listed in Table 1.

Accuracy

Accuracy of the method was established by carrying out recovery experiment to study if there is any interference of other constituents present in *Mirabilis jalapa* Linn. leaf powder on peak of trigonelline.

About 1.0 g of dried leaf micro powder of *Mirabilis jalapa* Linn. was accurately weighed in four separate 50 mL conical flasks. Known amounts of the standard trigonelline (0.0 mg, 0.1mg, 0.2 mg and 0.3 mg) respectively were added to each flask and extracted as described above. Each solution was analysed by developed HPTLC method, using the optimized chromatographic conditions, in seven replicates and the value of amount of trigonelline recovered from the sample for

each level, was determined. The value of percent recovery was determined.

Exactly same procedure was followed for the ultra fine powder. The results are listed in Table 1. The results indicate good accuracy of the method for quantitative determination of trigonelline from the dried leaf powder of *Mirabilis jalapa* Linn.

Results and Discussion

HPTLC method has been developed for quantitation of trigonelline from dried leaf powder of *Mirabilis jalapa* Linn. The linearity range of trigonelline was found to be 1.5 µg/band to 3.5µg/band, with correlation coefficient as 0.999. (regression equation Y=2265 X-31.84) When the method was validated in terms of instrumental precision, repeatability and intermediate precision, the percent relative standard deviation values for each solution were found to be less than 2, indicating that the proposed method is precise and reproducible.

The micro powder of *Mirabilis jalapa* Linn. had a diameter at 90% (90% particles have a size below) of 180 µm and a specific surface area of 0.415 m^2/g. After further grinding thrice through a jet mill and three cycles of ball milling, each of 45 minutes duration, the ultra fine powder had a diameter at 90% of 24.545 µm and a specific surface area of 1.55 m^2/g. The bulk density of micro powder was 0.332 g/cm^3 and that of ultra fine powder was 0.496 g/cm^3. The tapped density of micro powder was 0.462 g/cm^3 and that of ultra fine powder was 0.790 g/cm^3. Figure 1 shows FESEM image of ultra fine powder of *Mirabilis jalapa* Linn.

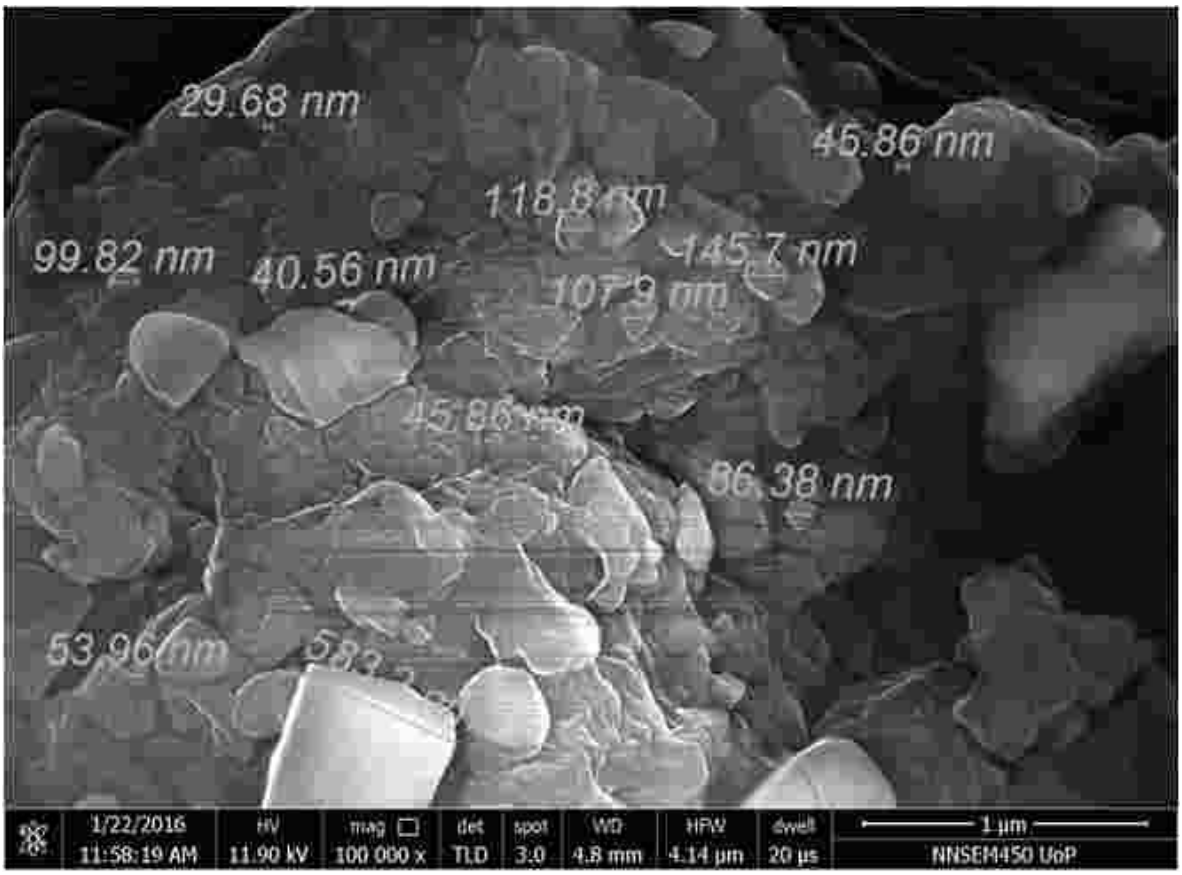

Fig. 1. Field Emission Scanning Electron Microscope image of *Mirabilis jalapa* Linn. dried leaf ultra fine powder

The amount of trigonelline found in the methanolic extract of dried leaf micro powder of *Mirabilis jalapa* Linn., by the proposed method, was found to be 0.7356 mg/g and in methanolic extract of ultra fine powder it was found to be 1.1147 mg/g. (Table 1).

The accuracy of the method was established by means of recovery experiment. The percent recovery of trigonelline at three different levels was found to be 98.36 for the micro powder and 98.48 for the ultra fine powder. (Table1).

The method is specific for trigonelline because it resolved the standard trigonelline (Rf=0.12) well in presence of other phytochemicals of *Mirabilis jalapa* Linn.

Figure 2, 3 and 4 show typical chromatograms of standard trigonelline, methanolic extract of micro powder of *Mirabilis jalapa* Linn.and methanolic extract of ultra fine powder of *Mirabilis jalapa* Linn. respectively. Figure 5 shows typical HPTLC plate illustrating the separation of trigonelline in the methanolic extract of micro and ultra fine powder of *Mirabilis jalapa* Linn. Figure 6 shows a three dimensional representation of HPTLC chromatograms for trigonelline on all tracks when the plate was visualized at λ=254nm.

Table 1: Results of developed and validated HPTLC method

Parameters	Results For Trigonelline	
Linear range (µg/band)	1.5-3.5	
Correlation Coefficient	0.999	
LOD (µg/band)	0.05	
LOQ (µg/band)	1.5	
System Suitability (%RSD)	Less than 2	
Stability of Standard Solution	Stable for minimum 48 hours	
	Micro Powder	Ultra fine Powder
Repeatability (% RSD) (n=6) (on same day)	0.9705	0.9457
Intermediate Precision (% RSD) (n=6) (For 3 successive days)	1.0069	0.9427
Assay (mg/g)	0.7356	1.1147
Percent recovery	98.36	98.48

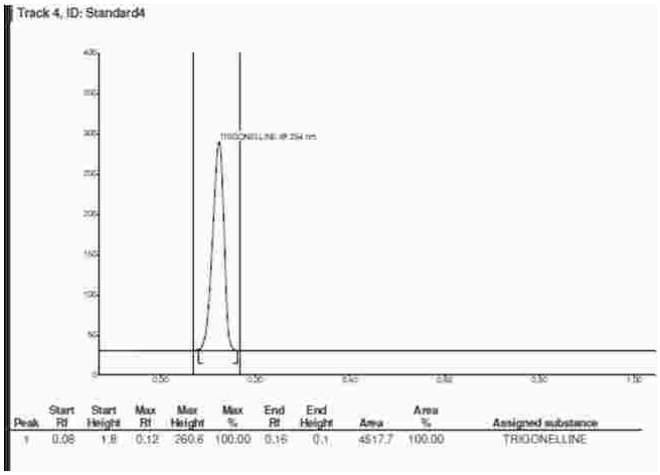

Fig. 2. Trigonelline standard (concentration 2.0 µg per band)

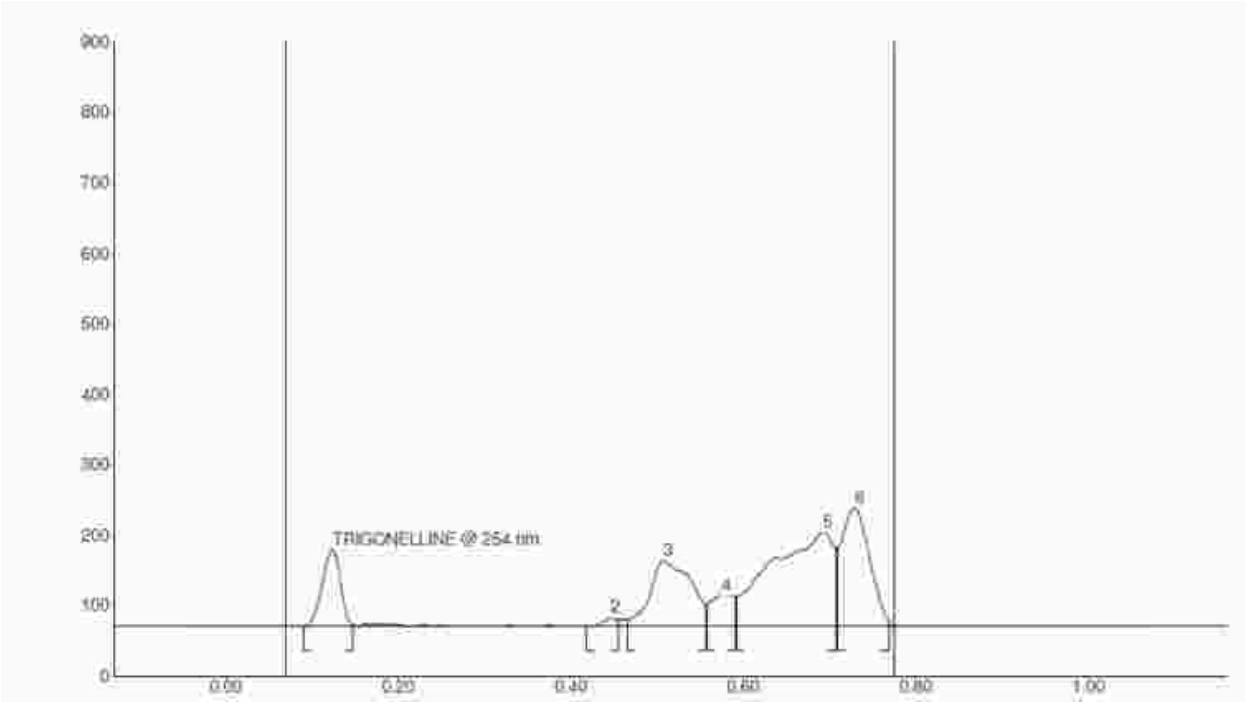

Peak	Start Rf	Start Height	Max Rf	Max Height	Max %	End Rf	End Height	Area	Area %	Assigned substance
1	0.09	0.2	0.12	109.8	19.47	0.15	2.9	1668.7	9.92	TRIGONELLINE

Fig. 3. 10 µL of methanolic extract of micro powder sample

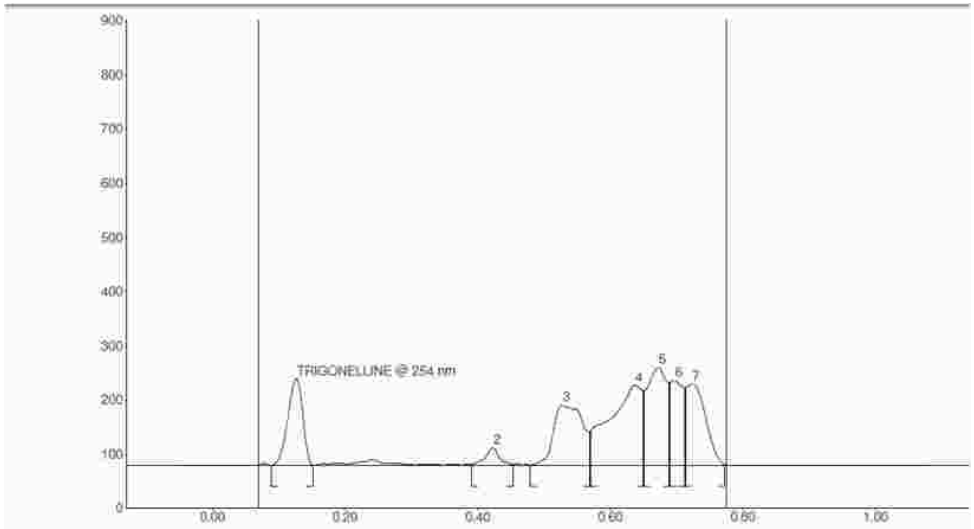

Peak	Start Rf	Start Height	Max Rf	Max Height	Max %	End Rf	End Height	Area	Area %	Assigned substance
1	0.09	0.2	0.13	159.5	17.03	0.15	0.3	2554.3	12.13	TRIGONELLINE

Fig. 4. 10 µL of methanolic extract of ultra fine powder sample

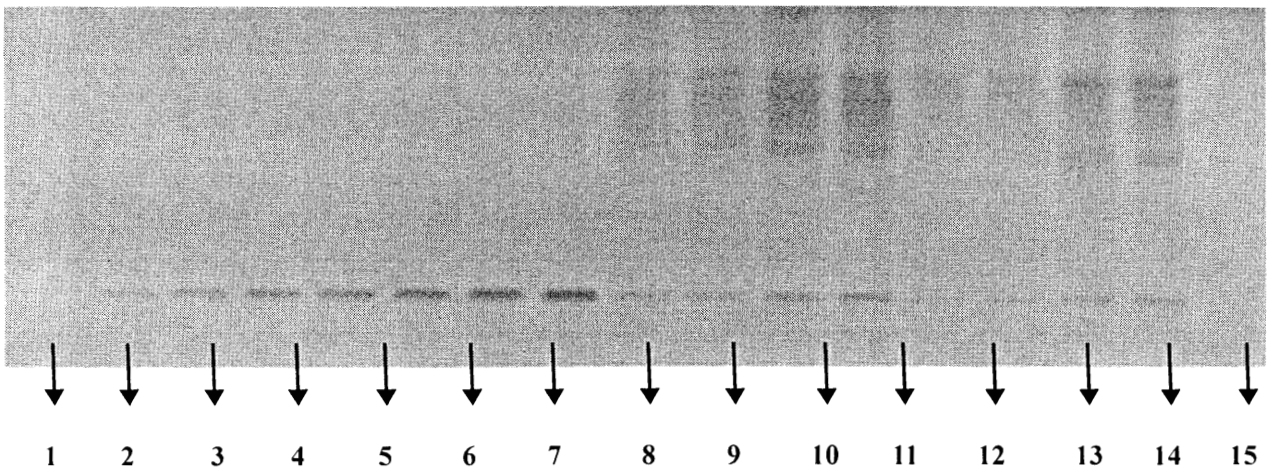

Fig. 5. Photograph of TLC plate

Track 1-7: standard trigonelline (conc. from 0.5 µg per band to 3.5 µg per band)
Track 8, 9: 5 µL each of methanolic extract of dried leaf ultra fine powder of *Mirabilis jalapa* Linn.
Track 10, 11: 10 µL each of methanolic extract of dried leaf ultra fine powder of *Mirabilis jalapa* Linn.
Track 12, 13: 5 µL each of methanolic extract of dried leaf micro powder of *Mirabilis jalapa* Linn.
Track 14, 15: 10 µL each of methanolic extract of dried leaf micro powder of *Mirabilis jalapa* Linn.

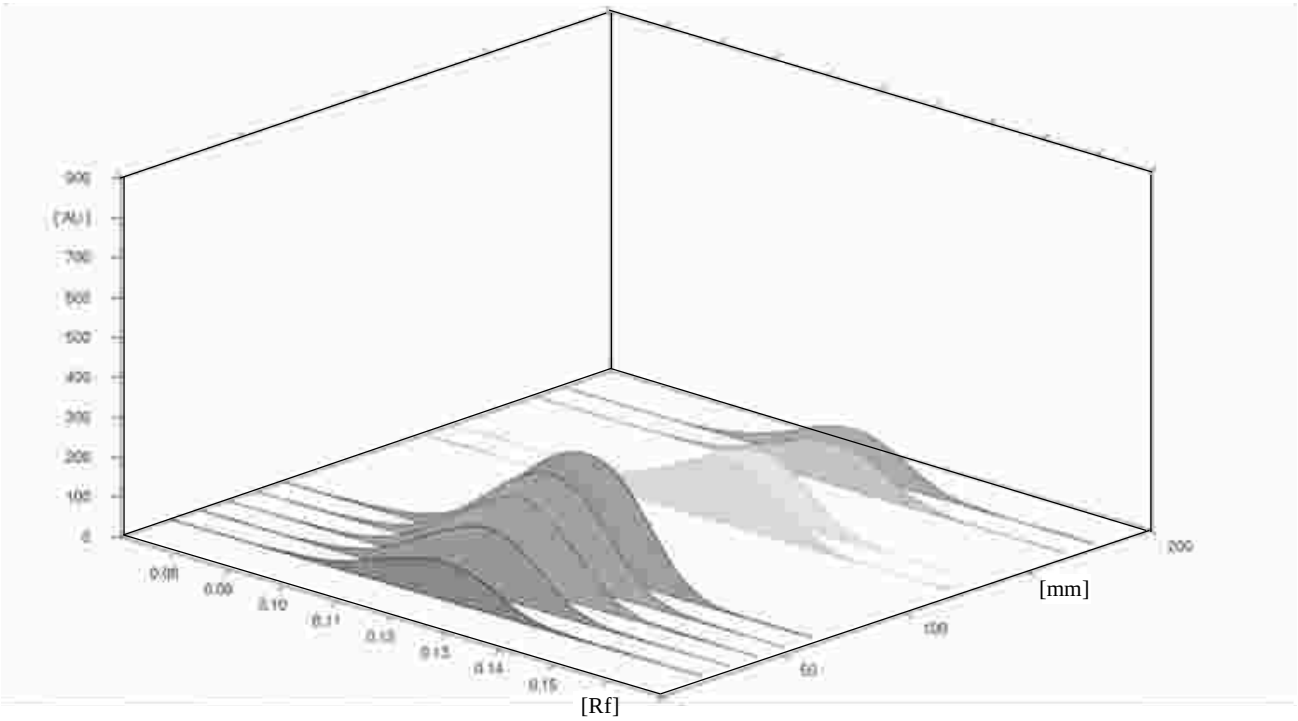

Fig. 6. HPTLC chromatograms of trigonelline from standard trigonelline (shaded in brown, pink and purple), methanolic extract of dried leaf ultra fine powder (shaded in green) and micro powder (shaded in orange red), of *Mirabilis jalapa* Linn.

Discussion

The extracting conditions were optimized to obtain maximum amount of trigonelline in the extract of leaf powder of *Mirabilis jalapa* Linn. Various solvent systems in different proportions of solvents were tried as mobile phases for the quantitation of trigonelline from the methanolic extract of dried leaf powder of *Mirabilis jalapa* Linn., but satisfactory separation of trigonelline from its sample matrix was achieved when mobile phase comprising of a mixture of n-butanol–methanol-water, in the volume ratio of (6: 2: 2) was used. Single development of the plate provided a good resolution of trigonelline from the other phytoconstituents present in the dried leaf powder of *Mirabilis jalapa* Linn. Detection was carried out densitometrically using a CAMAG TLC Scanner at λ = 254 nm since trigonelline showed maximum response at this wavelength.

The plate was scanned in absorbance mode, using Deuterium lamp at λ = 254 nm. The identity of the band of trigonelline in the sample solution was confirmed by comparing R_f value of trigonelline in micro powder sample ((R_f=0.12) and ultra fine powder sample ((R_f=0.13) of dried leaf powder of *Mirabilis jalapa* Linn. with that of reference standard trigonelline (R_f=0.12). Figure 6 shows a three dimensional representation of all the trigonelline peaks together and indicates matching of the R_f values of the standard and samples.

In literature, a normal phase HPTLC method has been developed and validated for quantitation of trigonelline in herbal extracts, using mobile phase comprising of n-propanol: methanol: water in the volume ratio of 4.0:1.0:4.0. Detection was done at λ=269 nm.[18]

In this work, n-butanol was used which gave a better resolution of the sample components.

HPTLC method for estimation of trigonelline in leaves of *Abrus precatorius* L. has been developed and validated.[19] Mobile phase used was toluene: ethyl acetate: formic acid: methanol in the volume ratio 2:3:1.8:3.8. Detection was done at 268 nm.

A simple, sensitive, and reproducible high-performance thin-layer chromatographic method has been established for simultaneous analysis of trigonelline and 4-hydroxyisoleucine from fenugreek seeds (*Trigonella foenum-graceum*). [20] Chromatography was performed on silica gel GF254 with n-butanol–methanol–acetic acid–water 4:1.5:1:1 as mobile phase.

In the present work, mobile phase used was simpler as neither formic acid nor acetic acid was needed to improve the peak shape of trigonelline.

In literature, HPTLC method for Fenugreek seed extract and its phytocompounds-trigonelline and diosgenin is reported.[21] Chromatography was done with Silica gel GF_{254} plates, pre-washed with methanol and activated at 55^0 C for 30 minutes. Absorbance was recorded at 254nm and 340 nm.

In the present research work, the method used is advantageous as it requires less time and minimum amount of solvent. No pre-washing or activation of the plates is required.

No HPTLC method has been reported in literature for quantitation of trigonelline from *Mirabilis jalapa* Linn. and in the present work, a high performance thin layer chromatographic method for the quantitative determination of trigonelline from the extract of dried leaf powder of *Mirabilis jalapa* Linn. has been developed. It has been applied in the quantitation of trigonelline from micro powder and ultra fine powder of dried leaf of *Mirabilis jalapa* Linn.

Conclusions

Trigonelline is one of the most important and effective anti diabetic molecules of recent times.

In the present research work, HPTLC method has been developed and validated for the quantitation of trigonelline from the methanolic extract of dried leaf powder of *Mirabilis jalapa* Linn., collected from Dombivli, District Thane, Maharashtra, India. It can be applied for the

quantitation of trigonelline from the methanolic extract of the dried leaf powder of *Mirabilis jalapa* Linn., collected from any other location. The HPTLC method developed with careful validation for the quantitation of trigonelline from the leaves of *Mirabilis jalapa* Linn. was found to be simple, precise, sensitive and accurate. Further, it is clearly established that ultra fine grinding enhances the amount of trigonelline extracted from the dried leaf powder of *Mirabilis jalapa* Linn.

References

1. Khare C.P., 2007, Indian Medicinal Plants: an Illustrated Dictionary. 1st Indian Reprint, Springer (India) Pvt. Ltd, p 417.

2. Dimayuga R.E., 1998, *Pharm. Biol.*, **36**, 33-43.

3. Chakraborthy G.S., 2009, *Journal of Pharmaceutical Sciences and Research.*, **1 (2)**, 79-82.

4. Vivanco J.M., Querci M. and Salazar L.F., 1999, *Plant Disease*, **83**, 1116-1121.

5. Subin M.Z., Aleykutty N.A., Vidya V. and Rachana V.G., 2012, *International Journal of Pharmaceutical Sciences Review and Research.*, **12 (1)**, Article 018.

6. Walker C., Trevisan G., Rossato M., Franciscato C., Pereira M., Ferreira J. and Manfron M., 2008, *J Ethnopharmacology*, **120,** 169-175.

7. Singh M., Kumar V., Singh I., Gauttam V. and Kalia A.N., 2010, *Pharmacognosy Res.*, **2(60)**, 364-367.

8. Gogoi J., Nakhuru K.S., Chattophadhayay P., Rai A.K., Gogoi H.K. and Veer V., 2014, *Oriental Pharmacy and Experimental Medicine*, **14(2),** 103–109.

9. Basini J., Mohanalakshmi S. and Anitha K., 2013, *Asian Journal of Pharmaceutical and Clinical Research*, **6(3)**, 221-224.

10. Liu An-jun, Wang Yun-xia, LI Hai-yan, MA Tian-jiao and Zheng Guo-qiang., 2011, *Modern Food Science & Technology*, **152(2),** 128-130.

11. Ji-Yin Zhou, Shi-Wen Zhou, Sheng- Ya Zeng, Jian-Yun Zhou, Ming- Jin Jiang and Yan He., 2012, *Evidence-Based Complementary and Alternative Medicine*, **2012,** Article ID 257374.

12. Maxia A., Sanna C., Salve B., Kasture A. and Kasture S., 2010, *Natural Product Research*, **24(18),** 1681-1686.

13. Mishkinsky J., Joseph B. and Sulman F., Hypoglycemic effect of trigonelline. 1967, *The Lancet.* **2 (7529),** 1311–1312.

14. Ashihara H. and Watanabe S., 2014, *Nat. Prod. Commun.*, **9(6)**, 795-798.

15. Song F., Zhang D., Zhong Y., Wang W. and Zeng S., 2005, *Traditional Chinese Drug Research and Clinical Pharmacology*, **3**, 189-190.

16. Chopra S., Ahmad F., Khar R., Motwani S., Mehdi S., Iqbal Z. and Talegaonkar S., 2006, *Anal. Chim. Acta.*, **577**, 46-51.

17. Kumbhalkar, B.B., Rajopadhye A.A. and Upadhye, A.S., 2012, *Acta Chromatographica*, **24(3)**, 511-518.

18. Gopu C., Gilda S., Paradkar A. and Mahadik K., 2008, *Acta Chromatographica*, **20 (4),** 709–719.

19. Nagore D., Patil P. and Kuber V., 2012, *International Journal of Green Pharmacy*, 315-320.

20. Kalaivani K. and Prasanna G., 2016, *International Journal of Current Microbiology and Applied Sciences*, **5(6)**, 642-654.

21. Borhan MZ, Ahmad R, Rusop M and Abdullah S., 2013, *Journal of Applied Chemistry.* **2013**, Article ID 460168.

22. Chen Q.M., Fu M.R., Yue F.L. and Cheng YY., 2015, *Food and Nutrition Sciences*, **6**, 1277-1284.

23. Rajkhowa R., Wang L., Kanwar J. and Wang X., 2009, *Powder Technology*, **191**,155–163.

24. Borhan MZ, Ahmad R, Rusop M and Abdullah S., 2013, *Journal of Nanostructure in Chemistry*, **3**, 79.

RNI No. MAHENG/2017/74063
ISSN No. (Print) 2581-5911

SERS study of two organophosphates: Dimethoate and methyl parathion

Praveen S.G.[1], Asenath Benitta T[1], Sudhir Kapoor*[2], Jayakumar V.S.[1], Bansal C[3] and Kumaran J T T*[1]

[1]Department of Physics, Nesamony Memorial Christian College, Marthandam India
[2] Radiation & Photochemistry Division, Bhabha Atomic Research Centre, Mumbai 400085, India
[3]School of Physics, University of Hyderabad, Hyderabad, India
Email: jthampi@vsnl.com
sudhirk@barc.gov.in

Abstract

Silver nanoparticles deposited on a glass substrate using modified mirror reaction were characterized using FE-SEM. The substrate was used to record surface-enhanced Raman scattering (SERS) of crystal violet (CV) dye as the probe molecule to detect the activity of Ag nanocubes substrate and then we used this substrate to detect two organophosphate pesticides, methyl parathion (MP) and dimethoate (DMT). Theoretical support was obtained with the assistance of DFT computed molecular parameters using the def-TZVP basis set of the Turbomole software. Low levels of MP and DMT can be detected by the SERS technique, which shows that the SERS substrate has excellent sensitivity and reproducibility. We were able to detect as amounts low as 100 picomolar for methyl parathion and dimethoate. The results can be useful in probing the presence of pesticide residues in food.

Keywords: *SERS, Nanostructures, Pesticides, Silver nanoparticles*

Introduction

In recent years, there has been a growing need for sensitive and selective assay for rapid detection and identification of terrorist threats including chemical and biological warfare agents, explosives, etc. In this regard, numerous attempts have been made to develop field-deployable detection techniques, a vital component of homeland and national security[1-6]. Pesticides are defined as substances or mixtures intended to prevent, destroy, repel or mitigate any pest, including insects, rodents and weeds.[7] Methyl parathion is one of the most hazardous insecticides, which is widely used to control insects which play havoc with a very wide range of crops such as cereals, fruits, vegetables, etc[8]. The detection limit of methyl parathion insecticide in vegetables is in the range 0.1 – 1.0 ppm according to recommendations from the Collaborative International Pesticide Analytical Council (CIPAC)[9]. A number of analytical methods, including gas chromatography-mass spectroscopy (GC-MS)[10], high-pressure liquid chromatography (HPLC)[11,12], Spectrophotometry[13], and electrophoresis[14],

have been reported. However, some disadvantages, viz., poor detection limit, lengthy measurement time, and indirect measurement, make these detection systems less attractive.

Surface-enhanced Raman spectroscopy (SERS) is a well-known analytical method that offers great potential for rapid and sensitive chemical or biological analysis[5,6,15-28]. It is well known that two mechanisms contribute to the SERS effect: (i) electromagnetic (EM) enhancement and (ii) chemical (charge transfer or CT) enhancement. EM enhancement stems from the enhancement of local electromagnetic field incident on adsorbed molecules on the noble metallic nanoparticles with the size scale of 10 – 200 nm[29]. On the other hand, in chemical enhancement Raman scattering cross section increases due to an increase of the polarizability of the molecule, which is highly dependent on the electronic resonance-charge transfer between absorbed molecules and metal surfaces[30]. Several methods for producing SERS substrate for the detection of insecticides, pesticides, chemical and biological agents are available in literature[5,6,31-39]. Using various methods of preparation of nanostructures detection limit of 10^{-7} – 10^{-12} M for methyl parathion[6,33-37] and 10^{-5} M for dimethoate[38,39] was achieved.

In the present study, the substrates were prepared by modified mirror reaction and by physical deposition method. The prepared substrates were then used to detect two organophosphate pesticides, methyl parathion and dimethoate. The SERS spectra was recorded and compared with the experimental and simulated Raman spectrum, using the Version 6.0 of the Turbomole software.

Materials and Methods

The chemicals used in this study were obtained from Sigma-Aldrich and used without further purification. Aqueous solutions were prepared using water filtered by a Millipore Milli-Q system having a resistivity of 18.0 mega-ohm/cm. Ultra high pure nitrogen and argon gases of 99.999% purity were used.

Preparation of SERS active substrates

The substrate for SERS detection was prepared using the modified mirror reaction by following the literature process with a slight modification[40]. For this, a fine brown precipitate of Ag_2O was produced by adding 20 μL of 3.2 wt % KOH solution in 18 mL of 2 wt % $AgNO_3$ solution. The precipitate was dissolved by adding ammonium hydroxide (29.5%) drop by drop. Then 6 wt % $AgNO_3$ solution was added till the solution turned yellow. On adding a drop of 6 wt % ammonium hydroxide solution, the solution became colourless. The solution was mixed with 3 mL methanol, 10 μL of 10 wt % $Na_3P_5O_{10}$, and 40μL of 5 wt % Na_2HPO_4 consecutively to form a yellow colloid. Finally, a colloidal solution was produced when 6 mL of 35 wt % glucose was added and mixed. The glass slides of 1 cm by 1 cm dimensions were cut and then cleaned with piranha solution for a few minutes or until the visible reaction of organic material with the solution stopped. The piranha solution is a mixture of three parts of concentrated H_2SO_4 and one part of H_2O_2 (29.5%) [3:1]. Glass slides were then rinsed with water. To clean the glass slides further, it was sonicated in propanol, acetone and water and then dried under nitrogen gas. The cleaned glass slides were immersed in the colloidal suspension prepared as explained above for 24 hours at room temperature to form Ag nano-film on them. Then, the substrates were taken out and rinsed with copious amount of Milli Q water (18.2 MΩ cm) and dried under nitrogen gas. It is to be noted that the cleaning of the above glass slides should be repeated till there was no visible white or black turbidity on the surface of the coated particles. These substrates were then annealed for 3 hours at 200^0C in a vacuum oven kept inside the anhydrous conditions of an argon glove box by maintaining O_2 and H_2O levels less than 0.1 ppm to remove oxidation product, if any.

The metal nanoclusters of silver were also prepared by inert gas condensation technique using Nanodep60 nanocluster deposition system obtained from Oxford Applied Research UK. In this deposition method, metal atoms are sputtered into a highly pure cooled inert gas

flow at relatively high pressure than the deposition chamber where the glass slides were kept for deposition. The super saturated metal atoms while flowing through the inert carrier gas, nucleate and form clusters of nanometer size. In the present study, nanoclusters formed in the aggregation chamber were made to flow through an aperture into a deposition chamber that was maintained at a slightly lower pressure than the aggregation chamber by differential pumping. The distance between the substrate and apertures was 55 cm. The base pressure achieved in this system before the start of deposition was $4x10^{-7}$ milli bar and a working pressure of $5x10^{-5}$ milli bar was obtained during the aggregation gas flow whose flow rate was maintained at 100 sccm. The current in the DC magnetron was kept constant at 0.2 A and the power level was about 70 watts.

All the samples for Raman analysis were prepared inside the argon glove box in order to prevent contamination. The SERS spectra were recorded at different concentrations of methyl parathion and dimethoate. SERS measurements were acquired from an average of ten randomly selected locations for each analyte concentration.

Characterization

The morphology of the micro structure of the deposited films of silver by modified mirror reaction and the deposited silver nanoclusters were obtained using the Carl Zeizz Ultra 55 FESEM. An excitation voltage of 5 kV was applied and a working distance around 5 mm was maintained for obtaining the SEM image. The Raman measurements were performed using LABRAM HORIBA micro Raman Spectrometer equipped with TE cooled CCD detector and an Argon Ion Laser of 9 mW power with excitation wavelength of 514.4 nm.

Computation Quantum chemical computations of methyl parathion using version 6.0 of Turbomole software was performed[41]. Density functional theory with the B3LYP functional and def-TZVP basis set[42] was used for the optimization of the ground state geometry and the simulation of the Raman spectra.

Results and Discussion

The morphology of Ag nanoparticles prepared by modified mirror method was examined using SEM. As seen from the SEM image in Fig. 1, Ag nanoparticles of the order of 20 nm were obtained and distributed uniformly on the slide surface. An attempt was also made to deposit silver nanoparticles using physical deposition method. The SEM of this substrate is shown in Fig. 2. It is seen from SEM that the silver nanoparticles were of the order of 30 nm. The efficiency of the substrate was then tested using crystal violet (CV) solution. For this, the required concentration of CV was transferred over the prepared substrate using a micro pipette. The substrate was kept for drying inside the glove box for a few hours and then these substrates were sealed in petri dishes using parafilm inside, the glove box to avoid contamination and taken out only at the time of recording the SERS spectra. SERS of CV on the modified mirror reacted slide is shown in Fig. 3 and it agrees well with the reported spectrum[43]. The optimized geometries of both methyl parathion and dimethoate are shown in Figures 4 and 5, respectively. The SERS spectra in the important region of 400-2000 cm^{-1} were recorded for both methyl parathion and dimethoate.

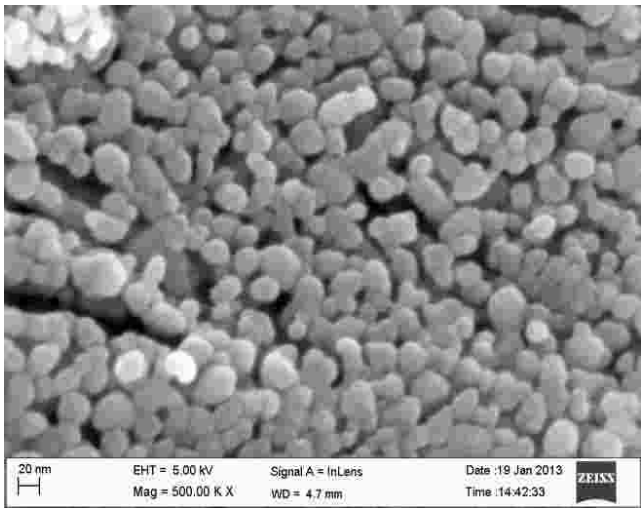

Fig.1 SEM image of the substrate having silver nanoparticles prepared by modified mirror reaction.

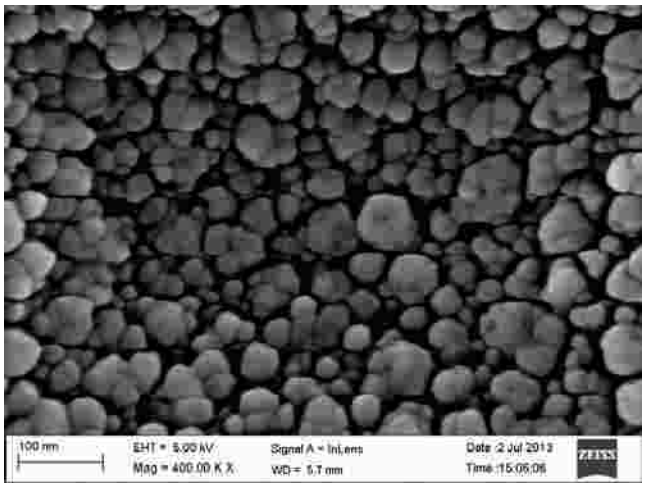

Fig.2 SEM image of the substrate having silver nanoparticles prepared by silver nanocluster deposition method.

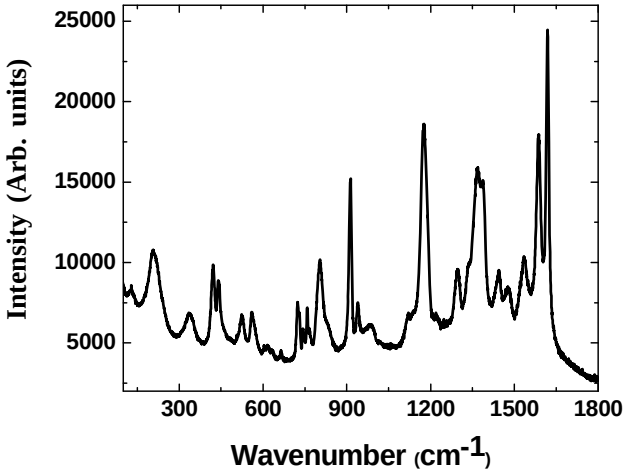

Fig. 3 SERS of 1 mM crystal violet on silver nanoparticles deposited by modified mirror reaction.

Figure 6 shows SERS spectra under different experimental conditions. Simulated Raman spectrum is also shown in the figures. It can be seen that SERS spectra of methyl parathion showed several Raman bands. The Raman bands showed similar features as reported in literature[36,37]. The intensity of Raman bands in SERS spectra varied with the type of support used[6,33-37]. It can be seen from Fig. 6 that the intensity variation also occurs as the concentration of methyl parathion is

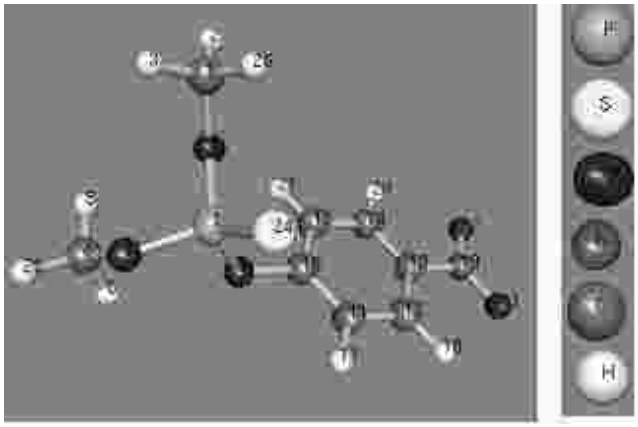

Fig. 4 Optimized geometry of methyl parathion.

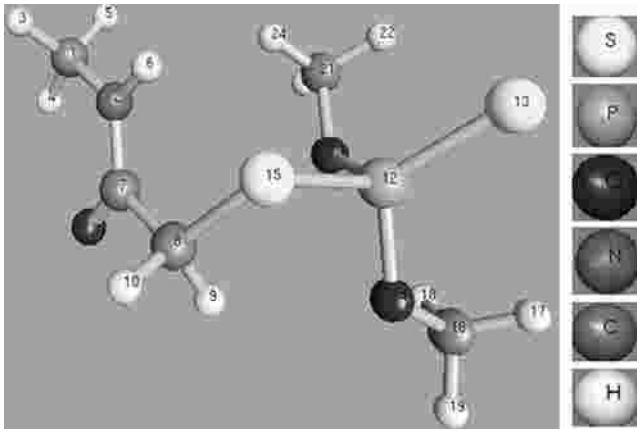

Fig. 5 Optimized geometry of dimethoate.

changed. This can occur due to the adsorption of monolayer on the surface of the particles[15-28]. The most interesting observation was that intensity of Raman bands was more when methyl parathion was adsorbed on silver nanoparticles prepared by modified mirror, reaction method as compared to when prepared by cluster method. The data corroborates the results reported in literature[6, 33-37]. Due to the more intense Raman bands in silver mirror modified method, the support was exploited to detect methyl parathion up to 10^{-10} M concentration. Due to the simplicity of the method, the present work offers a simple method to detect methyl parathion.

Figure 7 shows SERS spectra of dimethoate over silver

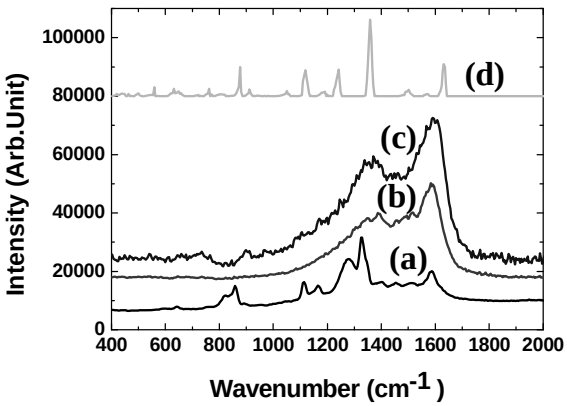

Fig.6 SERS spectra of methyl parathion (a) 1x10^{-3} M over silver nanoparticles prepared by deposition method. (b) 1x10^{-9} M over silver nanoparticles prepared by deposition method, (c) 1 x10^{-9} M over silver nanopaticles prepared by modified mirror method. (d) Simulated Raman spectrum of methyl parathion.

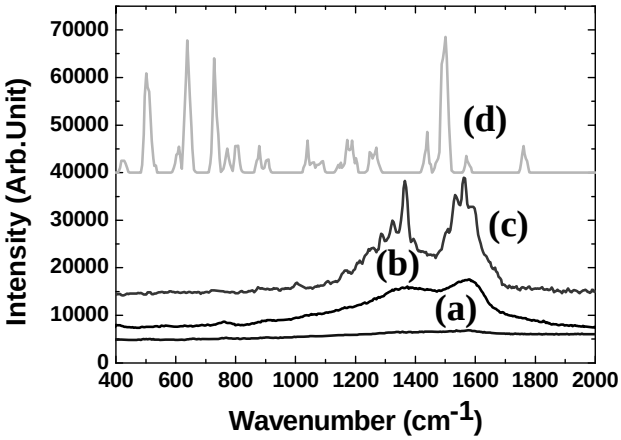

Fig 7 SERS spectra of dimethoate (a) 1x10^{-9} M over silver nanoparticles prepared by deposition method. (b) 1x10^{-3} M over silver nanoparticles prepared by deposition method. (c) 1x10^{-9} M over silver nanopaticles prepared by modified mirror method. (d) Simulated Raman spectrum of dimethoate.

nanoparticles prepared by cluster method and mirror modified reaction method. Simulated Raman spectrum is also shown in Fig. 7. The obtained spectra showed Raman peaks which agree well with that reported in literature[38,39]. The most intriguing result that was obtained in the case of dimethoate is that it was possible to detect it up to 10^{-10} M concentration over the silver particles prepared by mirror modified method. The representative SERS spectra under different experimental conditions are shown in Fig. 7. The sensitivity obtained in the present work is at least 4 orders of magnitude higher than that reported in literature[38].

Conclusions

The SERS spectra of methyl parathion and dimethoate from the substrates prepared by modified mirror reaction and by physical deposition method were obtained. Substrate with modified mirror reaction is highly sensitive and gives a detection limit of about 100 picomolar. Vibrational wavenumbers from turbomole, when compared with experimental SERS values gives results which are in good agreement. Highly enhanced SERS spectra of dimethoate and methyl parathion are obtained as a result of a strong interaction between the molecules and Ag hydrosols. This method offers rapid, cost effective and highly sensitive detection applicable to the quantitative evaluation of pesticides.

Acknowledgement

The authors would like to acknowledge the financial support of DAE-BRNS, Mumbai for the project no 2012/34/1/BRNS/No.122 dated 12 April 2012.

References

1. Alarie, J.P., Vo-Dinh, T., Miller, G.H., Ericson, M.N., Maddox, S.R. and Watts, W., 1993, *Rev. Sci. Instrum.*, **64**, 2541.

2. Vo-Dinh, T., Nolan, T., Cheng, Y.F., Sepaniak, M.J. and Alarie, J.P., 1990, *Appl. Spectrosc.*, **44**, 128.

3. Ray, M.D., Sedlacek, A.J. and Wu, M., 2000, *Rev. Sci. Instrum.*, **71**, 3485.

4. Skinner, H.T., Cooney, T.F., Sharma, S.K. and Angel, S.M., 1996, *Appl. Spectrosc.*, **50,** 1007.

5. Zhang, X.Y., Young, M.A., Lyandres, O. and Van Duyne, R.P., 2005, *J. Am. Chem. Soc.*, **127,** 4484.

6. Yan, F. and Vo-Dinh, T., 2007, *Sensors and Actuators B,* **121**, 61.

7. UN Food and Agricultural Organization: International Code of Conduct on the Distribution and Use of Pesticides. Rome, Italy (2002)

8. Pablos-Espana, M. C., Arrebola-Liebnas, F. J., Garrido-Frenich, A. and Martinez-Vidal, J. L., 1999, *Int. J. Environ. Anal. Chem.,* **75**, 165.

9. Collaborative International Pesticides Analytical Council (CIPAC) Handbook (CIPAC Ltd., 1994, **vol. 1B**, p. 1849.

10. Goncalves C. and Alpendurada, M.F., 2004, *J. Chromatogr., A,* **1026,** 239.

11. Paradopoulou-Mourkidou, E. and Patsias, J.J., 1996, *J. Chromatogr., A,* **726**, 99.

12. Valenzuela, A.I., Lorenzini, R., Redondo, M.J. and Font, G. 1999, *J. Chromatogr., A,* **839**, 101.

13. Naidu, U.V., Gangaiah, T., Ramadevi, P., Seshaiah, K. and Naidu,G.R.K., 1990, *Tantala,* **37,** 761.

14. Stockton, A.M., Chiesl, T.N., Scherer J.R. and Mathies, R.A., 2009, *Anal. Chem.,* **81**, 790.

15. Moskovits, M. **1985**, *Rev. Mod. Phys.,* **57,** 783.

16. Camden, J.P., Dieringer, J. A., Zhao, J. and Van Duyne, R.P., 2008, *Acc. Chem. Res.* **41,** 1653.

17. Maiti, N., Thomas, S., Jacob, J. A., Chadha, R., Mukherjee, T. and Kapoor, S., 2012, *J Coll. I n - terface Sci.,* **380,** 141.

18. Thomas, S., Biswas, N., Malkar, V. V., Mukherjee, T. and Kapoor, S., 2010, *Chem. Phys. Lett.,* **491,** 59.

19. Biswas, N., Thomas, S., Sarkar, A., Mukherjee, T. and Kapoor, S., 2009, *J. Phys. Chem. C,* **113,** 7091.

20. Biswas, N., Kapoor, S., Mahal, H. S. and Mukherjee, T., 2007, *Chem. Phys. Lett.,* **444,** 338.

21. Chadha, R., Maiti, N. and Kapoor, S, 2014, *J. Phys. Chem. C,* **118,** 26227.

22. Han, X.X., Kitahama, Y., Itoh, T., Wang, C.X., Zhao, B. and Ozaki, Y., 2009, *Anal. Chem.,* **81,** 3350.

23. Ko, H. and Tsukruk, V.V., 2008, *Small,* **4**, 1980.

24. Tripp, R.A., Dluhy R.A. and Zhao, Y.P., 2008, *Nano Today,* **3,** 31.

25. Wang, W., Ruan, C.M. and Gu, B.H., 2006, *Anal. Chim. Acta,* **567**, 121.

26. Alvarez-Puebla, R.A., Contreras-Cáceres, R., Pastoriza-Santos, I., Pérez-Juste, J. and Liz-Marzán, L. M., 2009, *Angew. Chem., Int. Ed.,* **48,** 138.

27. Sun, L.L., Song, Y.H., Wang, L., Guo, C.L., Sun, Y.J., Liu, Z.L. and Li, Z., 2008, *J. Phys. Chem. C,* **112,** 1415.

28. Alvarez-Puebla, R.A., Dos Santos Jr., D.S. and Aroca, R.F., 2007, *Analyst,* **132,** 1210.

29. McFarland, A.D., Young, M.A., Dieringer, J.A. and Van Duyne, R.P., 2005, *J. Phys. Chem. B,* **109,** 11279.

30. Otto, A., Mrozek, I. and Pettenkofer, C., 1990, *Surf. Sci.,* **238**, 192.

31. Wang, B., Zhang, L. and Zhou, X., 2014, *Spectrochim. Acta Part A* **121**, 63.

32. Cañamares, M.V. and Feis, A., 2013, *J. Raman Spectrosc.,* **44** 1126.

33. Zhang, L., 2013, *Applied Surface Science,* **270**, 292.

34. Ahn, W., Qiu, Y. and Reinhard, B.M., 2013, *J. Mater. Chem. C,* **1**, 3110.

35. Wang, J., Kong, L.T., Guo, Z., Xu, J.Y. and Liu, J.H., 2010, *J. Mater. Chem.,* **20,** 5271.

36. Yazdi, S.H. and White, I.M., 2013, *Analyst,* **138,** 100.

37. Lee, D., Lee, S., Seong, G.H., Choo, J., Lee, E.K., Gweon, D.-G. and Lee, S., 2006, *Applied Spectrosc.,* **60,** 373.

38. Guerrini, L., Sanchez-Cortes, S., Cruz, V.L., Martinez, S., Ristori, S. and Feis, A., 2011, *J. Raman Spectrosc.,* **42**, 980.

39. Kim, H.J., Lee, C.J., Karim, M.R., Kim, M.S. and Lee, M.S., 2011, *Spectrochim. Acta Part A,* **78,** 179.

40. Xu, Z., Hao, J., Li, F. and Meng, X., 2010, *J Coll. Interface Sci.,* **347**, 90.

41. TURBOMOLE V6.0 2009, A development of University of Karlsruhe and Forschungszentrum Karlsruhe GmbH, 1989-2007.

42. Schafer, A., Huber, C. and Ahlrichs, R., 1994, *J. Chem. Phys.,* **100,** 5829.

43. Cañamares, M.V., Chenal, C., Birke, R.L. and Lombardi, J.R., 2008, *J. Phys. Chem. C,* **112,** 20295.

Conference Alerts

1) 16th International Conference on Envirotech, Cleantech and Greentech (ECG)
July 14-15, 2017 Bali, Indonesia
Website: http://wasrti.org/16th -international-conference-envirotech-cleantech-and-greentech-ecg-14-15-July-2017-bali-indonesia-about-77

2) 2017 2nd International Conference on Green Energy Technology (ICGET – 2017)
July 18-20, 2017, Sapienza University of Rome, Rome, Italy
Website: http://www.icget.org/

3) 6th International Conference for Young Chemists (ICYC) Conference
August 16-18, 2017, George Town, Penang, Malaysia
Website: http://www.icy2017.com

4) 2017 4th International Conference on Advances in Biology and Chemistry (ICABC2017)
August 21-23, 2017, Singapore
Website: http://www.icbac.org/

5) International Conference on Chemical, Biological, Medical and Pharmaceutical Sciences (CBMPS-2017)
September 6-7, 2017, Budapest, Hungary
Website: http://earbm.org/conferences/CBMPS-2017

6) International Conference on Drug Discovery and Development (ICDDD2017)
September 12-13, 2017, Colombo, Sri Lanka
Website: http://drugdiscoveryconference.co/

7) World Congress on Drug Discovery and Development -2017 Conference
September 20-22, 2017, Kolkata, India
Website: http://www.drugdiscoveryconference2017.org

8) The Second Bandung International Conference on Medicinal Chemistry 2017
October 5-6, 2017 Bandung, West Java, Indonesia
Website://www/icmc-itb.org

9) International Conference on Applications in Chemistry and Chemical Engineering (CACCHE)
October 11-15, 2017, Sarajevo, Bosnia and Herzegovina
Website: http://www.icacche.com
Enquiries: info@icacche.com

10) 2017 6th International Conference on Chemical Science and Engineering (ICCSE-2017)
October 21-23, 2017, Philadelphia, USA
Website: http://www/iccse.org/

11) 6th International Conference on Nanostructures, Nanomaterials and Nanoengineering (ICNNN-2017)
October 27-30, 2017, Tokyo, Japan
Website: http://icnnn.org/

12) ASEAN Academic Network International Conference on Applied Chemistry and Physica Research 2017
October 27-28, 2017, Kuching, Malaysia
Website: http://aicacpr2017.weebly.com/

13) International Workshop on Chemistry (IWCH-2017)
October 28-29, 2017, Istanbul, Turkey
Website: http://cmf-scoop.org/science/iwch/

14) 2017 International Conference on Renewable Energy and Environment (ICREE-2017)
November 1-3, 2017, Toronto, Canada
Website: http://www.icree.org/

15) SQU-Chemistry Conference (2017): Green and Sustainable Chemistry
November 13-15, 2017, Sultan Qaboos University, Muscat, Oman
Website: http://confeence.squ.edu.om/Default.aspx?tabid=2560
Enquiries: gscc2017oman@gmail.com

16) 2017 6th International Conference on Environmental Chemistry and Biology (ICECB2017)
November 20-22, 2017, Queensland, Australia
Website: http://www.icecb.org

17) 9th International Conference on Research in Chemical, Agricultural, Biological and Environmental Sciences (RAABES-2017)
November 27-28, 2017, Parys (Near Johannesburg), South Africa
Website: http://earbm.org/conference/RCABES-2017

18) 3rd International Conference on Global Trends in Pure and Applied Chemical Sciences (ICGTCS-2017), organized by Asian Publication Corporation.
December 8-9, 2017 SRM University, Delhi-NCR, Ghaziabad, UP, India
Website: www.asianjournalofchemistry.co.in
http://icgtcs-2017.asianjournalofchemistry.co.in
Enquiries: asianicgtcs2017@gmail.com
Contact: Mrs Anjul Agarwal, Organizing Secretary, ICGTCS 2017,
Managing Director, Asian Publication Corporation
Prof. R.K. Agarwal, Editor-in-Chief, Asian Journal of Chemistry
Dr. Himanshu, Agarwal, Director, Asian Publication Corporation

19) 7th International Science Congress (ISC-2017)
December 8-9, 2017, Chukka, Bhutan
Website: www.isca.in, www.isca.net.co
Contact: Dr. Dipak Sharma, Director, ISCA

20) 15th EURASIA Conference on Chemical Sciences
December 15-18, 2017, Chicago, USA
Website: http://www.eurasia15.org

21) 4th International Conference on Applied Chemistry and Biology (ICACB2017)
December 29-30, 2017, Bandung, Indonesia
Website: http://icacb2017.weebly.com

G P GLOBALIZE RESEARCH JOURNAL OF CHEMISTRY

RNI No. MAHENG/2017/74063 ISSN No.(Print) 2581 5911

Volume 1 Issue 2 ❄ January-June 2018

CONTENTS

Papers

1. Catalytic aspects of Ruthenium in Redox Processes: A brief review **83 - 96**
   Santosh Bahadur Singh and Praveen Kumar Tandon

2. Computer colour matching data of synthesized monoazo disperse dyes, their dyeing performance on polyester fiber and antimicrobial activity **97 - 106**
   Sandip K. Patel, Pratixa K. Patel and G. M. Malik

3. Mechanistic aspect of Iridium(III) catalyzed oxidation of ethylene glycol by Chloramine-T in aqueous acidic medium: a kinetic model **107 - 115**
   Abhishek Verma, Jyoti Pandey, Sheila Srivastava and Kaman Singh

4. A mechanistic investigation of Pd (II) catalyzed oxidation of paracetamol by potassium bromate ($KBrO_3$) in presence of $HClO_4$ acid medium: A kinetic model **116 - 126**
   Reena Patel, Shailesh Kumar, Abhishek Verma and Sheila Srivastava

5. Development of nucleotide-bonded stationary phases for capillary liquid chromatography **127 - 133**
   Lee Wah Lim, Itsuya Kawase, Miki Watanabe, Nobuyuki Takayama and Toyohide Takeuchi

6. Ionic content of Hot spring water in Vajreshwari town of Maharashtra State, India **134 - 142**
   Dipak Shetty and Ganapathy Ramkrishnan

7. Effect of length of Spacer and carbonyl group on quantum yield of pyrene armed Calix[4]arene upon complexation with metal **143 - 163**
   Vrashali S. Kalyani and Dipali D. Malkhede

8. Oxidation of some aliphatic aldehydes by imidazolium dichromate: A kinetic and mechanistic study **164 - 172**
   Itishree Hedau, K. Kanwar, S. Panwar L. Mathur and Vinita Sharma

9. Differences in Triboluminescent Emission Properties of EuD_4TEA synthesized with Europium Nitrate and Acetate **173 - 182**
   Ross S. Fontenot, William A. Hollerman, Stephen A. Williams, Jacque A. Meche, Kamala N. Bhat, and Mohan D. Aggarwal

Conference Alerts **183 - 184**

RNI No. MAHENG/2017/74063
ISSN No. (Print) 2581-5911

Catalytic aspects of Ruthenium in Redox Processes: A brief review

Santosh Bahadur Singh[1] and Praveen Kumar Tandon[2]
[1]Department of Chemistry, National Institute of Technology Raipur, Raipur-492010, C.G., India
[2]Department of Chemistry, University of Allahabad, Allahabad-211002, U.P., India
E-mail: singhsbau2012@gmail.com

Abstract
Transition metals show fascinating ability to catalyze redox processes. Redox processes play a vital role in natural, biological and chemical changes. Out of all the elements of periodic table, ruthenium has the widest range of oxidation states. Since ruthenium has $4d^7 5s^1$ electronic configuration, it oxidation states vary from -2 in $Ru(CO)_4^{2-}$ to +8 in RuO_4. Out of these oxidation states, Ru(III) and Ru(VIII) complexes act as versatile catalysts in organic transformations. Mechanistic path of various ruthenium catalyzed reactions are quite complicated due to formation of different intermediate complexes and the different oxidation states of ruthenium. The mechanism of catalysis alters as per specification of reactions in which the catalysts are used. This review explores the catalytic aspects of ruthenium(III), ruthenium(VIII) and ruthenium nanoparticles in redox reactions.

Keywords: *Catalysis, Ruthenium complex, Ruthenium Nanocatalysis, Redox processes, Transition metals.*

Introduction

Catalysis by transition metals, have made a great contribution to organic synthesis. Since ruthenium has $4d^7 5s^1$ electronic configuration, it has the widest range of oxidation states (from -2 in $Ru(CO)_4^{2-}$ to +8 in RuO_4). Variety of ruthenium complexes have great potential both for catalyzed reactions and synthetic processes. Indeed, until 1980s the reported useful synthetic methods using ruthenium reagents and catalysts were limited to a few reactions which included oxidations with RuO_4, hydrogenation reactions, and hydrogen transfer reactions. But now days, a lot of reactions catalyzed by ruthenium complexes have been reported. $RuCl_3.nH_2O$ is frequently used as a starting material for the preparation of most of these ruthenium complexes and many ruthenium complexes are derived from it under ambient conditions. In addition to the higher economy of ruthenium compared to the other Group 8 transition metals such as rhodium and palladium, there is a larger availability of reactive ruthenium complexes which have proved as highly efficient reagents and catalysts for a variety of organic transformations[1]. This review mainly deals with the catalytic aspects of Ru(III), Ru(VIII) and ruthenium nanoparticles. Ruthenium(III) acts as a catalyst in the oxidation of many organic and inorganic substrates[2-7]. Ruthenium(VIII) catalyzed oxidation of many organics[8-10] have also been reported. Comparison of catalytic activities of ruthenium(III) chloride and ruthenium(VIII) oxide in acidic medium was first reported by Tandon and Krishna[11]. Thus, in the light of these facts the present article provides a brief review of the catalytic activity of

ruthenium(III) chloride and ruthenium(VIII) oxide in organic transformations[12].

Chemistry of Ruthenium

Platinum group elements includes ruthenium (Ru), rhodium (Rh), palladium (Pd), osmium (Os), iridium (Ir) and platinum (Pt) and all these are rare and valuable elements. These are also called as precious metals. Ruthenium (Ru) is one of most valuable elements of platinum group in the periodic table. Ruthenium has an electronic configuration of $1s^2 2s^2 2p^6 3s^2 3p^6 3d^{10} 4s^2 4p^6 4d^7 5s^1$. Redistribution or spacial re-arrangement of electrons within the atoms or molecules is responsible for any alteration in physical or chemical properties of the atoms or molecules. Thus, we can say that the chemistry of any element is directly affected by its electronic configuration. Here, in Table 1, we have summarized various oxidation states of ruthenium and their respective electronic configurations[13].

Table 1: Various oxidation states of ruthenium with their electronic configurations

Oxidation states	Electronic Configurations
-2	[Kr] $4d^{10}5s^0$
0	[Kr] $4d^7 5s^1$
1	[Kr] $4d^7 5s^0$
2	[Kr] $4d^6 5s^0$
3	[Kr] $4d^5 5s^0$
4	[Kr] $4d^4 5s^0$
5	[Kr] $4d^3 5s^0$
6	[Kr] $4d^2 5s^0$
7	[Kr] $4d^1 5s^0$
8	[Kr] $4d^0 5s^0$

The most important applications of ruthenium are for hardening alloys with palladium and platinum, use as an additive for some osmium alloys, use in catalysis and use in catalytic converters in automobiles[13] to reduce the direct emission of harmful nitrogen oxides (NOx), sulphur oxides (SOx) and carbon mono-oxide (CO).

Catalytic aspects of Ruthenium complexes

Catalytic activity of metals or metal complexes mainly depends on two quantities, viz. the electronic and geometric factors. Availability of d-orbitals which can accept electrons from the reactants comes under the category of electronic factors. In general, absence of vacant d-orbitals show negligible amount of catalytic activity because there is no reactive affinity between metal surface and reactants and large number of vacant d-orbital shows very less extent of catalysis due to formation of strong and stable bond between metallic surface and reactants which is non-reversible (reversibility of bond formed between catalyst and reactants during reaction period is an essential condition for catalytic activity of any catalysts) in nature. Therefore, it may be concluded that maximum catalytic activities of any transition metal or metal complexes is to be expected for those metals which possess the smallest number of vacant d-orbitals because this favors easy formation of reversible bonds between catalyst and reactants. Geometric arrangement of catalyst should be spaced in such a way that the transition-state complex has the lowest possible energy which ultimately lowers the activation energy of reaction and favors the catalysis. Electronic factor is more favorable for platinum group catalytic activity. This is second requirement of a catalyst and termed as geometric factor. It is very interesting to know that both these factors are optimal for platinum group metals which accounts for the catalytic activities of this group of metals[12]. Various oxidation states of ruthenium are mainly responsible for its broad spectrum of catalytic activity in redox processes[14, 1].

1. Catalysis by Ruthenium(III)

The ruthenium(III) catalyzed reaction mechanism can be quite complicated due to formation of different intermediate complexes and different aqueous species of ruthenium(III) chloride i.e. $[RuCl_4 (H_2O)_2]^-$, $[RuCl_3 (H_2O)_3]$, $[RuCl_2 (H_2O)_4]^+$ and $[RuCl (H_2O)_5]^{2+}$. Mechanism of catalysis depends on the nature of substrates, oxidants and experimental conditions; it has been shown[15] that metal ions act as catalysts by one of the

Some of most important characteristics, properties and importance of ruthenium[12] are summarized in Scheme 1 as given below:

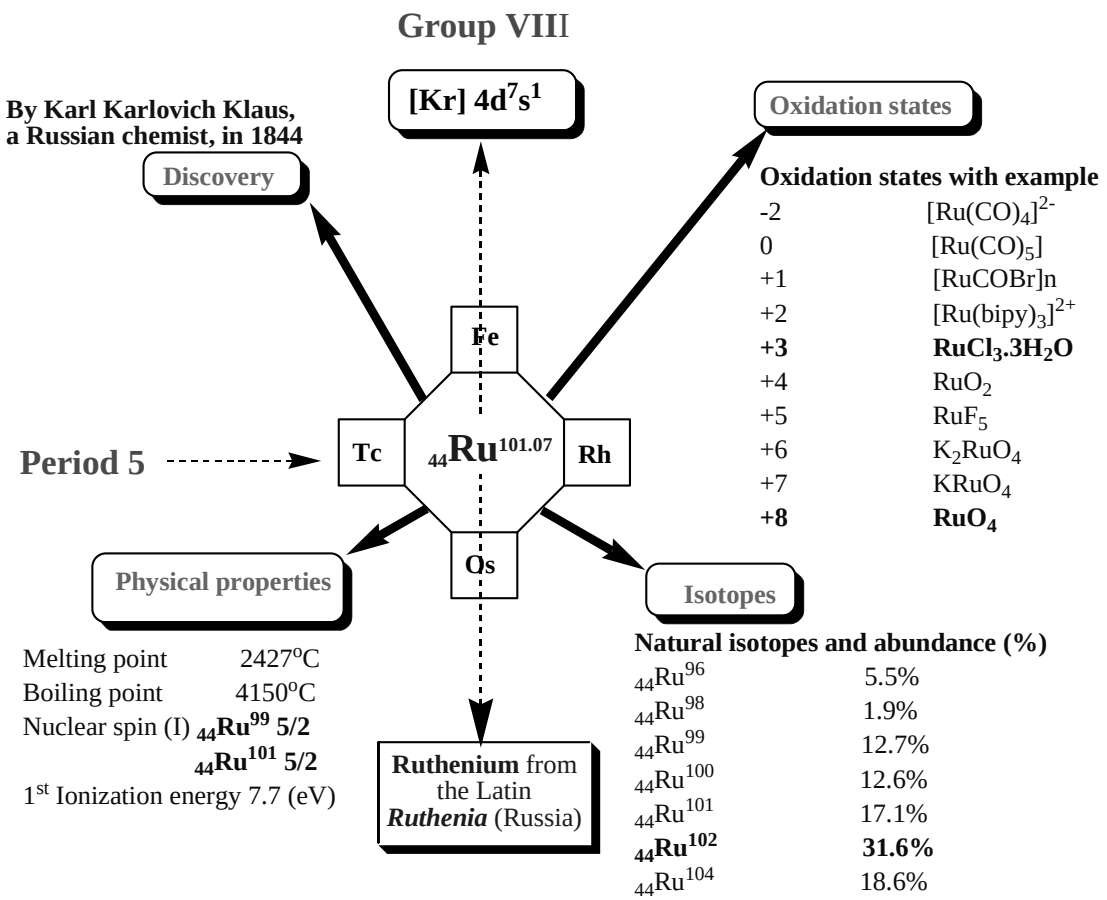

Ruthemium is a hard and white metal. It is a suspected to be a carcinogen and its compounds strongly stain the skin. Ruthenium tetroxide (RuO_4) is volatile, highly toxic and explosive. Its reactivity is due to high electron transfer ability, high Lewis acidity, low redox potential and stabilities of reactive metallic species.

Due to its ability to assume a wide range of oxidation states (from -2 to +8) and its unique coordination geometries, it shows wonderful properties for catalysis.

Scheme 1: A brief summary of Ruthenium Chemistry

different paths such as the formation of complexes with reactants or oxidation of a substrate itself or through the formation of free radicals. In earlier reports[16], it has been reported that Ru(III) forms a complex with the substrate, which gets oxidized to form a Ru(IV)–substrate complex followed by the rapid redox decomposition to regenerate Ru(III). In another report[17], it has been reported that there is formation of a Ru(III)– substrate complex with further cleavage in a concerted manner giving rise to a Ru(I) species, which gets rap-

idly oxidized to regenerate the catalyst. It is also reported that Ru(III) forms a complex with a substrate and is then oxidized with the regeneration of the catalyst.[18]

1.1 Oxidation of alcohols

Ruthenium(III) chloride catalyzed oxidation of alcohols[19] i.e. propanol-1, prpanol-2, butanol-1 and butanol-2 by hexacyanoferrate(III) in mild alkaline medium shows zero order reaction with respect to [oxidant] and first order reaction with respect to [substrate] and $[OH^-]$ at low concentrations. At higher concentration of substrate and hydroxyl ions, the rate of reaction gradually decreases. Increase in pH also retards the rate of reaction. Ruthenium(III) chloride exists in hydrated form[20] as $[Ru(H_2O)_6]^{3+}$. Metal ions of the type $[Ru(H_2O)_6]^{3+}$ are also known to exist as $[Ru(H_2O)_5\,(OH)]^{2+}$ in alkaline medium. Active species of ruthenium form complexes with substrate giving rise to corresponding carbonyl compounds which subsequently get oxidized into the corresponding carboxylic acids. On the basis of experimental observation, the final rate law for oxidation of alcohols may be given as:

$$\frac{-\,d[Fe(CN)_6^{3-}]}{dt} = \frac{2k_1K[Ru^{III}]_T\,[S]}{[OH^-] + K[S] + KK_1[S]^2} \quad .....(1)$$

1.2 Oxidation of glycols

Ruthenium(III) chloride acts as a homogeneous catalyst for oxidation of methyl glycol, ethyl glycol, diethylene glycol and tetraethylene glycol by alkaline hexacyanoferrate(III)[6]. The organic substrate forms anion with hydroxide ion which subsequently reacts with ruthenium(III) species to form complex. The complex, thus formed, slowly disproportionates into ruthenium(III) hydride species and intermediate product which further gets oxidized quickly by taking more of ferricyanide ions into the original ruthenium(III) species and the final oxidation product respectively. Schematic route for conversion into product is given in Scheme-2.

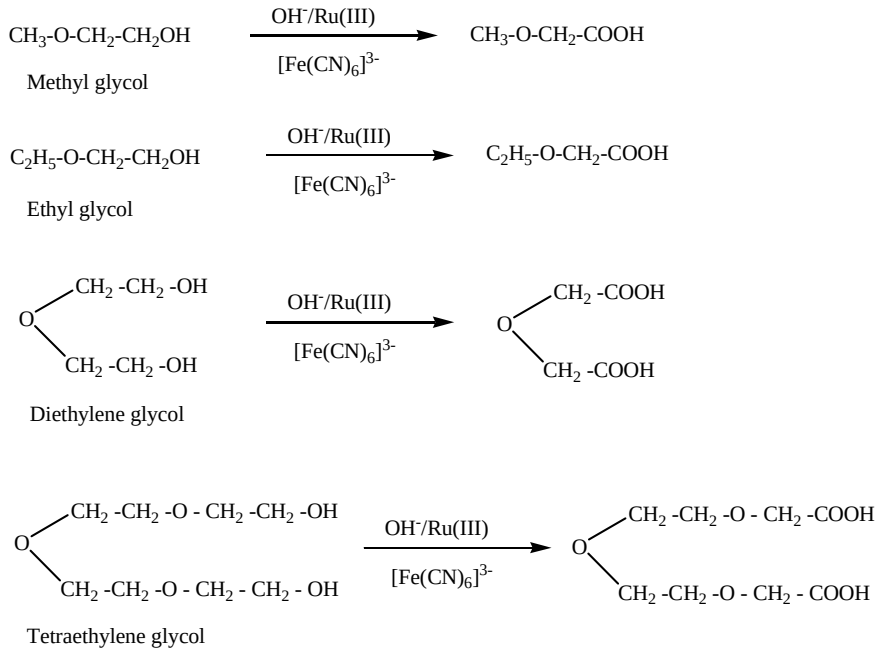

Scheme 2

1.3 Oxidation of cyclic alcohols

Oxidation of cyclic alcohols[5] i.e. cyclopentanol, cyclohexanol and cycloheptanol by cerium(IV) sulphate catalyzed by ruthenium(III) chloride in aqueous acidic medium, shows first order kinetics with respect to cycloalcohols at lower concentration and tend to zero order at higher concentrations of substrate. Rate of reaction shows first order kinetics with respect to ruthenium(III) chloride. Reaction proceeds by formation of activated complex between the protonated cycloalcohols and ruthenium(III) chloride. From the ion exchange technique, it has been confirmed that ruthenium(III) chloride forms $RuCl_6^{3-}$ species[21] in hydrochloric acid medium and its conversion into $[RuCl_5(H_2O)]^{2-}$ takes only a few seconds[22]. Thus, one might assume that $[RuCl_5(H_2O)]^{2-}$ is the only reacting species of ruthenium(III) chloride in acidic medium. The final oxidation products in case of cyclopentanol, cyclohexanol and cycloheptanol are glutaric acid, adipic acid and pimelic acid respectively.

1.4 Oxidation of carbonyl compounds

Oxidation of various aromatic aldehydes[23, 24] i.e. benzaldehyde, 4-chlorobenzaldehyde, 4-nitobenzaldehyde, 2-hydroxybenzaldehyde, 4-hydroxybenzaldehyde, 4-methoxybenzaldehyde, 4-hydroxy-3-methoxybenzaldehyde and cinnamaldehyde by hydrogen peroxide catalyzed by ruthenium(III) chloride in acetic acid medium gives quantitative to moderate yields (substrate:catalyst ratio 85400 to 387500:1). Ruthenium(III) chloride when heated at near reflux temperature with acetic acid gives rise to oxo-centered carboxylate $[Ru_3^{III}(\mu_3\text{-}O)(OOC.CH_3)_6(H_2O)_3]^+$ species, which may undergo reversible redox steps[25]. Trinuclear carboxylates have been reported to be effective catalysts for the aerobic oxidation of aliphatic alcohols[26]. Catalytic activities of these complexes are approximately ten times higher than that of $RuCl_3$ [27]. General conversion route may be given as-

$$\text{RCHO} \xrightarrow[\text{reflux}]{RuCl_3 / H_2O_2 / AcOH} \text{RCOOH}$$

yield = 14 to 100%

where R= C_6H_5-, 4-chloro-C_6H_4-, 4-nitro-C_6H_4-, 2-hydroxy-C_6H_4-, 4-hydroxy-C_6H_4-, 4-methoxy-C_6H_4-, 4-hydroxy-3-methoxy-C_6H_3-, $C_6H_5CH{=}CH$-

1.5 Oxidation of hydrocarbons

Aromatic hydrocarbons[23, 24] viz. anthracene, phenanthrene, naphthalene and methyl benzene have been oxidized to 9,10-anthraquionone, 9,10-phenanthraquinone, a-naphthol and o-, p-, m- cresols respectively by hydrogen peroxide catalyzed by ruthenium(III) chloride in acetic acid medium.

1.6 Oxidation of acids

Ruthenium(III) chloride shows catalytic activity in oxidation of various hydroxy acids[28] i.e. glycolic acid, sodium lactate, malic acid, sodium potassium tartarate and DL-mandelic acid by alkaline hexacyanoferrate(III). The stoichiometry of the reaction was studied by taking hexacyanoferrate(III) in sufficient amount compared to organic substrate and the reaction was studied for a sufficiently long period to ensure complete oxidation of the organic substrate under the experimental condition [hydroxyl acid] > [oxidant]. The total amount of potassium hexacyanoferrate(III) consumed by one mole of organic substrate for its complete oxidation was determined and it was found that in case of glycolic acid and sodium lactate, the equivalence was four while in case of malic acid, potassium sodium tartarate and DL-mandelic acid, the equivalence was two. Final oxidation products were oxalate ions in both the cases. In case of malic acid, potassium sodium tartarate and DL-mandelic acid, the final oxidation products were found to be

malonate ion, tartronate ion and benzaldehyde respectively. Rate of the reaction in different substrates was found to be in the order, malic acid > DL-mandelic acid > glycolic acid > sodium lactate > potassium sodium tartarate. Reaction proceeds through the formation of an activated complex between the substrate anion and ruthenium(III) species. The complex, thus formed, slowly breaks up giving ruthenium(III) hydride species and the intermediate product. This ruthenium(III) hydride species and intermediate product quickly get oxidized to the original ruthenium(III) hydroxy species and final oxidation product by incorporating more hexacyanoferrate(III) ions in the subsequent steps. The probable conversion route is given in Scheme 3.

$$\underset{\text{Glycollic acid}}{HOCH_2.COOH} \xrightarrow[K_3[Fe(CN)_6]]{RuCl_3 / OH^-} \underset{\text{Oxalate ion}}{^-OOC.COO^-}$$

$$\underset{\text{Sodium lactate}}{CH_3CH(OH).COONa} \xrightarrow[K_3[Fe(CN)_6]]{RuCl_3 / OH^-} \underset{\text{Oxalate ion}}{^-OOC.COO^-} + CO_2$$

$$\underset{\text{Malic acid}}{HOOC.CH_2.CH(OH).COOH} \xrightarrow[K_3[Fe(CN)_6]]{RuCl_3 / OH^-} \underset{\text{Malonate ion}}{^-OOC.CH_2.COO^-} + CO_2$$

$$\underset{\text{Potassium sodium tartarate}}{NaOOC.CH(OH).CH(OH).COOK} \xrightarrow[K_3[Fe(CN)_6]]{RuCl_3 / OH^-} \underset{\text{Tartronate ion}}{^-OOC.CH(OH).COO^-} + CO_2$$

$$\underset{\text{DL-Mandelic acid}}{C_6H_5.CH(OH).COOH} \xrightarrow[K_3[Fe(CN)_6]]{RuCl_3 / OH^-} \underset{\text{Benzaldehyde}}{C_6H_5.CHO}$$

Scheme 3

1.7 Oxidation of inorganic substrates

Ruthenium(III) chloride also catalyzes the oxidation of inorganic substrate such as iodide[29, 30] by hexacyanoferrate(III) acidic medium. It has been reported that in hydrochloric acid medium[21], ruthenium(III) chloride forms $RuCl_6^{3-}$ species. Using the ion – exchange technique, it has been confirmed that the half-life of loss of chloride from $[RuCl(H_2O)_5]^{2-}$ is of the order of a year, while the aquation of $RuCl_6^{3-}$ to $[RuCl_5(H_2O)]^{2-}$ takes only few seconds. Thus, one might safely assume that $[RuCl_5(H_2O)]^{2-}$ is the actual reacting species of ruthenium(III) chloride in acidic medium for the oxidation of potassium iodide. In this reaction, acid itself catalyzes the reaction between iodide and hexacyanoferrate(III) hence ruthenium(III) chloride further catalyzes the reaction as a co-catalyst. Reactions studied

separately in the presence as well as absence of $RuCl_3$ under similar conditions were found to follow second-order kinetics with respect to (I^-), while the rate showed first order kinetics with respect to $[Fe(CN)_6]^{3-}$, $[RuCl_3]$, and $[H^+]$. Mechanistic path for oxidation of iodide catalyzed by hydrogen ion and hydrogen ions with ruthenium trichloride is given in scheme 4.

$$H_2SO_4 + 2KI \underset{}{\overset{K'_1}{\rightleftharpoons}} \underset{(C_1)}{HI_2^- + HSO_4^- + 2K^+}$$

$$HI_2^- + Fe(CN)_6^{3-} \underset{k'_{-1}}{\overset{k'_1}{\rightleftharpoons}} \underset{(C_2)}{Fe(CN)_6^{4-} + [I\cdots H\cdots I]}$$

$$C_2 \xrightarrow[\text{slow}]{k'} H^+ + I^- + I$$

A- In absence of $RuCl_3$

$$H_2SO_4 + 2KI \underset{}{\overset{K'_1}{\rightleftharpoons}} \underset{(C_1)}{HI_2^- + HSO_4^- + 2K^+}$$

$$HI_2^- + Fe(CN)_6^{3-} \underset{k'_{-1}}{\overset{k'_1}{\rightleftharpoons}} \underset{(C_2)}{Fe(CN)_6^{4-} + [I\cdots H\cdots I]}$$

$$C_2 + [RuCl_5(H_2O)]^{2-} \underset{k_{-1}}{\overset{k_1}{\rightleftharpoons}} [\text{complex } C_3]^{2-}$$

$$[C_3]^{2-} \xrightarrow[\text{slow}]{k} [RuCl_5(H_2O)]^{2-} + H^+ + I^- + I$$

B- In presence of $RuCl_3$

Scheme 4

Some of the other recent and important Ru(III) catalyzed reactions are summarized in Table 2.

Table 2: Ruthenium(III) catalyzed some important redox reactions

Ruthenium(III) catalyzed redox reactions		
Various redox processes	**Reactions**	**References**
Oxidation of acids	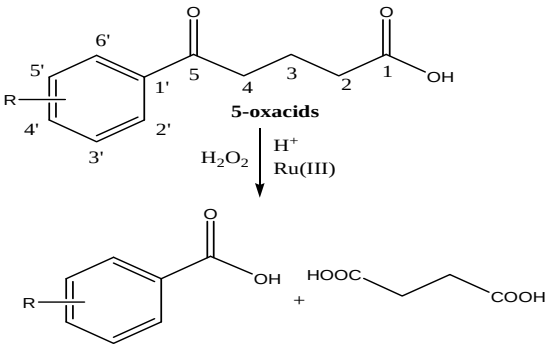	31
Oxidation of inorganic compounds	$SCN^- + H_2O_2 \xrightarrow{Ru(III)} SO_4^{--}/OCN^-$	32

Oxidation of water	$2H_2O + 4Ce^{IV}$ $\xrightarrow{Ru(III)}$ $4H^+ + 4Ce^{III} + O_2$	33
Selective reduction of dienes/ polyenes	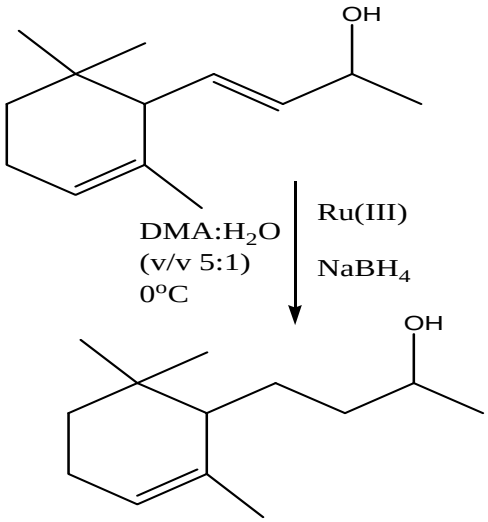	34
Oxidation of antibiotic drug	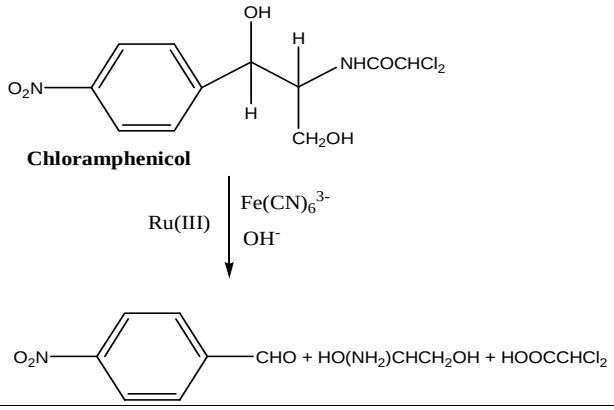	35
Oxidation of carbo-hydrate	$C_5H_{10}O_5 + OH^-$ L(+) arabinose Periodate $[IO_4^-]$ $\xrightarrow{Ru(III)}$ $C_4H_{10}O_5 + HCOOH$	36

2. Catalysis by Ruthenium (VIII)

Oxo-ruthenium complexes can be used to carry out a number of useful organic transformations. In a catalytic role some of them are particularly efficient for the mild and selectivc oxidation of alcohols, tolerating the presence of sensitive functional groups often attacked by other oxidizing reagents. The only well-defined oxo-complex of ruthenium(VIII) oxide is RuO_4. Over the past few decades, the use of ruthenium(VIII) oxide as a catalyst in organic transformation has become very important. The present review emphasizes the recent developments in the catalytic application of ruthenium(VIII) oxide in the oxidation of alcohols, diols, glycols and hydroxy acids. With the ruthenium catalysts so far developed, the oxidation of alcohols is effected with the greatest efficiency. Although this reaction is one of the commonest of organic transformations, few reagents will effect such reactions catalytically and without attacking sensitive linkages in the R group.

2.1 Oxidation of alcohols

RuO_4 gives $RuO_4(OH)_2^{2-}$ in alkaline medium[37] which may be assumed as reactive species in ruthenium tetroxide catalyzed oxidation of methanol, ethanol, propanol and butanol by hexacyanoferrate(III) in alkaline medium[8, 9]. Rate of reaction shows zero order kinetics with respect to $[Fe(CN)_6]^{3-}$ and direct proportionality with [catalyst] and [substrate] at low concentrations. Rate of reaction increases with increase in $[OH^-]$ at low concentrations and reaction is retarded at higher concentrations in case of propanol and butanol while in case of methanol and ethanol it shows inverse relation. In the light of these kinetic observations, the authors have proposed the formation of a reactive species of ruthenium(VIII) oxide complex with substrate molecules. At this stage, the hydride ion transfer takes place. Final oxidation products, viz. methanoic acid, ethanoic acid, propanoic acid and butanoic acid were reported in case of methanol, ethanol, propanol and butanol respectively. The general conversion route is given below:-

$$RCH_2OH \xrightarrow[{[OH^-]}]{RuO_4 / Fe(CN)_6^{3-}} RCOOH$$

2.2 Oxidation of glycols

Ruthenium(VIII) oxide catalyzed oxidation of glycols[8] i.e. hexylene glycol, diethylene glycol, triethylene glycol and glycerol by alkaline hexacyanoferrate(III) proceeds through $RuO_4(OH)_2^{2-}$ as reactive species. Kinetic data shows zero order with respect to [oxidant], inverse proportionality with respect to [OH-], first order with respect to [hexylene glycol] and [glycerol] while in case of the remaining two substrates, after showing first order kinetics initially, the reaction becomes independent of concentration at higher concentrations. Reaction proceeds through formation of complex between substrate and ruthenium(VIII) oxide reactive species.

2.3 Oxidation of diols

Ruthenium(VIII) oxide acts as a homogeneous catalyst in oxidation of various diols[38-39, 10], viz. ethan-1,2-diol, propan-1,2-diol, butan-1,2-diol, butan-1,3-diol, propan-1,3-diol,butan-1,4,-diol, pentan-1,5-diol, 2-methyl pentan-2,4-diol and hexan-1,6-diol by hexacyanoferrate(III) in aqueous alkaline medium. Reaction proceeds through the formation of a complex between alkoxide obtained from diols and ruthenium(VIII) oxide reactive species. The conversion path is given in Scheme 5.

2.4 Oxidation of acids

Ruthenium(VIII) oxide also catalyzes the oxidation of various sodium salts of hydroxyl acids[40], viz. glycolic acid, lactic acid, malic acid, tartaric acid and DL-mandelic acid by alkaline hexacyanoferrate(III). Rates of oxidation of these hydroxyl acids were compared when one of the hydrogen attached to α-carbon is successively replaced by the methyl and phenyl groups or in dicarboxylic acids when hydrogen atoms attached with both α and α' carbons are replaced by hydroxyl groups. Rates of reaction in different substrates was found to follow the sequence mandelic acid > glycolic acid > lactic acid > tartaric acid > malic acid.

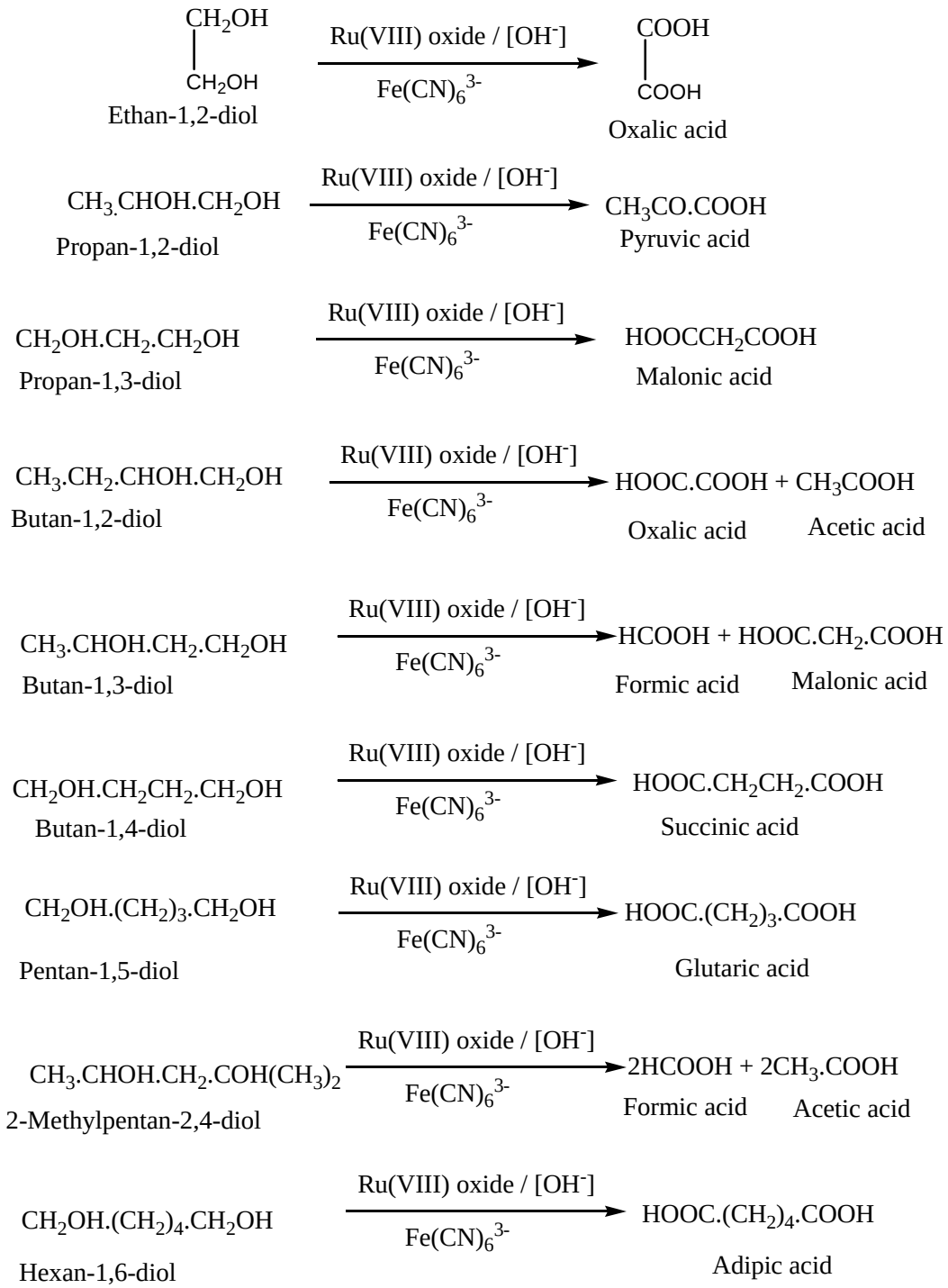
CH2OH
CH2OH
Ethan-1,2-diol
Ru(VIII) oxide / [OH-]
Fe(CN)6 3-
COOH
COOH
Oxalic acid
CH3.CHOH.CH2OH
Propan-1,2-diol
Ru(VIII) oxide / [OH-]
Fe(CN)6 3-
CH3CO.COOH
Pyruvic acid
CH2OH.CH2.CH2OH
Propan-1,3-diol
Ru(VIII) oxide / [OH-]
Fe(CN)6 3-
HOOCCH2COOH
Malonic acid
CH3.CH2.CHOH.CH2OH
Butan-1,2-diol
Ru(VIII) oxide / [OH-]
Fe(CN)6 3-
HOOC.COOH + CH3COOH
Oxalic acid
Acetic acid
CH3.CHOH.CH2.CH2OH
Butan-1,3-diol
Ru(VIII) oxide / [OH-]
Fe(CN)6 3-
HCOOH + HOOC.CH2.COOH
Formic acid
Malonic acid
CH2OH.CH2CH2.CH2OH
Butan-1,4-diol
Ru(VIII) oxide / [OH-]
Fe(CN)6 3-
HOOC.CH2CH2.COOH
Succinic acid
CH2OH.(CH2)3.CH2OH
Pentan-1,5-diol
Ru(VIII) oxide / [OH-]
Fe(CN)6 3-
HOOC.(CH2)3.COOH
Glutaric acid
CH3.CHOH.CH2.COH(CH3)2
2-Methylpentan-2,4-diol
Ru(VIII) oxide / [OH-]
Fe(CN)6 3-
2HCOOH + 2CH3.COOH
Formic acid
Acetic acid
CH2OH.(CH2)4.CH2OH
Hexan-1,6-diol
Ru(VIII) oxide / [OH-]
Fe(CN)6 3-
HOOC.(CH2)4.COOH
Adipic acid

Scheme 5

3. Ruthenium catalysis in special reference to nanocatalysis

At present, Nanocatalysis is the most promising field of research. At nanoscale size, large number of atoms are exposed on the surface resulting in increase in the surface activity and consequently the catalytic efficiency in a large number of chemical transformations. Ruthenium is a less expensive catalyst as compared to Gold, Palladium, Platinum and Rhodium[41, 42]. Ruthenium at nano size shows excellent catalytic activity for redox reactions[43]. In recent years, bi-metallic and tri-metallic nanocomposites have attracted considerable attention as highly active, eco-friendly and relatively economical catalysts for chemical transformations[44]. Recently, Veerakumar P. et.al.[45] published a broad review of catalytic aspects of Ruthenium nano particles in redox reactions. This review is mainly focused on synthesis, characterization and application of ruthenium nanoparticles as catalyst in redox reactions of heteroatom containing organic compounds and hydrogen peroxide (as a green oxidant). The review mainly concentrates on catalytic application of ruthenium nanoparticles (RuNPs) as a catalyst in oxidation of sulfides and amines, organic substrates and reduction reactions, reduction of sulfoxides and N-oxides. Due to its high surface to volume ratio, RuNps show good catalytic activity. Scheme 6 shows the importance of ruthenium nano particles catalysis in redox processes.

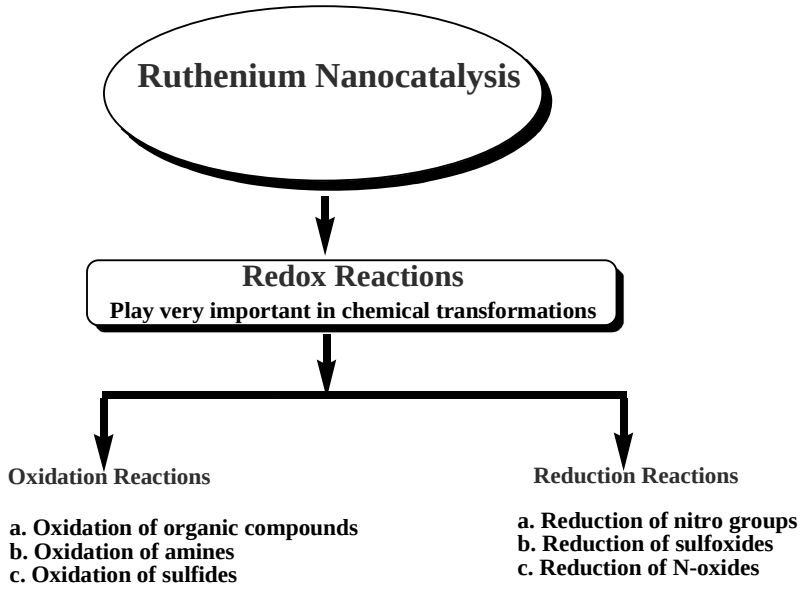

Scheme 6: Ruthenium nanocatalysis in redox processes

Conclusions

This review provides a survey of the catalytic aspects of Ru(III), Ru(VIII) and ruthenium nanoparticles in organic transformations. Ruthenium chemistry has progressed exponentially in the past decade and a large number of fundamental characteristics of ruthenium complexes have been reviewed. Ruthenium based redox catalysis is developing fast from an economic point of view. From the detoxification oxidation with ruthenium tetroxide as applied to the destruction of dioxins to the direct oxidation of methane, the research on ruthenium and its complexes is fast growing. Ruthenium based oxidation catalysts are expected to play a major role in finding renew-

able energy sources and efficient water splitting catalysts for the generation of oxygen.

Acknowledgement

Financial support from Council of Scientific and Industrial Research (CSIR), New Delhi {01(2538)/11/RMR-II} is gratefully acknowledged. Authors would like to thank Professor (Mrs.) Fahmida Khan, Head, Department of Chemistry, National Institute of Technology Raipur, Raipur, India for her support and inspiration.

References

1. Murahashi S.-I., 2004, Ruthenium in Organic Synthesis, WILEY-VCH VERLAG GmbH & KGaA, Weinheim.

2. Shivananda K. N., Lakshmi B., Jagdeesh R. V., Puttaswamy and Mahendra K. N., 2007, *Appl. Catal., A,* **326,** 202.

3. Puttaswamy, Shubha J. P. and Jagadish R. V., 2007, *Transition Met. Chem.,* **32**, 991.

4. Singh M.P., Singh H.S. and Verma M.K., 1980, *J. Phys. Chem.,* **84,** 256.

5. Tandon P.K., Manibala, Singh H.S. and Krishna B., 1984, *Z. Phys. Chemie, Leipzig,* **265,** 609.

6. Manibala, Tandon P.K. and Krishna B., 1985, *Z. Phys. Chemie, Leipzig,* **266,** 1153.

7. Tandon P.K., Mehrotra A., Singh A.P. and Singh M.P., 1983, *Proc. Indian Natn. Sci. Acad.,* **59A**, 87.

8. Singh H.S., Tandon P.K. and Singh K.K., 1994, *J. Indian Chem. Soc.,* **71**, 675.

9. Singh M.P., Singh R.M., Tandon P.K., Mehrotra A. and Thakur P., 1988, *J. Indian Chem. Soc.,* **LXV**, 720.

10. Singh H.S., Tandon P.K., Singh B.K. and Mehrotra A., 1990, *Proc. Indian Nats. Sci. Acad.,* **56A (5),** 447.

11. Tandon P.K. and Krishna B., 1985, *Kinetics and Catalysis (USSR),* **26,** 607.

12. Livingstone S. E., 1975, The Chemistry of Ruthenium, Rhodium, Palladium, Osmium, Iridium and Platinum in Comprehensive Inorganic Chemistry, Pergamon Press Ltd., Headington Hill Hall, Oxford, OX3 OBW, England.

13. Seddon E.A. and Seddon K.R., 1984, The Chemistry of Ruthenium in Topics in Inorganic and General Chemistry by Clark R.J.H., ELSEVIER SCIENCE PUBLISHERS B.V. Molenwerf 1 P.O. Box 211, 1000 A E Amsterdam, The Netherlands.

14. Bruneau C. and Dixneuf P. H., 2004, Ruthenium Catalysts and Fine Chemistry, Springer-Verlag, Berlin.

15. Singh A. K., Srivastava S., Srivastava J., Srivastava R. and Singh P., 2007, *J. Mol. Catal. A: Chem.,* **278,** 72.

16. Sondu S., Sethuram B. and Rao T. N., 1983, *J. Indian Chem. Soc.,* **60**, 198.

17. Panda H. P. and Sahu B. D., 1977, *Indian J. Chem.,* **15,** 1066.

18. Tegginamath V., Hiremath C. V. and Nandibewoor S. T., 2007, *J. Phys. Org. Chem.,* **20,** 55.

19. (a) Singh M.P., Tandon P.K., Mehrotra A., Gupta A. and Singh R., 1990, *Indian J. Chem.* **29A**, 590, (b) Singh M.P., Tandon P.K., Mehrotra A., Gupta A., Singh J.P. and Singh V.S., 1990, *J. Indian Chem. Soc.,* **67,** 424.

20. Connick R.E. and Fine D.E., 1960, *J. Am. Chem. Soc.,* **82,** 4187.

21. (a) Cady H.H. and Connik R.E., 1958, *J. Am. Chem. Soc.* **80**, 2646, (b) Connik R.E. and Fine D.A., 1961, *ibid* **83**,3414, (c) Connik R.E. and Fine D.A., 1960, *ibid* **82**, 4187.

22. (a) Helpern J., James B.R. and Kemp A.L.W., 1961, *J. Am. Chem. Soc.* **83**, 4097, (b) Harrod J.E., Cocone S. and Helpern J., 1961, *Can. J. Chem.* **39**, 1372.

23. Tandon P.K., Baboo R., Singh A.K. and Gayatri, 2006, *Appl. Organometal. Chem.* **20,** 20.

24. Tandon P.K., Baboo R., Singh A.K., Gayatri and Purwar M., 2005, *Appl. Organometal. Chem.* **19**, 1079.

25. Murahashi S-I., Komiya N., Oda Y. and Kuwabara T.T., 2000, *J. Org. Chem.* **65,** 9186.

26. Bilgrien C., Davis S. and Drago R.S., 1987, *J. Am. Chem. Soc.*, **109,** 3786.

27. Naota T., Takaya H. and Murahashi S-I.,1998, *Chem. Rev.*, **98,** 2599.

28. Tandon P.K., Mehrotra A., Singh A.P. and Singh M.P., 1993, *Proc. Indian Natn. Acad.*, **59A,** 87.

29. Tandon P.K., Mehrotra A., Singh A.K., Baboo R. and Dwivedi P.B., 2004, *Int. J. Chem Kinet.*, **36**, 545.

30. Tandon P.K., Mehrotra A., Srivastava M., Dhusia M. and Singh S.B., 2007, *Trans. Metal Chem.*, **32,** 74.

31. Devi S. S., Krishnamoorthy P. and Muthukumaran B., 2014, *Advances in Physical Chemistry* Hindawi Publishing Corporation **Volume 2014**, Article ID 879608, pp1-14.

32. Chatterjee D., Paul B. and Mukherjee R., 2013, *Dalton Trans.*, 42, 10056.

33. Murakami M., Hong D., Suenobu T., Yamaguchi S., Ogura T. and Fukuzumi S., *J. Am. Chem. Soc.*, 2011, **133 (30)**, 11605.

34. Babler J. H., Ziemke D. W. and Hamer R. M., 2013, *Tetrahedron Letters* **54**, 1754.

35. Meti M. D., Byadagi K. S., Nandibewoor S. T. and Chimatadar S. A., 2014, *Monatsh. Chem.* **145**, 1561.

36. Singh A. K., Chaurasia N., Rahmani S., Srivastava J. and Singh B., 2004, Catalysis Letters **95**, 135.

37. Connik R.E. and Harley C.R., 1952, *J. Am. Chem. Soc.*, **74,** 5012.

38. Verma M.K., Tandon P.K. and Singh M.P., 1987, *Z. Phys. Chemie., Leipzig* 268(3), S, 565.

39. Verma M.K., Tandon P.K., Singh H.S. and Singh M.P., 1986, *Z. Phys. Chemie., Leipzig* **267(6)**, S, 1219.

40. Tandon P.K., Singh A.K., Baboo, R.; Kumar S., Saxena A.K. and Singh M.P., 2005, *Oxidation Commun.* 28(3), 611.

41. (a) Liu J., Bai P. and Zhao X. S., 2011, *Phys. Chem. Chem. Phys.* **13**, 3758; (b) Zhao C., Luo C., Dyson P. J., Liu H. and Kou Y., 2006, *J. Am. Chem. Soc.* **128**, 8714; (c) Kobayashi H., Matsuhashi H., Komanoya T., Hara K. and Fukuok A., 2011, *Chem. Commun.*, **47,** 2366.

42. Sarmah P. P. and Dutta D. K., 2012, *Green Chem.* **14**, 1086.

43. (a) Mori S., Takubo M., Makida K., Yanase T., Aoyagi S., Maegawa T., Monguchi Y. and Sajiki H., 2009, *Chem. Commun.*, 5159; (b) Kantam M. L., Reddy R. S., Pal U., Sudhakar M., Venugopal A., Ratnam K. J., Figueras F., Chintareddy V. R. and Nishina Y., 2012, *J. Mol. Catal. A: Chem.* **359**, 1; (c) Yamaguchi K. and Mizuno N., 2002, *Angew. Chem. Int. Ed.* **41**, 4538; (d) Yamaguchi K. and Mizuno N., 2003, *Chem. Eur. J.* **9,** 4353; (e) Ho C.

M., Yu W. Y. and Che C. M., 2004, *Angew. Chem. Int. Ed.* **43,** 3303.

44. (a) Chen S., Zhang H., Wu L., Zhao Y., Huang C., Ge M. and Liu Z., 2012, *J. Mater. Chem.* **22**, 9117; (b) Zhou C., Wang H., Peng F., Liang J., Yu H. and Yang J., 2009, *Langmuir* **25**, 7711; (c) Haijie S., Zhihao C., Wei G., Xiaoli Z., Zhongyi L. and Shouchang L., 2011, *Chin. J. Chem.* **29**, 369; (d) Modibedi R. M., Masombuka T. and Mathe M. K., 2011, *Inter. J. Hyd. Eng.* **36**, 4664; (e) Park K. C., Jang I. Y., Wongwiriyapan W., Morimoto S., Kim Y. J., Jung Y. C., Toyad T. and Endo M., 2010, *J. Mater. Chem.* 20, 5345.

45. Veerakumar P., Ramdass A. and Rajagopal S., 2013, *Journal of Nanoscience and Nanotechnology*, **13**, 4761.

RNI No. MAHENG/2017/74063
ISSN No. (Print) 2581-5911

Computer colour matching data of synthesized monoazo disperse dyes, their dyeing performance on polyester fiber and antimicrobial activity

Sandip K. Patel[1], Pratixa K. Patel[2] and G. M. Malik[1].
[1]Department of Chemistry, Navyug Science College, Surat-395009, Gujarat, India
[2]Department of Chemistry, Narmada College of Science and Commerce, Zadeshwar, Bharuch-392011, India
E-mail: sandip942@yahoo.com, gmmalik2010@gmail.com

Abstract
Different monoazo disperse dyes from N-(3-methylphenyl)-2-((4-(3'-nitro phenyl)-1, 3-thiazol-2-yl)amino)acetamide have been synthesized using different diazotized aryl amines. These were characterized using elemental analysis, ^{1}H Nuclear Magnetic Resonance (NMR) and Infra Red spectra (IR). The visible absorption spectra of synthesized dyes were recorded in dimethyl formemide (DMF). Their dyeing performance on polyester fiber was assessed and fastness properties of these dyes were evaluated by applying them to polyester fibres. These dyes showed moderate anti-bacterial and anti-fungal activities. The computer colour matching data (L, a*, b*, C*, H* and K/S) was assessed.*

Keywords: *2-Amino-4-(3'-nitro phenyl) thiazole, antimicrobial activity, chloroacetylchloride, dyeing performance, Infra Red Spectra (IR), 3-methyl aniline, ^{1}H Nuclear Magnetic Resonance (NMR).*

Introduction

Disperse dyes are organic colorants with less water solubility which are applied in colloidal dispersions to hydrophobic textile fibers to produce desired colour[1,2]. 2-amino thiazole derivatives[3-7] have been utilized as heterocyclic components for many disperse dyes since long. Synthesized monoazo disperse dyes based on chloroacetyl chloride derivatives[8-10] have been reported. It was our main objective to synthesize monoazo disperse dyes based on 2-chloro-N-(3-methylphenyl) acetamide. The synthesized monoazo disperse dyes exhibited moderate to good light, washing and sublimation fastness. The synthesized dyes were screened for antibacterial activity against *Staphylococcus aureus, Escherichia coli*, *Bacillus subtilis* and *Pseudomonas aeruginosa* and antifungal activity against *Candida albicans*[11-16]. The computer colour matching data (L*, a*, b*, C*, H* and K/S) was also studied.

Materials and Methods

All reagents were of analytical reagent grade and were used without further purification. All the synthesized compounds were characterized by spectral analysis. The melting points of the compounds were determined using Stuart SMP 10 melting point apparatus and are uncorrected. The purity of dyes was determined by thin-layer chromatography (TLC) using silica gel-G coated Al-plates and spots were visualized under UV radiation. Infra Red spectra (IR) were recorded on FTIR spectrophotometer Perkin Elmer using KBr pellets. ^{1}H Nuclear

Magnetic Resonance (NMR) spectra were obtained on Bruker Avance-II 400 NMR spectrometer using dimethyl sulphoxide (DMSO) solvent and tetra methyl silene (TMS) as internal reference (chemical shifts in δ ppm). Elemental analysis was carried on Perkin Elmer (USA) 2400 series instrument. The synthesized dyes were screened for their antimicrobial activity using the Kirby-Bauer method. All the compounds were screened for their in vitro antimicrobial activity against bacterial strains, *Escherichia coli, Pseudomonas aeruginosa, Staphylococcus aureus, Bacillus subtilis* and fungi *Candida albicans* at 50μg/mL concentration using Ciprofloxacin and Flucanazole as standards respectively. A convenient laboratory method was used for dyeing polyester at high temperature (130°C) and high pressure (24-30psi.)[17]. The fastness to light, wash and sublimation was assessed in accordance with ISO 105[18-22]. The dye bath exhaustion (%E) of the dyed fiber was determined.

Preparation of 2-amino-4-(3'-Nitro phenyl) thiazole (1)

In 250 mL mixture of m-nitro acetophenone (16.5 g, 0.1 mole) and thiourea (7.6 g, 0.2 mole) bromine (23.97 g, 0.15 mole) was added drop wise and the reaction mixture was heated on water bath for 8-10 hours, cooled and the contents were washed with water. The residue left was dissolved in boiling water and filtered. The filtrate was made alkaline by addition of liquor ammonia. The solid **(1)** thus obtained was filtered, dried and recrystalized from ethanol.

Yield 81%, M.P.: 185-188°C IR (KBr $cm^{-1)}$ 3444 (N-H str.), 3287, 3113 (C-H str.), 1512 (NO_2 str.), 713 (C-S str.), 1339 (C-N str.).

Preparation of 2-chloro-N-(3-methylphenyl) acetamide (2)

3-methyl aniline (2.14 g, 0.02 mole) in 15 mL glacial acetic acid was taken in a 250 mL round bottom flask and cooled to 0-5°C. Chloroacetyl chloride (3.39 mL, 0.02 mole) was slowly added with continuous stirring. When addition was completed, the reaction mixture was stirred at room temperature for 3 hours. The reaction mixture was put into ice-cold 20% sodium acetate solution. The solid **(2)** thus obtained was filtered, washed with water, dried and recrystalized from 80% ethanol solution.

Yield: 90%, M.P.: 86-88°C. IR (KBr cm^{-1}) 3420 (N-H str.), 3115 (C-H str.), 2980 (CH_3), 1645 (C=O str.), 715 (C-Cl str.).

Preparation of N-(3-methylphenyl)-2-((4-(3'-nitro phenyl)-1, 3-thiazol-2-yl) amino acetamide (3)

2-chloro-N-(3-methylphenyl)acetamide **(2)** (1.83 g, 0.01 mole) and 2-amino-4-(3'-nitro phenyl) thiazole) **(1)** (2.21 g, 0.01 mole) in 30 mL glacial acetic acid was taken in a 250 mL round bottom flask, then K_2CO_3 (6.9 g, 0.05 mole) was added slowly into the reaction mixture. When addition was complete, the reaction mixture was heated for 6 hours at 85-90°C. The reaction mixture was put into ice-cold 20% sodium acetate solution. The solid **(3)** thus obtained was filtered and washed with water, dried and recrystalized from ethanol.

Yield: 80%, M.P.: 155-160°C. IR (KBr cm^{-1}) 3410 (N-H str.), 3120 (C-H str.), 2983 (CH_3 str.), 1642 (C=O str.), 1514 (NO_2), 1470 (C-S-C str.), 750(C-S str.).

Diazotization and coupling reaction (SN_1-SN_{15})

Different aryl amines (0.01 mole) were dissolved in HCl (5 mL, 50%) and cooled to 0-5°C in an ice-bath. A solution of sodium nitrite (0.01 mole, 0.69 g) in water (5 mL) previously cooled to 0-5°C was added over a period of 10 minutes with continuous stirring and maintaining the temperature at 0-5°C and further the reaction mixture was stirred for an hour. The excess of nitrous acid was then removed using sulfamic acid. The resulting solution was used for coupling reaction.

N-(3-methylphenyl)-2-((4-(3'-nitrophenyl)-1,3-thiazol-2-yl) amino) acetamide **(3)** (0.01mole) was dissolved in glacial acetic acid (30 mL) and cooled below 5°C in an

ice-bath. The above mentioned diazonium chloride solution was added drop wise over a period of 10-15 minutes, maintaining the pH at 7.0 to 7.5 by simultaneous addition of aqueous sodium acetate (10% w/v), and further the reaction mixture was stirred for 3 hours at 0-5°C. The solid dye obtained was filtered, washed with water to remove acid completely, dried and recrystalized from acetone.

Results and Discussion

Spectral Properties of Dyes

The visible absorption spectra of dyes were recorded in dimethyl formamide (DMF) and their results are shown in Table 1. From (Table-1), it is clear that the value of λ_{max} depends on the nature and position of coupling component used.

Infrared spectra (IR) of synthesized dyes are described in Table 3. Infra Red Spectra (IR) of dye (SN_7) showed N-H stretching vibrations at 3448 cm^{-1}, C-H stretching vibrations at 3078 cm^{-1} (aromatic), C-H stretching vibrations at 2991, 2725 cm^{-1} CH_3 (Asymmetric and symmetric stretching) C=O stretching vibrations at 1643 cm^{-1}, N=N stretching vibrations at 1577 cm^{-1} and C-S-C stretching vibration at 1469 cm^{-1}. C-S stretching in thiazole at 831 cm^{-1}, 1533 cm^{-1} is due to presence of NO_2 group. The ^1H Nuclear Magnetic Resonance (NMR) data of the dyes is given in Table 3. The ^1H Nuclear Magnetic Resonance (NMR) spectra of all dyes were recorded in dimethyl sulphoxide (DMSO). The compound (SN_1) exhibited multiplets in the region at δ 7.08-8.72 ppm for 13 aromatic protons. The methylene group attached to carbonyl group showed singlet at δ 3.79 ppm. The presence of –NH in thiazole and aromatic ring showed singlet at δ 4.09 ppm and δ 9.15 ppm, respectively. The methyl group showed singlet at δ 2.19 ppm.

Dyeing Properties

Dyeing method

All the synthesized dyes SN_1-SN_{15} were applied on polyester fabric in 2% depth by HTHP method at high temperature (130°C) and high pressure (24-30psi). Glycerin-bath high temperature beaker dyeing machine was used. 10 mL DMF was added and dispersion of the dye was produced by dissolving the appropriate amount of dye (2% depth) and which was added dropwise with continuous stirring to the dyebath (liquor ratio 20:1) containing 1% Setamol WS (BASF) as anionic dispersing agent. The pH of dye solution was adjusted to 4 to 5 using aqueous acetic acid. Previously wetted-out polyester fabric pieces were added. Dyeing was continued by raising the dyebath temperature upto 130°C at a rate of 2°C /minute and this temperature was maintained for 1 hour under (24-30 psi) pressure. After completion of the process, cooling upto 50°C was done and the dyed fabric pieces were rinsed with cold water and reduction was completed under the conditions: (1 g/L sodium hydroxide, 1 g/L sodium hydrosulphite, 10 minutes at 80°C). The dyed sample was rinsed with cold water and finally air-dried.

Fastness Properties

Light Fastness

The light fastness study was carried out using a xenon light fastness tester having a xenon arc lamp. The dyed sample was assessed by comparing change in colour of specimen with standard dye patterns of specific rating (1 to 8). The higher the rating, the better is the light fastness. The results are given in Table 2.

Wash Fastness

Fastness to washing was assessed under following conditions: the washing solution contained soap 5 g/L and anhydrous sodium carbonate 2 g/L, washing temperature was 95°C, the duration of washing was 30 minutes, and the material to liquor ratio was 5:1. After washing, the specimen was removed and rinsed with hot water (35°C) until the rinsed water showed no alkalinity. It was dried in air. The effect of the change in colour was expressed and defined by reference to grey scale. The results are given in Table 2.

Table 1 Physical properties of Dyes

Dye No.	R	Molecular Formula	Molecular Weight g/mole	Yield %	M.P. °C	λ_{max} (nm)	Nitrogen (%)	
							Found	Calcd.
SN_1	H-	$C_{24}H_{20}N_6O_3S$	472	77	170	453	17.70	17.79
SN_2	3-NO_2-	$C_{24}H_{19}N_7O_5S$	517	80	205	472	18.76	18.95
SN_3	4-NO_2-	$C_{24}H_{19}N_7O_5S$	517	79	190	504	19.05	18.95
SN_4	3-CH_3-	$C_{25}H_{22}N_6O_3S$	486	72	178	451	17.15	17.27
SN_5	4- CH_3-	$C_{25}H_{22}N_6O_3S$	486	74	182	465	17.38	17.27
SN_6	3-Cl-	$C_{24}H_{19}ClN_6O_3S$	506	83	232	467	16.63	16.58
SN_7	4-Cl-	$C_{24}H_{19}ClN_6O_3S$	506	81	204	468	16.45	16.58
SN_8	4-F-	$C_{24}H_{19}FN_6O_3S$	490	76	182	458	17.01	17.13
SN_9	3-OCH_3-	$C_{24}H_{19}N_7O_6S$	502	82	152	463	16.85	16.72
SN_{10}	4-OCH_3-	$C_{24}H_{19}N_7O_6S$	502	78	198	461	16.80	16.72
SN_{11}	2,4-$(NO_2)_2$-	$C_{24}H_{18}N_8O_7S$	562	82	152	528	19.82	19.92
SN_{12}	2-OH-	$C_{24}H_{20}N_6O_4S$	488	80	180	467	17.34	17.20
SN_{13}	2-OH,4-NO_2-	$C_{24}H_{19}N_7O_6S$	533	78	164	450	18.45	18.38
SN_{14}	2,6-$(Cl)_2$,4-NO_2-	$C_{24}H_{17}Cl_2N_7O_5S$	586	81	158	513	16.80	16.72
SN_{15}	4-$NHCOCH_3$-	$C_{26}H_{23}N_7O_4S$	529	76	172	485	18.40	18.51

Table 2 Fastness properties of Dyes

Dye No.	Shade on Polyester Fabric	Fastness to		Sublimation fastness at 180°C		Exhaustion %	Fixation %
		Light	Washing	Staining of Cotton	Staining of Polyester		
SN_1	Dark yellow	5	4	4-5	4	75.35	84.24
SN_2	Cream	3-4	4	3-4	4	72.20	79.63
SN_3	Orange	4	4	4	4	74.75	81.90
SN_4	Yellow	5	4-5	5	5	78.60	85.78
SN_5	Brown yellow	4-5	5	4-5	4	77.30	83.89
SN_6	Khakhi	5	5	4-5	5	85.27	90.67
SN_7	Yellow	5	5	4-5	4-5	83.76	88.54
SN_8	Brown	4-5	4-5	4	4-5	80.45	86.54
SN_9	Cream	5	4-5	4-5	4-5	82.10	84.90
SN_{10}	Turmeric yellow	4	3-4	4	4	72.24	79.50
SN_{11}	Red	4	4	3-4	4	76.21	81.67
SN_{12}	Light brown	3-4	4	4	3-4	70.72	78.45
SN_{13}	Cream	4	4	4	4	78.91	81.90
SN_{14}	Dark cream	5	3-4	4	4	78.38	80.34
SN_{15}	Light brown	3-4	4	4	4	74.29	82.74

Light fastness: 1- poor, 2- slight, 3- moderate, 4- fair, 5- good, 6- very good, 7-excellent
Wash and sublimation fastness: 1- poor, 2- fair, 3- good, 4- very good, 5- excellent

Table 3 IR and ^{1}H NMR results of SN_1-SN_{15} Dyes

Dye No.	IR (KBr) cm^{-1}	^{1}H NMR (DMSO) Chemical shift in δ ppm
SN_1	3442 (N-H), 3080 (C-H), 2985, 2735 (CH_3) 1643 (C=O), 1570 (N=N), 1525 (NO_2), 1472 (C-S-C), 765 (C-S)	2.19 (S, 3H, -CH_3), 3.79 (S, 2H, -$COCH_2$), 4.09 (S, 1H, -NH), 7.08-8.72 (M, 13H, Ar-H) 9.15 (S, 1H, -NH)
SN_2	3449 (N-H), 3085 (C-H), 2995, 2728 (CH_3) 1640 (C=O), 1578 (N=N), 1528 (NO_2), 1473 (C-S-C), 757 (C-S)	2.15 (S, 3H, -CH_3), 3.65 (S, 2H, -$COCH_2$), 4.14 (S, 1H, -NH), 7.08-8.79 (M, 12H, Ar-H), 9.00 (S, 1H, -NH)
SN_3	3446 (N-H), 3082 (C-H), 2998, 2730 (CH_3) 1647 (C=O), 1577 (N=N), 1530 (NO_2), 1478 (C-S-C), 759 (C-S)	2.17 (S, 3H, -CH_3), 3.45 (S, 2H, -$COCH_2$), 4.18 (S, 1H, -NH), 7.15-8.81 (M, 12H, Ar-H), 9.10 (S, 1H, -NH),
SN_4	3445 (N-H), 3075 (C-H), 2987, 2728 (CH_3) 1655 (C=O), 1568 (N=N), 1527 (NO_2), 1475 (C-S-C), 762 (C-S)	2.21 (S, 6H, -CH_3), 3.36 (S, 2H, -$COCH_2$), 4.16 (S, 1H, -NH), 7.04-8.75 (M, 12H, Ar-H), 9.06 (S, 1H, -NH),
SN_5	3440 (N-H), 3074 (C-H), 2986, 2728 (CH_3) 1648 (C=O), 1572 (N=N), 1525 (NO_2), 1476 (C-S-C), 756 (C-S)	2.25 (S, 6H, -CH_3), 3.28 (S, 2H, -$COCH_2$), 4.19 (S,1H, -NH), 7.13-8.85 (M, 12H, Ar-H), 9.13 (S, 1H, -NH),
SN_6	3442 (N-H), 3080 (C-H), 2993, 2723 (CH_3) 1652 (C=O), 1580 (N=N), 1528 (NO_2), 1478 (C-S-C), 758 (C-S),725 (C-Cl)	2.16 (S, 3H, -CH_3), 3.30 (S, 2H, -$COCH_2$), 4.20 (S, 1H, -NH), 7.07-8.90(M, 12H, Ar-H), 9.10 (S, 1H, -NH)
SN_7	3448 (N-H), 3078 (C-H), 2991, 2725 (CH_3) 1643 (C=O), 1577 (N=N), 1533 (NO_2), 1469(C-S-C), 831 (C-S), 734 (C-Cl)	2.21 (S, 3H, -CH_3), 3.32 (S, 2H, -$COCH_2$), 4.25 (S, 1H, -NH), 7.12-8.94 (M, 12H, Ar-H) 8.97 (S, 1H, -NH)
SN_8	3443 (N-H), 3085 (C-H), 2988, 2723 (CH_3) 1664 (C=O), 1578 (N=N), 1526 (NO_2), 1468 (C-S-C), 757 (C-S), 1125 (C-F)	2.1 (S, 3H, -CH_3), 3.26 (S, 2H, -$COCH_2$), 4.17 (S, 1H, -NH), 6.98-8.80 (M, 12H, Ar-H) 9.18 (S, 1H, -NH),
SN_9	3446 (N-H), 3113 (C-H), 2991 (CH_3), 2850 (OCH_3), 1641 (C=O), 1570 (N=N), 1525 (NO_2), 1477 (C-S-C), 788 (C-S)	2.12 (S, 3H, -CH_3), 3.17 (S, 3H, -OCH_3), 3.23 (S, 2H, -$COCH_2$), 4.17 (S, 1H, -NH), 7.10-8.78 (M, 12H, Ar-H) 8.94 (S, 1H, -NH)
SN_{10}	3444 (N-H), 3098 (C-H), 2997, 2729 (CH_3) 1674 (C=O), 1579 (N=N), 1530 (NO_2), 1475 (C-S-C), 764 (C-S)	2.16 (S, 3H, -CH_3), 3.21 (S, 3H, -OCH_3), 3.30 (S, 2H, -$COCH_2$), 4.23 (S, 1H, -NH), 7.14-8.85 (M, 12H, Ar-H), 9.10 (S, 1H, -NH)
SN_{11}	3445 (N-H), 3102 (C-H), 2987, 2728 (CH_3) 1648 (C=O), 1570 (N=N), 1525 (NO_2), 1465 (C-S-C), 757 (C-S)	2.11 (S, 3H, -CH_3), 3.25 (S, 2H, -$COCH_2$), 4.12 (S, 1H, -NH), 7.12-9.07 (M, 11H, Ar-H), 9.07 (S, 1H, -NH)
SN_{12}	3443 (N-H), 3445 (O-H), 3105 (C-H), 3003, 2735 (CH_3) 1648 (C=O), 1568 (N=N), 1528 (NO_2), 1463 (C-S-C), 756 (C-S)	2.27 (S, 3H, -CH_3), 3.61 (S, 2H, -$COCH_2$), 4.01(S, 1H, -NH), 5.41 (S, 1H, -OH), 7.09-8.68 (M, 12H, Ar-H), 9.12 (S, 1H, -NH)
SN_{13}	3448 (N-H), 3438 (O-H), 3103 (C-H), 2998, 2730 (CH_3) 1645 (C=O), 1559 (N=N), 1524 (NO_2), 1467(C-S-C), 759 (C-S)	2.17 (S, 3H, -CH_3), 3.37 (S, 2H, -$COCH_2$), 4.06 (S, 1H, -NH), 5.45 (S, 1H, -OH), 7.16-8.90 (M, 11H, Ar-H), 9.06 (S, 1H, -NH)
SN_{14}	3441 (N-H), 3095 (C-H), 2985, 2720 (CH_3) 1657 (C=O), 1575 (N=N), 1522 (NO_2), 1467 (C-S-C), 762 (C-S), 731 (C-Cl)	2.15 (S, 3H, -CH_3), 3.40 (S, 2H, -$COCH_2$), 4.12 (S, 1H, -NH), 7.08-8.99 (M, 10H, Ar-H), 9.10 (S, 1H, -NH),
SN_{15}	3445 (N-H), 3090 (C-H), 2994, 2728 (CH_3) 1667 (C=O), 1579 (N=N), 1530 (NO_2), 1475 (C-S-C), 756 (C-S), 1687 (C-$NHCOCH_3$)	2.09 (S, 3H, -CH_3), 2.23 (S, 3H, -CH_3), 3.36 (S, 2H, -$COCH_2$),4.12 (S, 1H, -NH), 7.10-8.78 (M, 12H, Ar-H), 9.02 (S, 2H, -NH)

Table 4 Antimicrobial properties of Dyes

Dye No.	Zone of inhibition (mm)				
	Antibacterial Activity				Antifungal Activity
	E. coli	*P. aeruginosa*	*S. aureus*	*B. subtilis*	*C. albicans*
SN_1	11	11	10	13	12
SN_2	14	12	12	13	11
SN_3	12	10	13	14	12
SN_4	9	10	13	12	13
SN_5	15	13	16	17	15
SN_6	11	12	`13	15	12
SN_7	11	11	12	12	11
SN_8	12	14	17	19	14
SN_9	11	10	12	12	12
SN_{10}	14	12	11	15	14
SN_{11}	10	11	12	13	12
SN_{12}	11	10	11	12	10
SN_{13}	12	11	10	11	11
SN_{14}	10	9	13	14	14
SN_{15}	9	10	12	12	12
Ciprofloxacin	20	18	23	27	-
Flucanazole	-	-	-	-	20

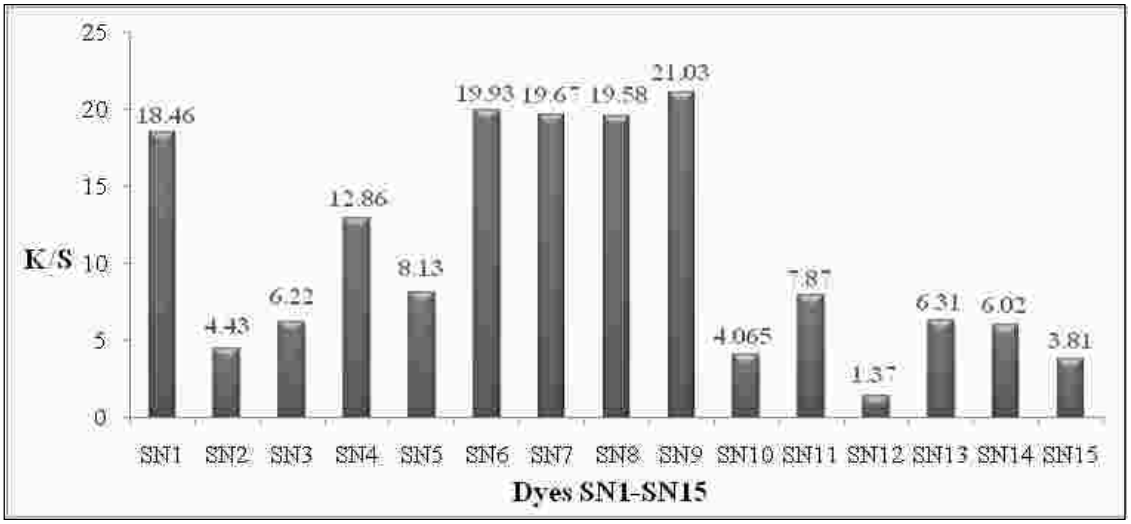

Fig. 1: Graph of K/S values of dyes SN_1-SN_{15} on polyester fibre, dye SN_9 has maximum K/S value and SN_{12} has minimum K/S value

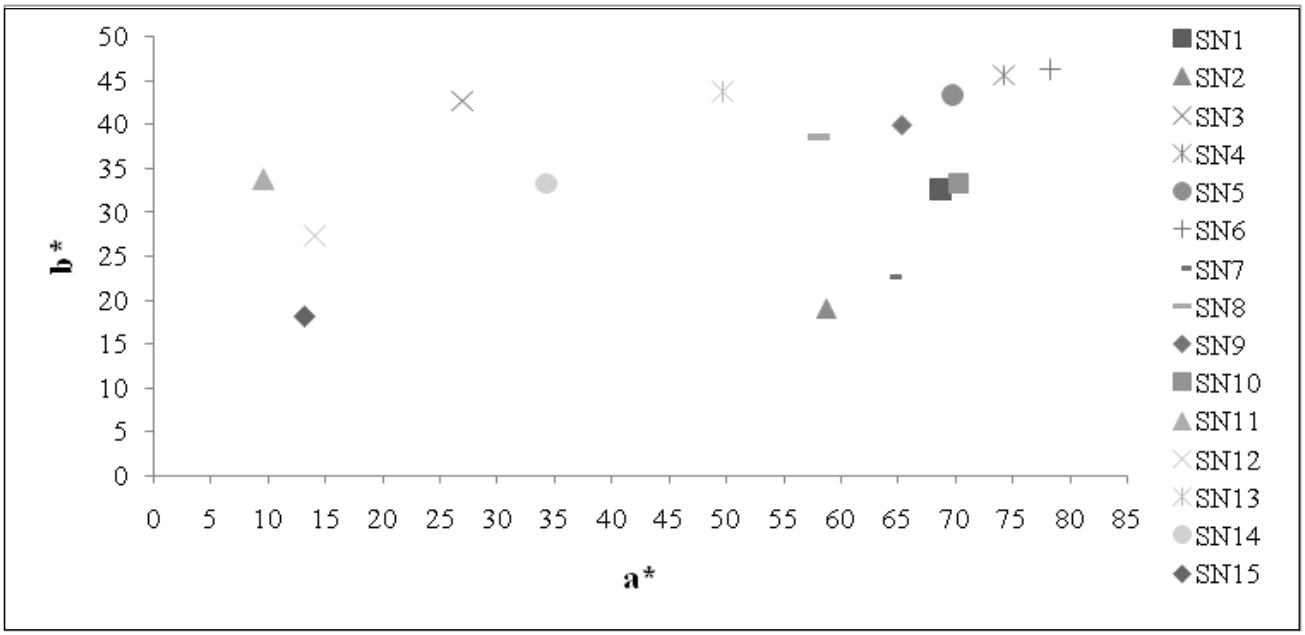

Fig. 2: Graph of b* vs a* for polyester fibre

Table 5: Colour difference data and K/S data of dyes on polyester fibre

Dye No.	L*	a*	b*	C*	H*	K/S	R
SN_1	59.35	32.54	68.68	76.00	64.65	18.46	17.43
SN_2	60.45	18.98	58.76	62.78	67.23	4.43	22.24
SN_3	52.68	42.62	26.92	50.41	32.28	6.22	21.34
SN_4	61.39	45.57	74.31	87.17	58.48	12.86	10.58
SN_5	58.56	43.34	69.78	84.36	55.87	8.13	12.96
SN_6	60.67	46.24	78.27	82.63	57.42	19.93	7.50
SN_7	67.67	22.58	64.41	68.25	70.68	19.67	7.78
SN_8	51.57	38.54	58.06	69.69	56.43	19.58	7.90
SN_9	65.25	39.87	65.37	70.27	53.02	21.03	6.56
SN_{10}	60.32	33.28	70.28	77.63	66.02	4.065	23.87
SN_{11}	40.12	33.77	9.49	35.07	15.70	7.87	12.78
SN_{12}	51.01	27.31	14.01	30.69	27.16	1.37	28.65
SN_{13}	53.98	43.65	49.64	63.62	45.59	6.31	21.20
SN_{14}	55.34	33.25	34.24	47.73	45.84	6.02	21.65
SN_{15}	49.09	18.10	13.08	22.33	35.86	3.81	23.30

Reaction scheme:

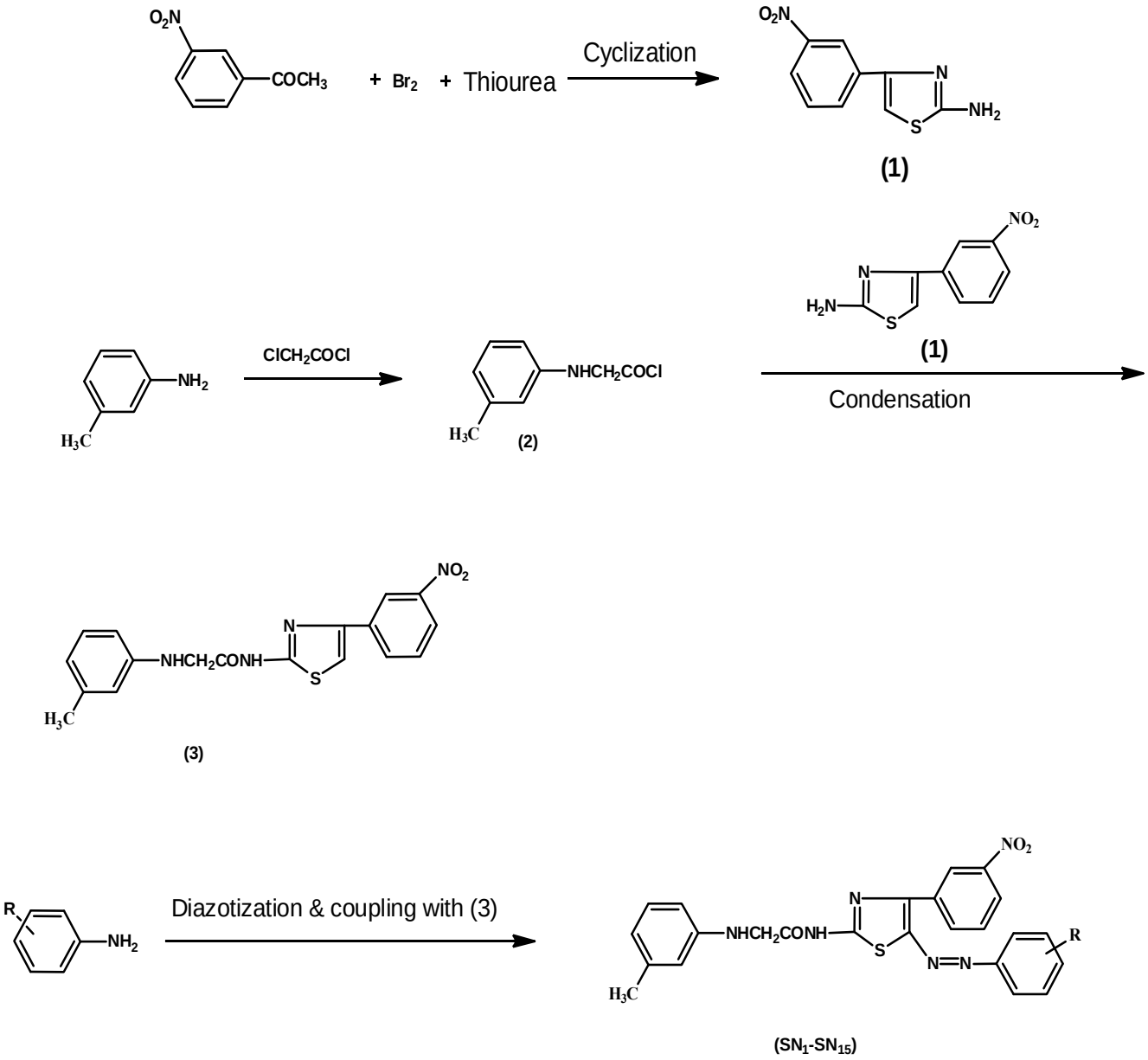

where, **R**= -H, $-NO_2$, $-CH_3$, -Cl, -F, $-OCH_3$, -OH, $-NHCOCH_3$.

Sublimation Fastness

The dyed fabric was stitched to undyed cotton fabric on one side and undyed polyester fabric on the other side. The composite dyeing specimens were placed in an electrical heating device (sublimation tester) for 30 seconds at 180°C. The dried fabric was then removed and kept in air for 4 hours. The effect of dyed fabric on the cotton and polyester fabric was studied and assessed with grey scales. (Table 2)

As shown in Table 2, the light fastness of each dye is rated as 3–5 for polyester, which shows that the light fastness is moderate to good. The wash fastness of each dye is rated as 3–5 for polyester showing that wash fastness is good to excellent. The sublimation fastness of each dye is rated as 3–5 for polyester, which also shows sublimation fastness is good to excellent.

Antimicrobial Activity

Antibacterial and antifungal activities of synthesized compounds were examined in vitro by Kirby-Bauer disc diffusion method. The zone of inhibition (mm) was determined using disc diffusion method according to the standard procedure at concentration 50 μg/mL. All the compounds were tested for activity against *Staphylococcus aureus*, *Escherichia coli*, *Bacillus subtilis, Pseudomonas aeruginosa* and *Candida albicans.* Ciprofloxacin and Flucanazole were employed as the standards (Table 4).

Colour Matching Data (CCM)

The colour on polyester fabric was expressed in terms of CIELab values and the coordinates measured were lightness (L*), chroma (C*) and hue angle from 0° to 360° (H*). a* values represent the degree of redness (positive) and greenness (negative) and b* values represent the degree of yellowness (positive) and blueness (negative). A reflectance spectraophotometer was used for the colorimetric measurement of the dyed samples. K/S value given by the reflectance spectrophotometer were calculated at λ_{max} and directly correlated with the dye concentration on the substrate according to the Kubelka-Munk equation[23,24].

The colorimetric data of polyester fabric for all the dyes are summarized in Table 5. The K/S values for dyes were found in the following order:

$SN_9 > SN_6 > SN_7 > SN_8 > SN_1 > SN_4 > SN_5 > SN_{11} > SN_{13} > SN_3 > SN_{14} > SN_2 > SN_{10} > SN_{15} > SN_{12}$

The K/S graph for all the dyes is shown in Figure-1 and graph of b* versus a* are shown in Figure 2.

Conclusions

The dyes gave generally yellow, turmeric yellow, orange, red, khakhi and cream shades with good depth and levelness on fabric. The variation in the shades of the dyed fabric and levelness resulted from both the nature and position of the substituent present in the aromatic amine. The synthesized dye SN_1 showed λ_{max} at 453nm. Introduction of electron donating groups -OH, $-OCH_3$, $-NHCOCH_3$, $-CH_3$ promoted bathochromic shift in dyes SN_4, SN_5, SN_9, SN_{10}, SN_{12} and SN_{15} to show λ_{max} values in the range 451 to 485nm. Chromphore $-NO_2$ group promoted bathochromic shift in dyes SN_2, SN_3, SN_{11}, SN_{14} to show λ_{max} in the range 472 to 528nm. Dyes SN_{13} both (-OH) and ($-NO_2$) group showed λ_{max} of 450nm.

The synthesis of monoazo disperse dyes derived from 2-chloro-N-(3-methylphenyl)acetamide was carried out by conventional methods and their different properties were studied by applying them to polyester fabric. The dyes showed good dyeing performance on polyester fabric. The dyes SN_1, SN_4, SN_6, SN_7, SN_9 and SN_{14} showed better light fastness properties. Sublimation fastness of the dyes was found to be fair to good. The wash-fastness of all the compounds was also of a very good order. All synthesized compounds were tested for microbial activity and showed mild to moderate antibacterial activity against *Escherichia coli, Pseudomonas aeruginosa, Staphylococcus aureus* and *Bacillus subtilis.* The dyes SN_3, SN_8 showed better activities against *Escherichia coli, Pseudomonas aeruginosa, Staphylococcus aureus* and *Bacillus subtilis* while SN_4, SN_5,

SN_8, SN_{11} and SN_{14} showed good antifungal activity against *Candida albicans*. Standard drugs like Ciprofloxacin and Flucanazole were used for the comparison purpose.

Acknowledgment

Authors are thankful to the Principal, Navyug Science College, Surat, India and Principal, V. S. Patel College of Arts and Science, Bilimora, India for laboratory facilities and Atul Limited for dyeing and computer colour matching facilities.

References

1. Griffiths J., 1981, *Rev. Prog. Coloration*, **11,** 37-57.
2. Devson J. F., 1978, *Rev. Rog. Coloration*, **9**, 27.
3. Hari Raghav Maradiya and Vithal Soma Patel, 2002, *Bulletin of the Chemists and Technologists of Macedonia*., **21(1),** 57–64.
4. Singh Kamaljit, Singh Sarbjit and Taylor John A., 2002, *Dyes and Pigments*. **54,** 189-200.
5. Miranda P.C., Rodrigues L.M., Goncalves MST., Costa SPG., Hardina R. and Oliveira AMF., 2001, *Advance in Colour Science and Technolog,* **4,** 1.
6. Metwally M. A., Abdel-Latif E., Amer F. A. and Kaupp G., 2004, *Dyes and Pigments*, **60,** 249-264.
7. Yadav J. S., Subba Reddy B.V., Gopala Rao Y., Narsaiah A.V., 2008, *Tetrahedron Letters*, **49,** 2381-2383.
8. S. K. Zadafiya, and G.M. Malik, 2013, *Fibers and Polymers*, **14 (6),** 904-908.
9. S. K. Zadafiya, J. H. Tailor. and G. M. Malik , J. of Chem., http://dx.doi.org10.1155/2013/ Article ID 851418.
10. Patel S. K., Patel P. K., and Malik G. M., 2014, *Journal of Applied Chemistry,* **7(10),** Ver II, 8-13.
11. Saravanan G., Alagarsamy V., Pavitra T. G. V., Chanukyakumar G., Savithri Y., Naresh L and Avinah P., 2010, *International J. Pharma and Biosciences*, **1,** 1-8.
12. Singh Deepak., Manish Srivastava., Gyananchandran A. K and Gokulan P. D., 2010, *Journal of Current Pharmaceuticals Research*, **4,** 16-19.
13. Prajapati *A. K and Modi Vishal. P.,* 2010, *J. Chil. Chem. Soc.* **55 (2)** 240-243.
14. Partan S. R., Dighe N. S., Nirmal S. A., Merekar A. N., Laware R. B., Shinde H. V., Musmade D. S., 2009, *Asian J. Research Chem.,* **2(2),** 196-201.
15. Saravanan G., Alagarsamy V., Prakash C. R., Panneer Selvam T., Karthick V and Dinesh Kumar P., 2009, *Rasayan J. Chem*. **2(3),** 746-752.
16. Bhosale P. P., Chavan R. S and Bhosale A.V., 2012, *Indian J. Chem*. **51B** 1649-1654.
17. Wurz, Melliand, 1956, *Textilber*, **37,** 566.
18. British Standard 1978, p.1006.
19. Park J and Smith D. J., 1974, *J. Soc. Dyers Colour*., **90,** 431.
20. Park J., 1976, *Int. Dyer Text. Print*., **155,** 220.
21. Standard Methods of Determining Fastness of Textiles and Leather (Bradford SOG), 4th edition, 1978.
22. Indian standard method for determination of colour fastness of textile materials to washing: Test 1 IS: 687-1979; Test 2 IS: 3361-1979; Test 3 IS: 764-1979; Test 4 IS: 765-1979; Test 5 IS: 3417-1979, 1979.
23. Billmeyer F. W. Jr and Abram R. L., 1973, *J. Paint Technol*., **45,** 31-38.
24. Allen E., 1966, *J. Opt. Soc. Am*., **56,** 1256-1259.

RNI No. MAHENG/2017/74063
ISSN No. (Print) 2581-5911

Mechanistic aspect of Iridium(III) catalyzed oxidation of ethylene glycol by Chloramine-T in aqueous acidic medium: a kinetic model

Abhishek Verma[1], Jyoti Pandey[1], Sheila Srivastava[2,*] and Kaman Singh[3]
[1]Department of Applied Chemistry, BBAU, Lucknow-226025, U.P., India
[2]Chemical Laboratories, Feroze Gandhi College, Raebareli-229001, U.P., India
[3]Department of Chemistry, Lucknow University-226007, U.P., India
Email: she_ila72@yahoo.com

Abstract
The kinetic investigation of homogeneously Ir(III) chloride catalyzed oxidation of Ethylene glycol by Chloramine-T [CAT] in perchloric acid medium has been carried out in the temperature range of 30 to 45 ^{0}C. The reaction was carried out in the presence of mercuric acetate as a scavenger for chloride ion. The reaction exhibits first order kinetics with respect to the oxidant [CAT] and catalyst [Ir(III)] while zero order with respect to substrate, i.e., Ethylene glycol (EG) was observed. The reaction shows negligible effect of [$Hg(OAc)_2$], [H^+] and ionic strength of the medium. Chloride ion positively influenced the rate of reaction. The various activation parameters have been calculated from the rate measurements at different temperatures (30 to 45^{0}C). The product of the reaction has been identified as the corresponding monocarboxylic acid. The reaction between Chloramine-T and Ethylene glycol in acid medium shows 2:1 stoichiometry. On the basis of kinetic studies, reaction stoichiometry and product analysis, a suitable mechanism has been proposed and rate law has been derived.

Keywords: *Kinetics, mechanism, Ir(III) catalysis , Ethylene glycol, Chloramine-T, acidic medium*

Introduction

The organic sulphonyl haloamines (N-haloamines), a group of mild oxidizing agents, has been extensively used for the oxidation of several organic compounds. The versatile nature of N-haloamines is attributed to the presence of halonium cations and nitrogen anions in their structure, which can act as base and nucleophile [1-5]. As a result, these compounds can react with a wide range of functional groups to cause many types of molecular changes. Sodium N-chloro-p-toluene-sulfonamide or Chloramine-T (CAT; p-$CH_3C_6H_4SO_2NClNa.3H_2O$) is one of the prime members of the organic haloamine family and behaves as an oxidizing agent in both acidic and alkaline media. Depending upon the pH of the medium, it forms various oxidizing species and thus gives a variety of kinetic results[6-9]. Several researchers have studied the oxidizing behavior of CAT[10-13] and numerous studies focus on the mechanistic aspects of the redox reactions in acidic media. In most of the studies, one of the species, RNHCl (R=$CH_3C_6H_4SO_2$), HOCl, or H_2OCl^+, has been considered as the reactive species[14]. It can behave both as electrophile and nucleophile depending on the reaction conditions.

A polyhydric alcohol (or polyalcohol) is a hydrogenated form of carbohydrate, whose carbonyl group (aldehyde or ketone, reducing suger) has been reduced to primary and secondary hydroxyl group. Glycol is widely used as a solvent, as an antifreeze agent and a raw material for synthetic vegetable oil and fats as the glycerol esters of higher acids. The study of oxidation of polyhydric alcohols has great importance in sugar chemistry. Various investigations on oxidation involving polyhydric alcohols and various oxidants i.e., periodic acid[15], lead acetate [16], permanganate[17], chloramine-B[18], potassium dichromate[19] in the presence/absence of catalyst in acidic medium have been reported by various workers. However, there are only few reports available in the literature on the oxidation of Ethylene glycol[20-21].

Various transition metal catalysts have been used in the N-haloamine oxidation of organic substrates [22]. Recently, the use of transition metal ions, such as osmium, ruthenium and iridium either alone or as binary mixtures, as catalyst in various redox processes has drawn considerable attention[23]. Iridium(III) chloride is an important platinum group metal ion and has been extensively used as homogeneous catalyst in a number of redox reactions[24]. Several studies have reported the use of Ir(III) chloride as a non-toxic and homogeneous catalyst[25-28]. Preliminary experimental results indicate that the reaction of Ethylene glycol with CAT in the acidic medium without a catalyst were very sluggish but the reaction becomes facile in the presence of Ir(III) catalyst.

In the present study, we examine the kinetic and mechanistic aspects of the Ir(III) catalyzed oxidation of Ethylene glycol by CAT in acidic medium with the following objectives: (i) to ascertain the reactive species of catalyst and oxidant, (ii) find the catalytic efficiency of Ir(III), (iii) identify the oxidation products, (iv) to elucidate the plausible reaction mechanism, (v) to deduce a rate law consistent with kinetic results and (vi) to calculate the activation parameters.

Materials and Methods

Materials

A stock standard solution of chloramine-T (S.D. Fine Chem. Ltd) was prepared by dissolving its known weight in doubly distilled water and its concentration was estimated iodometrically. In order to avoid photochemical deterioration, the solution of chloramine-T was preserved in black coated flask. The standard solution of Ethylene glycol (Thomas Baker) was freshly prepared. Iridium(III) chloride (Johnson Matthey) solution was prepared in HCl of known strength (0.018 N). Other reagents used were, A.R. grade and their solutions were also prepared in doubly distilled water. The reaction vessels were also black coated from outside to avoid photochemical effects.

Kinetic measurements

The kinetic runs were carried out at 35±0.1^{0}C. The reaction was initiated by mixing the already thermostated solution of Ethylene glycol to the thermally equilibrated reaction mixture containing required volume of solution of Chloramine-T, H^+, Ir(III) and other reagents. Aliquots (5mL) of the reaction mixture were pipetted out at regular intervals of time and poured into a conical flask containing 5mL of 4% KI solution and 5mL of dilute sulphuric acid. The liberated iodine equivalent to unconsumed oxidant was estimated using standard sodium thiosulphate solution with starch as an indicator. The initial rates were obtained from the slope of concentration vs. time graph in the initial stages of the reactions by plane mirror method.

Stoichiometry and product analysis

In order to ascertain the stoichiometry of the reaction, different sets of experiments with varying [RNHCl]:[EG] ratios were performed at 35^{0}C for 48 h and constant concentrations of all other reactants under the conditions [RNHCl] >> [EG]. Iodometric estimation of unconsumed [RNHCl] in different sets shows that 2 moles of RNHCl were consumed to oxidize 1 mole of Ethylene glycol. Accordingly, the following stoichiometric equations can be formulated:

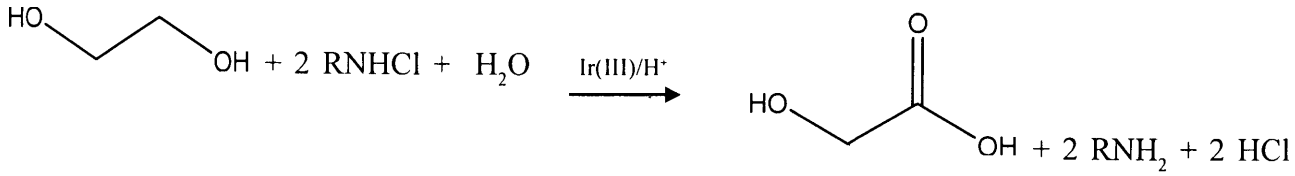

Ethylene glycol Glycolic acid

Glycolic acid (hydroxyacetic acid), the main product in the oxidation of were identified by the help of chromatography (TLC) and conventional spot test method. The nature of Glycolic acid was further confirmed by its IR spectrum.

Result and Discussion

Kinetics of Ir(III) catalyzed oxidation of Ethylene glycol by Chloramine-T in acidic medium was investigated at 35^0C. The kinetic results were recorded at several initial concentrations (Table1). First order kinetics was observed with respect to the oxidant, Chloramine-T (Figure 1). The order of reaction with respect to each reactant was determined by varying the concentration of oxidant, Ethylene glycol, Ir(III) chloride, H^+ ions, [CI^-] and mercuric acetate one by one in different sets, keeping concentration of all other reactants constant at constant temperature 35^0C (Table 1). In each kinetic run, the initial rate (i.e., –dc/dt) of the reaction was determined from the slope of the tangent drawn at a fixed concentration of Chloramine-T except for the Chloramine-T variation in which the slope of the tangent was drawn at fixed time. The first order reaction rate constants (k_1) for the variation of all the reagents were calculated using the equation

$$K_1 = \frac{-dc/dt}{[RNHCl]^*}$$

where [RNHCl]* denotes the [RNHCl] at which (-dc/dt) was determined.

A plot of (-dc/dt) versus [Chloramine-T] was linear with the slope value (0.98) near unity, which further confirmed first order dependence of reaction on Chloramine-T (Figure 1). A plot of (-dc/dt) versus [Ir(III)] gave a slope which is close to the average value of first order rate constant at 35^0C (Figure 2). Insignificant effect on the rate was observed on increasing the concentration of the substrate, indicating zero order with respect to substrate *i.e.* Ethylene glycol (Table 1). Variation of [KCl] concentration shows positive effect on reaction rate (Table 2). Negligible effect of mercuric acetate eliminate the probability of its involvement either as a catalyst or as an oxidant. Hence, the function of mercuric acetate is to act as scavenger for any chloride ion formed in the reaction[29]. Experimental data indicate negligible effect of ionic strength of the medium on the rate (affected by addition of $NaClO_4$). It helps to eliminate the parallel oxidation by Cl_2 which would have been formed as a result of interaction between Cl^- and RNHCl ion. In acidic solution of Chloramine-T, quick formation of RNHCl has been reported [30]. The reaction is unaffected by H^+ concentration (Table 2).

The kinetic measurements were also carried out in the temperature range of 30-45^0C and the rate constants were obtained at 30^0, 35^0, 40^0 and 45^0C. These rate constants were used to draw a plot of log k versus 1/T (Figure 3) which was linear. The various activation parameters were calculated from the slope of curves obtained from Figure-3. The value of Energy of activation (ΔE*), Arrhenius factor (A), entropy of activation (ΔS*), free energy of activation (ΔG*) and enthalpy of activation (ΔH*) were calculated from rate measurement and these values are shown in Table 3. Moderate ΔH* and ΔS* values are favorable for electron transfer reaction. The value of ΔH* was due to energy of solution changes in transition state. The high positive value of ΔG* represents highly solvated transition state. The negative value of ΔS* indicates that the intermediate

Table 1: Effect of variation of oxidant, Ethylene glycol and Ir(III) on rate of reaction at 35^{0}C

[Oxidant] x 10^3 M (Chloramine-T)	[Substrate]x 10^2 M (Ethylene glycol)	[Ir(III)] x 10^5 M	(-dc/dt)x10^7 $ML^{-1}s^{-1}$
0.83	2.00	8.02	2.65
1.00	2.00	8.02	3.30
1.25	2.00	8.02	4.12
1.67	2.00	8.02	5.40
2.50	2.00	8.02	8.25
5.00	2.00	8.02	16.45
1.00	0.33	8.02	2.75
1.00	0.40	8.02	3.20
1.00	0.50	8.02	3.00
1.00	0.66	8.02	2.90
1.00	1.00	8.02	3.12
1.00	2.00	8.02	3.30
1.00	2.00	2.67	1.12
1.00	2.00	4.01	1.68
1.00	2.00	5.34	2.25
1.00	2.00	6.67	2.78
1.00	2.00	8.02	3.30
1.00	2.00	9.35	3.90

Solution conditions: $[Hg(OAc)_2]$ = 1.25 x 10^{-3} M, $[HClO_4]$ =1.00 x 10^{-3} M, [KCl] = 1.00 x 10^{-3} M.

complex is more ordered than the reactants so the formation of activated complex occurs with reduction in the degrees of freedom. The observed modest enthalpy of activation and higher rate constant for the slow step show that oxidation presumably occurs by means of an inner sphere mechanism. This conclusion is supported by earlier observations. The activation parameters evaluated for the catalyzed reaction explain the catalytic effect on the reaction. Kinetic observations show that the reaction under investigation is a complex reaction, which usually takes place in more than one step.

Mechanism and derivation of rate law

The acidic solution of Iridium chloride exists as $[IrCI_6]^3$. It has also been reported that $[IrCI_6]^{3-}$ is involved in equilibrium [31]:

$$[IrCl_6]^3 + H_2O \rightleftharpoons [IrCl_5(H_2O)]^{2-} + CI^-$$

Table 2: Effect of variation of $HClO_4$, KCl and $NaClO_4$ on rate of reaction at 35^{0}C

$[HClO_4]$ x 10^3 M	[KCl] x10^3M	$NaClO_4$x10^3M	(-dc/dt) x 10^7ML^{-1}s^{-1}
0.83	1.00	1.00	3.48
1.00	1.00	1.00	3.30
1.25	1.00	1.00	3.55
1.67	1.00	1.00	3.20
2.50	1.00	1.00	3.15
5.00	1.00	1.00	3.62
1.00	0.83	1.00	2.95
1.00	1.00	1.00	3.30
1.00	1.25	1.00	3.52
1.00	1.67	1.00	3.85
1.00	2.50	1.00	4.15
1.00	5.00	1.00	4.45
1.00	1.00	0.83	3.45
1.00	1.00	1.00	3.30
1.00	1.00	1.25	3.60
1.00	1.00	1.67	3.15
1.00	1.00	2.50	3.08
1.00	1.00	5.00	3.34

Solution conditions: [Ir (III)] =8.02 x 10^{-5} M, [Chloramine-T] = 1.00 x 10^{-3} M, [Ethylene glycol] = 2.00 x 10^{-2}, $[Hg(OAc)_2]$ = 1.25 x 10^{-3} M.

Table 3: Activation parameters for the oxidation of Ethylene glycol

Parameters	Temperature(^{0}C)	Ethylene glycol
k_1x 10^4 s^{-1}	30	2.35
k_1x 10^4 s^{-1}	35	3.30
k_1x10^4 s^{-1}	40	4.72
k_1x 10^4 s^{-1}	45	6.58
log A	--	9.82
ΔE* (k J mol^{-1})	35	54.93
ΔG* (k J mol^{-1})	35	73.71
ΔH * (k J mol^{-1})	35	69.24
ΔS* (JK^{-1}mol^{-1})	35	-14.50

Solution conditions: [Ir (III)] = 8.02 x 10^{-5} M, [Chloramine-T] = 1.00 x 10^{-3} M, [Ethylene glycol] = 2.00 x 10^{-2} , $[Hg(OAc)_2]$ = 1.25 x 10^{-3} M, $[HClO_4]$ =1.00 x 10^{-3} M, [KCl] = 1.00 x 10^{-3} M.

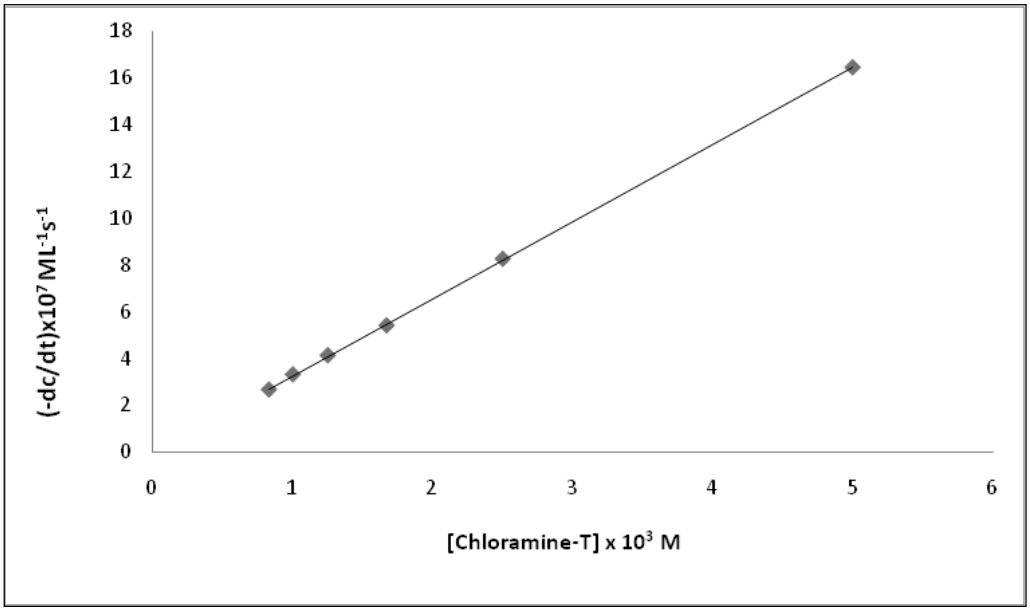

Fig. 1: Plot between (-dc/dt) and [Chloramine-T] for the oxidation of Ethylene glycol at 35 ^{0}C. [Ir (III)] = 8.02 x 10^{-5} M, [Ethylene glycol] = 2.00 x 10^{-2}, [$Hg(OAc)_2$] = 1.25 x 10^{-3} M, [$HClO_4$] =1.00 x 10^{-3} M, [KCl] = 1.00 x 10^{-3} M.

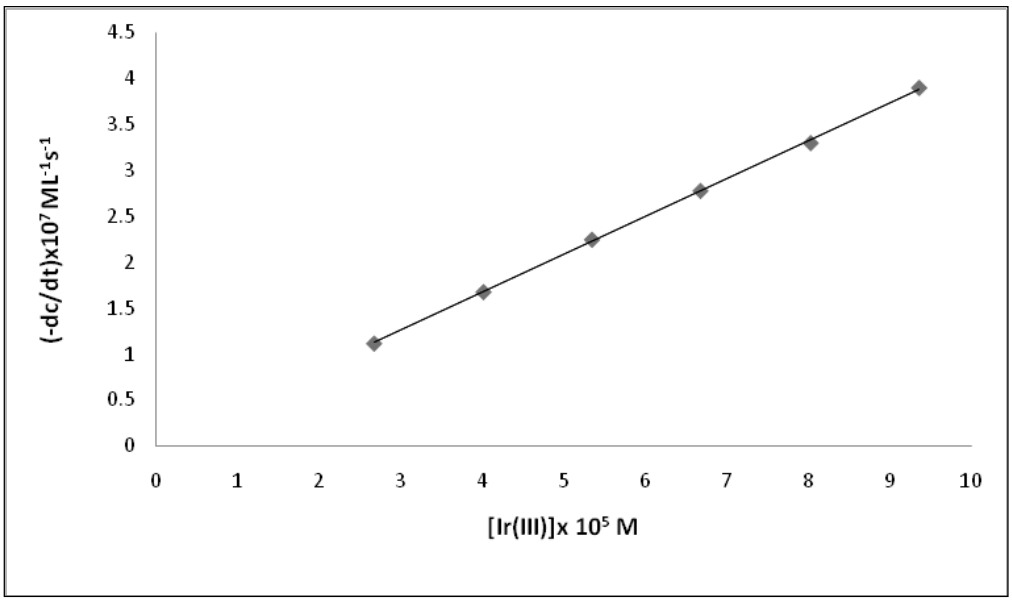

Fig. 2: Plot between (-dc/dt) and [Ir(III)] for the oxidation of Ethylene glycol at 35 ^{0}C . [Ethylene glycol] = 2.00 x 10^{-2} M, [Chloramine-T] = 1.00 x 10^{-3}, [$Hg(OAc)_2$] = 1.25 x 10^{-3} M, [$HClO_4$] =1.00 x 10^{-3} M, [KCl] = 1.00 x 10^{-3} M.

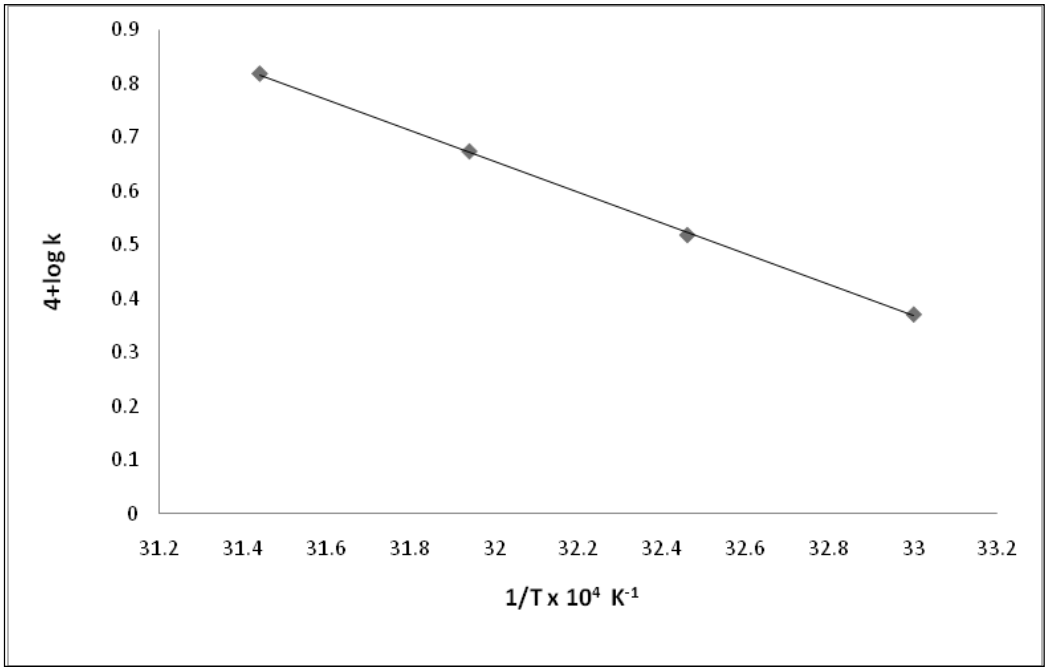

Fig. 3: Arrhenius plot for the oxidation of Ethylene glycol. [Ir (III)] = 8.02 x 10^{-5} M , [Chloramine-T] = 1.00 x 10^{-3} M, [Ethylene glycol] = 2.00 x 10^{-2} , [$Hg(OAc)_2$] = 1.25 x 10^{-3} M, [$HClO_4$] =1.00 x 10^{-3} M, [KCl] = 1.00 x 10^{-3} M.

Thus, either $[IrCI_6]^{3-}$ or $[IrCI_5H_2O]^{2-}$ may act as catalytic species[32]. If $[IrCI_5H_2O]^{2-}$ is taken as catalytic species, the rate law would require negative effect of chloride ion contrary to the observed positive effect of chloride ion on the oxidation rate $[IrCI_6]^{3-}$ which when assumed as reactive species of Iridium trichloride in acidic medium, explains the positive effect of chloride ion. The kinetic results reported in Tables 1, 2, 3 along with the above discussion lead us to suggest the following reaction scheme:

$$\underset{[C_1]}{[IrCI_5(H_2O)]^{2-}} + CI^- \underset{k_{-1}}{\overset{k_1}{\rightleftharpoons}} \underset{[C_2]}{[IrCI_6]^{3-}} + H_2O$$

$$\underset{[C_2]}{[IrCI_6]^{3-}} + RNHCl \xrightarrow[\text{slow step (r.d.s)}]{k_2} \underset{[C_3]}{[IrCI_6 \text{——} RNHCl]^{3-}}$$

$$[C_3] + RCH_2OH \longrightarrow [IrCl_5H]^{3-} + R\text{–}\overset{\overset{RNCl}{|}}{CH}\text{–}OH + HCl$$

$$[IrCl_5H]^{3-} + RNHCl \longrightarrow [IrCI_6]^{3-} + RNH_2$$

$$R\text{–}\overset{\overset{RNCl}{|}}{CH}\text{–}OH + H_2O \xrightarrow{\text{fast}} \underset{[P]}{R\text{–}COOH} + RNH_2 + HCl$$

where, [P] = Product i.e. Glycolic acid

Now, considering the above reaction steps and applying the steady-state treatment with reasonable approximation, the rate law may be written as

$$\text{Rate} = \frac{-d[RNHCl]}{dt} = k_2[C_2][RNHCl] \qquad (i)$$

$$[Ir(III)]_T = [C_1] + [C_2] \qquad (ii)$$

$$\frac{d[C_1]}{dt} = k_{-1}[C_2] - k_1[C_1][Cl^{-1}] \qquad (iii)$$

$$[C_1] = \frac{k_{-1}[C_2]}{k_1[Cl^-]} \qquad (iv)$$

$$[C_1] = \frac{[C_2]}{K_1[Cl^-]} \qquad (v)$$

where $K_1 = \frac{k_1}{k_{-1}}$

Putting the value of $[C_1]$ in Equation (ii) we get

$$[\text{Ir(III)}]_T = [C_1] + [C_2]$$

$$[Ir(III)]_T = \frac{[C_2]}{K_1[Cl^-]} + [C_2]$$

$$= \left[\frac{[C_2] + K_1[Cl^-][C_2]}{K_1[Cl^{-1}]}\right]$$

$$= [C_2]\left[\frac{1 + K_1[Cl^{-1}]}{K_1[Cl^-]}\right]$$

This gives

$$[C_2] = \frac{[Ir(III)_T K_1[Cl^{-1}]}{1 + K_1[Cl^{-1}]}$$

Putting the value of C_2 in Equation (i), we get

$$\text{Rate} = \frac{K_1 k_2[Ir(III)_T[Cl^-][RNHCl]}{1 + K_1[Cl^-]}$$

Conclusions

The following conclusions can be derived in the present study of Ir(III) catalyzed oxidation of Ethylene glycol by Chloramine-T in acidic medium. (a) Among the various species of Ir(III) in acidic medium, $[IrCl_6]^{3-}$ is considered as the reactive species, (b) RNHCl is the reactive species of Chloramine-T in acidic medium, (c) In the absence of catalyst, the oxidation of Ethylene glycol by Chloramine-T is very sluggish, but it becomes facile in the presence of Ir(III) catalyst, (d) The stoichiometry of the reaction was found to be 2:1 and the oxidation products of Ethylene glycol were identified, (e) Activation parameters were computed from the Arrhenius plots, (f) The observed results have been explained by a plausible mechanism and the related rate law has been deduced. It can be concluded that Ir(III) chloride act as an efficient catalyst for the oxidation of Ethylene glycol by Chloramine-T in acidic medium.

Acknowlegement

The first author thankfully acknowledges the University Grants Commission, New Delhi, India for providing financial assistance in the form of Research Fellowship.

References

1. Puttaswamy, Vaz N. and Jagadeesh R.V., 2008, *Chin. J. Chem.*, **26**, 536–542.
2. Vinod K.N, Puttaswamy and Gowda K.N.N., 2009, *Inorg. Chim. Act.*, **362**, 2044–2051.
3. Puttaswamy, Anuradha T.M., Ramachandrappa R. and Gowda N.M.M., 2000, *Int. J. Chem. Kinet.* **32 (4)**, 221–230.
4. Puttaswamy and Jagadeesh R.V., 2006, *Ind. Eng. Chem. Res.*, **45**, 1563–1570.
5. Puttaswamy and Jagadeesh R.V., 2005, *Int. J. Chem. Kint.*, **37(4)**, 201–210.
6. Singh A.K., Negi R., Katre Y. and Singh S.P., 2009, *J. Mol. Catal.*, **302,** 36-42.
7. Kambo N. and Upadhyay S.K., 2004, *Ind. J. Chem.*, **43A,** 1210-1215.
8. Shukla A., Gupta S. and Upadhyay S.K., 1991, *Int. J. Chem. Kinet.*, **23,** 279-288.
9. Puttaswamy, Jagadeesh R.V. and Vaz N., 2005, *J. Mol. Catal. A*, **229,** 211-22.
10. Filler R., 1963, *Chem. Rev,*. **63**, 21–43.
11. Campbell M.M. and Johnson G., 1978, *Chem. Rev.*, **78**, 65–79.
12. Wadhwani M. and Jain S., 2014, *Res. J. Chem. Sci.*, **4(7)**, 61-65.
13. Sarasan G. and Muktibodh S., 2015, *J. Chem. Pharm. Res.*, **7(2)**, 890-895.

14. Singh A.K., Negi R., Jain B., Katre Y., Singh S.P. and Sharma V.K., 2011, *Ind. Eng. Chem.* Res., **50**, 8407–8419.

15. Buist G.J., Bunton C.A. and Hipperson W.C.P., 1971, *J. Chem. Soc. B*, **25(1)**, 2128-2142.

16. Criegee R. et al, 1931, Ber., **64,** 260; 1940, **73**, 563, Annalar, 1933, **159**, 507.

17. Nath P. and Banerjee K.K., 1971, *Indian J. chem.*, **9(9)**, 954.

18. Shah B., Jain A.L. and Banerjee K.K., 1982, *Indian J. chem.*, **21(A)(1)**, 41.

19. Rohatgi, 1960, *Proc. Natl. Inst. Sci.*, **26(A)**, 507.

20. Bai Wei-Song, Zhai Yong-qing, Liu Hong-meri, Lu Hong-Ying and Song Wen Yu, 2008, *Ind. J. Chem.*, **47A**, 1194-1198.

21. Srivastava Sh. and Srivastava S., 2008, *Asian J. Chem.*, **20(8)**, 6228-6234.

22. Puttaswamy and Vaz N., 2003, *Trans. Met. Chem.*, **28,** 409-417.

23. Hiremath C.V., Kiran T.S. and Nandibewoor S.T., 2006, *J. Mol. Catal. A Chem.*, **248,** 163-174.

24. Uma V., Sethuram B. and Rao T.N., 1981, *React. Kinet. Catal. Lett.*, **18,** 283.

25. Song Wen-yu, Zhao Rong-hui and Jiang Qing-mei, 2005, *Acta. Phys.-Chim.Sin.*, **21(08)**, 929-933.

26. Singh A.K., Rahmani S., Singh B., Singh R.K. and Singh M., 2004, *J. Phys. Org. Chem.*, **17(3)**, 249-256.

27. Bai Wei-Song, Zhai Yong-qing, Liu Hong-meri, Lu Hong-Ying and Song Wen Yu, 2008, *Ind. J. Chem.*, **47A**, 1194-1198.

28. Singh A.K., Sachdev N., Srivastava A., Jain B. and Khtre Y., 2012, *Res. Chem. Intermed.*, **38,** 507-521.

29. Venkatasubramanian N. and Thiagarajan V., 1968, *Can. J. Chem.*, **47**, 694.

30. Grover N., Kambo N. and Upadhyay S.K.,2002, *Ind. J. Chem.*, **41(A),** 2482-2488.

31. Gopalakrishanan G., Pai B.R. and Venkatasubramaniam N., 1980, *Ind. J. Chem.* **19B**, 293.

32. Chang J.C. and Garner G.S., 1965, *Inorg. Chem.*, **4(2),** 209-215.

RNI No. MAHENG/2017/74063
ISSN No. (Print) 2581-5911

A mechanistic investigation of Pd (II) catalyzed oxidation of paracetamol by potassium bromate ($KBrO_3$) in presence of $HClO_4$ acid medium: A kinetic model

Reena Patel[1], Shailesh Kumar[1], Abhishek Verma[1] and Sheila Srivastava[*2]
[1]Department of Applied Chemistry B.B.A.U. Lucknow U.P.,India
[2]Department of Chemistry Feroze Gandhi College, Raebareli U.P., India
Email: she_ila72@yahoo.com

Abstract
The present paper deals with the kinetic and mechanistic investigation of Pd(II) catalyzed oxidation of paracetamol by Potassium bromate ($KBrO_3$) in presence of Perchloric acid medium at 303 K. The experimental results show a first order kinetics with respect to [Palladium] and [bromate]. The reaction showed negative effect of [H^+]. Paracetamol positively influences the rate of reaction. Negligible effects of [$(HgOAc)_2$] and ionic strength of the medium have been observed. Variation of [Cl^-] did not show any significant change on the rate of reaction. The values of rate constants observed at different temperatures (30 to 45^{0}C) were utilized to calculate the activation parameters. Quinoneoxime and acetic acid have been identified as the main oxidation products of the reactions. A suitable mechanism has been proposed conforming with the kinetics, stochiometry and products of the reaction. The rate law has been derived from the observed kinetic data.

Keywords: *Kinetics, Pd(II) chloride, oxidation, Paracetamol, Potassium bromate, acidic medium.*

Introduction

The kinetics of paracetamol (PAM) oxidation has been studied both spectrophotometrically and iodometrically. Spectrophotometric determination of paracetamol in drug formulation has been a subject of several investigators.[1-9] In this paper, an attempt has been made to consolidate the work done on the well-known drug that finds extensive application in pharmaceutical industries especially in the last few decades. Paracetamol (4-hydroxyace-tanilide or acetmidophenol) is a well known drug that is having extensive appliction in pharmaceutical industries. It is an antipyretic and analgesic compound of high therapeutic value [10-11]. It is also used as an intermediate for pharmaceuticals (as a precursor in penicillin) and azo dyes [12-15]. Oxidation reactions are important in the synthesis of organic compounds as they create new functional groups or modify existing functional groups in a molecule[16-17]. Various advanced oxidation processes such as electrochemical[18-20] ozonation and H_2O_2/UV oxidation[21-24] have been employed to remove aqueous paracetamol. The oxidation kinetics of Paracetamol drug is important to understand the mechanism of metabolic conversion of paracetamol in biological systems and also to identify the reactive species of the oxidant in aqueous acid/base. Till date the action of paracetamol at a molecular level is not completely understood but could be related to production of reactive metabolites by the peroxidase function of COX-2, which could deplete glutathione, a cofactor of enzymes such

as PGE synthase[25] which has high therapeutic value. The results of various studies are interpreted and consolidated. In recent years, platinum group metal ions including Ru(III), Os(VIII), Ir(III), Rh(III), and Pd(II) have been widely used as catalysts. Palladium (II) chloride is the most important salt in the catalytic chemistry of palladium. Several authors have carried out studies using Pd(II) because of the commercial importance of reactions catalyzed by Pd(II). The kinetics for the oxidation of ethylene by aqueous Pd (II) is an example[26-27]. In this study the effect of chloride ion on the reaction rate was studied in order to establish the active species of the catalyst. Generally the mechanism of catalysis depends on the nature of the substrate, the oxidant, and other experimental conditions [28-29]. In most of the catalytic studies of organic transformations, the nature of the active form of Pd(II) remain obscure. The kinetic methods of analysis are highly sensitive, selective, simple, accurate, and less expensive. In recent years, several kinetic catalytic techniques have been reported for the detection of biomolecules[30-32]. The present study examines, in detail the kinetic and mechanistic aspects of the Pd(II) catalyzed oxidation of paracetamol by $KBrO_3$ in acidic media with the following objectives in mind:

(i) To ascertain the reactive species of the catalyst and the oxidant.
(ii) To deduce the rate law consistent with the kinetic results.
(iii) To identify the oxidation products.
(iv) To determine activation parameters.
(v) To elucidate the plausible reaction mechanism based on the observed reacion rate law and stoichiometry.

Materials and Methods

Materials

Aqueous solutions of Paracetamol (CDH), potassium bromate (S.D. Fine A.R.) and mercuric acetate (E. Merck) were prepared by dissolving weighed amounts of the samples in triple distilled water. Perchloric acid (60% E. Merck) was used as a source of hydrogen ions. Palladium (II) Chloride (Johnson Matthey) was prepared by dissolving the sample in hydrochloric acid of known strength. All other reagents of analytical grade were used. Sodium perchlorate (E. Merck) was used to maintain the ionic strength of the medium. The reaction stills were blackened from outside to prevent photochemical effect.

Kinetic Procedure

A thermostated water bath was used to maintain the desired temperature within ± 0.1°C. Calculated amounts of the reactants i.e. paracetamol, perchloric acid, mercuric acetate, Pd (II) chloride, KCl and water, except potassium bromate were taken in a reaction vessel which was kept in a thermostatic water bath. After allowing sufficient time to attain the temperature of the experiment, requisite amount of potassium bromate solution, also thermostated at the same temperature was rapidly pipetted out and run into the reaction vessel. The total volume of reaction mixture was 50 mL in each case. Aliquots (5mL) of the reaction mixture were pipetted out at regular intervals of time and transferred to a conical flask containing 5 mL of 4% KI solution and 5 mL of dilute sulfuric acid. The liberated iodine equivalent to unconsumed oxidant was estimated with standard sodium thiosulphate solution using starch as an indicator. The rate of reaction (-dc/dt) was determined from the slope of the tangent drawn at a fixed [BrO_3^-] in each kinetic run. The order of reaction with respect to each reactant was calculated with the help of log (-dc/dt) versus log concentration.

Determination of stoichiometry and product analysis

Different sets of the reaction mixture containing Paracetamol, Pd(II) chloride, and $HClO_4$ with excess $KBrO_3$ were equilibrated for 72 h at 303 K. Estimation of unconsumed $KBrO_3$ in each set revealed that for the oxidation of 1 mol of Paracetamol, 2 mols of $KBrO_3$ were consumed. Accordingly, the stoichiometry equation may be expressed as-

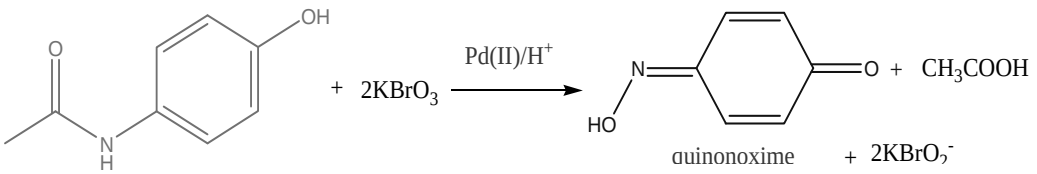

quinonoxime + $2KBrO_2$

The reaction products were extracted with ether after completion of the reaction (monitored by TLC). Evaporation of the ether layer was followed by column chromatography on silica gel using gradient elution (from dichloromethane to chloroform). After the initial separation, the products were further purified by recrystallization. Acetic acid and quinine oxime were identified as oxidation products of Paracetamol and $KBrO_2$ was the reduction product. The quinone oxime was identified by its IR spectrum (1652 cm^{-1}, C=O stretching; 1615 cm^{-1}, C=N stretching of oxime; 3332 cm^{-1}, O-H stretching). The identification was further confirmed by melting point, 131^{0}C (literature mp 132^{0}C). Quinone oxime was also analyzed via GC- MS (JEOL- JMS, Mate-MS system, Japan. GC - MS results were confirmed by extraction of the reaction mixture with diethyl ether and by concentrating the ether layer by a slow evaporation procedure. Acetic acid was identified by the spot test.

Results and Discussion

The kinetic results were recorded at several initial concentrations of reactants (Table 1). First order rate constant k_1 i.e. $\left(\frac{-dc}{dt}\right)$ were calculated from the plots of unconsumed potassium bromate vs. time. The plots of log (-dc/dt) versus log (oxidant) were linear indicating first order dependence on $KBrO_3$ (Fig-1). The first order kinetics with respect to $KBrO_3$ was also confirmed by least squares method (Fig. 2). No effect on the rate was observed on increasing the concentration of chloride ion, indicating zero order (Table 1). Kinetic result obtained by varying the concentration of [PA] indicated fractional positive order with respect to Paracetamol, which implies that rate of reaction increases when the concentration of [PA] is increased (Table 1) (Fig.3). The rate of reaction increased as the concentration of Palladium (II) chloride was increased, It was observed that the values of (-dc/dt) were doubled when the concentration of palladium(II) was doubled, showing first order dependence on $PdCl_2$ and first order dependence on catalyst i.e. Pd(II) chloride (Table 1) (Fig.4). With increase in the concentration of [H^+], the value of reaction rate decreased (Table 2). This showed negative effect of [H^+] on the rate of oxidation of paracetamol (Fig.5). The rate measurements were taken at 30^0-45^{0}C and specific rate constants were used to draw a plot of log k vs. 1/T which was linear (Fig-6). The value of Energy of Activation (ΔE^*), Arrhenius factor (A), Entropy of activation (ΔS^*) and Free energy of activation (ΔG^*) were calculated from rate measurements at 30^0, 35^0, 40^0, 45^{0}C and these values have been recorded in Table-3. Moderate ΔH^* and ΔS^* values are favourable for electron transfer reaction. The value of ΔH^* was due to energy of solution changes in the transition state. The observed modest enthalpy of activation and a higher rate constant for the slow step indicates that the oxidation presumably occurs via an inner-sphere mechanism. This conclusion is supported by earlier observations[33]. The high positive values of change in free energy of activation (ΔG^*) indicates highly solvated transition state, while fairly high negative values of change in entropy of activation (ΔS^*) suggest the formation of an activated complex with reduction in the degrees of freedom of molecule[34]. The activation parameters evaluated for the catalyzed and uncatalyzed reaction explain the catalytic effect on the reaction. Negligible effect of mercuric acetate excludes the possibility of its involvement either as a catalyst or as an oxidant because it does not help the reaction proceed in the absence of potassium bromate. Hence the function of mercuric acetate is to act as a scavenger for any Br^- ion formed in the reaction. It helps to eliminate the parallel oxidation by Br_2 which would have been formed as a result of interaction between Br^- and bromate ion.

Table 1: Effect of variation of oxidant, substrate and catalyst on oxidation rate at 35^{0}C

[Oxidant] x 10^3M (Potassium bromate)	[Substrate]x 10^2M (Paracetamol)	[Pd(II)] x 10^5M	(-dc/dt)x10^7ML^{-1}s^{-1}
0.83	1.00	11.2	1.92
1.00	1.00	11.2	2.60
1.25	1.00	11.2	2.82
1.67	1.00	11.2	3.81
2.50	1.00	11.2	5.32
5.00	1.00	11.2	10.60
1.00	0.40	11.2	1.32
1.00	0.50	11.2	1.60
1.00	0.66	11.2	2.10
1.00	1.00	11.2	2.60
1.00	2.00	11.2	4.25
1.00	4.00	11.2	6.20
1.00	1.00	5.60	1.33
1.00	1.00	11.2	2.60
1.00	1.00	16.8	4.60
1.00	1.00	22.4	5.18
1.00	1.00	33.6	8.35
1.00	1.00	44.8	10.21

Solution Conditions:
$[HClO_4]$ = 1.00 X 10^{-3} M, [KCl] = 1.00 X 10^{-3} M , $[Hg(OAC)_2]$ = 1.25 X 10^{-3} M

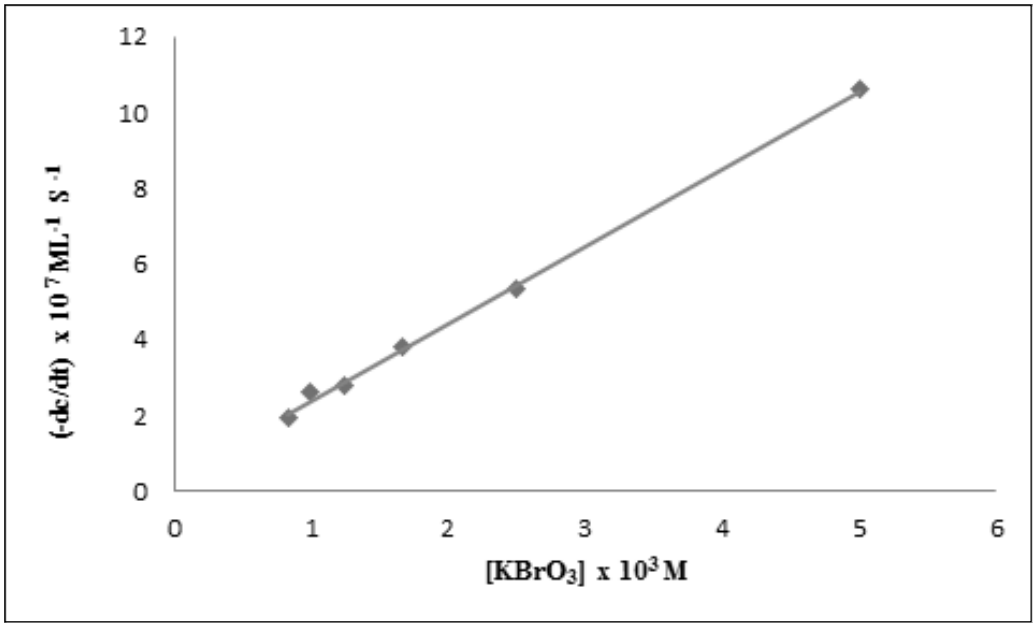

Fig. 1. Plot of rate of reaction (-dc/dt) vs $[KBrO_3]$ for the oxidation of paracetamol at 35^{0}C. $[HClO_4]$ = 1.00 x 10^{-3}M, [KCl] = 1.00 x 10^{-3} M, $[Hg(OAc)_2]$ = 1.25 x 10^{-3} M, Paracetamol [PAM] = 1.00 x 10^{-2} M, Pd(II) Chloride = 11.2 x 10^{-5} M

Table 2: Effect of Perchloric acid, Potassium chloride and Mercuric acetate on oxidation rate at 35^{0}C

$[HClO_4]$x 10^3 M	[KCl] x 10^3 M	$[Hg(OAc)_2]$ x 10^3 M	(-dc/dt)x10^7ML^{-1}s^{-1}
0.83	1.00	1.25	3.12
1.00	1.00	1.25	2.60
1.25	1.00	1.25	2.41
1.67	1.00	1.25	2.00
2.50	1.00	1.25	1.22
5.00	1.00	1.25	0.82
1.00	0.83	1.25	2.23
1.00	1.00	1.25	2.60
1.00	1.25	1.25	2.00
1.00	1.67	1.25	2.81
1.00	2.50	1.25	2.52
1.00	5.00	1.00	2.42
1.00	1.00	0.83	2.21
1.00	1.00	1.00	2.60
1.00	1.00	1.25	2.60
1.00	1.00	1.67	3.00
1.00	1.00	2.50	2.42
1.00	1.00	5.00	2.51

Solution Conditions:
Oxidant ($KBrO_3$) = 1.00 X 10^{-3} M, Paracetamol (PA) = 1.00 X 10^{-2} M,
Pd (II) Chloride = 11.2 X 10^{-5} M

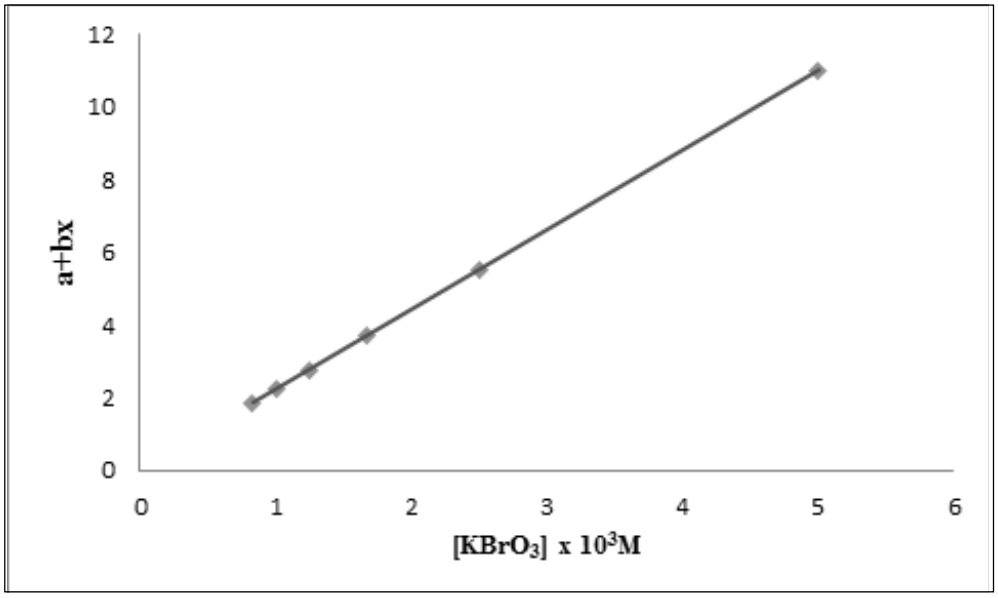

Fig. 2. Plot of rate of reaction (a+bx) vs $[KBrO_3]$ for the oxidation of paracetamol at 35^{0}C. $[HClO_4]$ = 1.00 X 10^{-3} M, [KCl] = 1.00 X 10^{-3} M, $[Hg(OAc)_2]$ = 1.25 X 10^{-3}M, Paracetamol [PA] = 1.00 x 10^{-2} M, Pd(II) = 11.2 x 10^{-5} M

Table 3: Activation parameters of Pd(II) chloride catalyzed oxidation of Paracetamol by $KBrO_3$ at 35^0C

Parameter	Temperature(T^0C)	Paracetamol(-dc/dt) x 10^7
k_1	30^0	1.55
k_1	35^0	2.60
k_1	40^0	3.18
k_1	45^0	5.18
log A	...	10.80
Ea* (k J mol^{-1})	35^0	60.98
Δ G* (k J mol^{-1})	35^0	74.63
Δ H * (k J mol^{-1})	35^0	71.45
Δ S* ($JK^{-1}mol^{-1}$)	35^0	-10.03

Solution Conditions: Pd(II) = 11.2 x 10^{-5} M, [$KBrO_3$] = 1.00 x 10^{-3} M, Paracetamol = 1.00 x 10^{-2} M, [$Hg(OAc)_2$] = 1.25 x 10^{-3} M, [$HClO_4$] = 1.00 x 10^{-3} M, [KCl] = 1.00 x 10^{-3} M,

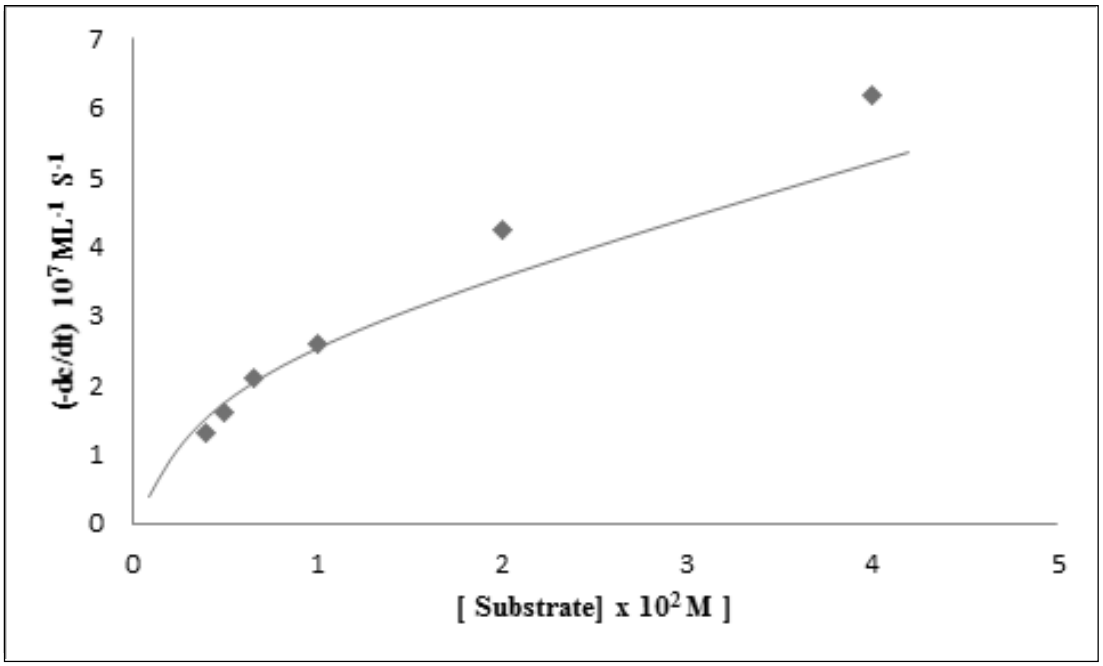

Fig. 3. Plot of rate of reaction (-dc/dt) vs [PA] on the reaction rate at 35^0C. [$HClO_4$] = 1.00 X 10^{-3}M, [KCl] = 1.00 X 10^{-3} M, [$Hg(OAc)_2$] = 1.25 X 10^{-3} M, [$KBrO_3$)] = 1.00 X 10^{-3} M, [Pd(II)] = 11.2 X 10^{-5} M

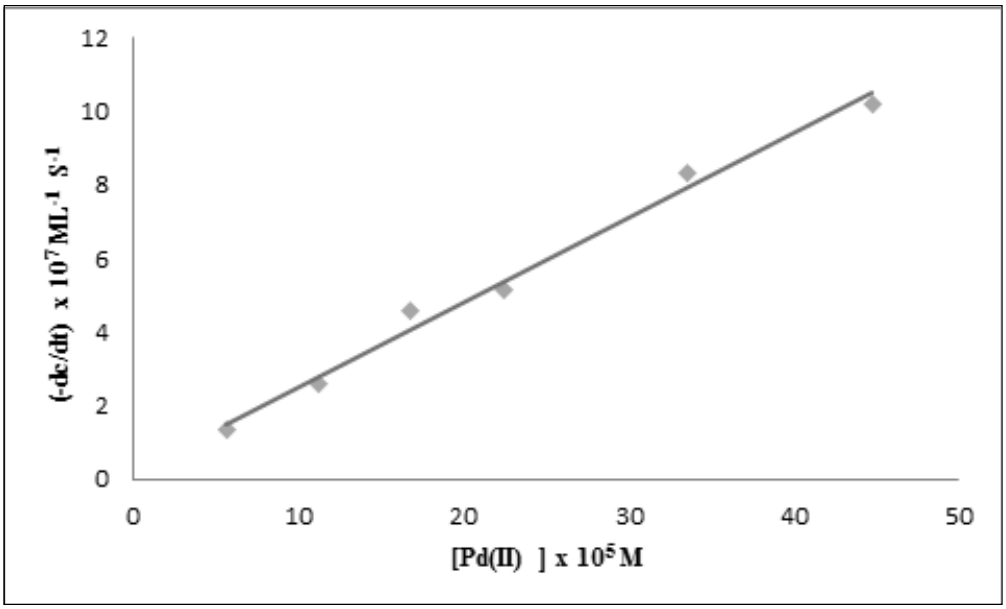

Fig. 4. Plot of rate of reaction (-dc/dt) vs [Pd(II)] on the reaction rate at 35^{0}C. [$HClO_4$] = 1.00 X 10 ^{3}M, [KCl] = 1.00 X 10^{-3} M, [$Hg(OAc)_2$] = 1.25 X 10^{-3} M, [$KBrO_3$] = 1.00 X 10^{-3} M , [Substrate(PA)] = 1.00 X 10^{-2} M

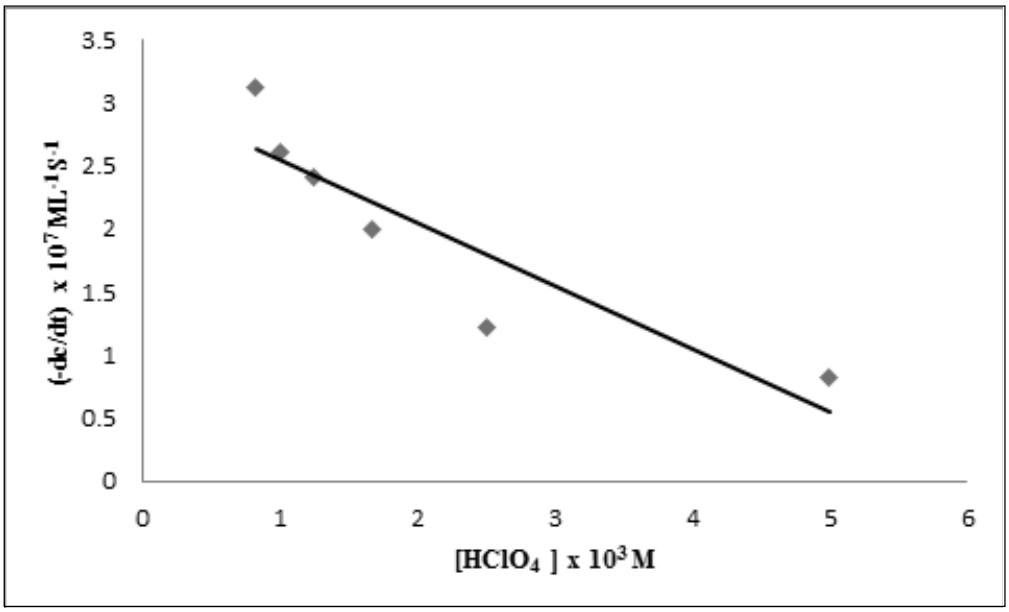

Fig. 5. Plot of rate of reaction (-dc/dt) vs [$HClO_4$] for the oxidation of paracetamol at 35^{0}C. [Pd(II) Chloride] = 11.2 X 10^{-5} M, [KCl] = 1.00 X 10^{-3} M, [$Hg(OAc)_2$] = 1.25 X 10^{-3} M, [Oxidant ($KBrO_3$)] = 1.00 X 10^{-3} M, [Substrate(PA)] = 1.00 X 10^{-2} M

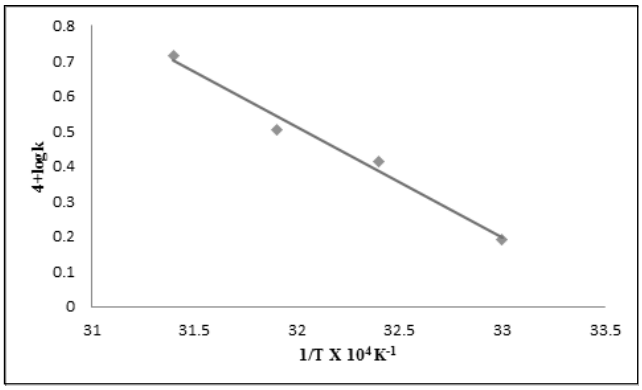

Fig. 6. Arrhenius plot for the effect of temperature on the oxidation of paracetamol

[Pd(II) Chloride]=11.2 x 10^{-5} M, [KCl]=1.00 x10^{-3} M,
[$Hg(OAc)_2$]=1.25 x 10^{-3} M
[Oxidant ($KBrO_3$)]=1.00 x 10^{-3} M,
[Substrate(PA)]=1.00X10^{-2} M, [$HClO_4$]=1.00 X10^{-3} M

Mechanism and derivation of rate law: In alkaline and acidic medium, potassium bromate is ionised:

$$KBrO_3 \rightarrow K^+ + BrO_3^-$$

The BrO_3^- species has been reported to act as an oxidising agent in acidic as well as in alkaline medium. Pd (II) chloride has been reported to give a number of possible chloro species dependent on pH of the solution. The kinetic results have been reported in Tables 1, 2 and 3.

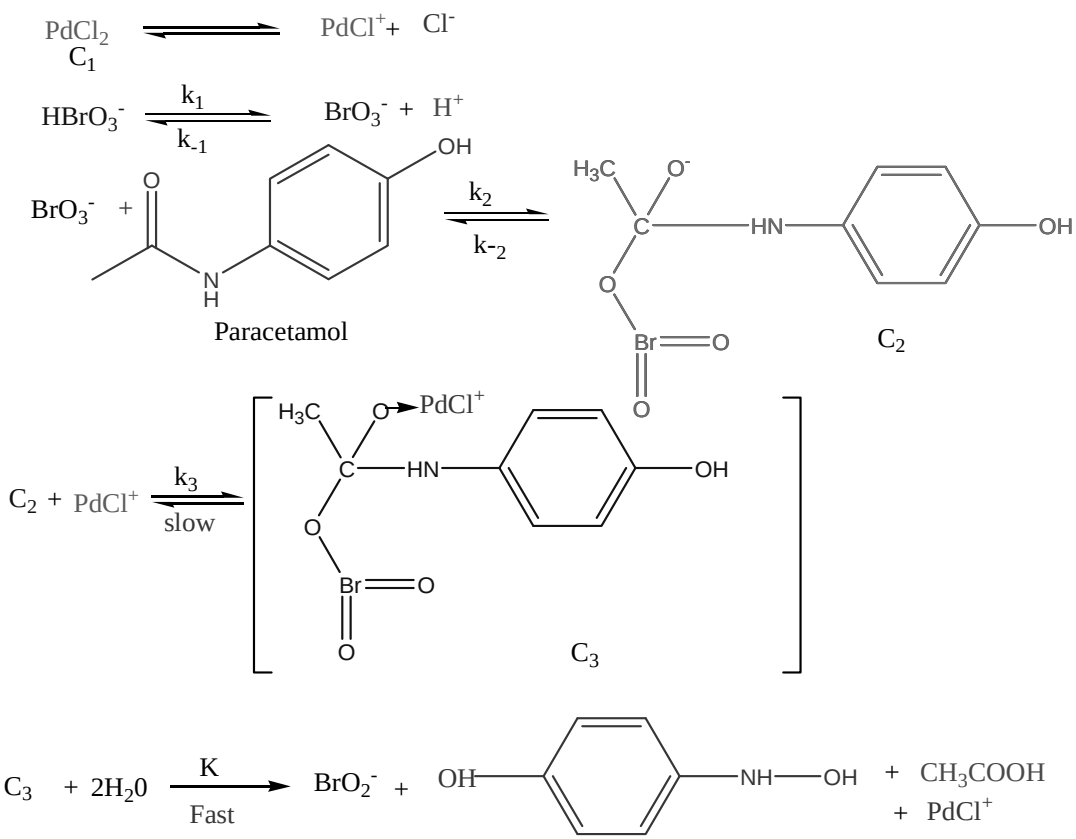

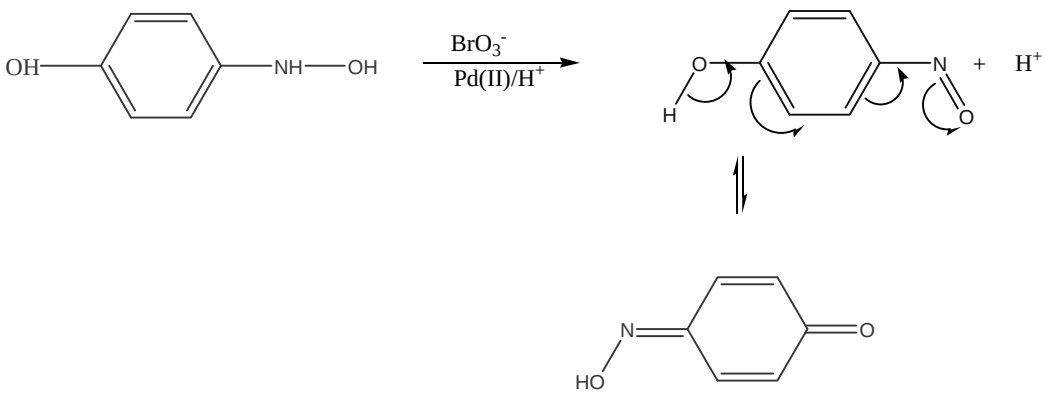

Quinoneoxime

Considering the fact that 1 mole of paracetamol is oxidised by 2 mole of bromate and applying the steady state treatment, with reasonable approximation, the rate law may be written as,

$$\text{rate (R)} = \frac{-d\,[BrO_3]^-}{dt} = 2k[C_3] \qquad (1)$$

On the basis of above step, Equations 2 to 5 can be obtained as follows:

$$\text{rate (R)} = \frac{2kK_1K_2K_3[Pd(II)][PA][HBrO_3]}{[H^+]} \qquad (2)$$

At any time during the reaction, the total concentration of $HBrO_3$ that is $[HBrO_3]_T$ can be expressed as-

$$[HBrO_3]_T = [HBrO_3] + [C_1] + [C_2] + [C_3] \qquad (3)$$

Substitution of $[C_1]$ $[C_2]$ and $[C_3]$ in Equation 3, gives Equation 4.

$$[HBrO_3] = \frac{[HBrO_3]_T}{[H]^+ + K_1 + K_1K_2[PA] + K_1K_2K_3[Pd(II)][PA]} \qquad (4)$$

Substituting the value of $[HBrO_3]$ in Equation 2 we get

$$\text{rate (R)} = \frac{2k\,K_1K_2K_3[Pd(II)][PA][HBrO_3]_T}{[H]^+ + K_1 + K_1K_2[PA] + K_1K_2K_3[Pd(II)][PA]} \qquad (5)$$

Conclusions

Oxidation of paracetamol by $KBrO_3$ does not proceed in the absence of catalyst, but becomes facile in the presence of Pd(II) catalyst. The reactive species of oxidant and catalyst have been identified. Oxidation products were identified and activation parameters were evaluated. The observed results have been explained by a plausible mechanism and the related law has been deduced. Therefore, it can be concluded that Pd(II) acts as an efficient catalyst for the oxidation of paracetamol. In the present study, a kinetic and mechanistic investigation of Pd(II) catalyzed oxidation of paracetamol by potassium bromate ($KBrO_3$) in presence of $HClO_4$ acid

medium has been done and the following conclusions drawn:

- $[PdCl]^+$ is the reactive species of Pd(II) in acidic medium.
- $HBrO_3$ is the reactive species of potassium bromate in acidic medium.
- The stoichiometry of the reaction was found to be 2:1 and the oxidation products of Paracetamol were identified.
- Activation parameters were computed from the Arrhenius plots.
- The observed results have been explained by a plausible mechanism and the related rate law has been derived.

References

1. Wallance, J. E. *Analytical Chemistry*, 1967, **39(4)**, 531-533
2. Plakogiannis, F.M. and Saad, A.M., 1975, *Journal of Pharmaceutical science*, **64(9)**, 1547-1549
3. Verma, K. K. Gulati, A. K. Palod S. and Tyagi, P., 1984, *The Analyst*, **109(6)**, 735-737
4. Sultan, S. M. Alzamil, I. Z. Aziz Alrahman, A. M. Altamrah S. A. and Asha, Y., 1986, *The Analyst*, **111(8)**, 919-921
5. Mohamed, F. A., AbdAllah, M. A. and Shammat, S. M., 1997, *Talanta*, **44(1)**, 61-68
6. Van Staden, J. F. and Tsanwani, M., 2002, *Talanta*, **58(6)**, 1095-1101
7. Oliva, M. Olsina, R. A. and Masi, A.N., 2005, *Talanta*, **66(1),** 229-235
8. Srivastava, M. K. Ahmad, S. Singh D. and Shukla, I.C., 1985, *The Analyst*, **110(6)**, 735-737
9. Gorle, Ashish Prakash, 2016, *International Research Journal of Pharmacy*, **7(3),** 30-34
10. Singh, A. K., Negi, Reena, Yokraj Katre, Singh S. P. and Sharma V. K., 2009, *J. Mol. Catal. A.*, **302,** 36–42.
11. Singh, A. K. Negi, Reena, Yokraj Katre, S. P. Singh, V. K. Sharma, 2009, *Catal. Lett.*, **132,** 285–291.
12. Yang, Liming. E Yu., Liya. Madhumita B. Ray, 2009, *Environ. Sci. Technol.*, **43,** 460–465.
13. Mulla, R. M. Gurubasavaraj and Nandibewoor, S.P., 2006, *Appl. Catal A*, **314,** 208–215.
14. Kiran, T. S. Hiremath, C. V. and Nandibewoor, S.T., 2006, *Appl. Catal A*, **305,** 79–89.
15. Kiran, T. S., Hiremath, C.V. and Nandibewoor, D.C., 2007, *Z. Phys Chem.*, **221,** 501–517.
16. Hudlicky, M., 1990, Oxidations in Organic Chemistry; ACS Monograph 186; American Chemical Society: Washington, DC, 838.
17. Russel, G. A. Janzen, E. G. Bemis, A. G. Geels, E. J. Moye, A. J. Mak, S. and Strom, E. T. 1965, Oxidation of Hydrocarbons in Basic Solution in Selective Oxidation Processes; Fields, E. K., Ed.; American Chemical Society; Washington, DC, **51,** 112-172.
18. Brillas, E. Sire's, I. Arias, C. Cabot, P. L. Centellas, F Rodr_iguez, R. M. and Garrido, J.A., 2005, *Chemospher.*, **58(4)**, 399–406.
19. Sir_es, I. Garrido, J. A. Rodr_iguez, R. M. Cabot, P. L. Centellas, F. Arias, C. and Brillas, E., 2006, *J. Electrochem. Soc.*, **153(1)**, D1–D9.
20. Waterston, K. Wang, J. W. J. Bejan, D. and Bunce, N. J., 2006, *J. Appl. Electrochem.*, **36(2)**, 227–232.
21. Vogna, D. Marotta, R. Napolitano, A. and d'Ischia, M., 2002, *J. Org. Chem.*, **67(17)**, 6143–6151.
22. Andreozzi, R. Caprio, V. Marotta, R. and Vogna, D., 2003, *Water Res.*, **37(5),** 993–1004.

23. Skoumal, M. Cabot, Centellas, P. L. F. Arias, C. Rodr_iguez, R. M. Garrido, J. A. and Brillas, E., 2006, *Appl. Catal. B.,* **66(3-4),** 228–240.

24. Yang, L. M. Yu, L. E. and Ray, M. B., 2008, *Water Res.,* **42(13)**, 3480–3488.

25. Graham G. G. and Scott K. F., 2005, *American journal of Therapeutic*., **12(1),** 46-55

26. Jagadeesh, R.V. and Puttaswamy., 2008, *J. Phys. Org. Chem*., **21(10),** 844–858.

27. Henry, P. M., 1980, Palladium (II) Catalysed Oxidation of Hydrocarbons. D. Reidal Publishing Company: Dordrecht, The Netherlands. p.2

28. Singh, Ashish. Singh, S. P. and Singh, A. K., 2007, *J. Mol. Catal. A*; **266,** 226–232.

29. Singh, A. K. Jain, Bhawana. Negi, Reena. Katre, Yokraj and Singh, S. P. 2009, *Open Catal. J.,* **2**, 12–20

30. Nandibewoor, S. T. and Morab, V. A., 1995, *Journal of the Chemical Society, Dalton Transactions*, **3,** 483–488

31. Imdadullah, T. F. and Kumamaru, T., 1994, *Analytica Chimica Acta.*, **292,** 151–157

32. Ensafi, A. A. and Keyvanfard, M., 2003, *Journal of Analytical Chemistry*, **58,** 1060–1064

33. Lewis, E. S., 1974, Investigation of Rates and Mechanism of Reactions in Techniques of Chemistry, A Weissberger, Ed.; Wiley, New York, p.421.

34. Onkar, A.S., Naik, P. N., Gunagi, S.D., Nandibewoor S.T. and Chimatadar, A.S., 2012, *Ind. J. Chem*., **51A,** 1574-1579.

RNI No. MAHENG/2017/74063
ISSN No. (Print) 2581-5911

Development of nucleotide-bonded stationary phases for capillary liquid chromatography

Lee Wah Lim, Itsuya Kawase, Miki Watanabe, Nobuyuki Takayama and Toyohide Takeuchi*
Department of Chemistry and Biomolecular Science, Faculty of Engineering,
Gifu University, 1-1 Yanagido, 501-1193, Gifu, Japan
E-mail: take-t@gifu-u.ac.jp

Abstract
Nucleotide-bonded zwitterionic stationary phases were prepared via *a two-step covalent modification. 3-glycidyloxypropyltrimethoxysilane (GPTMS) was first attached to dry silica gel (5 μm) in anhydrous toluene solvent and the mixture was heated at 110! for 18 h. After that, cytidine5'-monophosphate and adenosine5'-monophosphate were reacted to the glycidyl-bonded silica through epoxy-ring opening reaction under various conditions. The resulting nucleotide-bonded silica gels were then packed into 0.32 mm fused-silica tubes (10 cm in length) and the columns were evaluated for the separation of inorganic ions and polar compounds using a UV detector under ion-exchange and HILIC modes, respectively. The results showed that both cytidine- and adenosine-bonded columns could separate mono- and divalent cations, respectively, using indirect UV detection with copper sulfate used as the eluent. Adenosine-bonded column was found to have longer retention for organic acids under HILIC mode, and it was assumed that the distance between the phosphate and secondary amine groups in the structure plays an important role in the separation of these polar compounds.*

Keywords: *Zwitterionic stationary phases, Nucleotide-bonded column, Inorganic ions, Indirect UV detection, HILIC mode, Polar compounds*

Introduction

Miniaturization of chromatographic systems has attracted much attention since the 1970s[1] and the development of capillary-based separation systems has grown tremendously especially after the invention of fused-silica capillaries.[2] With the increasing concern of environmentally friendly analysis, capillary systems do not only reduce the amount of solvents, reagents and packing materials used, but we can also expect ultra-high sensitive and selective analysis of the most complex samples when it is directly connected to a mass spectrometer (MS) or a tandem MS/MS detection unit. Capillary columns also make the development of novel stationary phases so much easier and more importantly, affordable.[3-7]

Since ion chromatography was introduced in 1975, even though many types of stationary phases have been developed, ion-exchange chromatography still remains as the most common and widely used separation method especially for the separation of inorganic anions and

cations, and recently it has also been proven to be extremely useful for the separation of amino acids, as can be seen from the number of papers published in recent years.[8] Among these stationary phases, zwitterionic stationary phases, which contain both positive and negative charges, attract much attention due to their ability for higher efficient separations (caused by the shorter diffusion paths provided by the existence of oppositely charged layers on the surface) and wide range of selectivity (by using fixed concentrations of ligands and varying pH and ionic strength of mobile phases).[9] However, performing simultaneous separation of both anions and cations with high efficiency still remains a challenging task.

In this study, nucleotide-bonded zwitterionic stationary phases were prepared *via* a two-step covalent modification. Nucleotides are generally recognized as monomers or subunits of deoxyribonucleic acid (DNA) as well as ribonucleic acid (RNA), and they contain at least a nucleoside (which is a nitrogenous base) and a phosphate group. Therefore, under certain eluent conditions, nucleotides could be charged positively and/or negatively; and this characteristic favors their application in both ion-exchange and hydrophilic interaction chromatographic separations. Cytidine5'-monophosphate and adenosine5'-monophosphate were chosen in this study and their chemical structures are shown in Fig. 1.

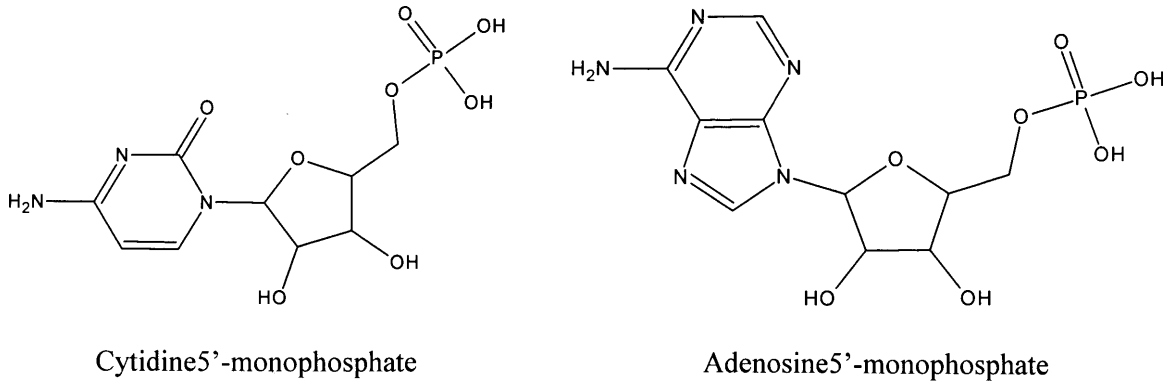

Fig. 1. Chemical structures of the nucleotides used in this study

Materials and Methods

Reagents and materials

Reagents employed were of guaranteed reagent grade and were obtained from Nacalai Tesque (Kyoto, Japan), unless otherwise stated. Sulfuric acid, *N*,*N*-dimethylformamide (DMF), tetrahydrofuran (THF), dimethyl sulfoxide (DMSO), sodium iodate, potassium sulfate, phenol, salicylic acid, adenine and thymine were purchased from Wako Pure Chemical Industries (Osaka, Japan), while Copper(II) sulfate pentahydrate was supplied by Yoneyama Yakuhin Kogyo (Osaka). Cytidine5'-monophosphate and 3-glycidyloxypropyltrimethoxysilane (GPTMS) were obtained from Tokyo Chemical Industry (Tokyo, Japan), whereas methanol, acetonitrile (ACN) and adenosine5'-monophosphate were obtained from Kanto Chemical, Tokyo, Japan. Ultrapure water was produced in the laboratory by using a Simplicity UV water purification system (Millipore, Molsheim, France), and all solutions used in this study were prepared using this ultrapure water.

The stationary phase materials employed were silica gels with average particle diameter and mean pore diameter of 5 ìm and 12 nm, respectively (Chemical Evaluation and Research Institute, Tokyo, Japan). The silica gels were dried at 120°C for 5 h before use. Toluene was dried in laboratory using molecular sieves 3A (1/16" pellets) for overnight (*approx.* 12 h), and stainless-steel tubing with 100 x 4.6 mm I.D. was used as the reaction vessel.

Apparatus

The capillary LC system used in this study was constructed by an L.TEX-8301 Micro Feeder (L.TEX corporation, Tokyo, Japan) equipped with an MS-GAN050 gas-tight syringe (0.5 mL, Ito, Fuji, Japan) as a micro pump, an M-435 micro valve injector (Upchurch Scientific, Oak Harbor, WA, USA) with an injection volume of 0.15 µL, a 100 mm x 0.32 mm I.D. microcolumn and a UV-2070 detector (JASCO, Tokyo, Japan). A capillary flow cell (75 µm; JASCO) was attached to the UV detector. All data was acquired using CDS-Lite ver5.0 data processor (LAsoft, Nagareyama, Chiba, Japan). Elemental analysis of the stationary phases was carried out by using a JM10 Micro Corder (J-Science Lab, Kyoto, Japan). A model 5220 centrifuge (Kubota, Tokyo, Japan) was used for washing the reaction products.

Preparation of stationary phases

The nucleotide-bonded stationary phases were prepared similar to those in our previous work with some modifications of each reaction step and the second reaction solvent was optimized in this study.[10-11] The dried porous silica gel was firstly reacted to GPTMS using dried toluene as the solvent and the reaction was carried out at 110°C for 18 h in the reaction vessel. The vessel was sometimes shaken manually during the reaction. After that, the GPTMS-bonded silica gel was washed with methanol and then dried at 75°C for 6 h. Cytidine5'-monophosphate and adenosine5'-monophosphate were reacted to the silica gel through epoxy-ring opening reaction under different solvents. Fig. 2 shows the series of the expected reactions when cytidine5'-monophosphate was used.

Results and Discussion

Elemental analysis

In order to optimize the amount of nucleotides bonded on the silica gel stationary phase, various reaction solvents such as toluene, DMF, DMSO, THF and ACN were used at different temperatures with the reaction time kept constant at 24 h. As can be seen from Tables 1 and 2, DMF as reaction solvent and reaction temperature 120°C were found to be the most suitable condition for bonding the nucleotides, *i.e.* with cytidine and adenosine contents calculated were 0.23 and 0.10 mmol/g, respectively.

Separation of anions

Figures 3 and 4 showed the separation of anions on cytidine- and adenosine-bonded stationary phases, respectively. As can be seen from the chromatograms, cytidine-bonded stationary phase did not have any retention on the analyte anions while adenosine-bonded stationary phase showed slight retention for the analytes.

Separation of cations

Figures 5 and 6 showed the separation of cations on cytidine- and adenosine-bonded stationary phases, respectively. As can be seen from the chromatograms, all monovalent and divalent cations were eluted as individual groups; and the resulted stationary phases did not have enough separation selectivity for each of the individual monovalent or divalent cations.

Under neutral eluent condition, *i.e.* when 1 mM BETMAC was used, however, the separation selectivity of the adenosine-bonded stationary phase was improved, and the separation profile is shown in Fig. 7. This drastic change in the retention of these cations, especially the sharp magnesium and calcium ions with base-line separation resolution, could be due to the less ionic repulsion caused by the eluent cations on the surface of the stationary phases.

Separation of organic acids

Figures 8 and 9 showed the separation of organic acids on cytidine- and adenosine-bonded stationary phases, respectively. As can be seen from the chromatograms, both stationary phases showed fairly good retention and separation efficiency for the analytes. The retention of organic acids increased with increasing ACN concentration, showing both stationary phases could be operated under typical HILIC conditions.

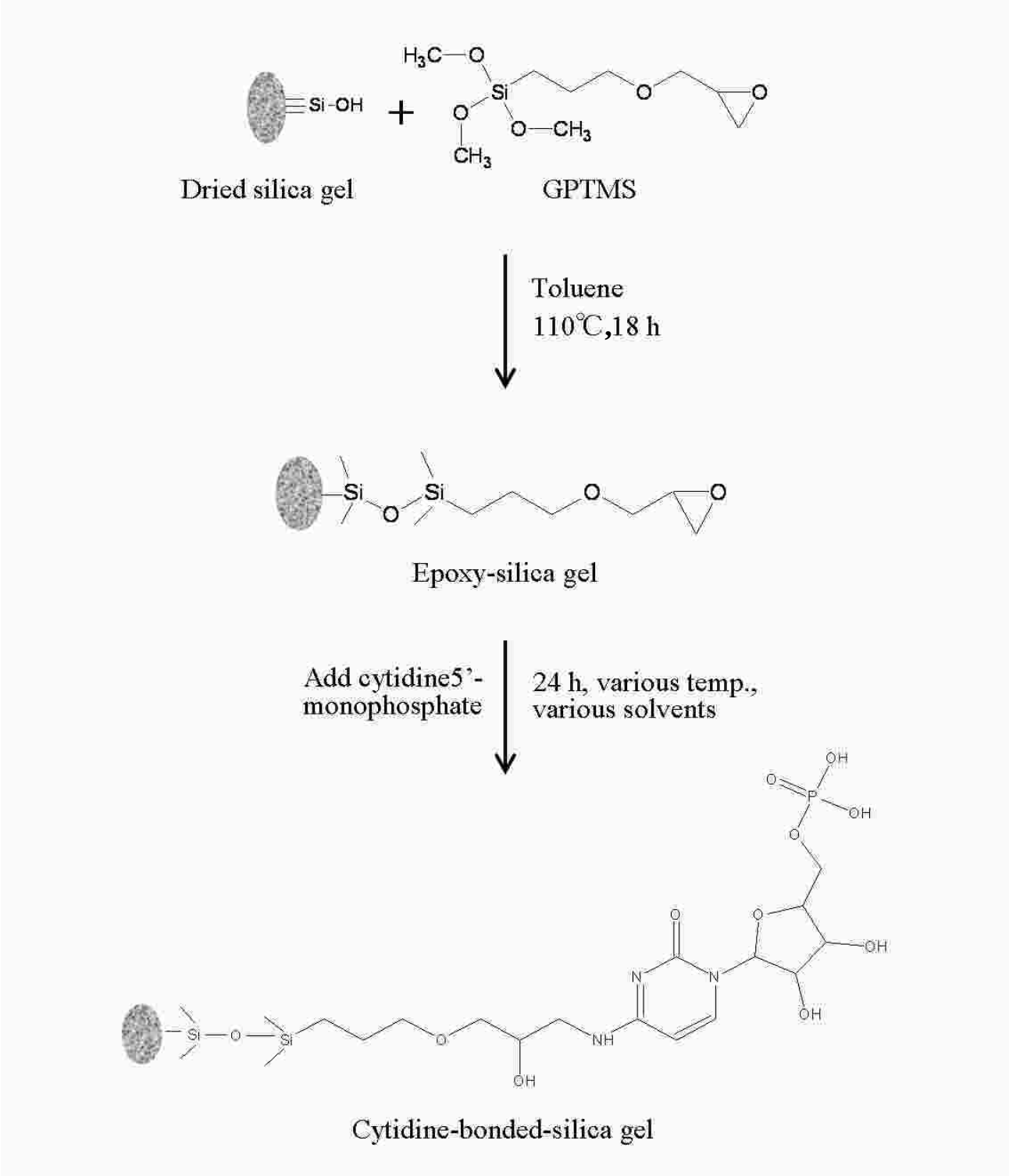

Fig. 2. Scheme for the expected reactions

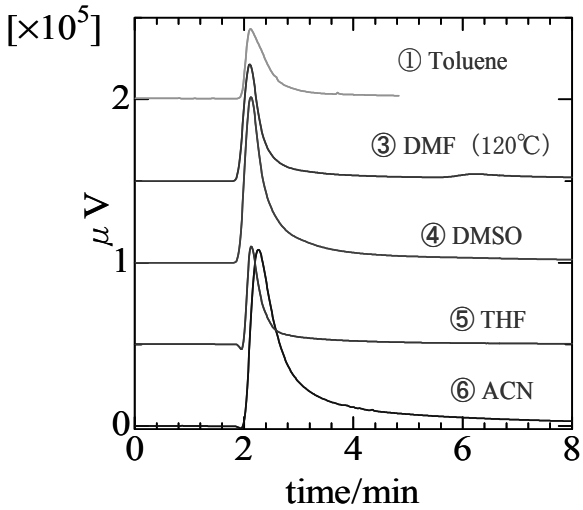

Fig. 3. Separation of anions on cytidine-bonded stationary phase

Column: Cytidine-bonded silica, 100 x 0.32 mm I.D.; Eluent: 10 mM NaCl + 1 mM HCl + 3% ACN; Sample: I^-, NO_3^-, IO_3^-, 0.5 mM each; Flow-rate: 4.0 μL/min; Wavelength of UV detection: 210 nm.

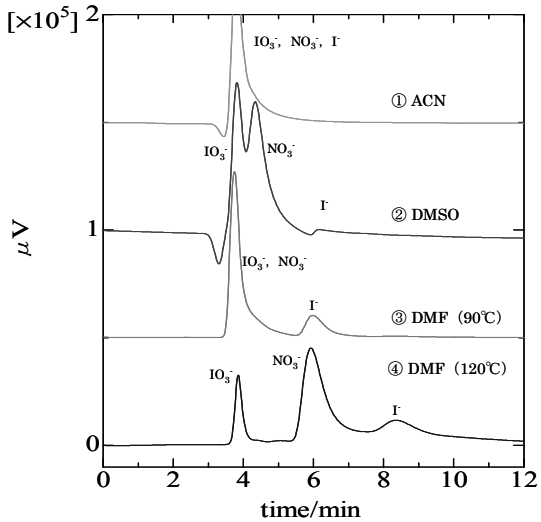

Fig. 4. Separation of anions on adenosine-bonded stationary phase

Column: Cytidine-bonded silica, 100 x 0.32 mm I.D.; Eluent: 10 mM NaCl + 1 mM HCl + 3% ACN; Sample: I^-, NO_3^-, IO_3^-, 0.5 mM each; Flow-rate: 2.0 μL/min; Wavelength of UV detection: 210 nm

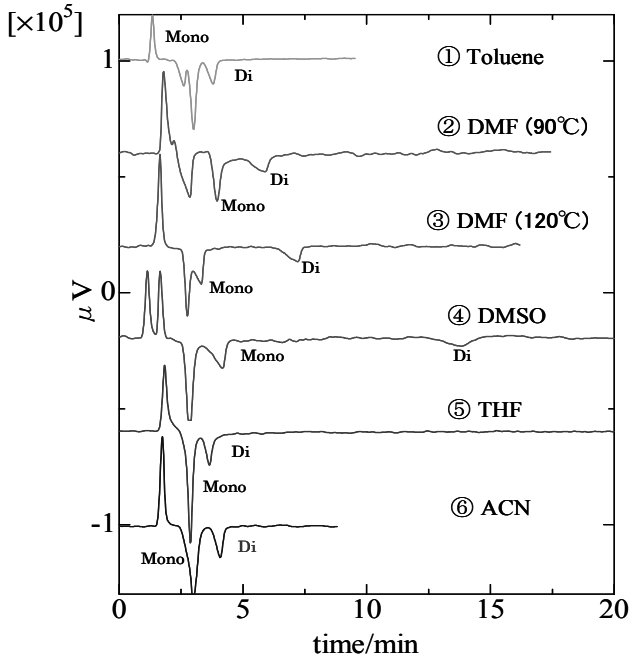

Fig. 5. Separation of cations on cytidine-bonded stationary phase

Column: Cytidine-bonded silica, 100 x 0.32 mm I.D.; Eluent: 1 mM $CuSO_4$; Sample: Na^+, K^+, NH_4^+, Mg^{2+}, Ca^{2+}, 0.5 mM each; Flow-rate: 4.0 μL/min; Wavelength of UV detection: 210 nm

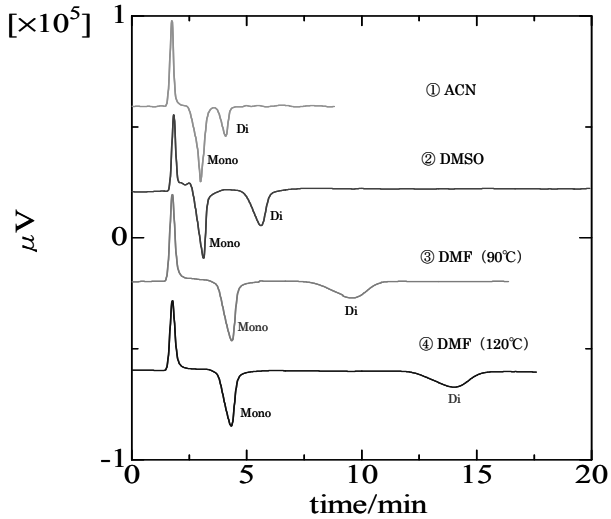

Fig. 6. Separation of cations on adenosine-bonded stationary phase

Column: Adenosine-bonded silica, 100 x 0.32 mm I.D.; Eluent: 1 mM $CuSO_4$; Sample: Na^+, K^+, NH_4^+, Mg^{2+}, Ca^{2+}, 0.5 mM each; Flow-rate: 4.0 μL/min; Wavelength of UV detection: 210 nm

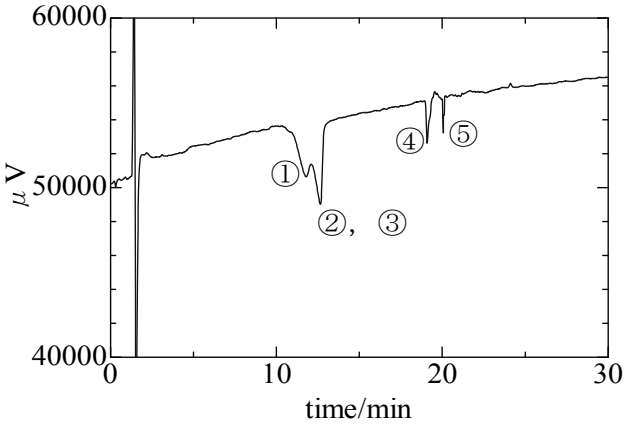

Fig. 7. Separation of cations on adenosine-bonded stationary phase under neutral eluent condition

Column: Adenosine-bonded silica, 100 x 0.32 mm I.D; Eluent: 1 mM BETMAC; Sample: ①Na^+, ②K^+, ③NH_4^+, ④Mg^{2+}, ⑤Ca^{2+}, 0.5 mM each; Flow-rate: 4.0 μL/min; Wavelength of UV detection: 210 nm.

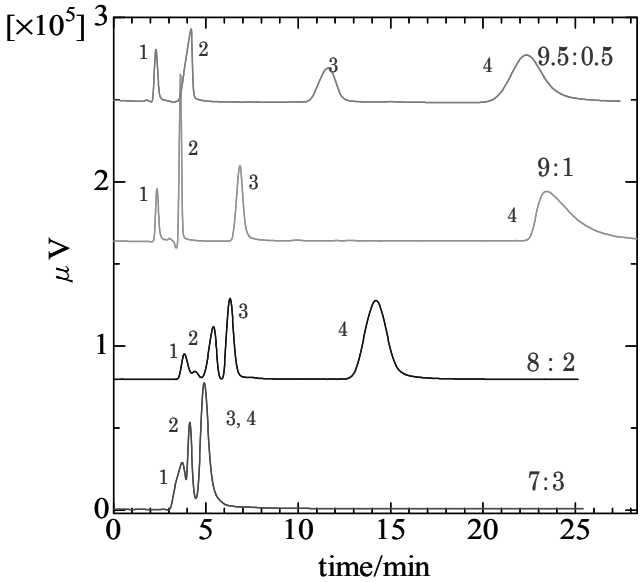

Fig. 9. Separation of organic acids on adenosine-bonded stationary phase

Column: Adenosine-bonded silica, 100 x 0.32 mm I.D.; Eluent: ACN:10 mM ammonium acetate, ratio as indicated; Sample: 1=phenol, 2=salicylic acid, 3=benzoic acid, 4=phthalic acid, 1 mM each; Flow-rate: 4.0 μL/min; Wavelength of UV detection: 254 nm.

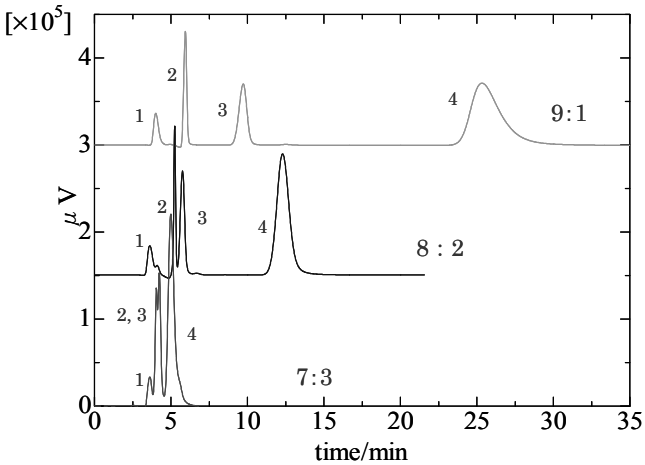

Fig. 8. Separation of organic acids on cytidine-bonded stationary phase

Column: Cytidine-bonded silica, 100 x 0.32 mm I.D.; Eluent: ACN:10 mM ammonium acetate, ratio as indicated; Sample: 1=phenol, 2=salicylic acid, 3=benzoic acid, 4=phthalic acid, 1 mM each; Flow-rate: 2.0 μL/min; Wavelength of UV detection: 254 nm.

Conclusions

Cytidine- and adenosine-boned bonded stationary phases were prepared *via* epoxy-ring opening reaction under various conditions. The resulting nucleotide-bonded silica gels were then packed into 0.32 mm fused-silica tubes (10 cm in length) and the columns were evaluated for the separation of inorganic ions (3 anions and 5 cations) and polar compounds (4 organic acids) using a UV detector under ion-exchange and HILIC modes, respectively. The results showed that both cytidine- and adenosine-bonded columns could separate mono- and divalent cations, respectively, using indirect UV detection with Copper sulfate used as the eluent. Adenosine-bonded column was found to have longer retention for organic acids under HILIC mode, and it was assumed that the distance between the phosphate and secondary amine groups in the structure plays an important role in the separation of these polar compounds.

Table 1 Elemental analysis of cytidine-bonded-silica gels under various conditions.

Reaction solvent/reaction temperature	Nitrogen / wt %	Nucleotide content / mmol g^{-1}
① Toluene / 110℃	0.14	0.03
② DMF / 90℃	0.86	0.20
③ DMF / 120℃	0.98	0.23
④ DMSO / 120℃	0.14	0.03
⑤ THF / 65℃	0.56	0.12
⑥ ACN / 80℃	0.91	0.22

Table 2 Elemental analysis of adenosine -bonded-silica gels under various conditions

Reaction solvent/reaction temperature	Nitrogen / wt %	Nucleotide content / mmol g^{-1}
① DMF / 90℃	0.47	0.07
② DMF / 120℃	0.66	0.10
③ DMSO / 120℃	0.35	0.05
④ ACN / 80℃	0.30	0.04

References

1. Ishii D. 1974, *Jasco Report*, **11**, 1.
2. Dandeneau R.D. and Zerenner E.H. 1979, *J. High Resolut. Chromatogr. Chromatogr. Commun.*, **2**, 351.
3. Takeuchi T. 2004, *Jasco Report*, **46**, 6.
4. Takeuchi T. 2004, *J. Ion Exchange*, **4**, 152.
5. Takeuchi T. 2005, *Chromatography*, **26**, 7.
6. Saito Y., Jinno K. and Greibrokk T. 2004, *J. Sep. Sci.*, **27**, 1379.
7. Lim L.W. 2015, *Chromatography*, **36**, 1.
8. Haddad P.R., Nesterenko P.N. and Buchberger W. 2008, *J. Chromatogr. A*, **1184**, 456.
9. Nesterenko P.N., Elefterov A.I., Tarasenko D.A. and Shpigun O.A. 1995, *J. Chromatogr. A*, **706**, 59.
10. Takeuchi T., Tokunaga K. and Lim L.W. 2013, *Anal. Sci.*, **29**, 423.
11. Lim L.W., Tokunaga T. and Takeuchi T. 2014, *Chromatography*, **35**, 95.

RNI No. MAHENG/2017/74063
ISSN No. (Print) 2581-5911

Ionic content of Hot spring water in Vajreshwari town of Maharashtra State, India

Dipak Shetty and Ganapathy Ramkrishnan*
SIES Institute of Chromatography and Spectroscopy,
Sri Chandrasekarendra Saraswathy Vidyapuram,
Plot 1C, Sector V. Nerul, Navi Mumbai - 400 706, India
E-mail: *director_ics@siesedu.net

Abstract

It is a very common belief that soaking in hot springs which are rich in sulphur content can cure some of the skin diseases.While we are not interested in learning the medical benefits of soaking in hot spring water, we are interested in studying the ionic content of the hotspring water.

This study focuses on the ion chromatographic analysis of Hot spring water to establish the current levels of anions and cations in hot springs of Vajreshwari town. As per our knowledge, this is the first time such a detailed study has been conducted using Ion chromatographic technique and reported.

In this study we propose two methods for identifying the origin of the stream of hot spring waters. Method 1 is by determining the ratio of monovalent cations to divalent cations and Method 2 is by calculating the ratio of Chloride to Sulphate ions present . Preliminary data shows that ratios calculated by both the methods (Method 1 and Method 2) are promising, but this has to be supported withfurther studies.

Keywords: *Vajreshwari town, Akloli,Ganeshpuri, Hot springs, Ion Chromatography, Anions, Cations*

Introduction

The beautiful town of Vajreshwari is an Indian tourist place mainly because of Vajreshwaridevi temple. The town is also called as Vadvali and Vajrayogini. Volcanic eruptions in Vajreshwari are the reason for such hot springs. Another spot of interest for travellers in the city is the shrine of Swami Nityananda and his samadhi located at Ganeshpuri nearly 2 km away from Vajreshwaridevi temple.

A hot water spring or a hydrothermal spring is a place where warm or hot groundwater comes out from the earth on a regular basis for at least a predictable part of the year and is significantly above the ambient ground temperature. Based on the geographical site and location, the heated water can hold more dissolved solids and especially a very high mineral content, containing everything from simple calcium to lithium, and even radium.[1]

It cannot be assumed that all spring water is pure, since many naturally occurring minerals are harmful or even dangerous to human andanimal health. A number of studies have found that the geothermal water may contain toxic elements such as arsenic and mercury, radioactive elements and pathogenic organisms such as the meningitis-causing *Naeglerias fowleri.*[2]

The purpose of this paper is to establish the current status of anions and cations in the Hot springs of Vajreshwari town in Maharashtra, India using Ion Chromatography.

Materials and Methods

Study area

Hot spring water samples were collected from different sites of Vajreshwari region (19.29°12.52" N, 73.01° 34.26" E), Maharashtra, India.Vajreshwari is at the foot of Mandakini Mountain, which was formed out of a volcanic eruption and it is this proximity that accounts for many hot springs in this region. It is reported that there are around twentyone hot water springs, just within a five kilometre radius of the temple.[3]

Vajreshwari is situated 80 km (2 hours) north of Bombay. It is 31 km away from the nearest railway station of Vasai. There are state transport buses running frequently from Vasai Road to Vajreshwari.

The climate is tropical in Vasai. In winter, there is very less rainfall in Vasai than in summer. This climate is considered to be Aw according to the Köppen-Geiger climate classification. The average annual temperature in Vasai is 26.7°C. The rainfall here averages 2317 mm. The driest month is January with 0 mm precipitation. With an average of 870 mm, the maximum precipitation occurs in July. With an average of 29.8°C, May is the warmest month. January has the lowest average temperature of the year (23.5°C). During the year, the average temperatures vary by 6.7°C.[4]

Fig.1. The study area (Image source: Google Earth)

Sampling strategy

Water samples were collected in December 2015. Water samples were collected in a high density polyethylene bottles previously washed with soap solution and rinsed with De-ionised water. Grab method of collection was used to collect water samples. The samples were kept in refrigerator at -4°C until analysis.

Sampling sites

Akloli: The hot springs at Akloli are located on the left bank of Tansa river. Ten hot springs are aligned along N10°W-S10°E and N55°W-S55°E.

A concrete well called "kund" is constructed at each hot spring site. Sampling was carried out in polythene bottles in seven kunds and one flowing stream and labelled as Station 1 to Station 9.Temperature of each sample was measured.

Ganeshpuri: Sampling was done at Garamkund situated near Nityanand Ashram and labelled as Station-10.

The samples collected from different stations with their names are presented in Table 1.

Station	Name
S-1	Shiv Kund
S-2	Surya Kund
S-3	Subhash Kund
S-4	Hot spring water stream near Chandra Kund
S-5	Chandra Kund
S-7	Seeta Kund
S-8	Ram Kund
S-9	Lakshman Kund
S-10	GaramKund - Ganeshpuri

Experimental

The Ion Chromatograph used was Metrohm 850 Professional IC (Switzerland), equipped with Metrohm Suppressor Module (MSM) and conductivity detector. Sample injection was done manually. The injection loop has a capacity of 20 µL. The anion exchange column focused on Fluoride (F^-), Chloride (Cl^-), Nitrite (NO_2), Bromide (Br^-), Nitrate (NO_3^-), Phosphate (PO_4^{3-}), Sulphate (SO_4^{2-}) and Iodide (I^-) and the cation exchange column focused on Lithium (Li^+), Sodium (Na^+), Ammonium (NH_4^+), Potassium (K^+), Calcium (Ca^{2+}) and Magnesium (Mg^{2+}). The anionic and cationic columns are useable over a pH range of 3-12 and 2-7 respectively. Table 2 shows the method parameters for anion and cation analysis.

Table 2. Anion and Cation Method parameters

Anion Method Parameters

Column	: Metrosep A supp5 150/4.0
Oven Temp.	: 27°C
Mobile Phase	: 3.2 mmol carbonate and 1 mmol bicarbonate
Flow rate	: 0.7 mL/min
Injection Volume	: 20 µl

Cation Method Parameters

Column	: Metrosep C4 150/4.0
Oven Temp.\	: 27°C
Mobile Phase	: 1.7 mmol nitric acid and 0.7 mmol Dipicolinic acid
Flow rate	: 0.9 mL/min
Injection volume	: 20 µl

Standard Preparation

1. Anions

1000 ppm stock solutions of F^-, Cl^-, NO_2^-,Br^-, NO_3^-, PO_4^3, SO_4^2 and I^- were prepared separately. Three standard calibration levels viz. level-I (1 ppm), level- II (5 ppm) and level- III (10 ppm)were prepared by serial dilutions of individual stock solutions.

2. Cations

1000 ppm stock solutions of Na^+, NH_4^+, K^+, Ca^{2+}, Mg^{2+} and Li^+ were prepared separately. Three standard calibration levels viz. level-I (1 ppm), level- II (5 ppm) and level- III (10 ppm) were prepared by serial dilutions of individual stock solutions.

Figure 2a and 2b represent typical chromatograms of calibration standard level-III for Anions and Cations. Fig. 2a represents Standard chromatogram of anion calibration level-III (10 ppm).

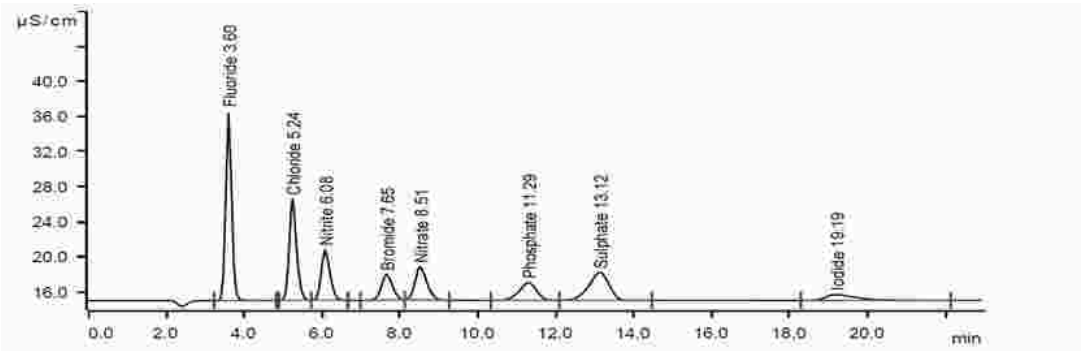

Fig. 2a. Standard chromatogram of anion calibration level-III (10 ppm)

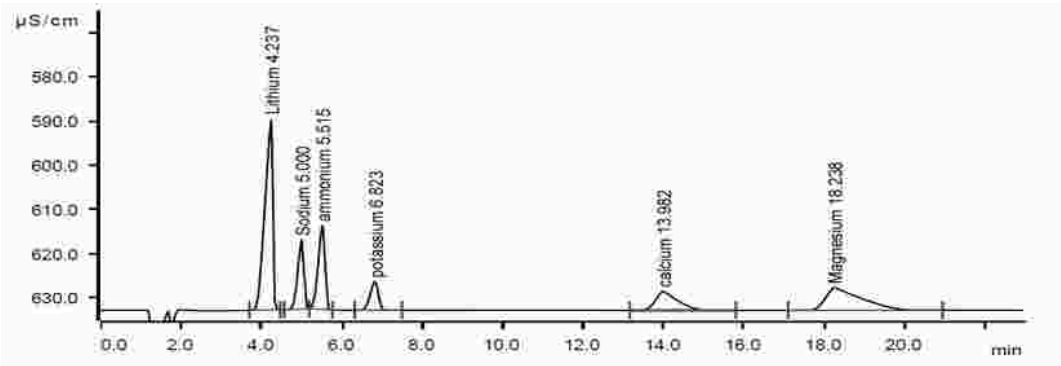

Fig. 2b. Standard chromatogram of cation calibration level-III (10 ppm)

Table 3a and 3b represents the Relative standard deviation and Correlation of anion and cation standard determinations.

Anions

Parameter	Fluoride	Chloride	Nitrite	Bromide	Nitrate	Phosphate	Sulphate	Iodide
RSD %	13.346	9.104	0.194	0.718	0.325	7.638	6.194	2.274
Correlation	0.9915	0.9962	0.9999	0.9999	0.9999	0.9958	0.9980	0.9997

Cations

Parameter	Lithium	Sodium	Ammonium	Potassium	Calcium	Magnesium
RSD %	6.112	4.421	1.106	0.160	1.046	2.562
Correlation	0.9975	0.9987	0.9999	0.9999	0.9999	0.9996

Sample Preparation

For Anions

The water sample was prepared by performing 10-fold dilution for first two samples and 20-fold dilution for remaining samples.

For Cations

For cation analysis 10 fold dilution was performed for all samples.

All cation and anion samples were further filtered using 0.2µm syringe filter before injecting into IC.

Results and Discussion

The temperature recorded for nine water samples were in between 42 to 60°C, the highest being at station 10. pH was in between 7.15 to 8.70.Conductivity was in the range of 1.028 to 1.640 mS cm^{-1}. The values for temperature, pH and conductivity are presented in Table 4a. The amount of anions and cations are represented in Tables 4b and 4c respectively.

All the water samples are highly mineralized chloride-sulphate waters.

Through this study we have compared the ionic composition of hot spring water from Akloli and Ganeshpuri regions in Vajreshwari town.

Table 4a: pH, temperature and electrical conductivity of water samples

Station	pH	Temperature (^{o}C)	Electrical Conductivity (mS cm^{-1}) at Room temperature (25^{0}C)
Station 1	7.80	46	1.572
Station 2	8.54	50	1.611
Station 3	7.48	50	1.551
Station 4	8.60	58	1.546
Station 5	7.18	50	1.593
Station 7	7.15	42	1.640
Station 8	7.35	44	1.610
Station 9	7.31	46	1.596
Station 10	8.70	60	1.028

The conductivity of station 10 water is substantially low as compared to that of the waters from Stations 1 to 9.

Table 4b: Concentration in ppm of anions in water samples from the study area

Sample	Fluoride	Chloride	Nitrite	Bromide	Nitrate	Phosphate	Sulphate	Iodide
*Station 1	1.3	495.0	ND	0.8	0.2	ND	37.7	ND
Station 2	2.3	1703.4	ND	2.8	0.1	ND	126.6	ND
Station 3	3.0	1515.3	ND	2.8	0.1	ND	129.8	ND
Station 4	2.5	1958.7	ND	3.3	1.4	ND	160.5	ND
*Station 5	0.6	180.0	ND	0.3	0.1	ND	21.0	ND
Station 7	0.1	1689.1	ND	2.5	0.5	ND	146.9	ND
Station 8	1.9	1586.4	ND	2.4	0.3	ND	138.9	ND
Station 9	2.0	1629.6	ND	2.5	ND	ND	142.4	ND
Station 10	2.6	1024.2	ND	2.4	0.3	ND	146.4	ND

Table 4c. Concentration in ppm of cations in water samples from the study area

Sample	Lithium	Sodium	Ammonium	Potassium	Calcium	Magnesium
Staion 1	0.04	496.3	3.2	10.9	371.5	0.8
Station 2	0.04	474.2	3.7	10.8	348.5	1.4
Station 3	0.03	396.0	3.4	8.6	316.7	0.4
Station 4	0.05	436.9	3.3	8.9	326.2	0.5
Station 5	0.05	447.5	4.6	10.5	331.3	1.0
Station 7	0.05	486.9	6.8	11.7	366.7	1.0
Station 8	0.05	448.3	6.4	10.0	337.9	0.8
Station 9	0.03	228.3	6.1	5.1	187.0	0.7
Station 10	0.05	343.1	4.1	7.0	152.8	1.8

***Note –** Anion content of Station -1 and Station-5 showed unexpectedly low values which could be due to manual error during analysis. This was confirmed by comparing the cation content of the same samples which are comparable to that of other samples. Anion values of Station-1 and Station-5 have been neglected in all the other comparisons.

Chloride content is rather high, ranging from 1024 ppm in Station-10 to 1959 ppm in Station-4. Sulphate content varies from 126.6 ppm in Station-1 to 161 ppm in Station-4. Sodium content varies from 228 ppm in Station-9 to 496 ppm in Station- 1, Calcium content varies from 152.8 ppm to 372 ppm, Potassium from 5 ppm to 11.7 ppm and Fluoride content varies from 0.1 ppm to 3 ppm. The thermal water contains high chloride content with appreciable amount of sulphate. The thermal springs in West Coast have high salinity as compared to ground water (Misissaleet al, 2000). High chloride content may suggest direct access to geothermal fluid reservoir or mixing of seawater with thermal water[5].

Table 4a and 4b shows the cation and anion composition of the study area and the corresponding chromatograms are given in Figures 3a and 3b. The result showed that Hot spring water is dominated by Sodium (Na^+) and Calcium(Ca^{2+})ions. The trend observed was $Na^+ > Ca^{2+} > K^+ > NH^{4+} > Mg^{2+} > Li^+$.Anions follows the trend $Cl^- > SO_4^{2-} > Br^- > F^- > NO_3^-$. Nitrite, Phosphate and Iodide were not detected.

Chloride ions(Cl^-) have a large migratory ability in connection with the very high solubility of chloride salts of sodium, magnesium and calcium. Their presence in water is naturally associated with the processes of leaching from minerals (e.g. gallite, sylvite, carnallite, bischofite), from rocks (e.g. nephelines), and from saline deposits. The main source of sulfate inwater is various sedimentary rocks which include gypsum and anhydride. Water enrichment by sulfates takes place both by the process of oxidation of sulfide, which is abundant in the Earth's crust and oxidation of hydrogen sulfide which is created during volcanic eruption and is present in atmospheric precipitation.

To show the distinction between the Akloli region hot spring water and Ganeshpuri region hot spring water, ratio of total monovalent cations (A^+) to divalent cations (B^{++}) and ratio of Cl^- to SO_4^{2-} was calculated as given below:

Table 4a shows that the conductivity of Ganeshpuri region water (station 10) is substantially low as compared to the waters from Akloli region (station 1 to 9) Table 5a shows the ratio of monovalent cations to divalent cations in the Akloli region hot spring water is low as compared to Ganeshpuri region hot spring water .

Table 5b shows that there is large difference between the Chloride to Sulphate ratio of Ganeshpuri hot spring water as compared to Akloli region hot spring water. The lower value of Chloride to Sulphate ratio in Ganeshpuri region could be attributed to the mixing of thermal water with marginal steam heated water or interactions with sulphur bearing environment during water rock reaction. Also, relatively high SO_4 content may be attributed to oxidation of sulphur released in gaseous activity and water rock interaction.[6]

Fig. 3a and 3b. Chromatograms showing the presence of anions and cations respectively in Hot springs samples

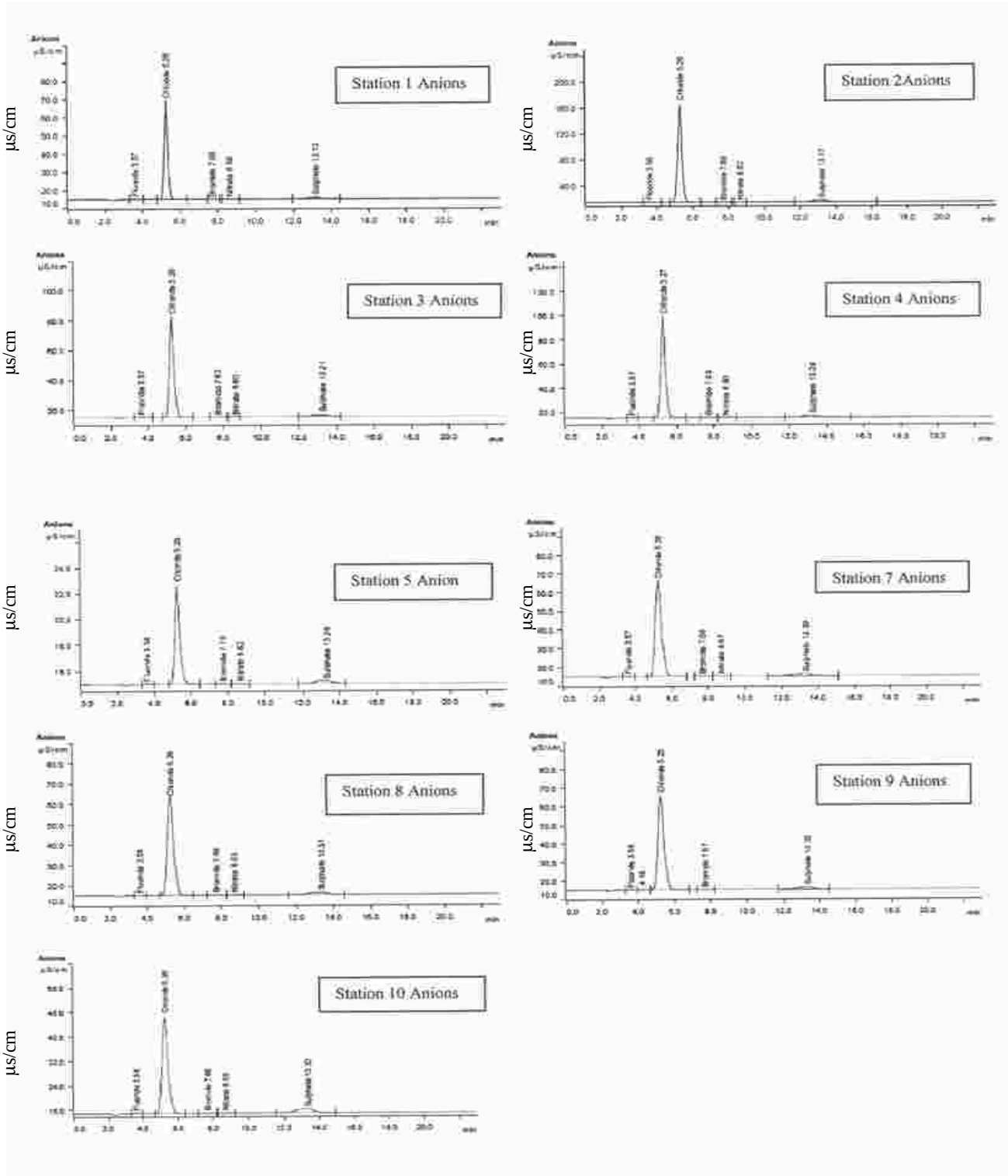

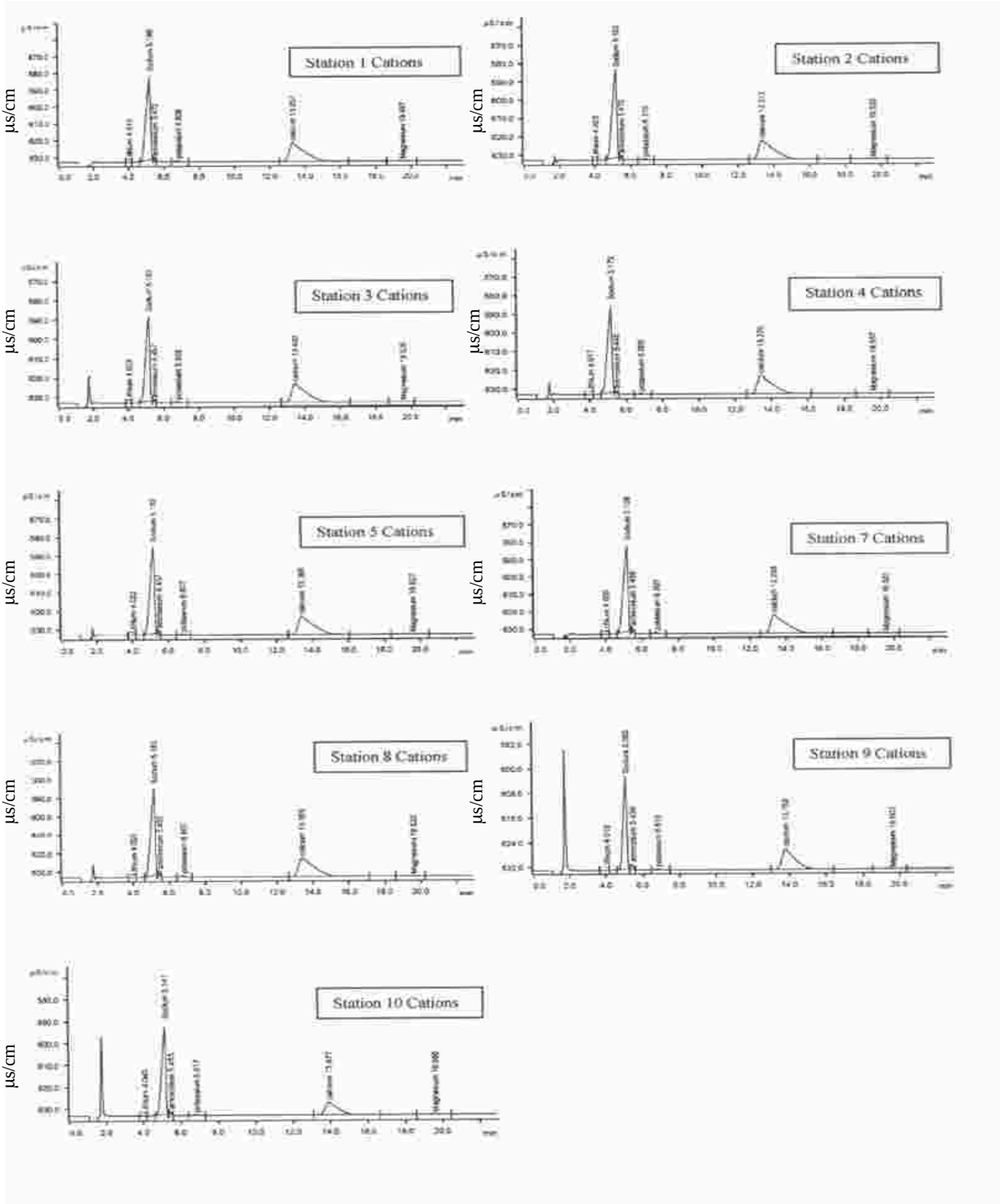
Station 1 Cations
Station 2 Cations
Station 3 Cations
Station 4 Cations
Station 5 Cations
Station 7 Cations
Station 8 Cations
Station 9 Cations
Station 10 Cations
µs/cm

Table 5a: Ratio of total monovalent cations to divalent cations

Sample	Total monovalent cations (A^+)	Total divalent cations (B^{++})	Ratio (A^+/B^{++})
Station 1	510.44	372.30	1.37
Station 2	488.74	349.90	1.40
Station 3	408.03	317.10	1.29
Station 4	449.15	326.70	1.37
Station 5	462.65	332.30	1.39
Station 7	505.45	367.70	1.37
Station 8	464.75	338.70	1.37
Station 9	239.53	187.70	1.28
Station 10	354.25	154.60	**2.29**

Table 5b: Cl^-/SO_4 Ratio

Sample	Chloride	Sulphate	Cl^-/SO_4
Station 2	1703.4	126.6	13.5
Station 3	1515.3	129.8	11.7
Station 4	1958.7	160.5	12.2
Station 7	1689.1	146.9	11.5
Station 8	1586.4	138.9	11.4
Station 9	1629.6	142.4	11.4
Station 10	1024.2	146.4	**7.0**

Conclusions

Common inorganic cations and anions in water samples of Vajreshwari town collected at two locations Akloli and Ganeshpuri were compared. The trends observed were almost matching for both the regions except one or two exceptions for bromide and fluoride contents.

The trend observed was $Na^+ > Ca^{2+} > K^+ > NH^{4+} > Mg^{2+} > Li^+$.Anions follows the trend $Cl^- > SO_4^{2-} > Br^- > F^- > NO_3^-$. Nitrite, Phosphate and Iodide were not detected.

There is a drastic difference in Chloride to Sulphate ratio and monovalent cation to divalent cation ratio in water samples fromAkloli and Ganeshpuri regions. Both these observations indicates that the source of the hot spring stream in Akloli region is different from that in Ganeshpuri region and may belong to a different fault line or fracture in the earth. These findings may play very important roles in indicating the origin and source of hot spring waters and offers scope for further research.

References

1. Satpal Singh Bisht, Nagendra Nath Das and Tripathy N.K., 2011, *Journal of Energy, Environment & Carbon Credits*, **1(1)**, 1-15.

2. Olivier. J., Venter J. S., and Jonker C. Z., 2011, *Journal Home*, **37,** http://dx.doi.org/10.4314/wsa.v37i4.1

3. Susie Harrison, 2015, Hot Springs of Maharashtra, Woozical World (1),

4. http://en.climate-data.org/location/6281/

5. P.B. Sarolkar, 2005, Proceedings of World Geothermal Congress, Antalya, Turkey, p.24-29.

6. Ayaka Homma and Hiroaki Tsukahara, 2008, *Bull. Earthq. Res. Inst.Univ., Tokyo*, **83,** 217-225.

RNI No. MAHENG/2017/74063
ISSN No. (Print) 2581-5911

Effect of length of Spacer and carbonyl group on quantum yield of pyrene armed Calix[4]arene upon complexation with metal

Vrashali S. Kalyani and Dipali D. Malkhede*
Department of Chemistry, Savitribai Phule Pune University, Pune, India-411007.
Email: ddm@chem.unipune.ac.in, vrashalikalyani@gmail.com

Abstract
Synthesis of mono and disubstituted pyrene derivatives of Calix[4]arene (MPCX4 and PCX4) was carried out. Its complexation with lanthanides, transition metal ions and potassium was studied by fluorescence technique and found to be selective towards specific metal ions. Among lanthanides, Eu^{+3} shows less quantum yield upon complexation with both MPCX4 and PCX4. While Ni^{+2} gave more quenching with MPCX4Cu^{+2} gave more quenching with PCX4. Ion-ion interaction and Van der waals interaction play important roles in binding. Quenching constants and quantum yield of complexation have been calculated.

Keywords: *pyrene, calixarene, metal ions, complexation quenching constants, quantum yield*

Introduction

In current research, a potent activity is synthesis and design of molecules with such functional groups which can be used for sensing of specific ions. This complexation has applications in various fields of chemical, biological and environmental processes[1]. Various techniques are available for sensing, among them detection by fluorescence technique has been widely used because of some distinct advantages in terms of sensitivity, in-situ monitoring, discrimination, response time etc.

However, macrocyclic ligands are good options for molecular sensors because of their incredible selectivity towards various metal ions. In this regard, calixarenes are very attractive because modifications of calixarene give rise to different derivatives with various functional groups, which furnish a highly preorganized framework for the accumulation of binding sites.

In this regard, calixarenes, which are macrocyclic oligomers made up of phenol units linked by methylene bridge are found to be very suitable because of their capacity to bind variety of ions[2]. Calix[4]arenes are most favoured because of their inflexible structures, which make them suitable for complexation with metal ions[3]. Complexation of metal ion can be carried out by both upper and lower rims of calixarene. These macrocycle show ion-selectivity which is directed by various components such as binding sites, steric hindrance, confirmation, size of the cavity and solvents used in the complexation study.

It is interesting to note that fluorescent sensors are constructed by attaching two aromatic fluorophores in proximity so that they are close enough (within van der Waals contact) to make π–π stacking interaction possible. Under such conditions, electronic excitation of one ring can cause an enhanced interaction with its neighbour, leading to excited-state dimer or excimer[4]. To establish this category of fluoroionophore, molecular

sensors including calix[4]arene derivatives (in cone and 1,3-alternate confirmation) as ionophore and two pyrene moieties in close proximity as fluorophore were constructed and their ion binding study carried out with alkali and alkaline metals[5].

The f-block elements have distinctive luminescent and magnetic properties and are widely utilized in luminescent imaging[6], medical diagnostics[7] and biochemistry and structural biology[8]. Macrocyclic ligands form complexes with Europium (III) and Terbium (III) which have prospective advantages as labels in bio affinity assays; these are depending on time-resolved measurements of the metal luminescence upon ligand excitation. Ungaro's and Sabbatini's group have investigated 2,2'- bipyridine lariat calixcrown macrocycles which form strongly luminescent Eu (III) and Tb (III) and Gd (III) complexes[9,10].

There is great interest in quantification of Cu^{2+} by using selective and sensitive organically derivatized synthetic receptors in the biological as well as in the environmental media[11]. There are many calix[4] arene based fluorescence sensors which have been outlined in literature for Cu^{2+}, but ratiometric ones are very rare[12-14].

Alkali and alkaline earth metal ions are identified by a new category of hybrid molecules which have been evolved by integrating crown ethers into calix[4] arene[15,16]. Among different confirmations of the calixarene, 1,3- alternate conformers have been studied as it is complexing agent for alkali-metal ions[17]. Particularly for Na^{+} and K^{+}, the calixarene containing crown-5 and crown-6 cavity are found more suitable for complexation [18].

We have elaborated in our previous study the effects of length of spacer and adjacent electron withdrawing group on fluorophore, and number of substitution on ionophore by fluorophore. We have synthesized and characterised monosubstituted pyrene derivative of calix[4]arene (MPCX4) and disubstituted pyrene derivative of calix[4]arene (PCX4) as shown in Figure 1. Complexation study of these ligands (MPCX4 and PCX4) with lanthanides La^{+3}, Eu^{+3}, Tb^{+3}, Dy^{+3}, $Nd^{+3}$and transition metal ions Cu^{+2}, Ni^{+2}, Co^{+2}, K^{+1} was carried out by using fluorescence technique. Quenching constant and quantum yield of complexation have been calculated. Study of effect of length of spacer, electron withdrawing group adjacent to fluorophore on quantum yield was carried out.

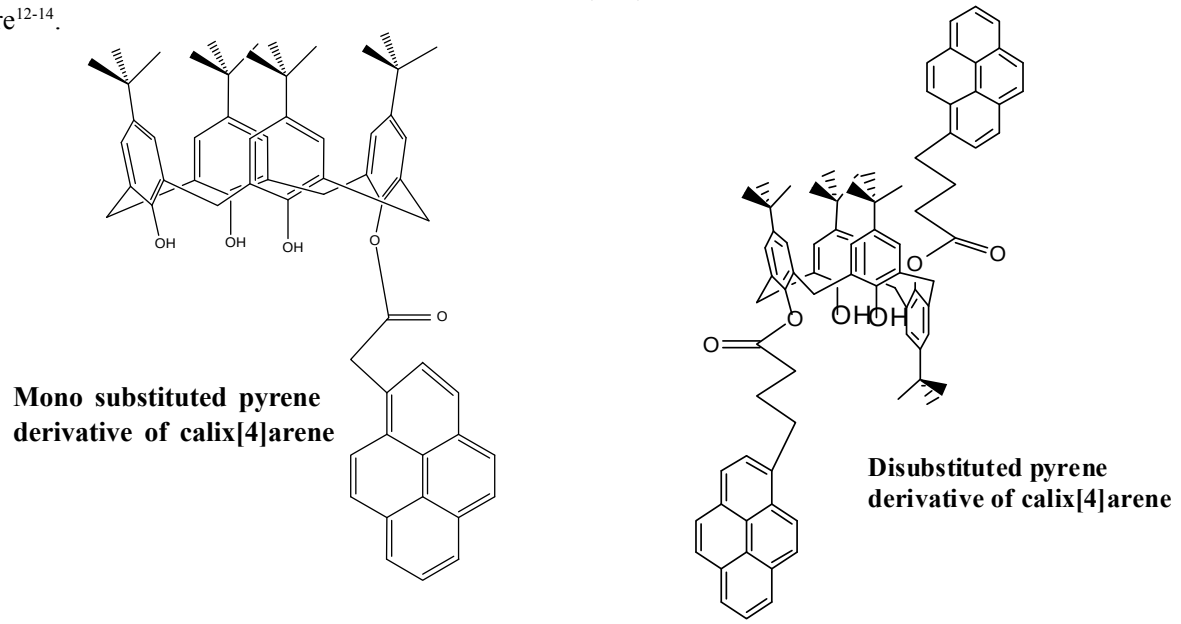

Fig. 1: Schematic representation of mono and di substituted pyrene derivative of calix[4]arene (MPCX4 and PCX4).

Materials and Methods

Synthesis and characterization of MPCX4 and PCX4
Synthesis of MPCX4 was carried out as per the procedure given by Yukihiro Nishimura[19]. The compound was characterized by ^{1}H NMR, ^{13}C NMR, and MALDI spectral analysis. ^{1}H NMR of MPCX4 is similar with that reported in literature which is shown in Figure S1. Figure S2 represents HR-MS spectra of MPCX4.

Synthesis of pyrene derivative of calix[4]arene (PCX4) was carried out as per the reported procedure by Kalyani *et al* [20a, 20b]. Purity of PCX4 was checked by TLC and melting point. PCX4 obtained was in partial cone confirmation, which was proved by ^{1}H NMR. It shows two singlets and two pairs of doublet for aromatic proton as well as one pair of doublet for bridging $-CH_2$ as reported by C. David Gutsch[21, 22] splitting of singlet of tertiary butyl group at 1.25 ppm proves partial cone confirmation of PCX4.

^{1}H-NMR (500Hz, $CDCl_3$): 1.25 (singlet split ter. butyl 36H), 1.95 (m 4H), 2.4 (t 4H), 3.4 (t 4H), 4.06 (t, 8H), 7.4 -7.9 (two singlets and two pairs of doublet Ar-H 8H), 8.0-8.4 (m 8H Py), 9.5 (s 2H). (Figure S3)

^{13} C-NMR: 27, 33, 125,135,137,174. (Figure S4)

HR-MS Spectra (Acetonitrile): 1238, 1192, 1076, 975, 833,671. (Figure S5)

FT-IR*í* max (KBr, cm^{-1}): 3321, 2956, 1680, 1593, 1481, 842 cm^{-}1. (Figure S6)

Measurement
UV-Vis absorption spectra were performed using Varian Cary 3E spectrophotometer. Fluorescence spectra were recorded on Shimadzu Spex Fluorolog 2 spectro-fluorometer. Data were collected with 1 nm interval and excitation slit width 2.5 nm and emission slit width 5 nm. All measurements were taken with stock solution of MPCX4 (1 x 10^{-6} M) and PCX4 (1 x 10^{-6} M) dissolved in acetonitrile and complexation titrations were carried out with salt solution of Eu, Nd, La, Dy, Tb, Cu, K (1 x 10^{-3} M) in Milli-Q. Florescence graph plotting and curve fitting was done on Sigma plot 12 version.

Reagents and Materials
All metal salts were purchased from Sigma Aldrich with 98% purity. Acetonitrile was 99.8% pure (HPLC grade). All reagents employed for the synthesis and purification were of AR grade. Nitrate salts of all Lanthanides metal ions and chloride salts of all transition metal ions were used for complexation studies which were purchased from Sigma Aldrich.

Results and Discussion

Fluorescence properties of Complex of lanthanides (La^{+3}, Eu^{+3}, Tb^{+3}, Dy^{+3}, Nd^{+3}) and metal ions (Cu^{+2}, Ni^{+2}, Co^{+2}, K^{+1}) with MPCX4:
There are many pyrene derived calixarene used as chemical sensors for various cations and anions (Cs^{+2}, Ag^{+2}, Pb^{+2}, Cu^{+2}, In^{+2}, F^{-})[23]. But pyrene derived calixarene as sensor for lanthanides has been less studied. So we tried to find out more a favourable structure of calixarene to bind lanthanide ions.

The emission spectra of MPCX4 were recorded in aqueous solution with addition of salt solution of metal ions by using excitation wavelength of 340 nm. The characteristic peaks for monomer emission at 385, 406 nm are observed which is shown in corresponding Figure 2. Titration of MPCX4 against M^{3+} and M^{2+} results in a gradual quenching of the fluorescence emission at λ=386 nm band. In order to find the selectivity of MPCX4 towards metal ions, quenching constants of complex were calculated in aqueous solution by using Equation (1). The titration results suggest that the MPCX4 shows dynamic quenching in presence of all metal ions. However, the quenching constants of Nd^{+3} and Co^{+2} with MPCX4 are highest.

Figure 2 (a) represents the fluorescence spectra of MPCX4 as a function of concentrations of nitrate salt of Nd^{+3} in water at 25°C and Figure 2b represents curve fitting for calculation of binding constant. Free MPCX4 gave monomer emission centred at approximately 385

nm. Upon addition of M^{3+} in the solution, the fluorescence peak at 385 nm showed decrease in intensity. The monomer emission intensity decreased when the concentration of M^{3+} was increased. These results clearly indicate that there is structural change of MPCX4 upon complex formation. The pyrene moiety in a MPCX4 is quenched by Photoinduced Electron Transfer from pyrene of MPCX4 to M^{3+} ion. Binding may be because of ion-ion interaction between +vely charged M^{+3} ion and π electron rich cavity of MPCX4 as well as partially –vely charged oxygen of lower rim of calixarene. An expected structural change of MPCX4 before and after the addition of M^{3+} is represented in Scheme 1. The plots of fluorescence intensity (I) at 385 nm of MPCX4 *vs.* concentrations of different lanthanides, transition metal ions and alkali metal ions, including La^{+3}, Eu^{+3}, Tb^{+3}, Dy^{+3}, Nd^{+3} Cu^{+2}, Ni^{+2}, Co^{+2}, K^{+1} are shown in (Figures S7a and S7b to S13a and S13b). The intensity at 385 nm vs. concentration profile of MPCX4 to M^{3+} is similar to that of other lanthanides La^{+3}, Eu^{+3}, Tb^{+3}, Dy^{+3}, Nd^{+3}. MPCX4 is specific towards Eu^{+3} and Ni^{+2} while other metal ions cause no fluorescence or slight fluorescence change. Metal-ion concentration dependence of the emission intensity with Co^{+2} represented in Figure 3a and 3b which allowed us to determine the association constant (*K*) by the non-linear curve-fitting method by using following equation and the data are listed in Table 1. For non linear curve fitting Equation 1 is used as follows:

$$x = \mathrm{K1.\ a}\left(\frac{\mathrm{b}}{1+\mathrm{K1\,x\,b}}\right)$$

$$x1 = \frac{x}{1+alfa\,x\,b}$$

$$f = P2\,x\,x1 + P1x(a-x) \text{.....(1)}$$

where

constant for quenching, alfa = 0,

a = concentration of MPCX4,

b = concentration of Metal ion, and

p1 = fluorescence intensity before complexation,

p2 = fluorescence intensity of MPCX4 after complexation

K1 = Association constant (K1 = K).

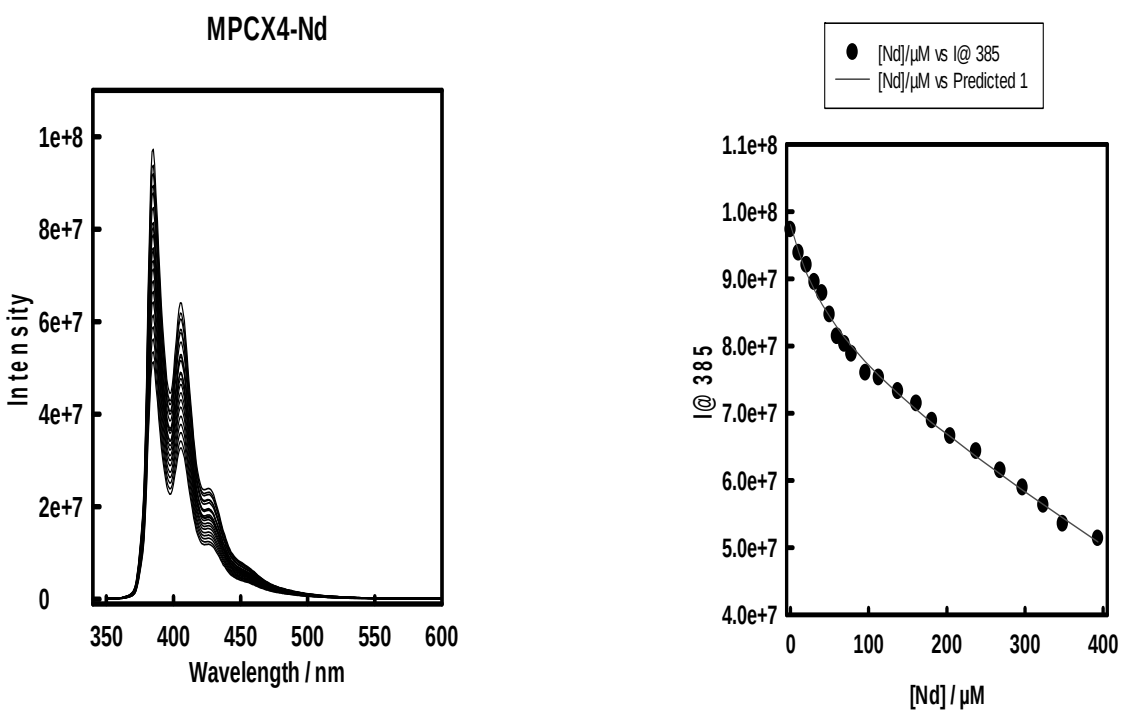

Fig. 2: a) The changes in the fluorescence spectra of MPCX4 (1 × 10^{-6} M in H_2O) upon addition of different concentrations of Neodium Nitrate. λex = 340 nm. B) The binding curve for the respective MPCX4: Nd^{+3} systems.

The order of *K* value for different metal ions with MPCX4 is Nd^{+3} > La^{+3}> Dy^{+3} > Tb^{+3} > Eu^{+3} and in transition metals Co^{+2} > Cu^{+2} > Ni^{+2}, K^{+1}. While in terms of quantum yield MPCX4 shows selectivity for Eu^{+3} and Ni^{+2}. The order of quantum yield in lanthanides is Eu^{+3}> Tb^{+3}> Nd^{+3}> Dy^{+3}> La^{+3} and in transition metals Ni^{+2}> Cu^{+2} > Co^{+2}. Figure 4 represent the bar graph for all metal ions with reference to quantum yield. These results suggest that MPCX4 is specific quenching for Eu^{+3} and Ni^{+2}.

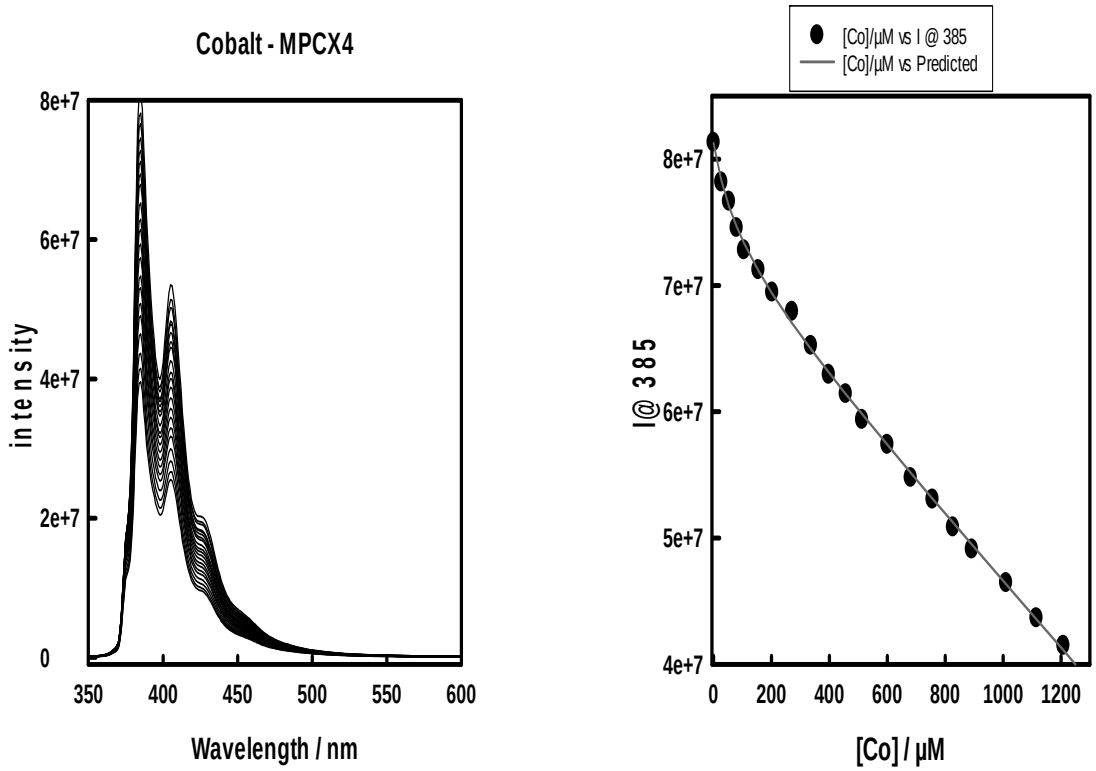

Fig. 3: A) The changes in the fluorescence spectra of MPCX4 (1×10^{-6} M in H_2O) upon addition of different concentrations of Cobalt Nitrate. λex = 340 nm. B) The binding curve for the respective MPCX4: Co^{+3} systems.

Table 1: The quenching constants and quantum yield for complex of MPCX4 and metal ions.

MPCX4	La^{+3}	Nd^{+3}	Eu^{+3}	Tb^{+3}	Dy^{+3}	Co^{+2}	Ni^{+2}	Cu^{+2}	K^{+1}
$K/\mu M^{-1}$	0.0108	0.0175	0.001	0.004	0.0054	0.0112	0.0028	0.0033	0.0042
ϕ_0	4.4e+7	6.3e+7	1.4e+7	6.3e+7	4.7e+7	6.9e+7	1.0e+8	6.4e+7	4.9e+7
ϕ_1	3.6e+7	4.9e+7	8.1e+6	4.7e+7	3.8e+7	6.1e+7	4.0e+7	3.3e+7	3.9e+7
ϕ_1/ϕ_0	0.8337	0.7925	**0.5723**	0.7415	0.7949	0.8852	**0.3988**	0.5153	0.8005

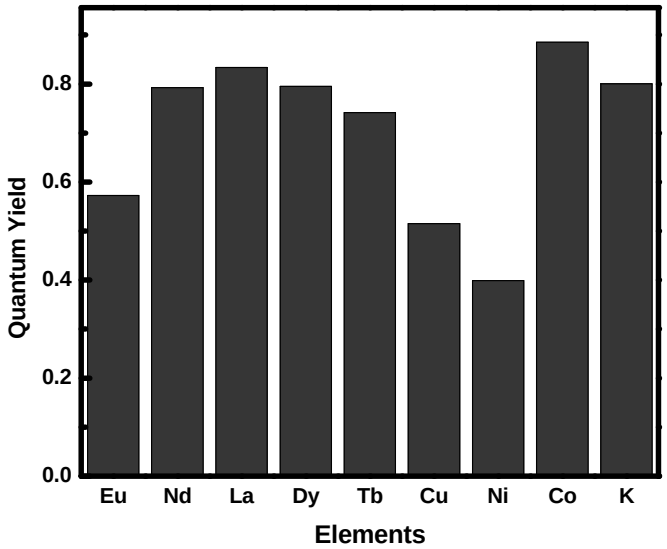

Fig. 4: The fluorescence intensity of MPCX4 (2.5 µM) at 385 nm upon the addition of Eu^{+3} (1 mm) and other metal ions (1 mm) in ACN/H_2O (1:9).

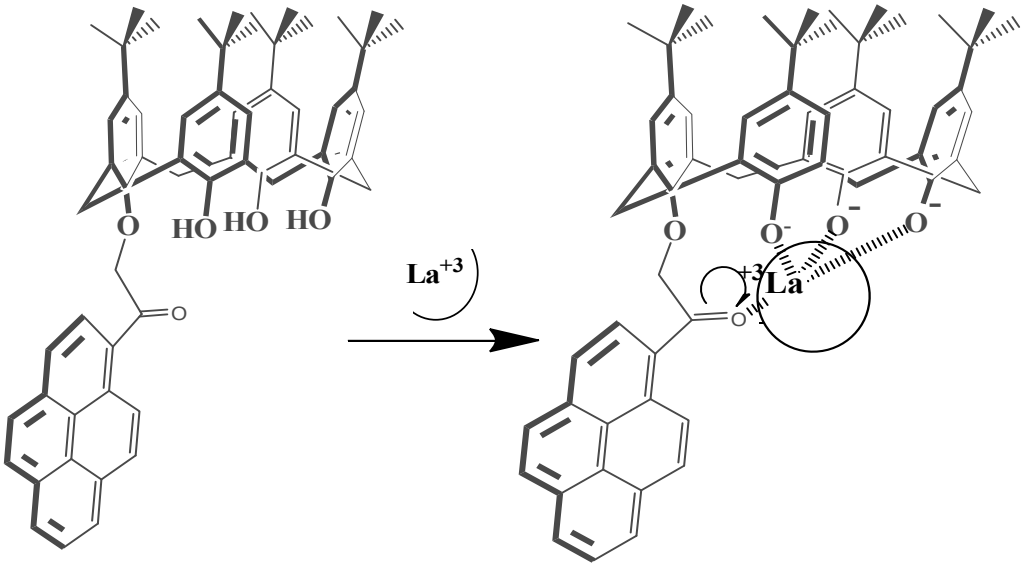

Scheme 1: Possible binding modes of complexation of MPCX4 and La^{+3}.

Fluorescence properties of complexes of lanthanides (La^{+3}, Eu^{+3}, Tb^{+3}, Dy^{+3}, Nd^{+3}) and metal ions (Cu^{+2}, Ni^{+2}, Zn^{+2}, Co^{+2}, K^{+1}) with PCX4:

The fluorescence spectra of PCX4 were determind with addition of salt solution of metal ions in aqueous solution by using excitation wavelength of 350 nm. Figure 5 represents characteristic peaks for monomer emission at 377, 395 nm. As PCX4 is in partial cone confirmation, two pyrenes are apart from each other therefore there is no excimer formation. There is gradual quenching of the fluorescence emission at λ = 377 nm band in titration of PCX4 with M^{3+} and M^{2+}. Quenching constants of complex were calculated in aqueous solution by using above Equation 1 and it was found

that PCX4 has specificity of metal ions.

It is observed from the titration results that PCX4 gives dynamic quenching with all metal ions. However the quenching constant of Dy^{+3} and K^{+1} with PCX4 is highest. *K* values for different metal ions are in the following order: Dy^{+3}> La^{+3}> Nd^{+3} > Tb^{+3} > Eu^{+3} and in transition metals, Co^{+2} e" Cu^{+2} > Ni^{+2}, K^{+1}.

Figure 5 (a) represents the fluorescence spectra of PCX4 as a function of concentrations of nitrate salt of Dy^{+3} in water at 25°C and Figure 5b shows its non linear curve fitting for determine quenching constant. Free PCX4 gave monomer emission which has maximum peak intensity at approximately 377 nm. Addition of M^{3+} in the solution of PCX4, results in the decrease in intensity of fluorescence peak at λ=377 nm. As the concentration of M^{3+} increased, there was decrease in monomer intensity. There is possibility of structural change of PCX4 upon complex formation. Quenching is due to PET (Photoinduced electron transfer) from pyrene moiety in PCX4 to M^{3+} ion. The driving force for complexation is ion-ion interaction between +vely charged M^{+3} ion and π electron rich cavity. There may be strong ion interaction between partially –vely charged oxygen of lower rim of calixarene and + vely charged metal ion. Scheme 2 represents an expected structural change of PCX4 before and after the addition of M^{3+}. Figures S14a and S14b to S19a and S19b) show the plots of fluorescence intensity (I) at 377 nm of PCX4 *vs.* concentrations of different lanthanides, transition metal ions and alkali metal ions, including La^{+3}, Eu^{+3}, Tb^{+3}, Nd^{+3}, Cu^{+2}, Ni^{+2}, Co^{+2}. Figure 6a represents the change in fluorescence intensity of PCX4 with addition of K^{+} and Figure 6b gives non linear curve fitting for complexation. Other metal ions cause no fluorescence or slight change fluorescence intensity after complexation. Association constant (*K*) were calculated by the non-linear curve-fitting method by using above Equation 1 and the data are tabulated in Table 2.

Binding constant of PCX4 shows more affinity for Lanthanides than the transition metals. This may be because of featured length of spacer and absence of adjacent carbonyl group to fluorophore. PCX4 gives remarkable quenching for Eu^{+3} and Cu^{+2} ions and affects the quantum yield. The order of quantum yield for lanthanides is Eu^{+3}> La^{+3} >Dy^{+3}> Tb^{+3}> Nd^{+3} and for transition metals Cu^{+2} > Ni^{+2} > Co^{+2}, K^{+1}. Figure 7 shows bar graph of all elements with reference to quantum yield.

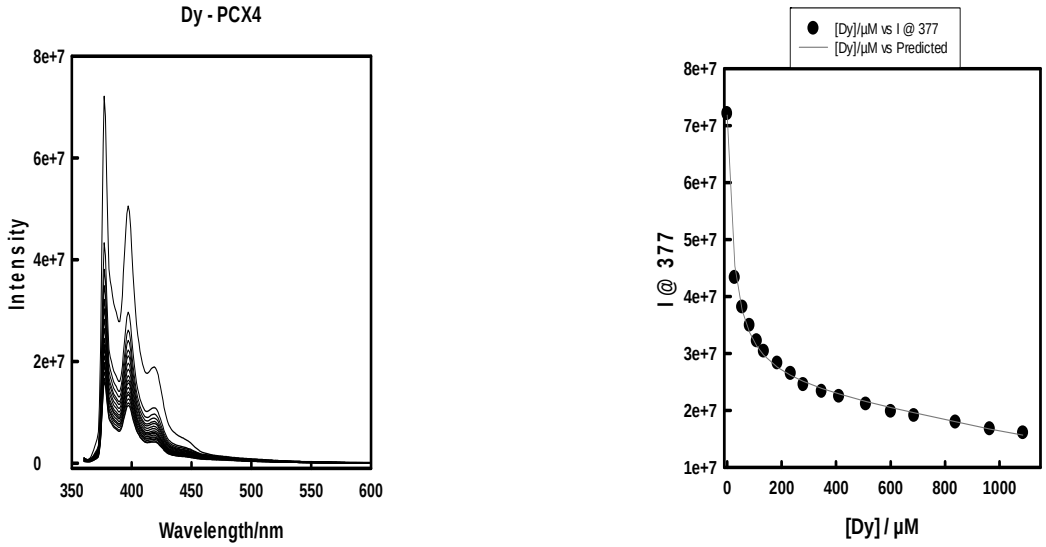

Fig. 5: A) The changes in the fluorescence spectra of PCX4 (1 × 10^{-6} M in H_2O) upon addition of different concentrations of Dysprosium Nitrate. λex = 350 nm. B) The binding curve for the respective PCX4: Dy^{+3} systems.

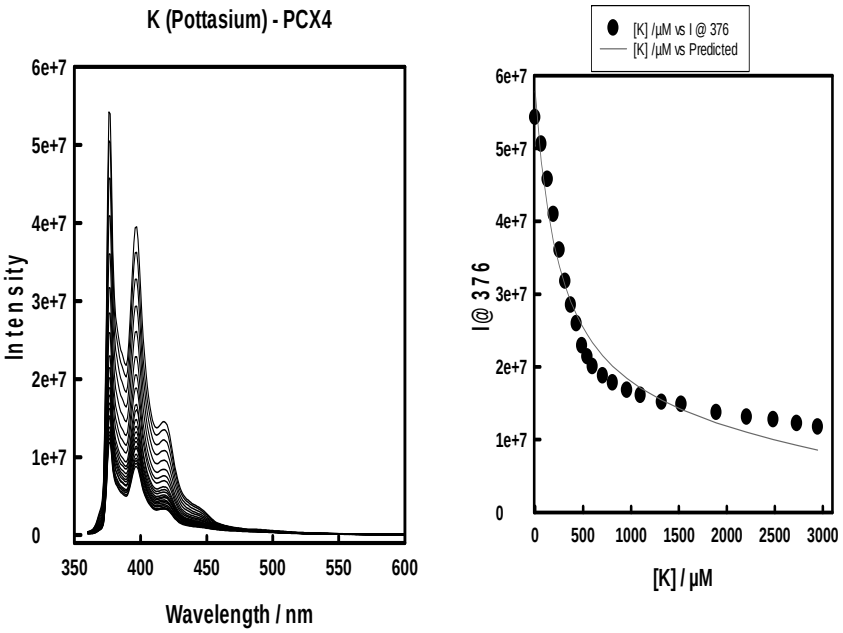

Fig. 6: A) The changes in the fluorescence spectra of PCX4 (1×10^{-6} M in H_2O) upon addition of different concentrations of Dysprosium Nitrate. λex = 350 nm. B) The binding curve for the respective PCX4: Dy^{+3} systems.

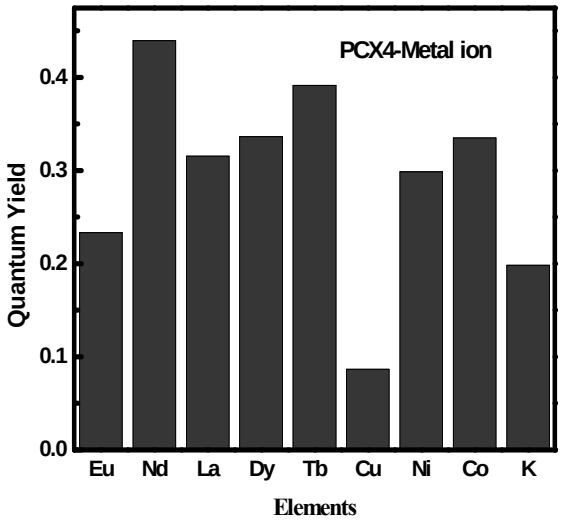

Fig. 7: The fluorescence intensity of PCX4 (2.5 µM) at 377 nm upon the addition of Eu^{+3} (1 mm) in the presence of other metal ions (1 mm) in ACN/H_2O (1:9).

Table 2: The quenching constants and quantum yield for complex of PCX4 and metal ions.

PCX4/M	La^{+3}	Nd^{+3}	Eu^{+3}	Tb^{+3}	Dy^{+3}	Co^{+2}	Ni^{+2}	Cu^{+2}	K^{+1}
$K/\mu M^{-1}$	0.042	0.035	0.0137	0.0285	0.0431	0.0044	0.002	0.0044	0.038
ϕ_0	3.6e+7	3.1e+7	1.9e+7	4.0e+7	7.2e+7	4e+7	7e+7	2.5e+9	3.5e+7
ϕ_1	1.1e+7	1.3e+7	4e+7	1.6e+7	1.6e+7	1e+7	2e+7	1.3e+7	7e+6
ϕ_1/ϕ_0	0.3155	0.4393	**0.2332**	0.3912	0.3362	0.3349	0.2985	0.0865	0.198

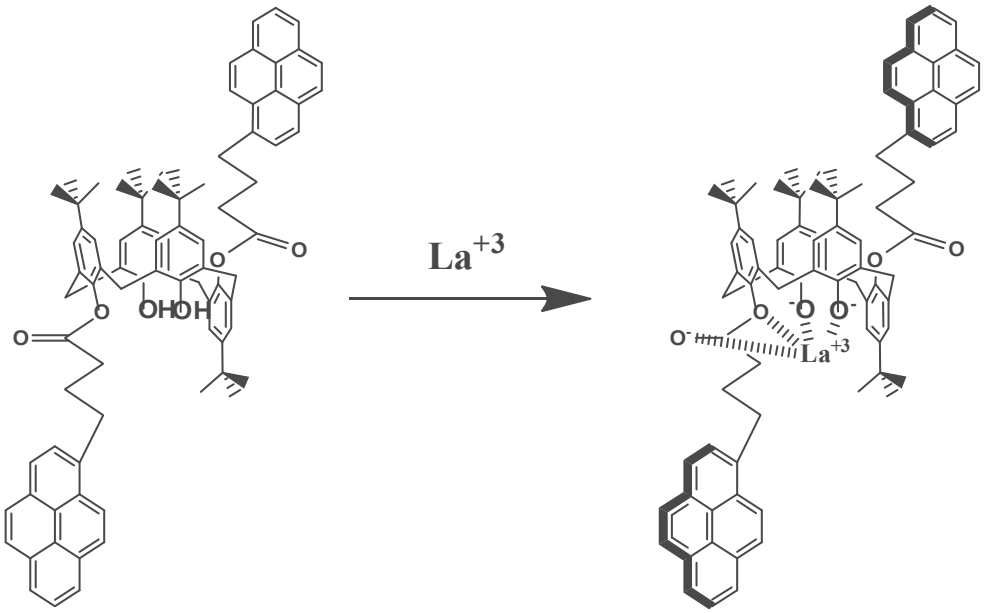

Scheme 2: Possible binding modes of complexation of PCX4 and La^{+3}.

Conclusions

From the data obtained from quenching constants of MPCX4 and PCX4 with all above metal ions it is observed that the constants for PCX4 complex are higher than that of MPCX4 complex except Co^{+2}. It means that PCX4 structure is more favourable for complexation than that of MPCX4. As PCX4 has longer length of spacer with both pyrene units it may show conjugation effect through covalent bonding for Photo Induced electron transfer process from pyrene to M^{+3}. Further MPCX4 has electron withdrawing carbonyl group adjacent to fluorophore and therefore there will be deficiency of electron in pyrene for PET process which affects the quenching process in MPCX4.

Again if we compare quantum yield of MPCX4 and PCX4 complexes with metal ions, it is noticed that quantum yield of PCX4 complexes are lower than that of MPCX4 complexes. It indicates that quenching is more effective in PCX4 than in MPCX4. As PCX4 has two pyrene units with electron rich centres for PET process, higher will be quenching.

In case of metal ions if we compare complexation of lanthanides and transition metal ions with MPCX4 and PCX4, quantum yield of transition metal ions is less than that of lanthanides. It means that transition metal ions give more quenching than lanthanides. This may be because the size of transition metal ions ie smaller than the lanthanides which approximately matches the size of calixarene cavity.

Among all lanthanides, the quantum yield of Eu^{+3} complexes with both MPCX4 and PCX4 is lower producing more quenching. This may be because of unusual behaviour of europium as compared to other lanthanides. Trivalent Eu^{+3} readily oxidises in water and form divalent compound. Divalent europium with +2 oxidation state with half filled f orbital gives more stability and hence can form more stable complex with MPCX4 and PCX4. In case of transition metals, MPCX4 forms complex with Ni^{+2} with low quantum yield and similarly PCX4 complexation with Cu^{+2} gives more quenching. PCX4 forms a more stable complex with Cu^{+2} with very low quantum yield as compared to Ni^{+2} and Co^{+2} ions.

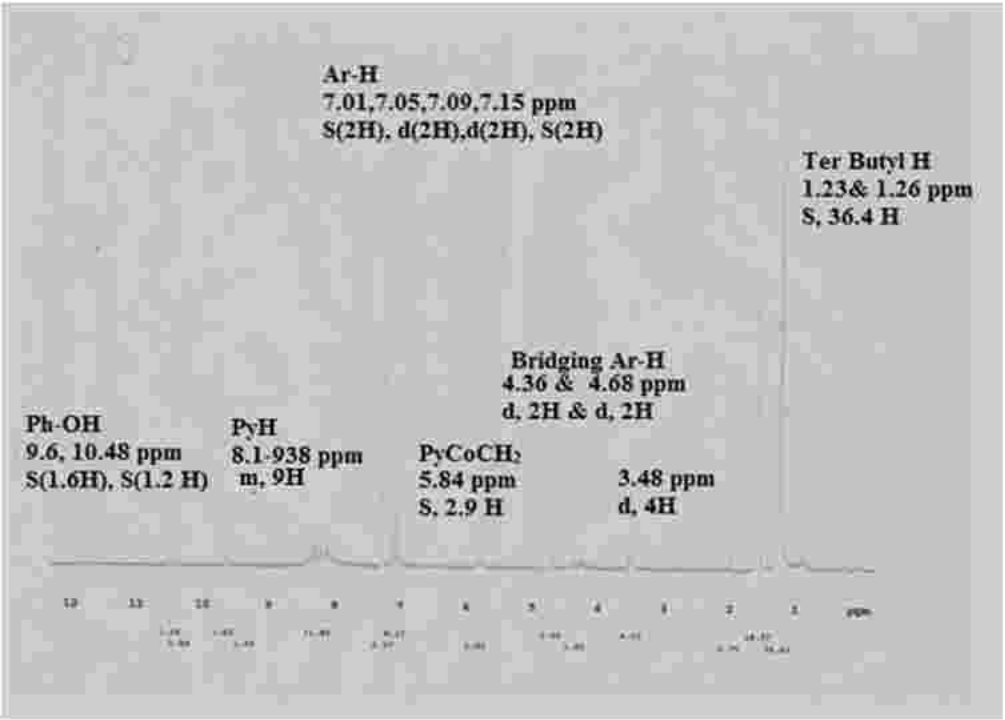

Fig. S1: ^{1}H-NMR of MPCX4 in $CDCl_3$ solvent.

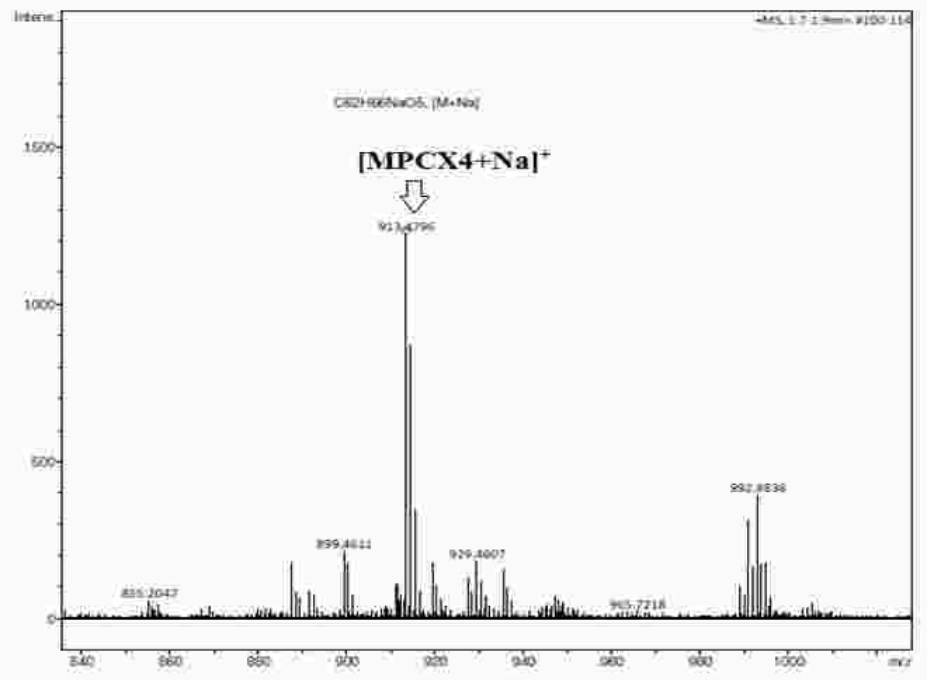

Fig. S2: HR-MS spectrum of MPCX4.

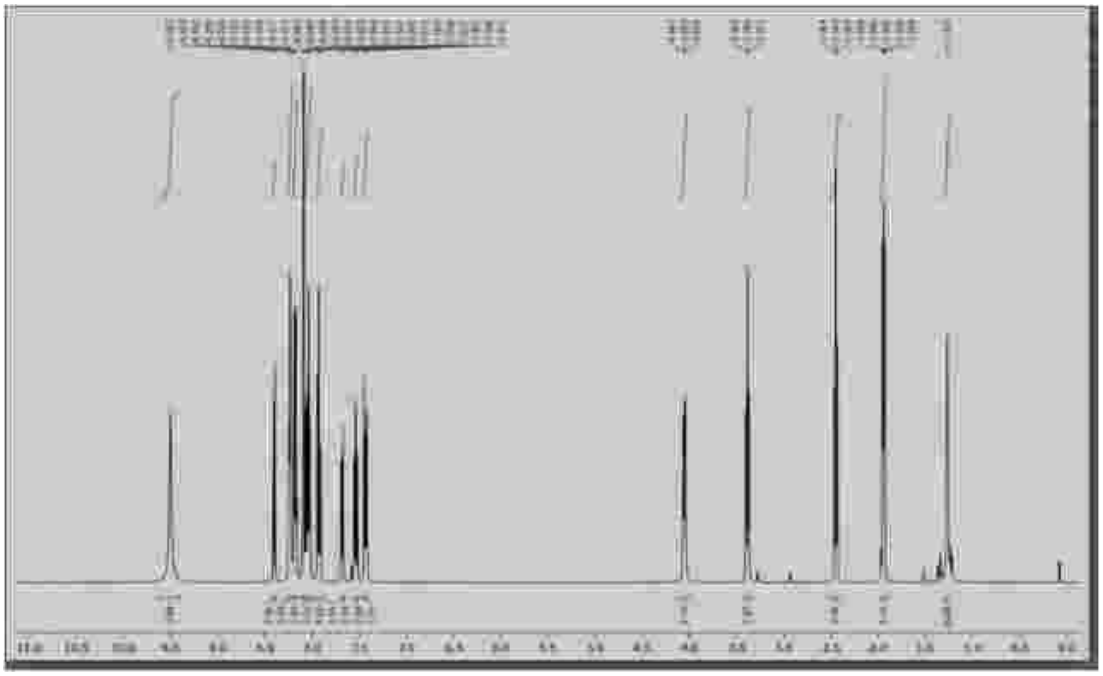

Fig. S3: ^{1}H-NMR of PCX4.

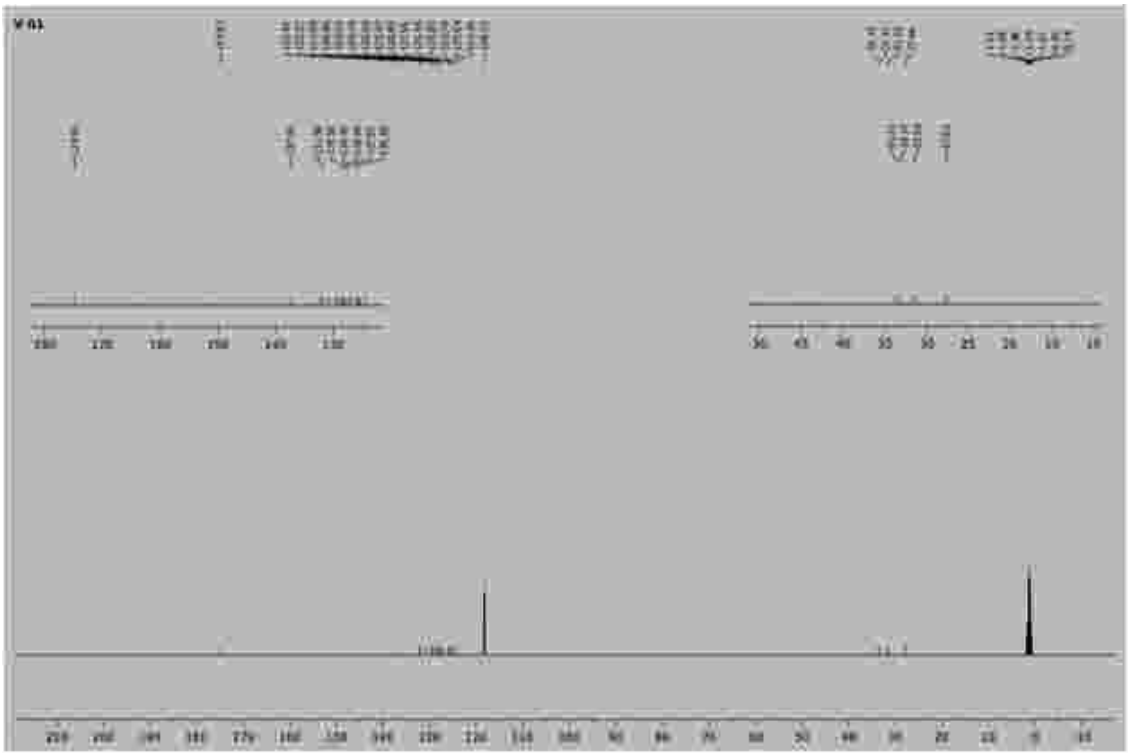

Fig. S4: ^{13}C-NMR Spectra of PCX4.

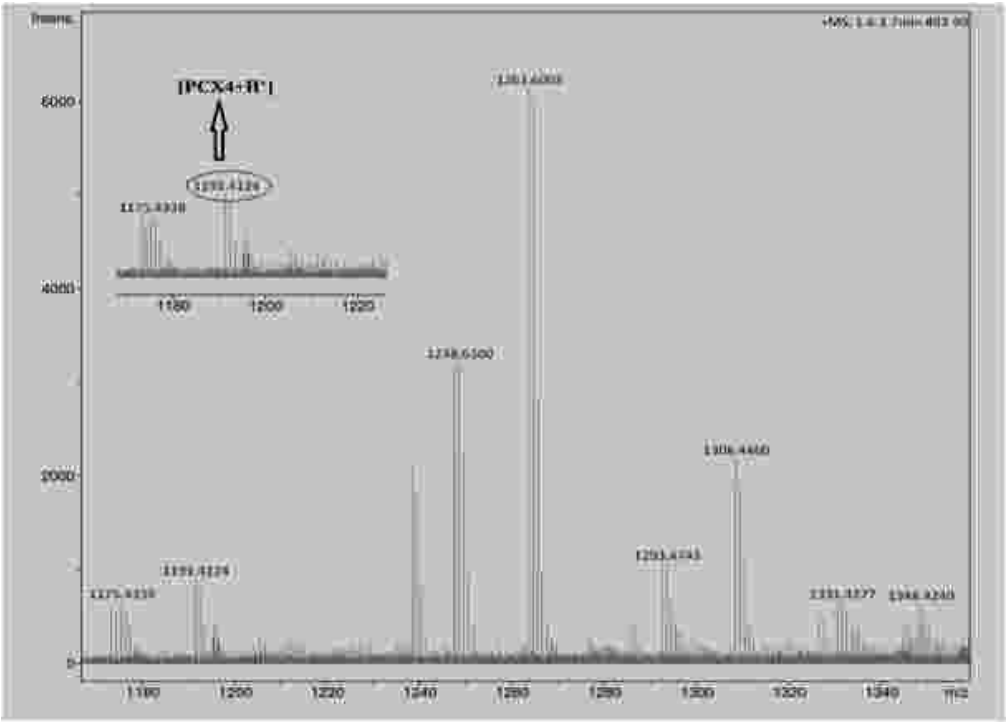

Fig. S5: Enlarged portion of HR-MS spectra of PCX4.

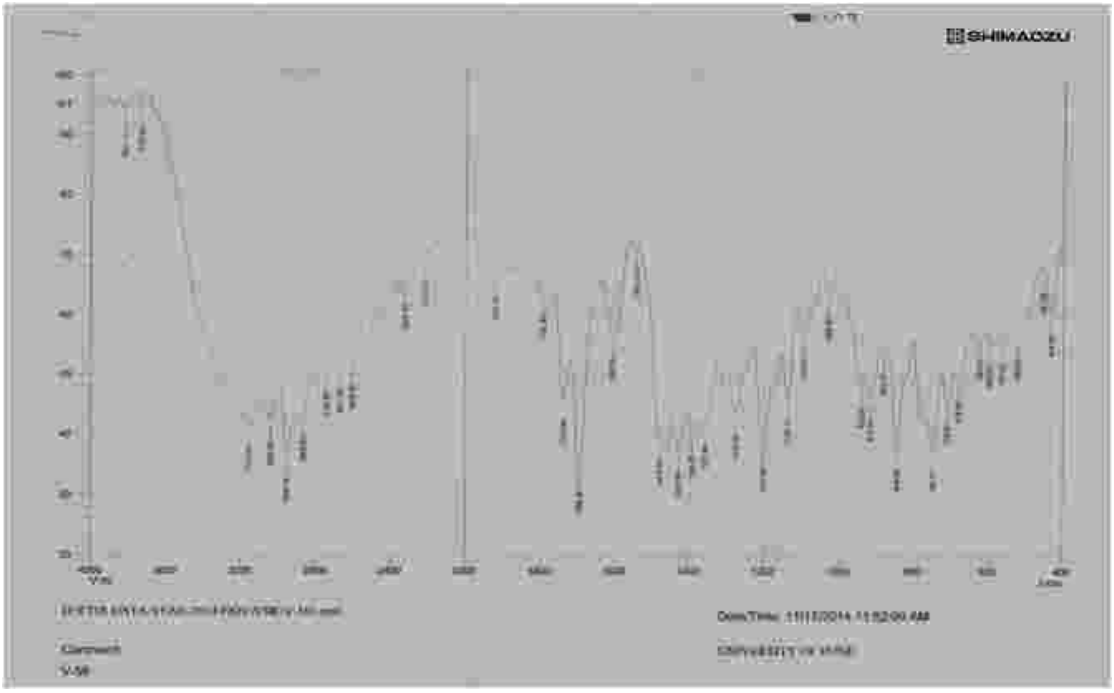

Fig. S6: FT-IR spectra of PCX4.

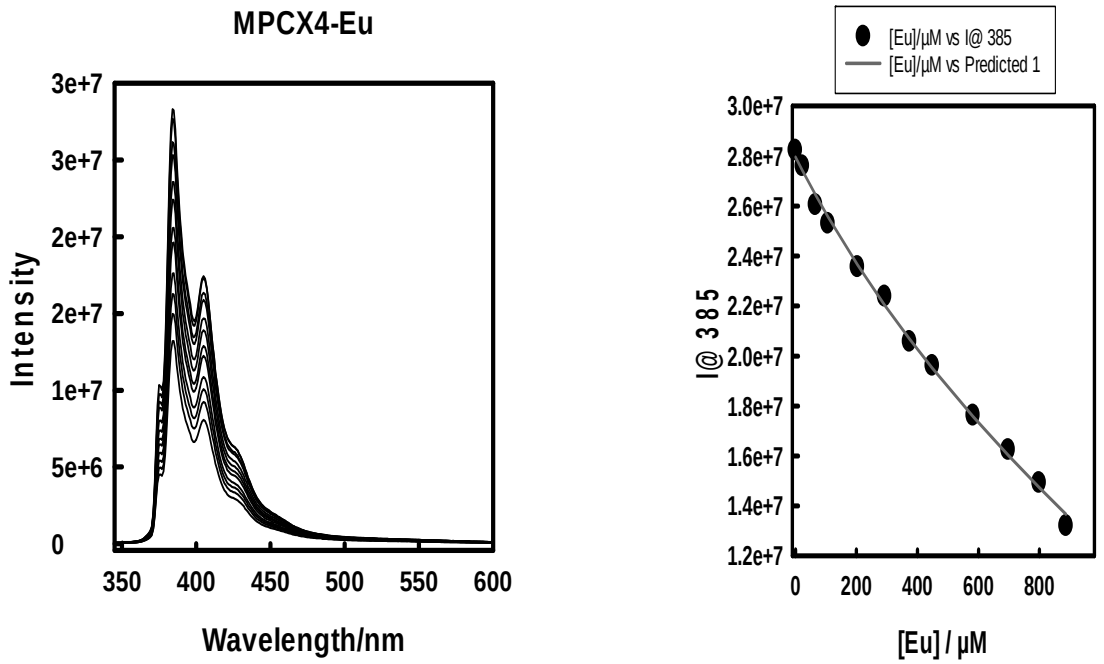

Fig. S7a) Changes in the fluorescence spectra of MPCX4 (1 × 10^{-6} M in H_2O) upon addition of different concentrations of Europium Nitrate λex = 340 nm. b) The binding curve for the respective MPCX4: Eu^{+3} systems.

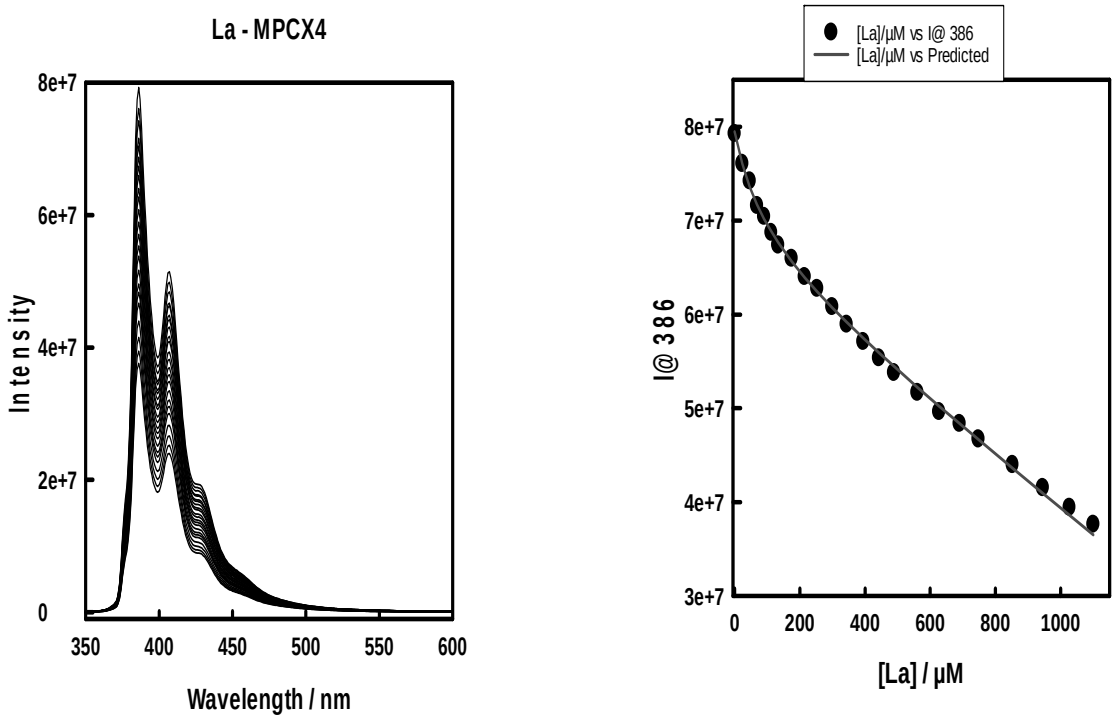

Fig. S8a) Changes in the fluorescence spectra of MPCX4 (1 × 10^{-6} M in H_2O) upon addition of different concentrations of Lanthanum Nitrate λex = 340 nm. b) The binding curve for the respective MPCX4: La^{+3} systems.

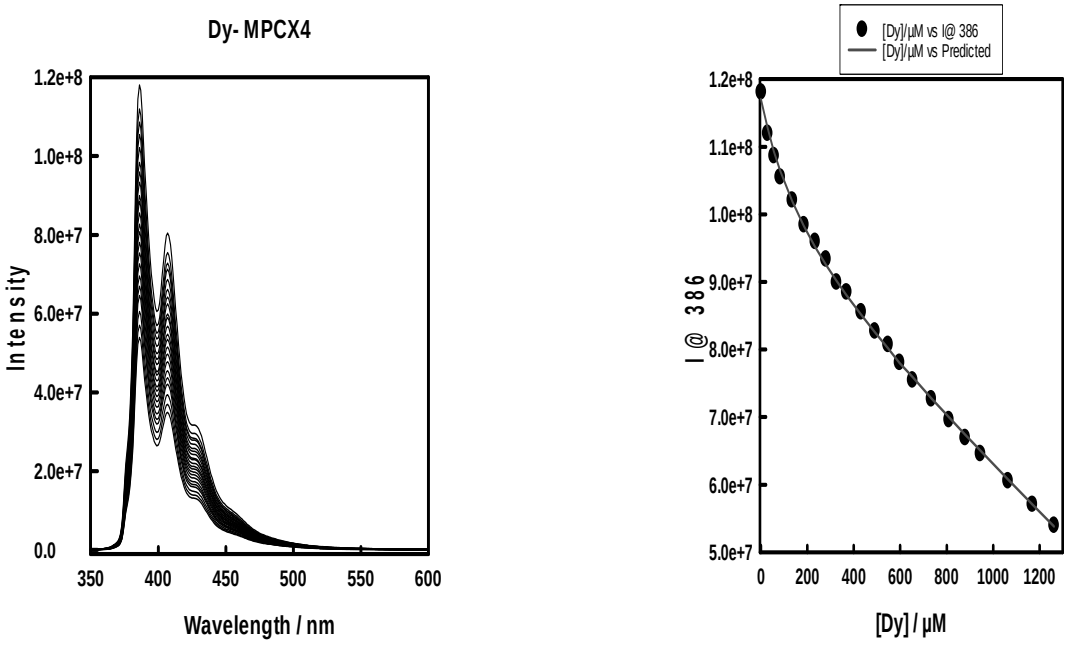

Fig. S9a) Changes in the fluorescence spectra of MPCX4 (1 × 10^{-6} M in H_2O) upon addition of different concentrations of Dysprosium Nitrate λex = 340 nm. b) The binding curve for the respective MPCX4: Dy^{+3} systems.

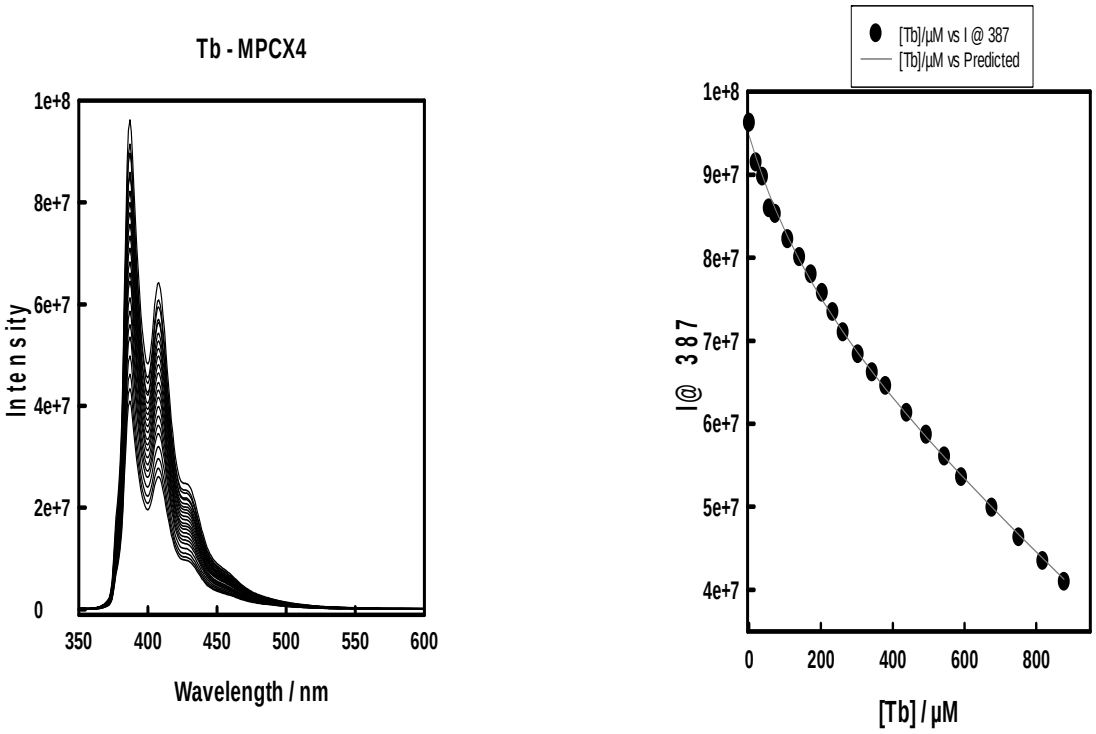

Fig. S10a) Changes in the fluorescence spectra of MPCX4 (1 × 10^{-6} M in H_2O) upon addition of different concentrations of Terbium Nitrate λex = 340 nm. b) The binding curve for the respective MPCX4: Tb^{+3} systems.

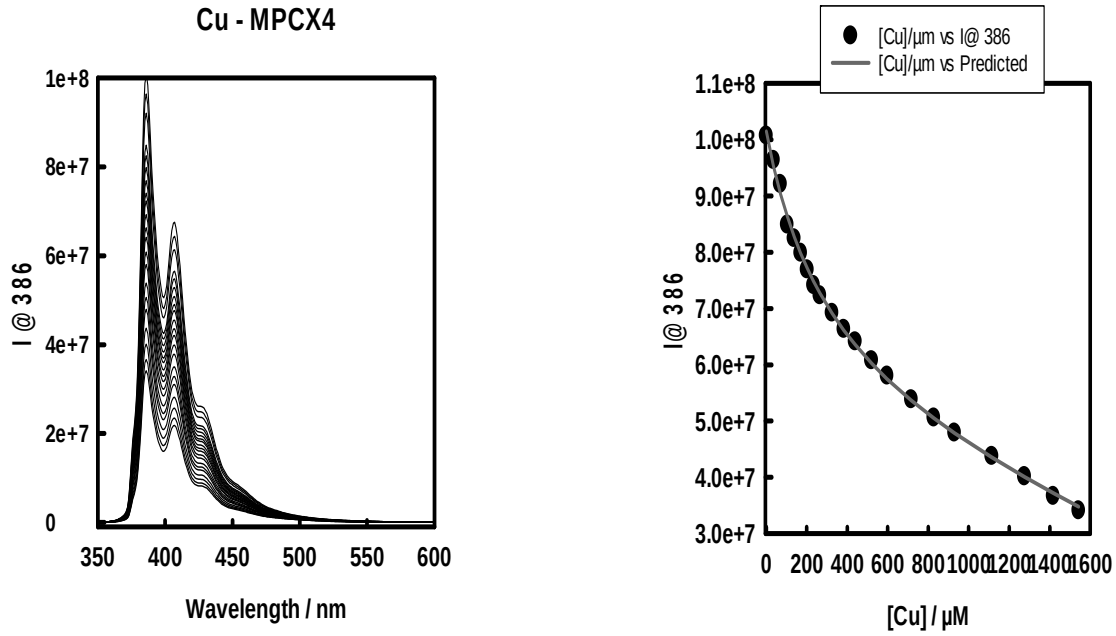

Fig. S11a) Changes in the fluorescence spectra of MPCX4 (1 × 10^{-6} M in H_2O) upon addition of different concentrations of Cupper Chloride λex = 340 nm. b) The binding curve for the respective MPCX4:Cu^{+2}system.

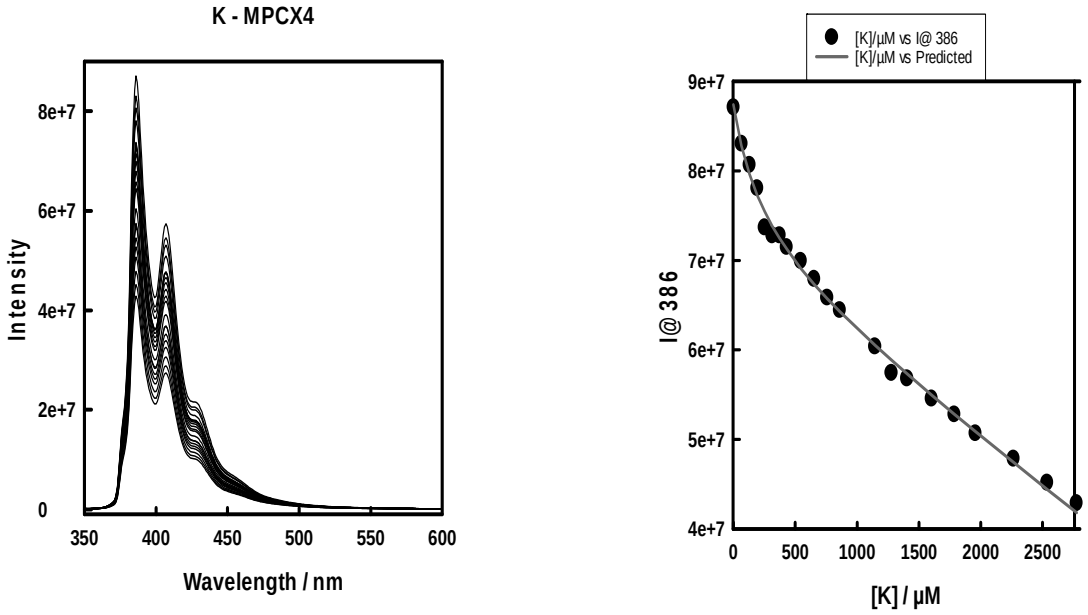

Fig. S12a) Changes in the fluorescence spectra of MPCX4 (1 × 10^{-6} M in H_2O) upon addition of different concentrations of Lanthanum Nitrate λex = 340 nm. b) The binding curve for the respective MPCX4: K^{+1} system.

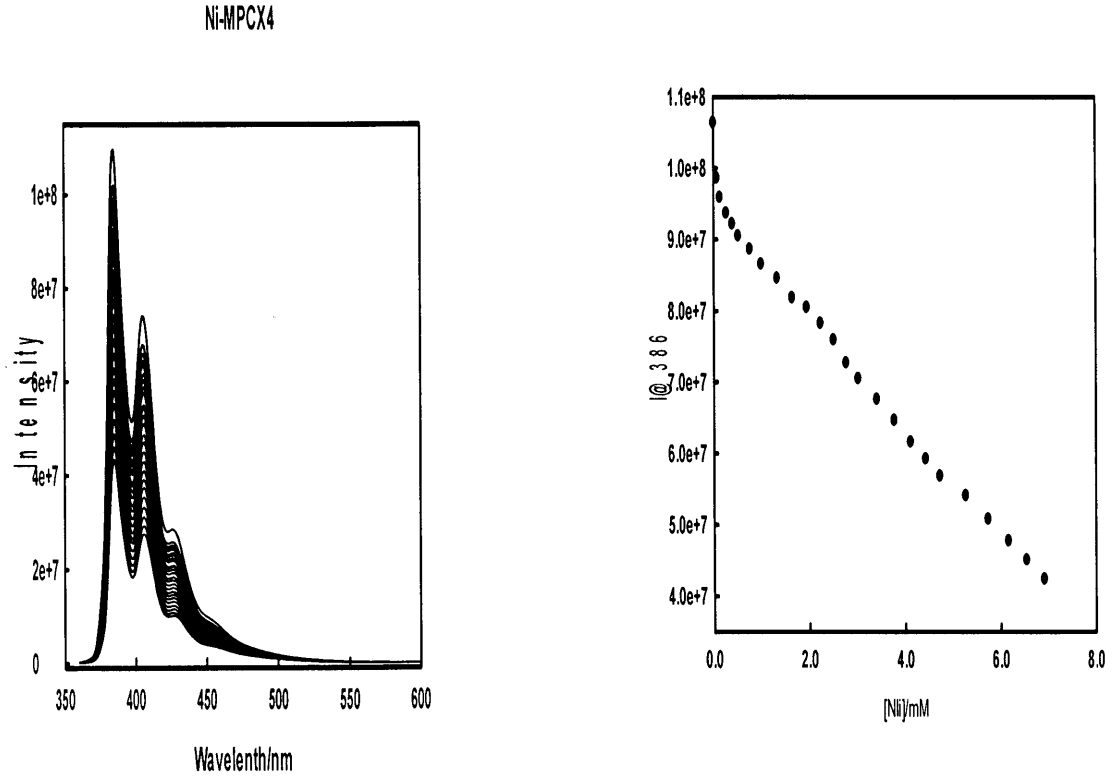

Fig. S13a) Changes in the fluorescence spectra of MPCX4 (1 × 10^{-6} M in H_2O) upon addition of different concentrations of Lanthanum Nitrate λex = 340 nm. b) The binding curve for the respective MPCX4: Ni^{+2} system.

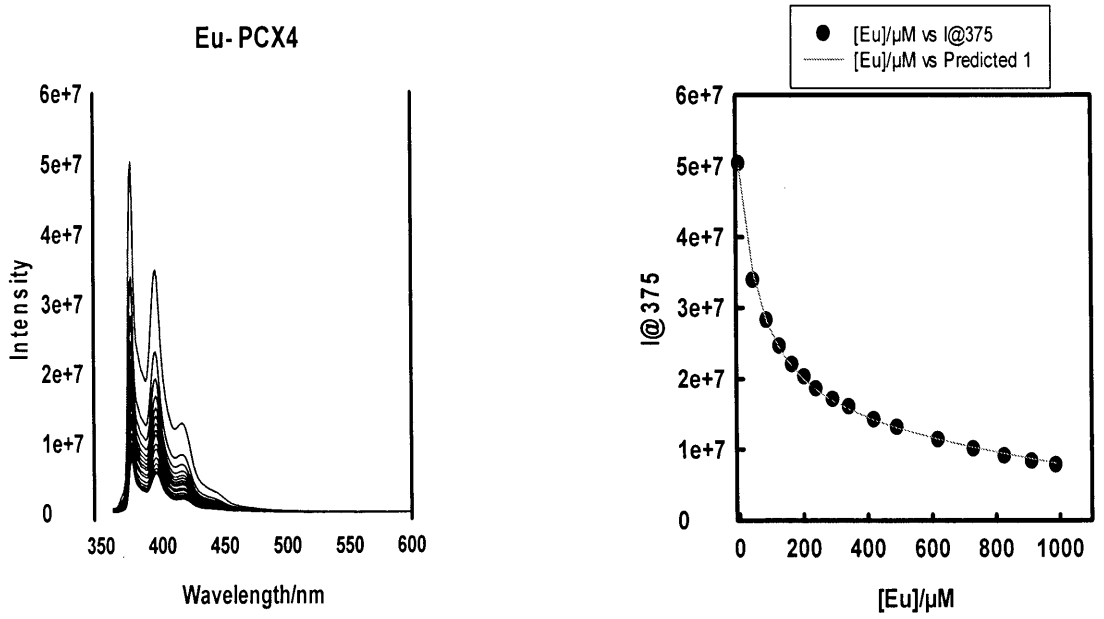

Fig. S14a) Changes in the fluorescence spectra of MPCX4 (1 × 10^{-6} M in H_2O) upon addition of different concentrations of Europium Nitrate λex = 350 nm. b) The binding curve for the respective PCX4: Eu^{+3} systems.

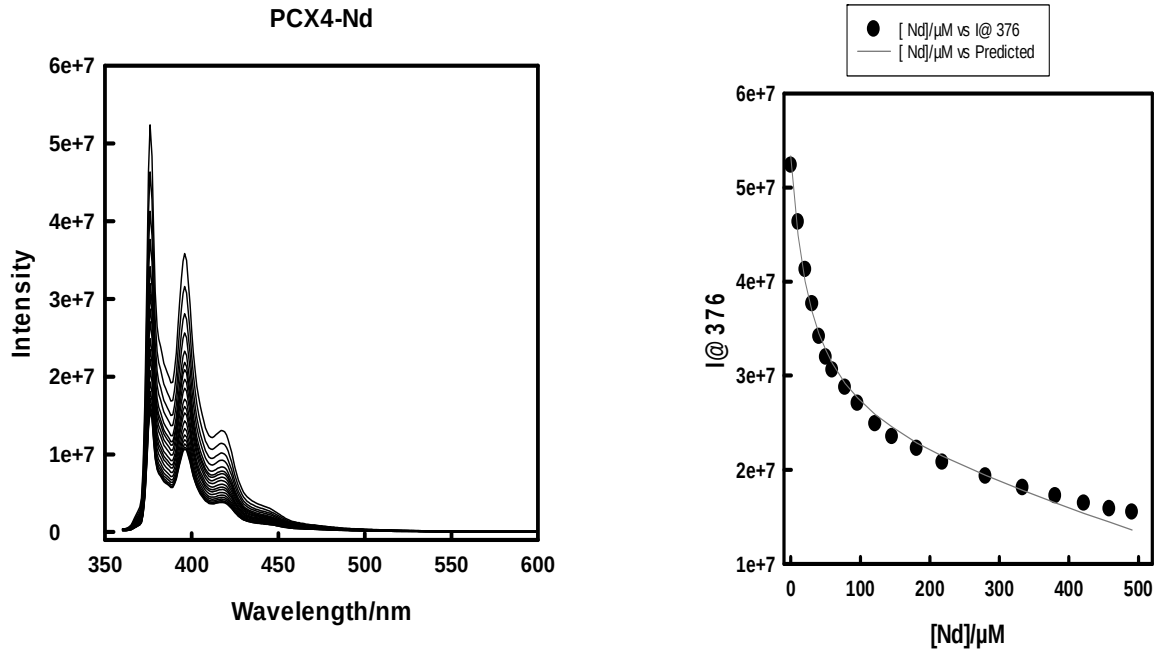

Fig. S15a) Changes in the fluorescence spectra of PCX4 (1 × 10^{-6} M in H_2O) upon addition of different concentrations of Lanthanum Nitrate λex = 350 nm. b) The binding curve for the respective PCX4: Nd^{+3} system.

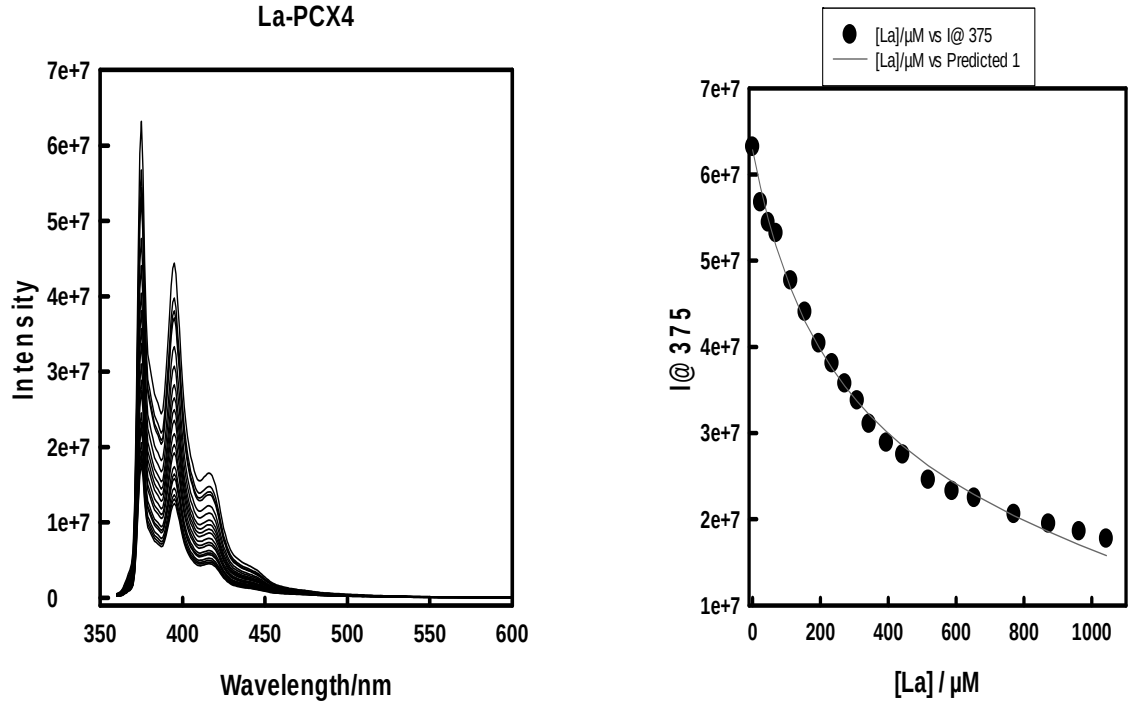

Fig. S16a) Changes in the fluorescence spectra of PCX4 (1 × 10^{-6} M in H_2O) upon addition of different concentrations of Lanthanum Nitrate λex = 350 nm. b) The binding curve for the respective PCX4: La^{+3} system.

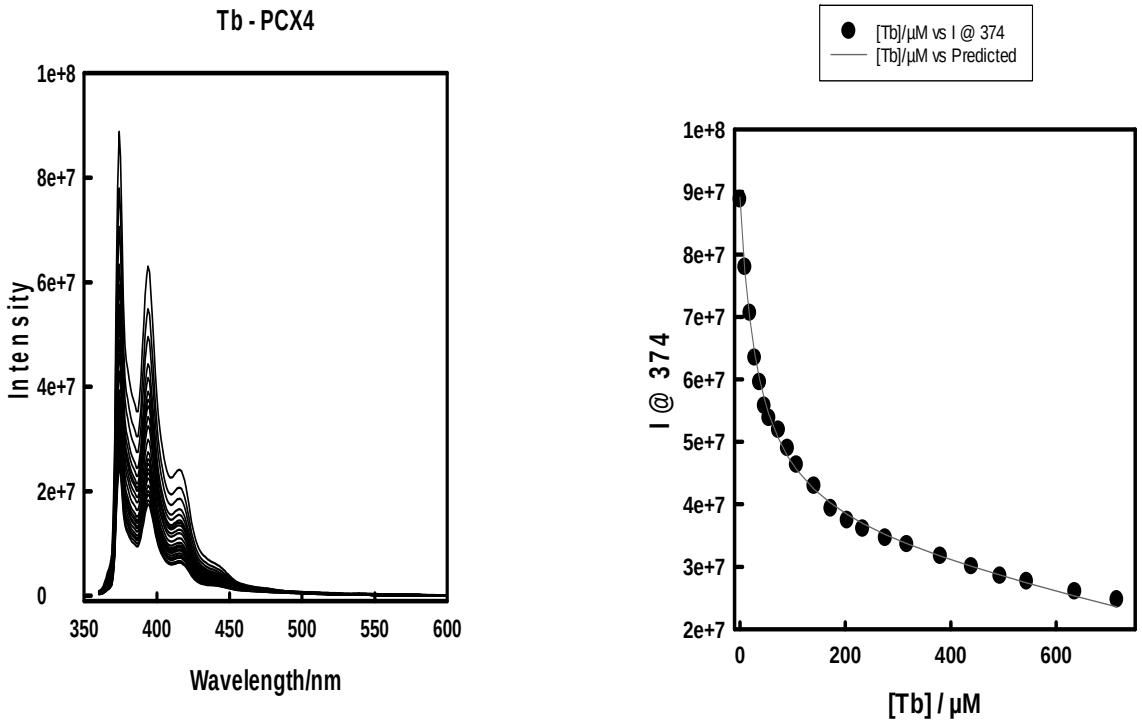

Fig. S17a) Changes in the fluorescence spectra of PCX4 (1 × 10^{-6} M in H_2O) upon addition of different concentrations of Terbium Nitrate λex = 350 nm. b) The binding curve for the respective PCX4: Tb^{+3} system.

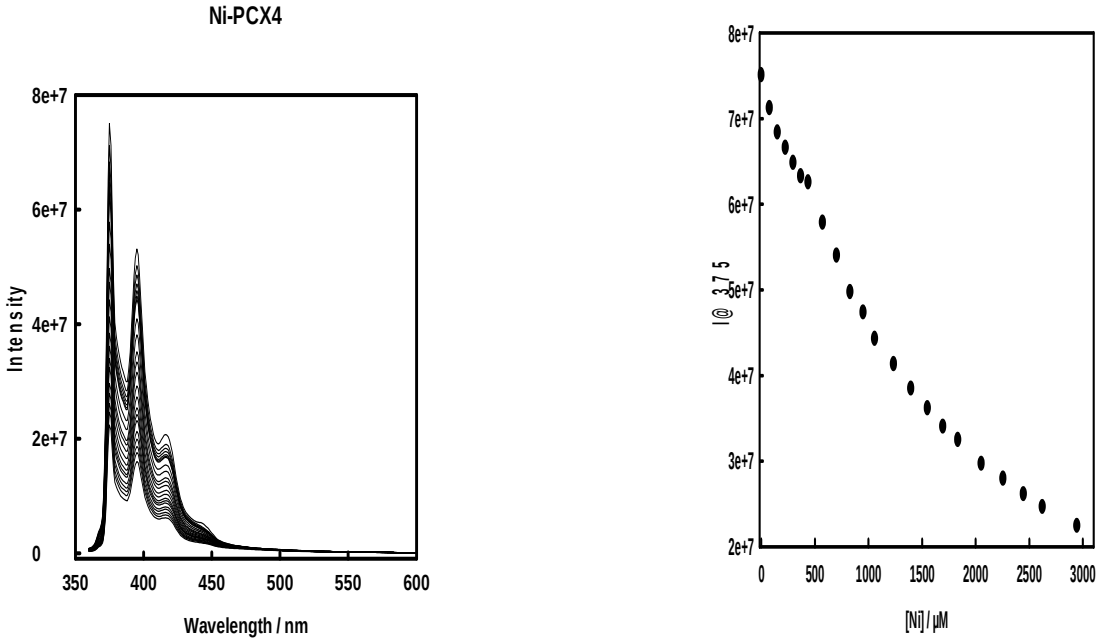

Fig. S18a) Changes in the fluorescence spectra of PCX4 (1 × 10^{-6} M in H_2O) upon addition of different concentrations of Nickel Nitrate λex = 350 nm. b) The binding curve for the respective PCX4: Ni^{+2} systems.

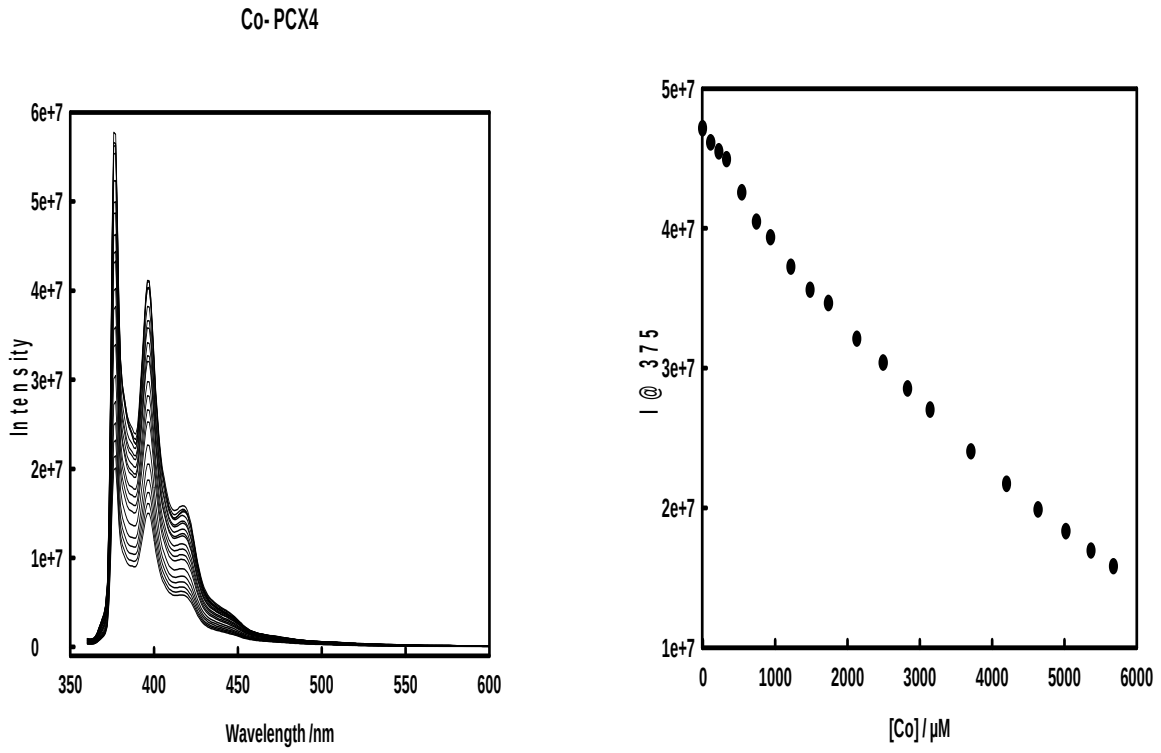

Fig. S19a) Changes in the fluorescence spectra of PCX4 (1 × 10^{-6} M in H_2O) upon addition of different concentrations of Cobalt Nitrate λex = 350 nm. b) The binding curve for the respective PCX4: Co^{+2} systems.

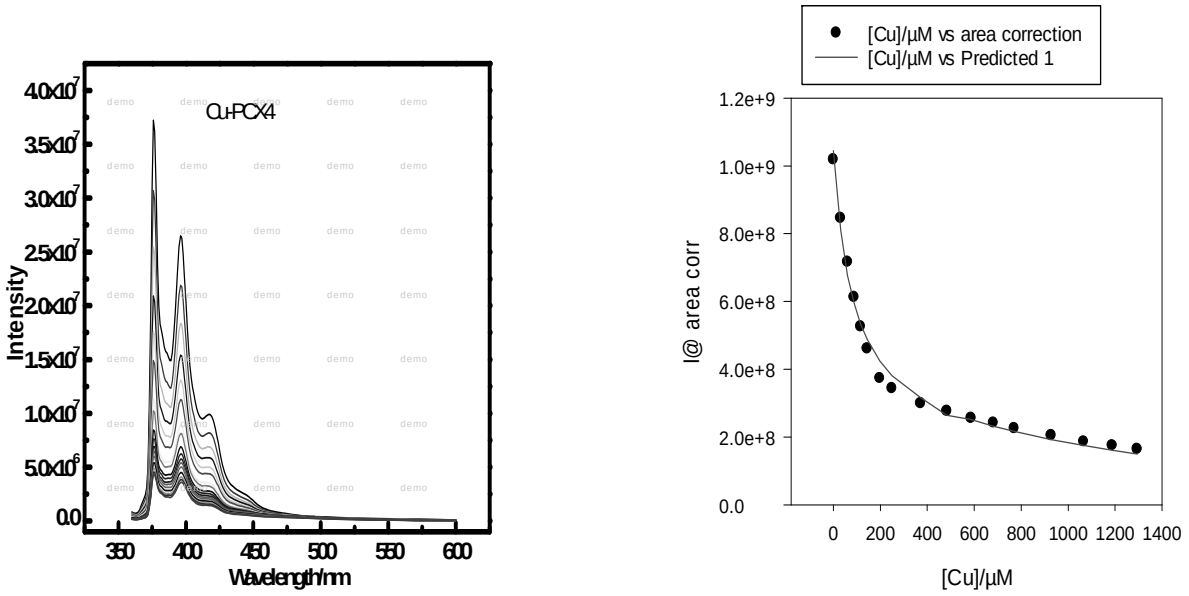

Fig. S20a) Changes in the fluorescence spectra of PCX4 (1 × 10^{-6} M in H_2O) upon addition of different concentrations of Cupper Nitrate λex = 350 nm. b) The binding curve for the respective PCX4: Cu^{+2} system.

Acknowledgment

We are thankful to Dr. Flor Rodriguez-Prieto and Dr. Manuel Mosquera Gonzalez, University of Santiago de Compostela Santiago, Spain for their guidance. Thanks are due to Department of Chemistry, S. P. Pune University, Pune for providing NMR, FTIR and HR-MS facilities.

References

1. (a) Beer P. D. and Gale P. A., 2001 *Angew. Chem. Int. Ed.*, **40,** 486; (b) de Silva A. P., Gunaratne H. Q. N, Gunnlaugsson T., Huxley J. M., Mchoy C. P., Rademacher J. T. and Rice T. E. 1997, *Chem. Rev.*, **97,** 1515; (c) Yoon J., Kim S. K., Sing N. J. and Kim K. S. 2006,*Chem. Soc. Rev.*, **35,** 355; (d) Kim J. S. and Quang D. T. 2007, *Chem. Rev.*, **107,** 3780; (e) Liu Y., Li Z. and Guo D. S. 2009, *Supramolecular Chem.*, **21,** 465. f) Kim, J. S. and Quang, D.T., 2007, *Chem. Rev.* **1073,** 780.

2. (a) Gutsche C. D. 1991, Calixarenes, A versatile class of macrocyclic compounds (eds) J. Vicens and V. B. Öhmer) (Dordrecht, Netherlands: Kluwer); (b) B. Öhmer V. 1995, *Angew.Chem. Int. Ed. Engl.* **34,** 713; (c) Gutsche C. D. 2000, Calixarenes in action (eds) L. Mandolini and R. Ungaro (London: Imperial College Press); (d) Casnati A, Sansone F. and Ungaro R. 2003 Calixarene receptors in ion recognition and sensing: Advances in Supramolecular Chemistry, (ed.) G. W. Gokel (Miami, FL, USA: Cerberus Press Inc.) vol. **9,** p. 165; (e) Gutsche C. D. 2008 Calixarenes: An introduction, 2nd edition, (UK: The Royal Society of Chemistry, Cambridge)

3. (a) Kim H. J., Lee M. H., M. Lucia, Vicens J. and J. S. Kim 2012, *Chem. Soc. Rev.*, **41,** 1173; (b) J. Roymon and R. C. Pulla 2011, *Chem. Rev.*, **111,** 3433.

4. Lee S. H., Kim S. H., Kim S. K., Jung J. H. and Kim J. S. *J.* 2005, *Org. Chem.* **70,** 9288; (b) Kim S. K., Kim S. H., Kim H. J., Lee S. H., Lee S. W., Ko J., Bartsch R. A. and Kim J. S. 2005, *Inorg. Chem.,* **44,** 7866; (c) Choi J. K., Kim S. H., Yoon J., Lee K.H., Bartsch R. A. and Kim J. S. 2006, *J. Org. Chem.,* **71,** 8011; (d) Kim H. J., Quang D. T., Hong J., Kang G., Ham S. and Kim J. S. 2007, *Tetrahedron,* **63,** 10788.

5. Debdeep M., Chakraborty A., Gunupuru R. and Paul P. 2011, *Inorg. Chim. Acta.,* **372,** 126.

6. (a) Bünzli J. C. G., 2010, *Chem. Rev.,* **110,** 2729. (b) C. P. Montgomery, B. S. Murray, E. J. New, R. Pal and D. Parker, 2009, Acc. *Chem. Res*., **42,** 925.

7. (a) Major J. L. and Meade T. J., 2009, *Acc. Chem. Res.,* **42,** 893. (b) Caravan P., 2009, *Acc. Chem. Res.,* **42,** 851; (c) Caravan P., Ellison J. J., McMurry T. J. and Lauffer R. B., 1999, *Chem. Rev.,* **99,** 2293.

8. (a) Silvaggi N. R., Martin L. J., Schwalbe H., Imperiali B. and Allen K. N., *J. 2007, Am. Chem. Soc*., **129,** 7114. (b) Wöhnert J., Franz K. J., Nitz M., Imperiali B. and Schwalbe H., 2003, *J. Am. Chem. Soc.,* **125,** 13338.

9. Fischer C., Sarti, G., Casnati A., Carrettoni, B., Manet, I., Schuurman, R., Guardigli, M., Sabbatini, N. and Ungaro, R. 2000, *Chem. Eur. J.,* **6,** 1026.

10. Casnati, L., Baldini, Sansone, F., Ungaro, R., Armaroli, N., Pompei, D. Barigelletti, F. 2002, *Supramol. Chem.,* **14,** 281.

11. Quang D. T. and Kim, J. S. 2010, *Chem. Rev*., **110**, 6380. (b) Domaille, D. W., Que E. L., and Chang, C. J., Nat. 2008, *Chem. Biol.,* **4,** 168. (c) Que, E. L., Domaille D. W., and Chang, C. J. 2008, *Chem. Rev*., **108,** 1517.

12. (a) Wu Q. and Anslyn, E. V. 2004, *J. Am. Chem. Soc.,* **126,** 14682 (b) Dai, M. Royzen Z. and Canary, J. W. 2005, *J. Am. Chem. Soc.,* **127,** 1612. (c) Wen, Z. C., Yang, R. He H. and Jiang, Y. B. 2006,

Chem. Commun. **106** (d) Kim, J., Shin I. and Yoon, J. 2008, *Chem. Commun*., 5915.

13. (a) Ho I. T., Chu J. H. and Chung W.S., 2011, *Eur. J. Org. Chem.,* **8,** 1472–1481; (b) Leray I. and Valeur, B. 2009, *Eur. J. Inorg. Chem.,* **24,** 3525; (c) Ke. G., Li, Z. Xu X., Chen C. F. and Huang, Z. T. 2008, *Chem. Commun.,*1774 (d) Senthilvelan, A., Ho I. T., Chang K. C., Lee G. H., Liu Y. H. and. Chung W. S, 2009, *Chem. Eur. J.,* **15,** 6152; (e) Joseph R., Chinta J. P. and Rao C. P., 2010, *Inorg. Chim. Acta.,* **363,** 2833.

14. (a) Liu J. M., Zheng Q. Y, Yang J. L, Chen C. F. and Huang Z. T., 2002, *Tetrahedron Lett.,* **43,** 9209; (b) Liang Z., Liu Z., Jiangc L.and. Gao Y, 2007, *Tetrahedron Lett.,* **48,** 1629.

15. Agnihotri P., Suresh E., Paul P. and Ghosh P. K. 2006, *Eur. J. Inorg. Chem.,* **57**, 3369.

16. Patra S. and Paul P. 2009, *Dalton Trans.,* 8683.

17. Patra S., Maity D., Sen A., Suresh E., Ganguly B. and Paul P. 2010, *New J. Chem.,* **34,** 2796.

18. Casnati A., Pochini A., Ungaro R., Bocchi C., Ugozzoli F., Egberink R. J. M., Struijk H., Lugtenberg R., Jong F. D. and Reinhoudt D. N. 1996, *Chem. Eur. J.,* **2,** 436.

19. Nishimura Y., Takemura T. and Arai S., 2007,*ARKIVOC,* xiii**,** 259-268.

20. a) Kalyani V. S., *et al.* γ-Cyclodextrin-Templated Excimer Emission From Pyrene-ArmedCalix[4]arene (manuscript in process of publication) b) Banerji B., Mallesham B., Kiran S., Kumar, Kunwar A. C. and Iqbal J. 2002, *Tetrahedron Letters,* **43,** 6479 - 6483.

21. Gutsche C. D., Alramd B. Hawanj, E., L. Kwanghyunno and Bauer L. J. 1983, *Tetrahedron,* **39,** 3, 409-426.

22. Gutsche C. D. and Lee G. L. 1986, *Tetrahedron,* **42,** 6, 1633-1640.

23. Kim J. S., and Quang D. T. 2007, *Chem. Rev.,* **107,** 3780-3799.

RNI No. MAHENG/2017/74063
ISSN No. (Print) 2581-5911

Oxidation of some aliphatic aldehydes by imidazolium dichromate: A kinetic and mechanistic study

Itishree Hedau, K. Kanwar, S. Panwar L. Mathur and Vinita Sharma*
Chemical Kinetics Laboratories, Department of Chemistry,
J.N.V. University, Jodhpur 342 005, India
E-mail: drvsharma29@gmail.com

Abstract
The oxidation of six aliphatic aldehydes by imidazolium dichromate (IDC) in dimethyl sulfoxide (DMSO) leads to the formation of corresponding carboxylic acids. The reaction are of first order with respect to IDC. A Michaelis-Menten type of kinetics is observed with respect to the aldehydes. The reaction is catalysed by hydrogen ions, the hydrogen ion dependence has the form: $k_{obs} = a + b[H^+]$. The oxidation of deuteriated acetaldehyde, MeCDO, exhibited a substantial primary kinetic isotope effect ($k_H/k_D = 5.78$ at 298 K). The oxidation of acetaldehyde has been studied in nineteen different organic solvents. The solvent effect has been analysed using Taft's and Swain's multiparametric equations. The rate constants correlate well with Taft's s^* values; reaction constants being negative. A mechanism involving transfer of hydride ion has been suggested.

Keywords: *aldehydes, correlation analysis, halochromate, kinetics, mechanism, oxidation.*

Introduction

Salts of Cr(VI) have long been used as oxidizing reagents in synthetic organic chemistry. However, these salts are drastic and non-selective oxidants in nature. Further, they are insoluble in most of the organic solvents also. and hence miscibility is a problem. To overcome these limitations, a large number of organic derivatives of Cr(VI) have been prepared and used in synthetic organic syntheses as mild and selective oxidants in non-aqueous solvents[1-4]. One such compound is imidazolium dichromate (IDC)[5] used for the oxidation of alcohols to carbonyl compounds. It is known that the mode of oxidation depends on the nature of the counter-ion attached to the chromium anion. We have been interested in kinetic and mechanistic aspects of oxidation by complexed Cr(VI) species and several reports, by halochromates have already been reported[6-10]. Therefore, in continuation of our earlier work, we report herein the kinetics and mechanism of oxidation of nine aliphatic primary alcohols by IDC in dimethylsulphoxide (DMSO) as solvent. The mechanistic aspects are discussed.

The main aims of the present investigation are to (i) determine kinetic parameters and to evaluate the rate laws, (ii) to study the correlation analysis of effect of structure on and (iii) to postulate a suitable mechanism for the oxidation process.

Materials and Methods

Materials

IDC was prepared by the reported method[5] and its purity checked by an iodometric determination. Solutions of formaldehyde were prepared by heating paraformaldehyde and passing its vapours in DMSO. The amount of HCHO in DMSO was determined by chromotropic acid method[11]. Other aldehydes were commercial products and were used as such. p Toluenesulphonic acid (TsOH) was used as a source of hydrogen ions. Deuteriated acetaldehyde (MeCDO) was obtained from Sigma Chemicals. Solvents were purified by their usual methods[12].

Product analysis

The product analysis was carried out under kinetic conditions. In a typical experiment, acetaldehyde (4.4 g, 0.1mol) and IDC (1.88 g, 0.01mol) were dissolved in DMSO (100 mL) and the reaction mixture was allowed to stand for *ca*. ≈ 24 to ensure completion of the reaction. It was then rendered alkaline using NaOH, filtered and the filtrate was reduced to dryness under pressure. The residue was acidified with perchloric acid and extracted with diethyl ether (5%, 50 mL). The ether extract was dried ($MgSO_4$) and treated with 10 mL of thionyl chloride. The solvent was allowed to evaporate. Dry methanol (7 mL) was added and the HCl formed was removed in a current of dry air. The residue was dissolved in diethyl ether (200 mL) and the ester content was determined colorimetrically as Fe (III) hydroxymate by the procedure of Hall and Schaefer[13]. Several determinations indicated a 1:1 stoichiometry. The oxidation state of chromium in a completely reduced reaction mixture, determined by iodometric titrations was 3.90 ± 0.15.

Kinetic Measurements

Pseudo first order conditions were attained by keeping an excess (x 15 or greater) of the [aldehyde] over [IDC]. The solvent was DMSO, unless mentioned otherwise. All reactions were carried out in flasks blackened from the outside to prevent any photochemical reactions. The reactions were carried out at constant temperature (±0.1 K) and were followed up to 80% of the extent of reaction, by monitoring the decrease in [IDC] at 352 nm. The pseudo first order rate constant, k_{obs}, was computed from the linear least squares plot of log [IDC] *versus* time. Duplicate runs showed that the rate constants were reproducible to within ±3%. The second order rate constant, k_2, was calculated from the relation: $k_2 = k_{obs}$/[aldehyde].

Results and Discussion

The rate and other experimental data were obtained for all the aldehydes. Since the results are similar, only representative data are reproduced here.

Stoichiometry

The oxidation of aliphatic aldehydes by IDC leads to the formation of corresponding carboxylic acids. The overall reaction may be written as:

$$2\ RCHO + Cr_2O_7^{-2} + 14\ H^+ \rightarrow 2\ RCOOH + 7\ H_2O + 2Cr^{+3} \qquad \ldots.1$$

Rate-laws

The reactions are of first order with respect to IDC. Further, the pseudo-first order rate constant, k_{obs} is independent of the initial concentration of IDC. The reaction rate increases with increase in the concentration of the aldehydes but not linearly (Table 1). The Figure 1 depicts a typical kinetic run. A plot of $1/k_{obs}$ against 1/[aldehyde] is linear (r > 0.995) with an intercept on the rate ordinate (Figure 2). Thus, Michaelis Menten type kinetics is observed with respect to the aldehydes. This leads to the postulation of the following overall mechanism (2) and (3) and rate law (4).

Table 1: Rate constants for the oxidation of acetaldehyde by IDC at 298 K

10^3 [IDC] mol dm^{-3}	[MeCHO] mol dm^{-3}	[TsOH] mol dm^{-3}	10^4 k_{obs} s^{-1}
1.00	0.10	0.00	10.3
1.00	0.20	0.00	15.5
1.00	0.40	0.00	20.8
1.00	0.60	0.00	23.5
1.00	0.80	0.00	25.1
1.00	1.00	0.00	26.1
1.00	1.50	0.00	27.7
1.00	3.00	0.00	29.5
2.00	0.40	0.00	21.6
4.00	0.40	0.00	19.8
6.00	0.40	0.00	18.9
8.00	0.40	0.00	21.0
1.00	0.20	0.00	16.2*

* contained 0.001 mol dm^{-3} acrylonitrile

Table 2: Dependence of the reaction rate on hydrogen-ion concentration

[Aldehyde] 0.10 mol dm^{-3} ;	[IDC] 0.001 mol dm^{-3} ;				Temp. 298 K	
[TsOH]/ mol dm^{-3}	0.10	0.20	0.40	0.60	0.80	1.00
10^4 k_{obs}/s^{-1}	12.6	14.4	18.0	21.6	25.2	29.7

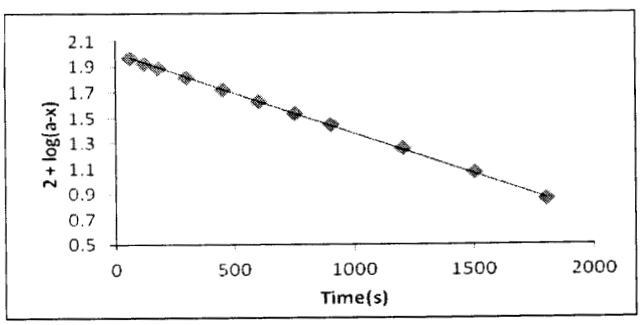

Fig. 1. Oxidation of Acetaldehyde by IDC: A typical kinetic run

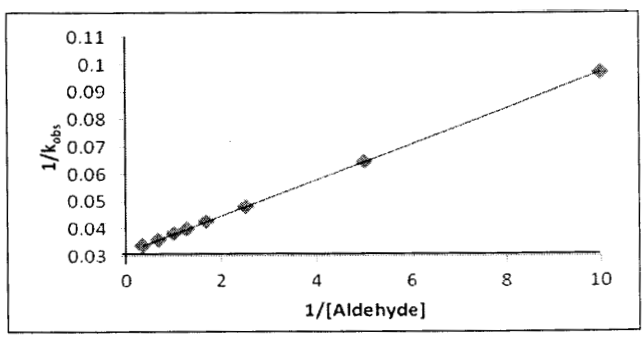

Fig. 2. Oxidation of Aldehyde by IDC: A double reciprocal plot

$$\text{Aldehyde} + \text{IDC} \overset{K}{\leftrightarrows} [\text{Complex}] \quad \ldots 2$$

$$[\text{Complex}] \xrightarrow{k_2} \text{Products} \quad \ldots 3$$

$$\text{Rate} = k_2 \text{ K [Aldehyde] [IDC]/(1+K [Aldehyde])} \ldots 4$$

The dependence of reaction rate on the reductant concentration was studied at different temperatures and the values of K and k_2 were evaluated from the double reciprocal plots. The thermodynamic parameters of the complex formation and activation parameters of the decomposition of the complexes were calculated from the values of K and k_2 respectively at different temperatures (Tables 3 and 4).

Table 3: Rate constants and activation parameters of the oxidation of aliphatic aldehydes – IDC complexes.

Subst.	$10^4\ k_2$ / ($dm^3\ mol^{-1}\ s^{-1}$)				ΔH^*	$-\Delta S^*$	ΔG^*
	288 K	298 K	308 K	318 K	(kJ mol^{-1})	(J mol^{-1} K^{-1})	(kJ mol^{-1})
H	1.17	2.79	6.39	14.4	61.1± ± 0.5	108± ± 2	93.3± ± 0.4
Me	14.4	31.5	65.7	135	54.2± ± 0.3	112± ± 1	87.2± ± 0.4
Et	24.3	52.2	106	213	52.4± ± 0.3	113± ± 1	86.0± ± 0.2
Pr	26.1	55.8	117	225	52.3± ± 0.3	113± ± 1	85.8± ± 0.2
Pr^i	38.7	81.0	162	324	51.3± ± 0.4	113± ± 1	84.9± ± 0.3
$ClCH_2$	0.063	0.18	0.45	1.13	70.4± ± 0.5	100± ± 2	99.9± ± 0.4
MeCDO	2.39	5.48	11.9	25.7	57.6± ± 0.4	115± ± 1	91.6± ± 0.3
k_H/k_D	6.03	5.75	5.52	5.25			

Table 4: Formation constants and thermodynamic parameters of the oxidation of aliphatic aldehydes – IDC complexes

Subst.	K ($dm^3\ mol^{-1}$))				$-\Delta H^*$	$-\Delta S^*$	$-\Delta G^*$
	288 K	298 K	308 K	318 K	(kJ mol^{-1})	(J mol^{-1} K^{-1})	(kJ mol^{-1})
H	6.03	5.33	4.55	3.90	13.6± ± 0.4	24± ± 1	6.60± ± 0.3
Me	5.58	4.88	4.14	3.45	14.7± ± 0.5	28± ± 2	6.38± ± 0.4
Et	6.39	5.69	4.98	4.23	12.9± ± 0.5	21± ± 2	6.77± ± 0.4
Pr	5.94	5.25	4.53	3.80	13.8± ± 0.6	25± ± 2	6.56± ± 0.4
Pr^i	5.76	5.07	4.35	36.0	14.3± ± 0.7	27± ± 2	6.47± ± 0.5
$ClCH_2$	6.15	5.45	4.70	3.95	13.7± ± 0.6	24± ± 2	6.65± ± 0.5
MeCDO	5.67	4.98	4.25	3.53	14.5± ± 0.6	28± ± 2	6.43± ± 0.5

Induced Polymerization of Acrylonitrile/ test for free radicals: The oxidation of aldehydes, in an atmosphere of nitrogen, failed to induce polymerisation of acrylonitrile. Further, the addition of acrylonitrile did not affect the reaction rate. This indicates that a one electron oxidation, giving rise to free radicals, is unlikely in the present reaction (Table 1). To further confirm the absence of free radicals in the reaction pathway, the reaction was carried out in the presence of 0.05 mol dm^{-3} of 2,6-di-t-butyl-4-methylphenol (butylated hydroxytoluene or BHT). It was observed that BHT was recovered unchanged, almost quantitatively.

Kinetic isotope effect: To ascertain the importance of the cleavage of the aldehydic C–H bond in the rate determining step, the oxidation of deuteriated

acetaldehyde (MeCDO) was studied. The oxidation of deuteriated acetaldehyde exhibited a substantial primary kinetic isotope effect (Table 3).

Effect of acidity: The reaction is catalysed by hydrogen ions (Table 2). The hydrogen ion dependence has the following form $k_{obs} = a + b[H^+]$. The values of *a* and *b*, for acetaldehyde, are $4.05 \pm 0.12 \times 10^{-4}$ s^{-1} and $7.46 \pm 0.21 \times 10^{-4}$ $dm^3 mol^{-1} s^{-1}$ respectively ($r^2 = 0.99708$).

$$\text{Rate} = k_2 \text{ [IDC] [Aldehyde]} + k_3 \text{ [IDC] [Aldehyde] [TsOH]} \quad \ldots 5$$

Effect of solvents: The oxidation of acetaldehyde was studied in 19 different organic solvents. The choice of solvents was limited due to the solubility of IDC and its reaction with primary and secondary alcohols. There was no reaction with the solvents chosen. The kinetics was similar in all the solvents. The values k_2 are recorded in Table 5.

Table 5: Effect of solvents on the oxidation of acetaldehyde-IDC complex at 298 K

Solvents	K (dm^3 mol^{-1})	10^4 k_2 (s^{-1})	Solvents	K (dm^3 mol^{-1})	10^4 k_2 (s^{-1})
Chloroform	6.01	8.91	Toluene	4.32	2.82
1,2 Dichloroethane	5.55	10.5	Acetophenone	5.09	14.8
Dichloromethane	5.90	12.0	THF	4.74	5.25
DMSO	4.88	31.5	t-butylalcohol	5.65	4.27
Acetone	5.69	9.77	1,4 Dioxane	4.90	6.03
DMF	6.21	18.2	1,2 Dimethoxyethane	6.03	3.31
Butanone	5.96	7.94	CS_2	4.59	1.78
Nitrobenzene	5.45	14.1	Acetic acid	5.60	2.29
Benzene	5.80	3.47	Ethyl acetate	5.57	3.98
Cyclohexane	5.66	0.44			

There is a fair correlation between the activation enthalpies and entropies of the oxidation of aldehydes ($r^2 = 0.9998$), indicating the operation of a compensation effect[14]. A correlation between the calculated values of enthalpies and entropies is often vitiated by the experimental errors associated with them. The reaction, however, exhibited an excellent isokinetic relationship, as determined by Exner's method[15]. An Exner's plot between log k_2 at 288 K and at 318 K was linear ($r^2 = 0.9999$) (Figure 3). The value of isokinetic temperature evaluated from the Exner's plot was 1412±108 K. The linear isokinetic correlation implies that all the aldehydes are oxidized by the same mechanism and the change in the rate of oxidation is governed by changes in both the enthalpy and entropy of the activation.

Table 6: Temperature dependence of the reaction constant

Temp./ K	$-\rho^*$	r^2	sd	ψ
288	2.24±0.01	0.9999	0.005	0.01
298	2.14±0.02	0.9998	0.004	0.02
308	2.06±0.01	0.9999	0.006	0.01
318	1.98±0.01	0.9989	0.004	0.04

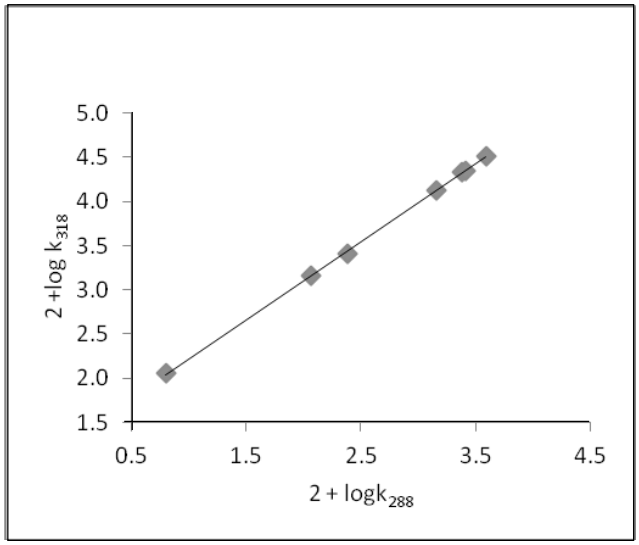

Fig. 3. Exner's Isokinetic Relationship in the oxidation of aldehydes by IDC

Solvent effect: The rate constants, k_2, in eighteen solvents (CS_2 was not considered, as the complete range of solvent parameters was not available) were correlated in terms of the linear solvation energy relationship (6) of Kamlet et al.[16].

$$\log k_2 = A_0 + p\pi^* + b\beta + a\alpha \quad .....6$$

In this equation, π^* represents the solvent polarity, β the hydrogen bond acceptor basicity and α is the hydrogen bond donor acidity. A_0 is the intercept term. It may be mentioned here that out of the 18 solvents, 12 have a value of zero for α. The results of correlation analyses in terms of Equation 6, a biparametric equation involving π^* and β, and separately with π^* and β are given below as Equations 7-10.

$$\log k_2 = -3.72 + 1.56\ (\pm 0.17)\ \pi^* + 0.20\ (\pm 0.14)\ \beta + 0.10\ (\pm 0.14)\ \alpha \quad .....7$$

$R^2 = 0.8806$; sd = 0.16; n = 18; $\psi = 0.38$

$$\log k_2 = -3.69 + 1.60\ (\pm 0.16)\ \pi^* + 0.17\ (\pm 0.13)\ \beta \quad .....8$$

$R^2 = 0.8757$; sd = 0.16; n = 18; $\psi = 0.37$

$$\log k_2 = -3.73 + 1.64\ (\pm 0.16)\ \pi^* \quad .....9$$

$r^2 = 0.8631$; sd = 0.16; n = 18; $\psi = 0.38$

$$\log k_2 = -3.38 + 0.45\ (\pm 0.34)\ \beta \quad .....10$$

$r^2 = 0.0978$; sd = 0.41; n = 18; $\psi = 0.98$

Here *n* is the number of data points and is the Exner's statistical parameter[17].

Kamlet's[16] triparametric equation explains *ca.* 88% of the effect of solvent on the oxidation. However, by Exner's criterion[17] the correlation is not even satisfactory (cf. Eq. 7). The major contribution is due to solvent polarity. It alone accounted for *ca.* 86% of the data. Both β and α play relatively minor roles.

The data on the solvent effect were analysed in terms of Swain's equation[18] of cation and anion solvating concept of the solvents (Equation 11).

$$\log k_2 = aA + bB + C \quad .....11$$

Here A represents the anion solvating power of the solvent and B the cation solvating power. C is the intercept term. (A + B) is postulated to represent the

solvent polarity. The rates in different solvents were analysed in terms of Equation 8, separately with A and B and with (A + B).

$$\log k_2 = 0.65\ (\pm 0.04)\ A + 1.62\ (\pm 0.03)\ B - 4.47 \qquad \text{.....12}$$

$R^2 = 0.9950;\ sd = 0.03;\ n = 19;\ \psi = 0.07$

$$\log k_2 = 0.42\ (\pm 0.53)\ A - 3.35 \qquad \text{.....13}$$

$r^2 = 0.0356;\ sd = 0.43;\ n = 19;\ \psi = 1.01$

$$\log k_2 = 1.57\ (\pm 0.12)\ B - 4.25 \qquad \text{.....14}$$

$r^2 = 0.9111;\ sd = 0.13;\ n = 19;\ \psi = 0.31$

$$\log k_2 = 1.30 \pm 0.12\ (A + B) - 4.44 \qquad \text{.....15}$$

$r^2 = 0.8629;\ sd = 0.16;\ n = 19;\ \psi = 0.38$

The rates of oxidation of acetaldehyde in different solvents showed an excellent correlation in Swain's equation [cf. Eq. 12] with the cation solvating power playing the major role. In fact, the cation solvation alone accounts for *ca.* 99% of the data. The correlation with the anion solvating power was very poor. The solvent polarity, represented by (A + B), also accounted for *ca.* 86% of the data. In view of the fact that solvent polarity is able to account for *ca.* 86% of the data, an attempt was made to correlate the rate with the relative permittivity of the solvent. However, a plot of $\log k_2$ against the inverse of the relative permittivity is not linear ($r^2 = 0.5447$; sd = 0.30; $\psi = 0.69$).

Correlation analysis of reactivity: The rates of the oxidation of six aldehydes show an excellent correlation with Taft's σ^* substituent constants[19], the reaction constant being negative (Table 6). The negative polar reaction constant indicates an electron-deficient carbon centre in the transition state of the rate-determining step.

Mechanism

In aqueous solutions most aliphatic aldehydes exist predominantly in the hydrate form[20] and in many oxidations, in aqueous solutions, it has been postulated that the hydrate is the reactive species. However, owing to the non aqueous nature of the solvent in the present reaction, only the free carbonyl form can be the reactive species. The presence of a substantial primary kinetic isotope effect ($k_H/k_D = 5.75$ at 298 K), confirms that the aldehydic C–H bond is cleaved in the rate determining step. The large negative value of the polar reaction constant together with the substantial deuterium isotope effect indicates that the transition state approaches a carbocation in character. Hence, transfer of a hydride ion from the aldehyde to the oxidant is suggested. The hydride ion transfer mechanism is also supported by major role of cation solvating power of the solvents.

High values of activation indicate that in the rate determining step bond breaking is more important in transition state. Large negative entropy of activation supports a transition state formed from two independent molecules.

Conclusions

The reaction is proposed to proceed through a hydride-

Acid-independent Path (Scheme-1)

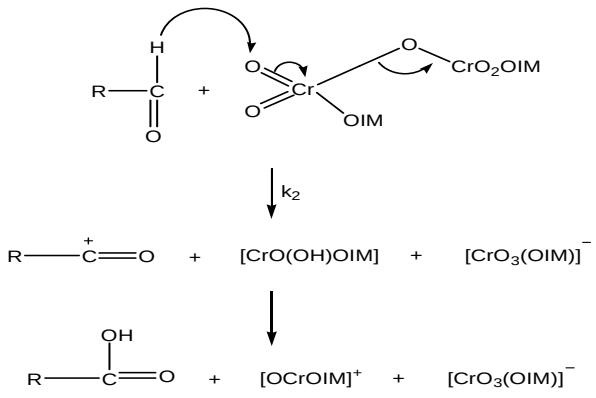

Acid-independent Path (Scheme-2)

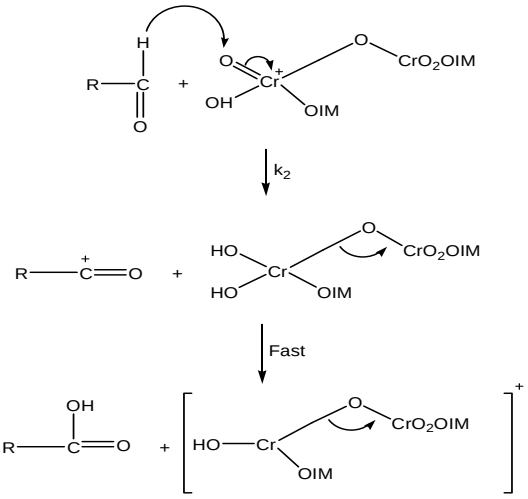

ion transfer from aldehyde to the oxidant. The hydride ion transfer mechanism is also supported by major role of cation solvating power of the solvents. Both deprotonated and protonated forms of IDC are the reactive oxidising species. An aldehydic C-H bond is cleaved in the rate-determining step.

References

1. Cainelli G. and Cardillo G., 1984, Chromium oxidations in Organic Chemistry, (Springer-Verlag, Berlin) Vol. 19.
2. Firouzabadi H. and Sharifi A., 1992, *Synthesis*, 999.
3. Li M. and Johnson M.E., 1995, *Synth..Communn.*, **25**, 533.
4. Mahanti M.K. and Banerji K.K., 2002, *J. Indian Chem. Soc.*, **79**, 31.
5. Kim S. and Chim D.C., 1986, *Bull. Chem. Soc. Jpn.*, **59**, 3297.
6. Sharma D., Panchariya P., Vadera K. and Sharma P.K., 2011, *J. Sulfur Chem.*, **32(4),** 315.
7. Sharma D., Panchariya P., Purohit P. and Sharma P.K., 2012, *Oxid. Commun.*, **35(4),** 821.
8. Purohit T., Patel M., Prakash O. and Sharma P. K., 2013, *Int. J. Chem.*, **2(4),** 436.
9. Mathur L., Choudhary A., Prakash O. and Sharma P.K., 2014, *Asian J. Chem.*, **26(9),** 2597.
10. Soni U., Yajurvedi D., Vyas S., Prakash O. and Sharma P. K., 2015, *Eur. Chem. Bull.*, **4(9),** 449.
11. J. Mitchell Jr., 1954, Organic Analysis, Vol. II, Interscience, New York, 273.
12. Perrin D.D., Armarego W.L., Perrin D.R., 1966, Purification of Organic Compounds, Oxford, Pergamon Press, 1966.
13. R.T. Hall and W.E. Schaefer, 1954, *Organic Analysis*, Vol II, Interscience, New York, 55.
14. Liu L. and Guo Q-X, 2001, *Chem. Rev.*, **101**, 673.
15. Exner O., 1964, *Collect. Chem. Czech. Commun.*, **29**, 1094.

16. Kamlet M.J., Abboud J L M, Abraham M.H., Taft R.W., 1983, *J. Org. Chem.*, **48**, 2877.

17. Exner O., 1966, *Collect. Chem. Czech. Commun.*, **31**, 3222.

18. Swain C.G., Swain M.S., Powel A.L. and Alunni S., 1983, *J. Am. Chem. Soc.*, **105**, 502.

19. R.W. Taft, 1956, Steric effects in Organic Chemistry, Ed. M.S. Newman, Wiley, New York, p.13.

20. R.P. Bell, 1966, *Adv. Phys. Org. Chem.*, **4**, 1.

RNI No. MAHENG/2017/74063
ISSN No. (Print) 2581-5911

Differences in Triboluminescent Emission Properties of EuD_4TEA Synthesized With Europium Nitrate and Acetate

Ross S. Fontenot[1*], William A. Hollerman[1], Stephen A. Williams[1], Jacque A. Meche[1], Kamala N Bhat[2], and Mohan D Aggarwal[2]
[1]University of Louisiana at Lafayette, Department of Physics,
P.O. Box 44210, Lafayette, LA 70504, USA
[2]Alabama A&M University, Department of Physics, Chemistry, and Mathematics,
P.O. Box 1268, Normal, Alabama 35762, USA
***E-mail: rsfontenot@hotmail.com**

Abstract
Europium tetrakis dibenzoylmehtide triethylammonium (EuD_4TEA) is one of the most intense triboluminescent (TL) materials currently known. In 2011, the authors have reported that the triboluminescent yield can be enhanced by changing the starting europium salt from europium chloride to europium nitrate by 82%. Unfortunately, europium nitrate has been classified as a hazardous material that cannot be shipped by air, which limits the availability of manufacturers and increases the cost. In an effort to further reduce the synthesis cost of EuD_4TEA, we explore the effects of europium acetate on the triboluminescent properties of EuD_4TEA by comparing the triboluminescent yield. The photoluminescent spectra as well as crystal structure using an optical microscope will also be explored.

Keywords: *Triboluminescence, Fractoluminescence, Mechanoluminescence, Europium tetrakis dibenzoylmehtide triethylammonium, Materials Synthesis, Solution Growth, Luminescence*

Introduction

Triboluminescence (TL) is the light emitted from a material when it undergoes fracture.[1] While this unique phenomenon has been known for over 400 years, no theory has yet been advanced to predict whether a material will emit TL. However, this has not stopped scientists from coming up with many unique applications. One such application is the use as the active element for impact and damage sensors.[1–13] For example, in 1999, Sage and Geddes used TL to patent a sensor capable of discerning the locations of an impact.[8,9,14] Their simple design involved coating a structure with a triboluminescent material or creating a composite triboluminescent object.[8,9,14] A sensor would then be embedded within the structure or mounted on its surface.[14] Impacts to the structure would produce light, which would be recorded and analyzed to determine the location.[14] In addition, Sage *et al.* proposed that several different triboluminescent materials could be used and arranged at various locations.[8,9,14] The advantage is that when an impact takes place, its location could be determined by the wavelength emitted.[14] For example, by placing two different triboluminescent materials at known distances from the detector, it is possible to determine the approximate location of the impact by measuring the emitted wavelength.

Unfortunately, the triboluminescent emission yield for most materials is small; therefore, the resulting light can be difficult to detect. For the last few years, Fontenot and Hollerman *et al.* have been investigating europium tetrakis dibenzoylmethide triethylammonium (EuD_4TEA),[2,15,16] which is also sometimes known as triethylammonium tetrakis (dibenzoylmethanato) europate.[17] This material is bright enough to be seen in daylight and has 206% of the triboluminescent emission yield of ZnS:Mn when subjected to low energy impacts.[2,18] In fact, recently, Fontenot *et al.* showed that adding dibutyl phosphate can increase the triboluminescent emission yield by 500 or 600%, i.e., it has an triboluminescent emission yield between 700 and 800% of ZnS:Mn.[19]

While emission from this material is very bright, it uses europium compounds as precursors, which are expensive in today's market. Just a few years ago, europium nitrate (99.999% pure) could be purchased for about $3-5 per gram (not including shipping costs). Since the 1990s, a large fraction of rare earth elements (such as europium) have come from China. Since 2007, the Chinese government has restricted mining and production of rare earth elements to conserve resources and to give supply preference to their manufacturers. For this reason, the cost of compounds made with rare earth elements has greatly increased. Currently, the most economical europium nitrate (99.9% pure) costs about 300% of what it did a few years ago. Adding to this increase, europium nitrate is now considered to be a hazardous material (oxidizer) in the United States.

To reduce the cost of synthesizing EuD_4TEA, we decided to use europium acetate instead of europium nitrate as the precursor material. Europium acetate was chosen because it can be dissolved in ethanol, it is the same europium ion state as common europium nitrate, and is significantly less expensive. This paper will compare the TL properties of EuD_4TEA made from both europium nitrate and acetate precursors.

Methods and Materials

Synthesis of EuD_4TEA

The synthesis of EuD_4TEA was based on reported procedures[2]. The process began by pouring 25 mL of HPLC grade anhydrous denatured ethanol (Alfa Aesar, 22930) into an Erlenmeyer flask and placed onto a hotplate. Afterwards, 4 mmol of 99.9% (REO) europium (III) acetate hydrate (Alfa Aesar, 42878) was added to the hot solution. Then, 13 mmol of 99% (GC) 1,3-diphenyl-1,3-propanedione (Chem-Impex, 00693) also known as dibenzoylmethane (DBM) was added. This addition caused the clear solution to turn dark yellow. Once the DBM was dissolved, the flask was removed from the hotplate and 14 mmol of ≥99.5% triethylamine (TEA) (Sigma Aldrich, 471283) was added. The solution was then kept aside to cool at ambient temperature. The EuD_4TEA powder that formed were light yellow in color, clumpy, and hard as shown in Fig 1(a). The same procedure was then repeated using 99.9% (REO) europium (III) nitrate hexahydrate (Alfa Aesar, 15290), which produced a light yellow powder that was very sparkly as shown in Fig. 1(b).

Triboluminescent Testing

Once the crystals were completely dried, they were stored in a small clear round wide-mouth jar. Using a custom built drop tower[18], the crystalline products were tested for their triboluminescent properties. The measurement began by placing 0.10 g of sample powder on the Plexiglass plate. The powder was arranged so that it was positioned around the center of the tube with a minimum height. A 130 g steel ball was positioned on a pull pin at a set distance of 42 inches (1.1 m) above the material. The pin was pulled and the ball fell and impacted the sample material producing TL. After each test, the drop tube was removed, the ball was cleaned, and the sample powder was redistributed near the center of the target area.[18]

To determine the triboluminescent yield for a given sample, a United Detector photodiode was positioned

(a) (b)

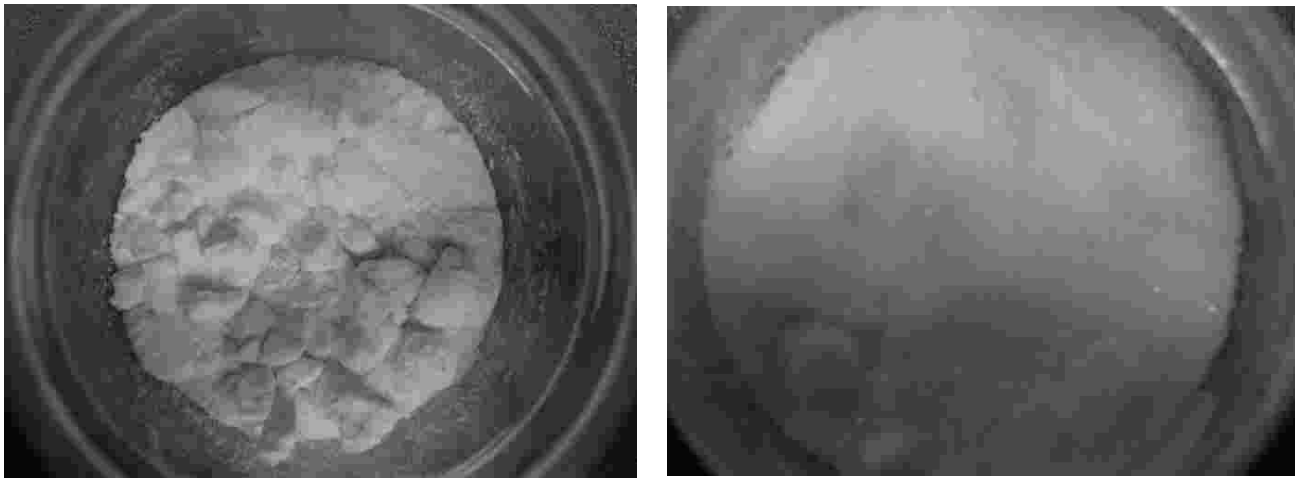

Fig. 1. Pictures of the finished EuD_4TEA samples synthesized with (a) europium acetate and (b) europium nitrate. These pictures were taken under standard white room light.

under the Plexiglass plate 2.25 cm below the sample. A Melles Griot large dynamic range linear amplifier set to a gain of 20 µA increased the signal amplitude. A Tektronix 2024B oscilloscope recorded the signal in single sequence mode with a 500 µs measurement time. Once the signal was acquired, it is analyzed using custom LabVIEW program that integrated the area under the curve and calculated the decay time for the particular emission.[18]

Photoluminescent Testing

Unlike fluorescence, phosphorescence utilizes both the singlet and triplet excited states.[20] The europium complex has an emission mechanism consisting of: the ligand absorbs energy, undergoes intersystem crossing into a triplet state, and then transfers its energy to the Eu^{3+} ion.[20] The phosphorescence of each material was excited using a 4 W 365 nm Raytech UV lamp (LS-7CB). It should be noted that each material was fresh, i.e., not tested for TL. The photoluminescence was recorded using an Ocean Optics USB 2000 spectrometer. The integration time was controlled using the SpectraSuite program and increased by using software until the photoluminescent emission spectrum reached its maximum that was just below the saturation limit of the spectrometer. Once this was determined, the dark background was subtracted and one hundred spectra were recorded and averaged.

Microscopy

To better understand the crystal structure, the samples were examined using a standard light microscope as well as a JOEL-6300FV field emission scanning electron microscope (SEM). The unused samples were first attached to metal stubs using carbon tape. Then they were gold coated so that they could be analyzed using SEM. An Electron Microscopy Sciences 550x sputter coater was used to coat a 12 nm gold layer on each sample. Once the thin coats were dry, they were placed inside the SEM. The working distance, till, accelerating voltage, and emission current were then set to 22 mm, 300 mm, 15 kV, and 8 µA, respectively.

Results and Discussion

Using the drop tower and LabVIEW VI tools described above, the effects of europium acetate on the triboluminescent properties of EuD_4TEA are shown in Fig 2. Due to this being a relative measurement, all the data was normalized to the europium nitrate result. The error

in normalized TL light yield was estimated to be 7% which is the error from synthesizing the material and the drop tower apparatus.[21] From these results, it is evident that europium acetate provides about half of the triboluminescent yield as the nitrate version. It should be noted that while the triboluminescent yields were different, the decay times are statistically identical. The measured triboluminescent decay time for the acetate based EuD_4TEA was 522.7 ± 10.1 µs, while the nitrate based EuD_4TEA decay time was 524.3 ± 17.7 µs.

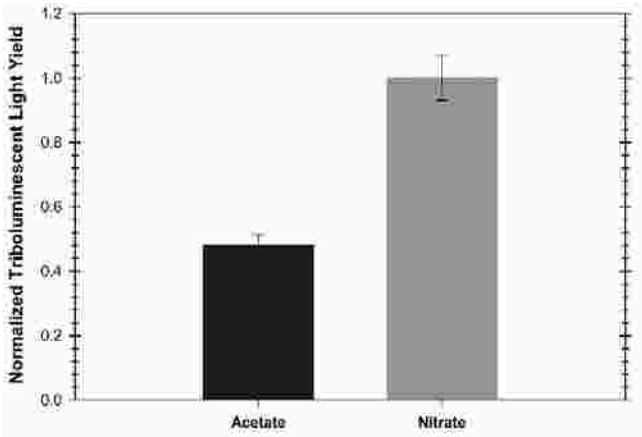

Fig. 2. Comparison of the TL produced by EuD_4TEA synthesized with europium acetate and nitrate precursors.

To better understand why the acetate provides a lower triboluminescent yield, we first used a standard optical microscope to investigate the crystals. As you can see in Fig. 3(a), the crystals formed by the acetate are cloudy. Meanwhile, the crystals produced by the nitrate are clear as shown in Fig. 3(c). This could be explained using the solubility. When acetate was used to create EuD_4TEA, the acetate had a very low solubility with ethyl alcohol (it was completely insoluble with acetone). This in turn caused a quick precipitation and rougher crystals. Conversely, the europium nitrate has a higher solubility with ethyl alcohol, which slows the precipitation and allows for a better crystal to form. This is verified by the SEM images shown in Fig. 4 as well as supplemental plots Figs. S1 and S2. Notice how the acetate based EuD_4TEA looks dirty, i.e., it is typically a rod shape with many smaller rods growing around it [Figs. 4(a) and S1]. Conversely, the nitrate based EuD_4TEA tends to be more plate-like and cleaner [Figs. 1(b) and S2]. More research is needed to fully understand these results.

(a) (b)

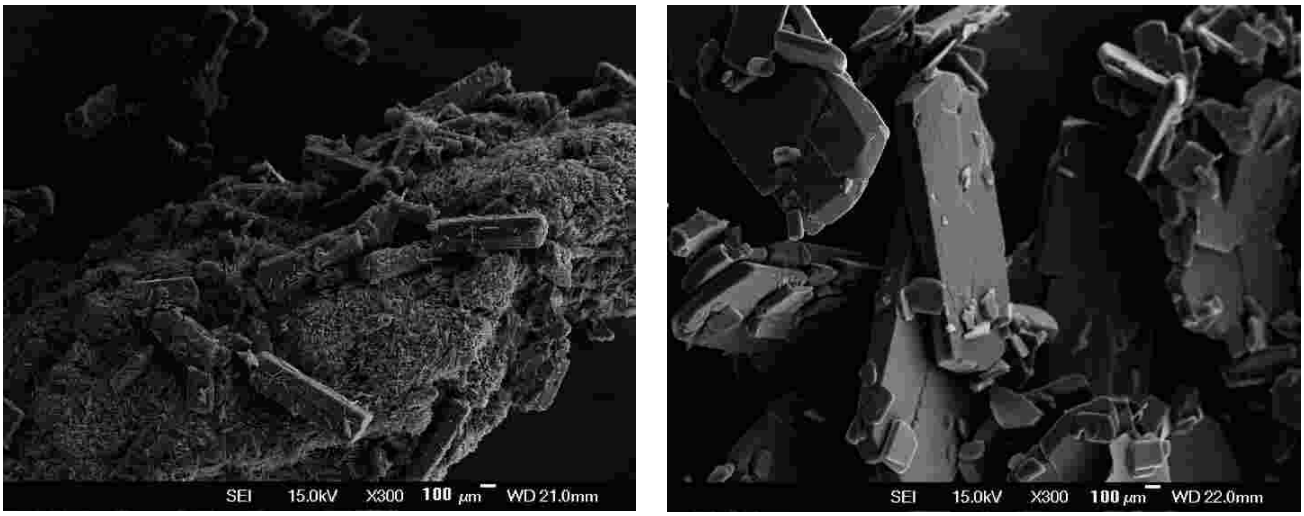

Fig. 4. Scanning electron microscope (SEM) images of EuD_4TEA crystallites made with (a) europium acetate and (b) europium acetate precursors at a magnification of 300.

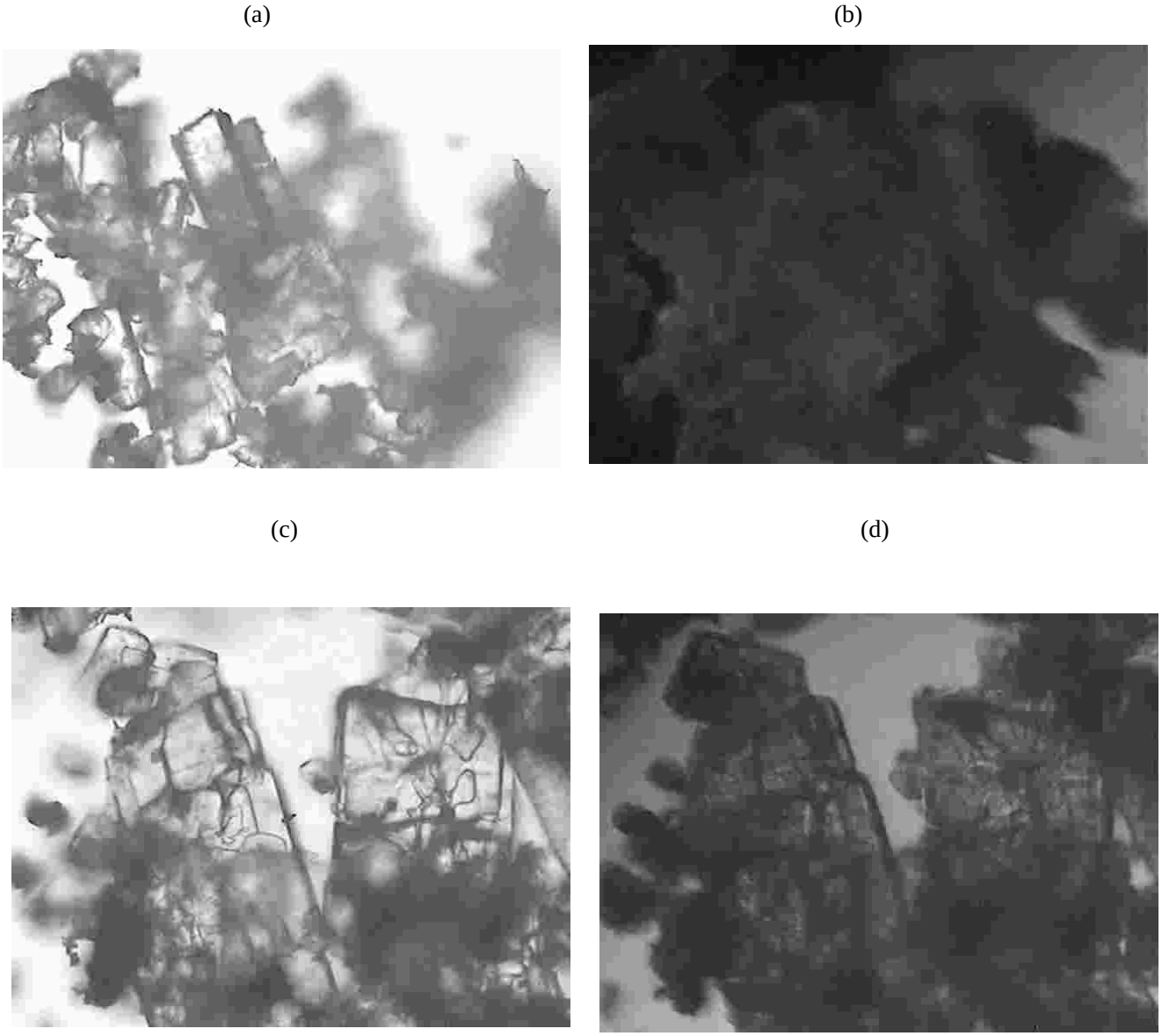

Fig. 3. Optical microscope pictures of EuD_4TEA crystallites made with europium acetate and nitrate at a magnification of 40. EuD_4TEA made with europium acetate is shown under (a) regular white light and (b) ultraviolet light. EuD_4TEA made with europium nitrate is shown under (c) regular white light and (d) ultraviolet light. EuD_4TEA

The measured photoluminescent (PL) and triboluminescent emission spectra for EuD_4TEA are shown in Figs. 5 and 6, respectively. Notice that the PL and TL excited emissions for both the acetate and nitrate precursor samples have the same peak wavelengths and are very bright. The spectra indicate that the luminescence from EuD_4TEA originates from the typical Eu^{3+} centered transitions from the $^5D_0$ levels to the lower$^7 F_{0-4}$ levels.[22] The main emission occurred from the $^5D_0 \rightarrow F_2$ transitions.

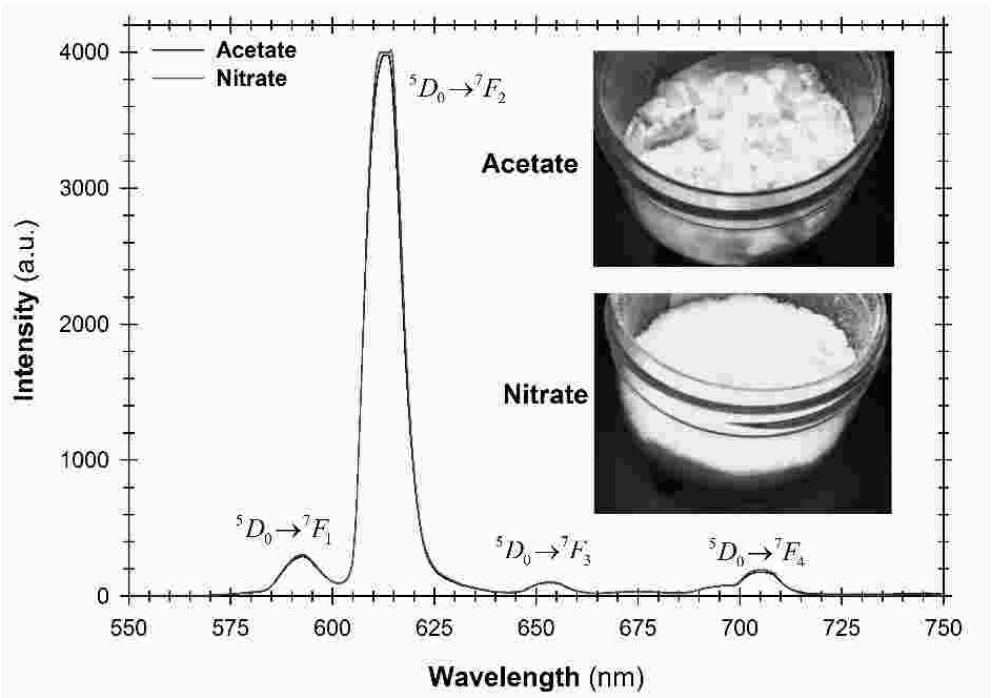

Fig. 5. Photoluminescent emission spectrum of EuD_4TEA synthesized with europium acetate and nitrate precursors. The inset pictures show the PL emitted from the samples under the UV light.

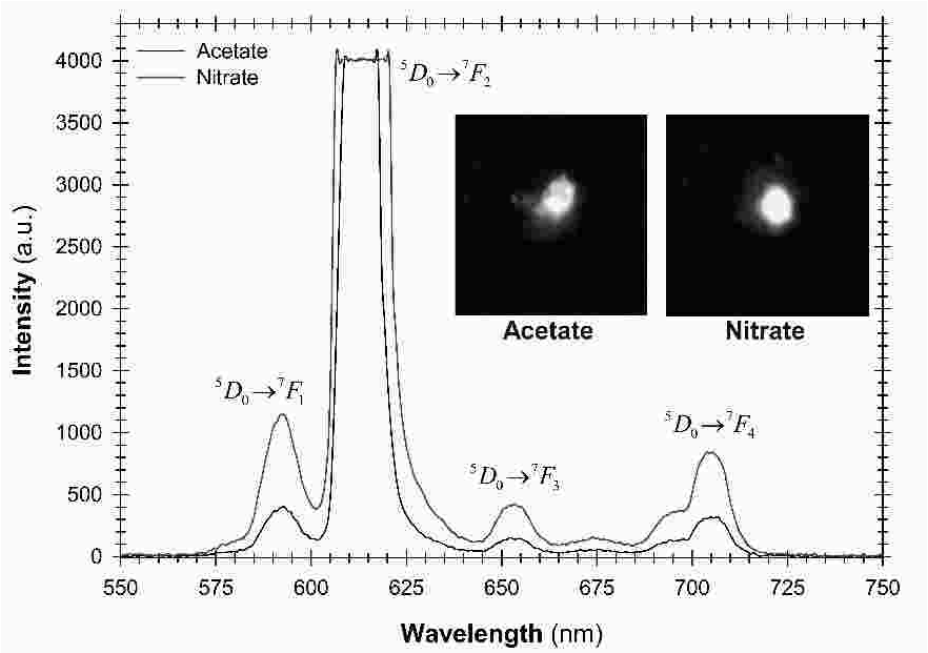

Fig. 6. Triboluminescent emission spectrum of EuD_4TEA synthesized with europium acetate and nitrate precursors. The inset pictures show the TL emitted upon impact.

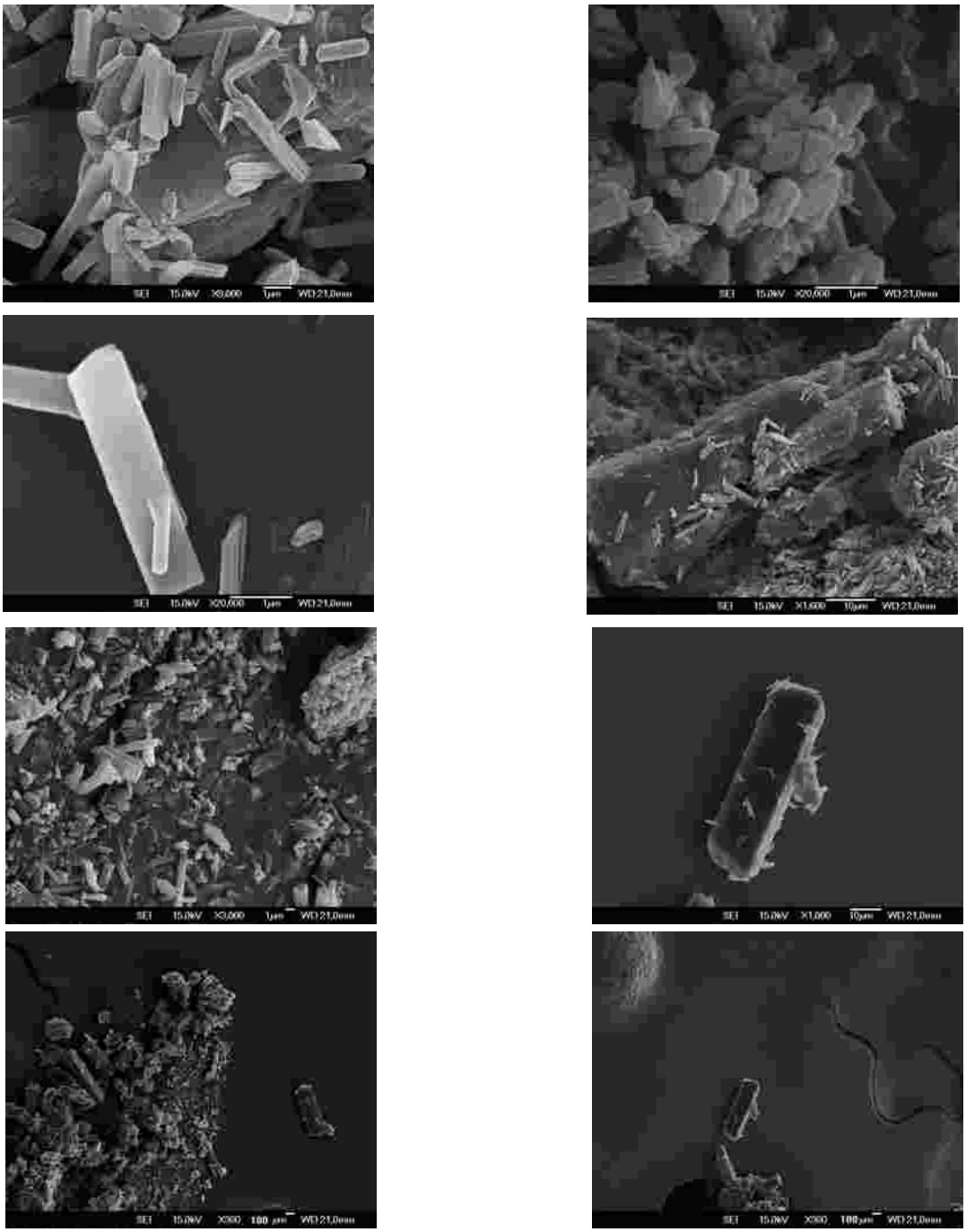

Fig. S1. Scanning electron microscope images of EuD_4TEA crystallites made with europium acetate. The given magnifications and scale bar sizes are shown on each image. A 12 nm gold layer was deposited on each sample.

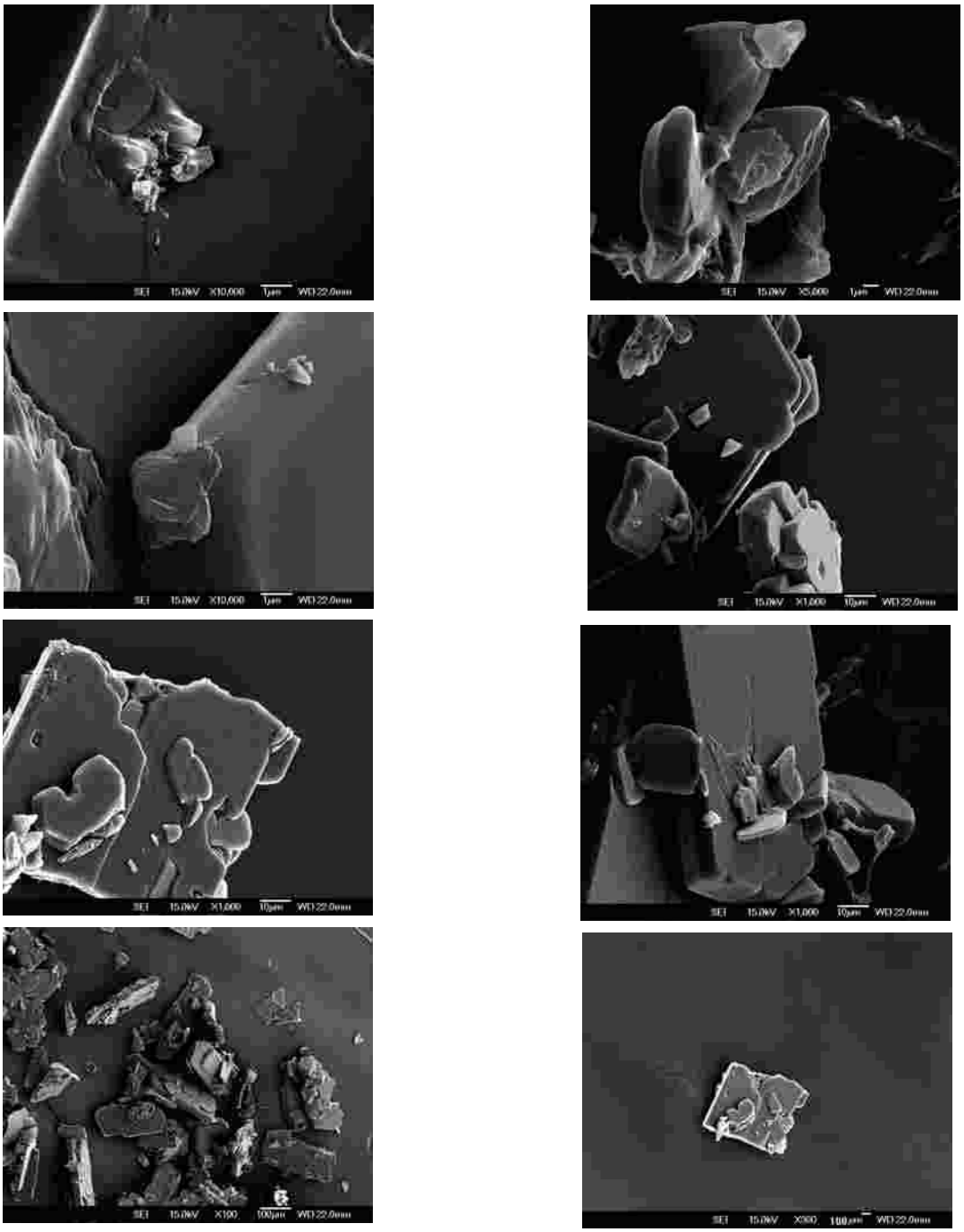

Fig. S2. Scanning electron microscope images of EuD_4TEA crystallites made with europium nitrate. The given magnifications and scale bar sizes are shown on each image. A 12 nm gold layer was deposited on each sample.

Conclusions

In order to reduce cost, europium acetate was used to synthesize EuD_4TEA. It was found that the triboluminescent yield for EuD_4TEA made with europium acetate was approximately half of what was measured for the sample made with europium nitrate. In addition, the EuD_4TEA precursor crystals produced with the acetate are cloudy and only emit luminescence near the edges. Emission peaks from both the acetate and nitrate precursor samples have the same peak wavelengths, when excited by both PL and TL. The spectra indicate that the luminescence from EuD_4TEA originates from the typical Eu^{3+} centered transitions from the $^5D_0$ levels to the lower $^7F_{0-4}$ levels. The main emission occurred from the $^5D_0 \rightarrow {}^7F_2$ transitions. As a result, the use of europium acetate to synthesize EuD_4TEA using ethyl alcohol is not practical, even with its reduced cost. Additional research needs to be completed to further quantify the best precursor materials for synthesizing EuD_4TEA.

Acknowledgement

This research was funded by the Louisiana Space Grant Consortium under the grant "Feasibility of EuD_4TEA-Based Sensors to Detect Space Radiation, 2014-2015." We would also like to thank the Louisiana Accelerator Center for allowing us the use of their chemistry center for the synthesis.

References

1. Walton, A. J., *Adv. Phys.*, 1977, **26**, 887–948.

2. Fontenot, R. S., Bhat, K. N., Hollerman W. A. and Aggarwal, M. D., *Mater. Today*, 2011, **14**, 292–293.

3. Fontenot, R. S., Hollerman, W. A., Broussard B. M. and Steuart, M. S., 2010, in *Earth and Space*, eds. Song G. and Malla, R. B., 2010, American Society of Civil Engineers, Honolulu, Hawaii, pp. 2560–2567.

4. Goedeke, S.M., Allison, S.W., Womack, F.N., Bergeron N.P. and Hollerman, W.A., 2001, Triboluminescence and its application to space-based damage sensors, Oak Ridge, TN.

5. Hollerman, W.A., Goedeke, S. M., Bergeron, N. P., Moore, R. J., Allison S. W. and Lewis, L. A., 2005, in Photonics for Space Environments *X*, ed. E. W. Taylor, SPIE, San Diego, CA, USA, vol. 5897, p. 58970F–10.

6. Olawale, D. O., Dickens, T., Sullivan, W. G., Okoli, O. I., Sobanjo J. O. and Wang, B.,2011, *J. Lumin.*, **131**, 1407–1418.

7. Sage I. C. and Bourhill, G., 2001, *J. Mater. Chem.*, **11**, 231–245.

8. Sage, I. C., Badcock, R., Humberstone, L., Geddes, N. J., Kemp M. and Bourhill, G., 1999, *Smart Mater. Struct.*, **8**, 504.

9. Sage, I. C., Humberstone, L., Oswald, I., Lloyd P. and Bourhill, G., 2001, *Smart Mater. Struct.*, **10**, 332–337.

10. Xu, C. N., Watanabe, T., Akiyama M. and Zheng, X. G., 1999, *Appl. Phys. Lett.*, **74**, 1236.

11. Xu, C. N., Zheng, X. G., Akiyama, M., Nonaka K. and Watanabe, T., 2000, *Appl. Phys. Lett.*, **76**, 179.

12. Yoo, C. S., Radousky, H. B., Holmes N. C. and Edelstein, N. M., 1991, *Phys. Rev. B*, **44**, 830–833.

13. Zink, J. I. 1978, *Acc. Chem. Res.*, **11**, 289–295.

14. Bhat, K. N., Fontenot, R. S., Hollerman W. A. and Aggarwal, M. D., 2012, *Int. J. Chem.*, **1**, 100–118.

15. Hurt, C. R., Mcavoy, N., Bjorklund S. and Flipescu, N., 1966, *Nature*, **212**, 179–180.

16. Sweeting L. M. and Rheingold, A. L., 1987, *J. Am. Chem. Soc.*, **109**, 2652–2658.

17. Fontenot, R. S., Hollerman, W. A., Aggarwal, M. D., Bhat K. N. and Goedeke, S.M., 2012, *Measurement*, **45**, 431–436.

18. Fontenot, R. S., Bhat, K. N., Owens, C. A., Hollerman W. A. and Aggarwal, M.D., 2015, *J. Lumin.*, **156**, 428–434.

19. Takada, N., Peng J. and Minami, N., 2001, *Synth. Met.*, **121**, 1745–1746.

20. Hollerman, W. A., Fontenot, R. S., Bhat K. N. and Aggarwal, M. D., 2012, *Metall. Mater. Trans. A*, **43**, 4200–4203.

21. Carnall, W. T., Fields P. R. and Rajnak, K., 1968, *J. Chem. Phys.*, **49**, 4450–4455.

Conference Alerts

1) International Conference on Chemistry and Environmental Science, 2018 (ICCES 2018)
January 5-6, 2018, Kota, Kinabalu, Malaysia
Website: http://icces2018.weebly.com/

2) 3rd World Research Journals Congress-World Environment Congress
January 10-12, 2018, Bangalore, India
Website: http:worldresearchjournals.com/conferenceinvitation.aspx
Enquiries: congress@worldresearchjournals.com

3) 6th International Conference on Nano and Materials Science (ICNMS-2018)
January 19-21, 2018, Orlando, USA
Website: http://www.icnms.org/

4) 1st Alpine Winter Conference on Medicinal and Synthetic Chemistry
January 28-February 1, 2018, St. Anton am Arlberg, Austria
Website: http://go.evvnt.com/128374-1

5) International Conference on Clean and Green Chemistry (ICCGE2018)
February 7-9, 2018, Paris, France
Website: http://www.iccge.org/

6) 3rd International Conference on Research in Science and Technology (ICRST2018)
Organised by World Association for Scientific Research and Technical Innovation (WASRTI)
February 20-21, 2018, Dubai, UAE
Enquiries: info@wasrti.org

7) 20th International Conference on Materials Chemistry and Catalysis (ICMCC-2018)
February 23-25, 2018, Mumbai, India
Website: http://www.waset.org/conference/2018/mumbai/ICMCC

8) 8TH International Conference on Chemistry and Chemical Process (ICCCP-2018)
February 23-25, 2018, Nha Trang, Vietnam
Website: http://www.icccp.org/

9) 5th International Conference on Chemical and Biological Sciences (ICCBS 2018)
March 7-9, 2018, Bucharest, Romania
Website: http://www.iccbs.org/

10) International Conference and Expo on Nanotechnology
April 19-20, 2018, Dubai, UAE
Website: http://scientificcognizance.com/Conference/Nanotechnology/Home

11) 11th Global Experts Meeting on Chemistry and Computational Catalysis
May 18-19, 2018, Singapore
Enquiries: chemistry@conferencesworld.org

12) World Agriculture Congress (4th World Research Journals Congress)
May 24-26, 2018, Banat's University of Agricultural Sciences and Veterinary Medicine "King Michael 1", Timisoara, Romania
Website: www.worldresearchjournals.com

13) 22nd Annual Green Chemistry and Engineering Conference
Hosted by ACS Green Chemistry Network
June 18-20, 2018, Portland, Oregon, USA
Website: www.acs.org/gce
Enquiries: gceconference@acs.org

ORDER FORM

I/We wish to subscribe to **G P Globalize Research Journal of Chemistry**

(Please fill in the form in BLOCK Letters).

Name:……

Address:……..

-……

-……

….....……..…Pin code:……..…

Tel No:…….....……....Email:…….....……....…….....

DD No. …..……....Dated……....Amount.....……...(₹ ….....…)

For Online payment:

Name of the Bank:	**Axis Bank**
Branch Name:	**Tardeo, Mumbai (MH)**
Account No.	**916020066451552**
IFSC Code:	**UTIB0001345**

Note :
All Payments by Bank Draft/Multicity Cheque (please add ₹ 75/- for outstation cheque) should be drawn in favour of "Gaurang Publishing Globalize Pvt. Ltd" payable at Mumbai.

RNI No. MAHENG/2017/74063
ISSN No. 2581–5911

Send your orders to - - - - -
Gaurang Publishing Globalize Private Limited
1, Plot 72, Pandit Madan Mohan Malviya Marg,
Tardeo, Mumbai-400034, India
● Mobile: 9969 392 245 ● E-mail: gpglobalize@gmail.com